AD 662003

FINAL REPORT

TO

NATIONAL SONIC BOOM EVALUATION OFFICE

RESPONSE OF STRUCTURES TO

SONIC BOOMS

PRODUCED BY XB-70, B-58 AND F-104 AIRCRAFT

BASED ON SONIC BOOM EXPERIMENTS
AT
EDWARDS AIR FORCE BASE

CONTRACT NO. AF 49(638) - 1739

OCTOBER 1967

D D C

NOV 3 0 1967

JOHN A. BLUME & ASSOCIATES RESEARCH DIVISION

SAN FRANCISCO

378

CLEARINGHOUSE

N O T I C E

Unless otherwise provided by contract, the Government is not responsible for, nor has any obliga-
tion whatsoever respecting the use of, or reliance upon, drawings, specifications or other data
contained herein. The fact that the Government may have formulated, furnished, or in any way
supplied the said drawings, specifications, or other data is not to be regarded by implication or
otherwise as in any manner licensing the holder or any other person or corporation, or conveying
any rights or permission to manufacture, use, or sell any patented invention that may in any way
be related thereto.

The information contained herein is a part of the President's Office of Science and Technology's
national sonic boom research program funded by the Federal Aviation Agency under the supersonic
transport development program. This research effort was conducted under the Executive Manage-
ment of the United States Air Force through the National Sonic Boom Evaluation Office with tech-
nical support provided by the Department of Defense, the National Aeronautics and Space Admini-
stration, the U. S. Department of Agriculture, the Environmental Science Services Administration,
and the Federal Aviation Agency. Advice and support were also provided by the National Academy
of Sciences.

Qualified requesters may obtain copies of this report from the Defense Documentation Center (DDC),
Cameron Station, Building 5, 5010 Duke Street, Alexandria, Virginia, 22314.

This report has been released to the Clearinghouse for Federal Scientific and Technical Informa-
tion, U. S. Department of Commerce, Springfield, Virginia, 22151, in stock quantities for sale to
the general public.

That portion of this report which reflects the views of the contractors does not necessarily reflect
the official views or policy of the Government. This report does not constitute a standard, speci-
fication or regulation.

Distribution of this document is unlimited.

FINAL REPORT

TO

NATIONAL SONIC BOOM EVALUATION OFFICE

NSBEO-2-67

RESPONSE OF STRUCTURES TO SONIC BOOMS
PRODUCED BY XB-70, B-58 AND F-104 AIRCRAFT

By

J. A. Blume, R. L. Sharpe
G. Kost, J. Proulx

BASED ON SONIC BOOM EXPERIMENTS
AT
EDWARDS AIR FORCE BASE

OCTOBER 1967

JOHN A. BLUME & ASSOCIATES RESEARCH DIVISION
SAN FRANCISCO, CALIFORNIA

CONTRACT NO. AF 49(638)-1739

ABSTRACT

The response of test structures and structure elements to sonic booms produced by XB-70, B-58 and F-104 aircraft was studied. These aircraft produced sonic booms of different signature durations. They were flown at several flight track offsets, altitudes and Mach numbers so as to generate different overpressure levels and signature characteristics. Free field signature data and the effects of free field signature parameters on structural response were analysed. Studies were made of the plate response (lateral deformation) and racking response (in-plane deformation) of the test structures. Damage complaints resulting from the test missions were investigated and the results analysed. The implications of the magnitudes of the responses of the test structures and the investigation of the damage claims resulting from the test missions on possible damage caused by supersonic flights were discussed.

I

TABLE OF CONTENTS

TABLE OF CONTENTS (Cont'd)

LIST OF TABLES

LIST OF TABLES (Cont'd)

LIST OF FIGURES

LIST OF FIGURES (Cont'd)

LIST OF FIGURES (Cont'd)

LIST OF FIGURES (Cont'd)

RESPONSE OF STRUCTURES TO SONIC BOOMS
PRODUCED BY XB-70, B-58 AND F-104 AIRCRAFT

I. SUMMARY OF MAJOR FINDINGS AND RECOMMENDATIONS

This report was prepared as partial fulfillment of the requirements
of Contract AF 49(638)-1739. The report summarizes the work performed by
John A. Blume & Associates Research Division during the sonic boom experi-
ments at Edwards Air Force Base. A detailed discussion of findings derived
from analyses of the data measured and recorded is presented.

The general objective of the structure response portion of the
Edwards Air Force Base Program, "determine the response of typical struc-
tures to sonic booms having different signature characteristics and
evaluate damage resulting from the program overflights", was accomplished.
The response of test structures and structure elements to sonic booms
produced by XB-70, B-58 and F-104 aircraft was studied. These aircraft
produced sonic booms of different signature durations. They were flown
at several flight track offsets, altitudes and Mach numbers so as to
generate different overpressure levels and signature characteristics. Free
field signature data and the effects of free field signature parameters on
structural response were analysed. Studies were made of the plate response
(lateral deformation) and racking response (in-plate deformation) of the
test structures. Damage complaints resulting from the test missions were
investigated and the results analysed. The implications of the magnitudes
of the responses of the test structures and the results of the investiga-
tions of damage claims resulting from the test missions on possible damage
caused by supersonic flights were evaluated.

This chapter presents a summary of major findings and recommendations,
and Chapter II presents a detailed summary of this report. Detailed dis-
cussions of the analyses performed are covered in Chapters III through XI.

The findings presented in this report are based on detailed analyses
of structure response and free field overpressure data for seventeen com-
parable XB-70, B-58, and F-104 missions flown within minutes of each other.

The measured plate response of three gypsum board/wood stud/wood siding walls and one large plate glass window, and the measured racking response of two typical wood frame houses, one one-story and one two-story house, were analysed in detail and compared with response predicted using boom signatures. In addition, the plate and racking response of a long-span steel frame-metal siding building were analysed.

MAJOR FINDINGS

Free field signature data and the effects of free field signature parameters on structural response were analysed and the following are major findings:

1. Sonic booms from large aircraft such as the XB-70 and the future Supersonic Transport will affect a greater range of structure elements (those elements with frequencies below approximately 5 cps) than will sonic booms from smaller aircraft such as the B-58 and F-104. These results are predictable if the boom and structure element characteristics are known. The natural frequency at which the maximum DAF occurred was primarily a function of the time from start of boom to negative peak T_2. As T_2 increased, the maximum DAF occurred at a lower natural frequency. T_2 increased as size of aircraft increased.

2. The Dynamic Amplification Factors (DAF) computed from free field signatures and peak positive free field overpressures were independent of the channel on which the signatures were recorded. Therefore, a single free field microphone would have supplied sufficient data to predict structure element response.

3. The ratio P_2/P_1 (absolute value of peak negative overpressure to peak positive overpressure) decreased as the offset of the aircraft increased for XB-70 missions. The magnitude of the maximum DAF decreased as the ratio P_2/P_1 decreased.

4. The DAF spectra obtained using a wave model described by free field signature parameters P_1, P_2, T_1, and T_2 (peak positive overpressure, peak negative overpressure, rise time, and time from start of boom to negative peak, respectively) were equal at the 95 percent confidence level to the DAF spectra obtained from digitized free field signatures. The wave model can be used to

1.2

predict structure response if these parameters and the characteristics of the structure element are known.

5. In the analysis of the effects of lateral offset of aircraft, the ratio P_2/P_1 in the recorded free field signatures caused the predominant effect on DAF. The recorded signatures showed little change in rise times (T_1) or in durations (τ) for overhead and offset missions for each type of aircraft. Therefore the influence of lateral offset on DAF spectra was limited to the effect of the ratio P_2/P_1.

The plate and racking response of the one-story and two-story test houses (E-1 and E-2, respectively) and of the long span steel frame structure (E-3) to sonic booms generated by the Edwards AFB test flights were analysed. The major findings were as follows:

6. Peak plate displacements of three typical walls in the two test houses were less than 0.034 inches for sonic boom overpressures of approximately 2 psf. Racking displacements at the roof line of the northeast corners of Test Houses E-1 and E-2 were extremely small (less than 0.0018" for E-1 and less than 0.005" for E-2) for sonic booms on the order of 2 psf overpressure.

7. Measured displacements of the three typical walls were nearly equal to predicted displacements based on either free field or net pressure signature data. Racking displacements predicted from free field peak overpressures and DAF spectra calculated from free field pressure signatures were in good agreement with measured displacements. The response of the large glass window in E-1 was predictable using free field signature data.

8. Structure response could be adequately predicted by using peak overpressures and DAF spectra calculated from free field signatures.

9. The future SST for peak overpressures of about 2 psf should produce racking displacements of typical houses that will be of similar magnitude, or possibly smaller, than those caused by the XB-70 missions. These racking displacements should be negligible and far less than those required to cause damage.

10. No sonic boom damage was observed in the test structures prior to or after the test flights. There were minor shrinkage cracks in the test structures prior to start of test flights. However, no discernible extension or widening of these cracks was observed although observations were made and recorded daily.

11. Damage to properly designed and constructed houses from low magnitude sonic booms is extremely unlikely. Damage should not occur to structure elements such as glass windows from racking motions caused by low magnitude sonic booms.

The supersonic test missions subjected a large number of buildings and structures at Edwards AFB and in communities near Edwards to sonic booms. A survey was made of all glass windows and doors in buildings and structures at Edwards to provide a basis for determining the extent of glass damage caused by the test program. An engineering investigator inspected each complaint received from Edwards and the adjacent communities. The major findings were as follows:

12. As the condition of the glass panes at Edwards AFB was determined prior to the test program, the number of damaged panes caused by booms from test missions should be an indicator of glass damage to be expected from future level supersonic flights gene   ng sonic boom peak overpressures of 2 to 3 psf. The rate was one damag.._,ane per 7.9 million boom-pane exposures. This rate was 27 percent of the rate for buildings in communities adjacent to Edwards which were not condition surveyed prior to test missions.

13. During Phase I, the 110,390 glass panes in structures at Edwards were subjected to more booms from test missions than were the 605,000 glass panes in the adjacent communities; however, the aircraft while over Edwards were flying straight courses and then made turns at supersonic speeds over adjacent communities. Some focusing of the boom overpressure (or super booms) may therefore have been produced with peak overpressures greatly exceeding those produced on the Base. As a resuit, the valid glass damage rate per mission during Phase I was 8.8 times the rate during Phase II when aircraft generally flew straight courses while at supersonic speeds.

14. Fifty-eight percent of all incidents of damage for which complaints were received during Phases I and II were listed as possibly caused by sonic booms generated by test program flights. Of these valid incidents, 80 percent were for glass, 5.5 percent for plaster or stucco, 0.0 percent for structural, and 14.5 percent for bric-a-brac or other fallen object damage.

1.4

As stated previously, the general objective of the structure response portion of the Edwards Program was accomplished. Measured response of structures and structure elements agreed quite closely with response predicted using free field signature data and computed structure characteristics. The magnitudes of the measured response to sonic booms with peak overpressures in the order of 2 psf were very small. Results of these tests and of others have indicated that damage to properly designed and constructed houses from low magnitude sonic booms is unlikely. However, judging from the large number of damage complaints which have been filed since 1955, some damage must be caused by low overpressure sonic booms.

Factors that could explain the apparent discrepancy between results of tests and actual damage claims received are the possible range of material properties and environmental conditions and also the variation in boom characteristics. Investigations of damage complaints and claims indicate that failure or damage may occur as a result of a combination of factors. Therefore, the problem of damage evaluation does not appear to have an absolute solution. The evaluation of damage claims could be based, however, on a determination of the most probable cause of failure when the factors affecting failure such as the environmental conditions and material properties of the element and the sonic boom loading on the element are known. The application of statistical techniques and engineering procedures to data developed from detailed examinations and engineering evaluations of damage complaints and claims plus selective laboratory testing of damaged elements could be used to establish the most probable cause and amount of damage.

The ultimate objective of the studies of structure response to sonic booms is to understand the mechanism of failure under sonic boom loading so that damage claims can be evaluated and a prediction of future damage can be made with a good degree of reliability. The Edwards Air Force Base tests and others have furnished sufficient data to establish the description of the loading mechanism of sonic booms on structure elements and to predict the dynamic response of structure elements. In order to understand the mechanism of element failure and to determine the most likely cause of damage due to sonic boom load-

ing, data are needed on in situ strengths and modes of failure of structure elements.

It is, therefore, recommended that the following studies be implemented to obtain the data and knowledge necessary to establish most probable or most likely cause of damage for sonic boom damage claims:

1. Several cities in the United States should be selected that are or will be overflown by numerous supersonic flights. All complaints of glass damage and major plaster and stucco damage that occur in these selected cities should be investigated in depth by trained and experienced research-oriented engineering personnel to determine the most likely cause of damage. Environmental conditions that might affect the strength of the structure element and thus cause or contribute to the damage should be evaluated. Samples of damaged glass, plaster or plasterboard should be taken, as appropriate, and tested for failure strength.

2. Overpressure levels in each of the selected cities should be measured by instruments capable of measuring the N-wave in detail. A number of simpler peak overpressure measuring gages should also be installed. The overpressure measurements are necessary to provide a basis for evaluating damage.

3. Structure element populations, at least glass panes, should be determined in the selected cities.

4. Statistical methods should be applied in analysing the data to determine probable amounts and types of damage from future supersonic flights.

5. A program of laboratory testing to determine average strengths and variations therefrom of in situ glass, plaster, plasterboard and stucco should be developed and implemented. The data and knowledge gained would strengthen the criteria for determining most likely cause of damage.

6. A "Guide for Sonic Boom Damage Investigation and Evaluation" should be prepared.

As discussed in Chapters VI and IX, additional analyses of the data recorded by NASA during the Edwards tests for XB-70 and B-58 missions at varying distances from the measuring-recording systems should be performed to de-

termine if trends in the ratios P_2/P_1 (peak positive overpressure to numerical value of peak negative overpressure) and T_1/τ (rise time to boom duration) can be established and hence determine the effect of these ratios on structure response. These data could help establish the effective width of the "boom swath" under an aircraft flying at supersonic speed and hence the area subjected to damaging conditions.

II.   INTRODUCTION

Sonic boom experiments were conducted at Edwards Air Force Base from 4 June to 23 June 1966 (Phase I) and from 31 October 1966 to 17 January 1967 (Phase II).   The general objectives of the program were to:

1.   Evaluate the judgments by human observers of the relative ac- ceptability of sonic booms and noise of different intensities from various types of aircraft.

2.   Determine the response of typical structures to sonic booms having different signature characteristics and evaluate damage resulting from the program overflights.

3.   Obtain detailed measurements of sonic boom signatures as functions of the type of aircraft and mode of operation and the atmosphere and ground through which the waves were propagated.

4.   Observe the response of animals to sonic booms.

Completion of objectives 1, 3 and 4 was the responsibility of other participants in the program and are covered in their reports.   The work per- formed by John A. Blume & Associates Research Division (JABARD) in fulfilling general objective 2 including the results of analyses of structure response data measured and recorded during the test program and the evaluation of damage reported during the test program are presented in this report.

The test program was designed to subject instrumented structures to sonic booms of different signature characteristics.   The aircraft utilized were the XB-70, B-58, and F-104, each of which produced sonic booms of dif- erent signature durations.   These aircraft were flown at several flight track offsets, altitudes and Mach numbers so as to generate different overpressure levels and signature characteristics.

The JABARD effort involved four major phases of work:

a.   Construction of three test structures and installation of instrumentation;

b.   Recording and reduction of data from test program aircraft missions;

2.1

c. Analyses of structural response data; and

d. Investigation and evaluation of complaints of damage resulting from the test program supersonic overflights.

A brief summary is presented in this chapter of the construction of the test structures; procedures for instrumentation, data recording and data reduction; analyses of structure response data; investigation of complaints of damage from test program missions; and findings resulting from the analyses of data concerning free field signatures, structure response and damage to structure elements.

TEST STRUCTURES

Two wood frame test house structures were built at Edwards AFB, a two-story house and a one-story house. They were complete homes with all services and standard built-in items. Both were built in accordance with plans obtained from a large housing developer and home builder and are representative of typical contemporary midwestern construction. The houses were furnished and equipped with appliances, drapes, rugs and dishes. Both of the test houses were instrumented to measure and record the loading on and the response of the house and certain elements.

In addition to the two test houses, the Bowling Alley on the Base was selected as a representative structure with a long-span roof. Instruments were installed to measure and record the response of the roof structure and the building frame to sonic booms.

During Phase I of the program, a two-story house identical to the two-story test structure at Edwards was built and leased in Lancaster, California. Furnishings and instrumentation were similar to those installed in the two-story test structure at Edwards AFB. A detailed discussion of the test structure is presented in Chapter III.

DATA RECORDING AND DATA REDUCTION

Instrumentation was installed in and on the test structures to measure acceleration and displacements of the structures and various structure elements, overpressure levels on the exterior and interior of the structures, strain of certain structure elements such as window panes and flanges of the long-span roof girders, acoustical levels at different locations in the test house structures and free field overpressures near the houses; and to provide data on the acoustical and vibrational signals transmitted to the human subjects (in test houses only). In order to make these measurements, three basic types of instruments (transducers) were installed: microphones, accelerometers, and strain gages. Each instrument was selected to be compatible with the characteristics (frequency response and size) of the structural element on which it was mounted.

The instrumentation locations were selected to measure as many critical parameters as possible with the number of channels and types of transducers available. The structural response data recorded during Phase II at test structures E-1, E-2 and E-3 totalled 2160 boom channels for comparable XB-70, B-58 and F-104 flights, 307 boom channels for SR-71 flights and over 300 boom channels of free field data. In addition, 6832 boom channels of acoustic microphone and high frequency accelerometer data were recorded for use by others. In order to acquire this large amount of data in reliable and useable form, detailed coordination, high standards of quality control and careful maintenance of equipment were instituted and followed. The quality of the recordings and recoverability of data recorded during Phase II were extremely high. Practically all data were recoverable with over 90 percent of the records of excellent quality.

The signals generated by the transducers when subjected to sonic booms were recorded on analog magnetic tape by precision recorders. In order to evaluate and analyse the data, the recorded data on the analog tapes were reproduced on oscillographic photo-sensitive paper. The recordings on paper provided a visual record of the pressures, accelerations, etc., produced by the booms and were used to make comparative judgments of the different instrument measurements. The analog data was also converted to digital form so that it could be processed by digital computers. Several different computer programs were developed and used in the analyses of the data.

2.3

All pertinent data such as aircraft mission characteristics, instrument locations and calibrations, and summaries of free field signature data were logged daily and punched on data cards to facilitate summarization, printing and distribution of the data. Chapter IV presents a detailed discussion of instrumentation and procedures followed in recording and reducing data.

ANALYSES OF STRUCTURE RESPONSE DATA

The primary purposes of the analyses of the structure response data were to determine and compare the response of test and other structures to sonic booms produced by XB-70, B-58, and F-104 aircraft; to compare predicted response with actual or measured response as determined from the instrumented test structures; and to develop a means of predicting structure response due to sonic booms generated by the future SST based on data from presently available aircraft.

A comprehensive analysis of the response of a structure or structure element to sonic boom overpressure loading involves consideration of the free field pressure wave as it envelopes the structure so as to determine the actual loading on the structure. This procedure is quite complex and time consuming. It was recognized that a method of approximating structure response that was based on free field signature data, thereby eliminating the fabrication of the loading waveform on the structure, would be extremely valuable.

Examination of the pressure signature data showed that the free field pressure signatures were quite similar to the exterior and interior loading pressure signatures. Preliminary analyses of the data indicated that a direct relation between predicted response based on free field data and predicted response based on exterior loading data should exist. As the actual or net loading pressure on a wall or window is the exterior pressure minus the interior pressure it seemed reasonable that a direct relationship between free field and net pressure loading existed. Further analyses showed that the response spectra or Dynamic Amplification Factors (DAF) computed from free field, exterior and net pressure signatures were similar. DAF represents the influence on structure response of the change in the magnitude of the load with respect to time. A DAF spectrum covers 1) the natural frequencies for which the response is impulse sensitive (low frequencies), 2) the natural frequencies for

2.4

which the response is pressure and duration sensitive (middle frequencies) and
3) the natural frequencies for which the response is only pressure sensitive
(high frequencies). Therefore the DAF concept was used in the analyses of the
data.

Since the advantages of being able to predict response using free field
data were readily apparent, an analysis plan was developed to determine if
structural response calculated using free field data was a good approximation
of the actual or measured response of elements of the test structures. The
comparison of predicted response based on net loading with measured response
was also included.

Concurrently with the analyses of structure response, the free field
data was studied to determine if the data from the five microphone channels
were consistent and to determine the effects on structural response of varia-
tions in free field signature parameters. The study included a determination
of the relative effects of the different parameters on structural response.
If one or two parameters were predominant, a simple gage measuring these
parameters could supply adequate information to predict response. It was
apparent that a wave model described by free field signature parameters
(peak positive overpressure, P_1, peak negative overpressure, P_2, rise time,
T_1, and time from start of boom to peak negative overpressure, T_2) would be
necessary to evaluate the effects of variations in the parameters on DAF
spectra. However, DAF spectra calculated from the wave model would have to
be equal to spectra obtained from actual digitized free field signatures.
The model would make it possible to predict the response of a structure ele-
ment knowing the free field siganture parameters P_1, P_2, T_1, T_2, and the
structural properties of the element. The wave model was also used to study
the effect on structure response of variations in free field siganture pa-
rameters beyond those in the recorded data and, therefore, provide a basis
for prediction of structure response to sonic booms produced by larger air-
craft such as the SST.

A generalized DAF spectrum was also developed, with which it is
possible to approximate response knowing only peak positive overpressure
and signature duration and the structural properties of the element. This
spectrum is useful when preliminary results are required. For more detailed
answers the wave model with values of the required parameters may be used.

2.5

In summary, a direct relationship between structural response and free field signatures is extremely valuable because free field signatures are easier and less costly to obtain than structural response data; free field signature parameters such as peak overpressures, rise time and duration can be predicted using available procedures; and the effect of the variations of the free field signature parameters have been investigated and the results known.

In the analysis of the response data, Phase II data were used for the major portion of the structural analysis, with Phase I data used where appropriate. Phase I missions were analysed only where the data could be used to validate findings from Phase II missions. This procedure was followed because the Phase II data contained measurements of comparable overhead and offset missions of XB-70, B-58, and F-104 aircraft flown within minutes of each other, while Phase I data contained measurements of only three XB-70 missions, two of which were test program missions.

INVESTIGATION OF COMPLAINTS OF DAMAGE

During the planning phases of the Edwards Test Program it became evident that many of the supersonic missions would subject a large number of buildings and structures at Edwards AFB and in communities near Edwards to sonic booms. Based on past experience, some damage was expected to occur. Therefore, to provide a fairly reliable basis for determining the extent of glass damage caused by the test program, a survey was made of all glass windows and doors in buildings and structures at Edwards. Provisions were also made to have an engineering investigator inspect each complaint received from Edwards and the adjacent communities. The findings of the engineering investigator were evaluated and then compared with the missions flown.

SUMMARY OF FINDINGS
RESULTING FROM THE ANALYSES OF EDWARDS AFB DATA

The findings resulting from the analyses of free field signature data, effects of free field signature parameters on dynamic amplification factors, test structure plate response, test structure racking response,

structure damage, generalized DAF spectrum, and damage complaint investigations are presented below. Detailed discussions can be found in the respective chapters. Analyses were based on data that was recorded at Edwards AFB and obtained from seventeen comparable XB-70, B-58, and F-104 missions that were flown within minutes of each other.

Analyses of Free Field Signature Parameters (Chapter V)

The free field signature parameters were analysed to determine if the channels were statistically equal or if the measured values of a parameter were independent of the channel on which it was recorded; to determine which parameters most influenced the Dynamic Amplification Factor (DAF); and to determine the number of samples necessary for studies of structure response data. The analytical techniques were such that the findings are stated with a 95 percent confidence level; that is, there is a 95 percent probability that the findings are correct. Following are the findings resulting from these analyses:

1. For the XB-70 missions the peak negative overpressure, P_2, and the ratio of the absolute value of peak negative overpressure to peak positive overpressure, P_2/P_1, were not independent of the channel on which they were recorded. All other parameters studied (positive overpressure, P_1, rise time, T_1, and time from start of boom to negative peak, T_2) were independent of the channels.

2. For the B-58 missions P_2 was not independent of the channel on which it was recorded. All other parameters studied (P_1, T_1, T_2, and P_2/P_1) were independent of the channels.

3. For the F-104 missions all parameters (P_1, P_2, T_1, T_2, and P_2/P_1) were independent of the channels on which they were recorded. A single channel would have been adequate to measure free field signatures.

4. The magnitude of P_1 and of the absolute value of P_2 decreased as the lateral offset and/or altitude of the aircraft increased.

5. The ratio P_2/P_1 decreased as the offset of the aircraft increased for XB-70 missions.

6. There was little difference between rise times (T_1) of overhead and offset missions for each type of aircraft.

7. There was little difference between times from start of boom to negative peak (T_2) of overhead and offset missions for each type of aircraft.

8. The Dynamic Amplification Factors (DAF) computed from free field signatures were independent of the channel the signatures were recorded on. Therefore, a single microphone would have been sufficient to evaluate DAFs.

9. The magnitude of the maximum DAF decreased as the ratio P_2/P_1 decreased.

10. The natural frequency at which the maximum DAF occurred was a function of the time from start of boom to negative peak T_2. As T_2 increased, the maximum DAF occurred at a lower natural frequency.

11. Sonic booms from large aircraft such as the XB-70 and the future SST will affect a greater range of structure elements than will sonic booms from smaller aircraft such as the B-58 and the F-104.

12. The number of missions needed in the study of the response of structure elements varied depending on the degree of precision in the results and on the confidence level.

Effects of Free Field Signature Parameters on Dynamic Amplification Factors (Chapter VI)

The effects of free field signature parameters on DAF were studied in order to develop a wave model from free field signature parameters (overpressures, rise time, duration) that could be used to make an accurate evaluation of DAF, and to analyse the effects on DAF of values of free field signature parameters beyond the range of the recorded data. The findings of this study are presented below:

1. The DAF spectra obtained using a wave model described by free field signature parameters P_1, P_2, T_1, and T_2 were equal at the 95 percent confidence level to the DAF spectra obtained from digitized free field signatures.

2. Using the derived wave model it was found that:

2.8

a. the magnitude of the maximum DAF decreased as the ratio P_2/P_1 decreased,

b. the magnitude of the maximum DAF increased as the ratio T_1/τ increased, and

c. the magnitude of the maximum DAF decreased as the damping coefficient increased.

3. In the analysis of the effects of lateral offset of aircraft, the ... P_2/P_1 in the recorded free field signatures caused the predominant ... on DAF. The recorded signatures showed little change in rise times ... or in durations (τ) for overhead and offset missions for each type of aircraft. Therefore, the influence of lateral offset on DAF spectra was limited to the effect of the ratio P_2/P_1.

Analysis of Structural Response Data - Plate Response (Chapter VII)

The analysis of structural response data was divided into two sections: plate response and racking response. Plate response was defined as the normal deformation of individual structure elements and was primarily of a bending mode. Racking response was defined as the deformation of the structure as a whole and was primarily of a shearing mode. The findings from the analyses of plate response are presented under three headings: A. Wall Plate Response in Test Houses E-1 and E-2; B. Window Plate Response in Test House E-1; and C. Response of Roof Frame of the Bowling Alley, E-3.

A. Wall Plate Response in Test Houses E-1 and E-2:

Predicted displacements were computed and compared with measured displacements for three walls. The effects of flight track offset, Mach number and aircraft vector on plate response were investigated. In addition, the results of Phase II tests were compared with those from previous tests. The findings of these analyses were as follows:

1. Peak plate displacements of three typical walls in the two test houses were less than 0.034 inches for sonic boom overpressures of approximately 2 psf. Results from Phase I were of similar magnitude.

2. The DAF spectra curves determined from the free field, exterior and net pressure loading signatures were in significant agreement for structure element natural frequencies from 10 to 40 cps.

3. There was an indication that plate response may decrease with an increase in offset for flights of the same altitude and Mach number.

4. Plate response decreased slightly with an increase in Mach number for flights of the same altitude and offset. An increase in Mach number from 1.8 to 2.5 for overhead flights of the XB-70 caused a decrease in plate response of approximately 10 percent.

5. Peak displacements of a wall subjected to nearly side-on vectors (flight track nearly parallel to the wall surface) were 50 percent of the displacements of an equivalent wall subjected to nearly head-on vectors (flight track nearly perpendicular to the wall surface). Similar results were also found at White Sands.[3]

6. Measured displacements of three typical walls compared very well with predicted displacements based on either free field or net pressure signature data. For predicted displacements computed using free field data, the average ratios of predicted to measured displacements were equal to 1.03, 1.05, and 1.00 at the 95 percent confidence level for the BRI-1, DR-2, and BRI-2 walls respectively. For predicted displacements computed using net pressure data, the average ratios of predicted to measured displacements were equal to 1.00 at the 95 percent confidence level for both the BRI-1 and DR-2 walls. These findings applied to comparable overhead missions of XB-70, B-58, and F-104 aircraft (flights flown within a few minutes of each other), and to XB-70 missions with different offset and Mach number.

7. Plate response could be adequately predicted using peak overpressures and DAF spectra calculated from free field signatures.

B. Window Plate Response in Test House E-1:

Predicted displacements based on peak overpressures and DAF spectra calculated from free field signatures were computed and compared with the measured displacements. The findings are as follows:

l.   Measured displacements compared well with predicted displacements computed from free field data when the free field overpressure data were reduced by an appropriate factor to account for transmissibility, geometry, and orientation of the structure.   For the E-l window it was determined that the average ratio of the predicted to measured displacement was equal to 1.05 at the 95 percent confidence level for XB-70, B-58, and F-104 missions.

2.   Large glass windows such as the one in E-l garage respond to a sonic boom loading primarily in the fundamental mode of vibration.   A minor excitation of the second symmetrical mode also occurs.

3.   For the E-l garage window, the maximum stress determined from the strain data for the missions investigated was 790 psi.   The corresponding theoretical predicted stress was 980 psi.

4.   Greater response of the E-l window was measured for B-58 missions than for XB-70 and F-104 missions.   This was expected, since the DAF spectra curves obtained from B-58 signature data peaked at about 5 cps and the frequency of the fundamental mode of vibration of this window was approximately 5.7 cps.

5.   Window plate response could be adequately predicted using peak overpressure and DAF spectra calculated from free field signatures.   For windows located on the trailing vector side of the structure, the free field data was reduced by an appropriate factor to account for orientation and geometry of the structure.

C.   Response of the Roof Frame of the Bowling Alley, E-3:

One of the main steel roof girders (118 foot span) was instrumented to record strain in the bottom flange, vertical acceleration of the girder and roof structure and overpressures on the roof.   These records were analysed and the following findings resulted:

l.   The maximum stress due to sonic boom loading in the bottom flange of the building frame at midspan was approximately 450 psi.

2.   Peak vertical displacements of the center of the building frame for XB-70 mission 12-2 and B-58 mission 12-1 were 0.19" and 0.'1" respectively. Free field peak overpressures near E-2 for these missions were 2.19 psf and 2.39 psf respectively.

2.11

3. The shape of net overpressure signatures on the roof of the Bowling Alley measurably differed from those for typical free field N-waves.

4. DAF spectra determined from net overpressure signatures differed from spectra determined from typical free field N-waves.

Analysis of Structural Response Data - Racking Response (Chapter VIII)

Racking response was defined as the deformation of the structure as a whole and was primarily of a shearing mode. The findings resulting from the analyses of racking response data are presented under A. Test Houses E-1 and E-2, and B. Bowling Alley E-3.

A. Test Houses E-1 and E-2:

Predicted response using free field peak overpressures a $\cdot$ DAF spectra computed from free field signatures was compared with measured racking response. The results of the Phase II tests were also compared with those from Phase I[19,20] and White Sands[2] tests. The following findings resulted from these analyses:

1. Racking displacements at the roof line of the northeast corners of Test Houses E-1 and E-2 were extremely small (less than 0.0018" for E-1 and less than 0.005" for E-2) for sonic booms on the order of 2 psf overpressure.

2. Racking displacements of E-1 and E-2 recorded during Phases I and II were of similar magnitudes for similar overpressures.

3. The racking displacements of E-1 and E-2 recorded during Phase II were of magnitude similar to displacements obtained at White Sands[2] for structures of similar construction and for similar overpressures.

4. Racking displacements predicted from free field peak overpressures and DAF spectra calculated from free field pressure signatures were in good agreement with measured displacements. For both the east-west and north-south racking of House E-1 the average ratio of the predicted to measured displacement was equal to 1.0 at the 95 percent confidence level for comparable XB-70, B-58, and F-104 missions. These findings applied to both head-on and side-on vectors.

2.12

5. Racking response could be adequately predicted by using peak overpressures and DAF spectra calculated from free field signatures.

6. The future SST, for peak overpressures of about 2 psf, should produce racking displacements of typical houses that will be of similar magnitude, or possibly smaller, than those caused by the XB-70 missions. These racking displacements should be negligible and far below those required to cause damage.

B. Bowling Alley E-3:

As free field signatures were not measured near the Bowling Alley, a comparison could not be made of displacements predicted from free field data versus measured displacements. The magnitude of the racking displacements were less than the maximum measured for E-2.

Structure Damage (Chapter IX)

A review of the results of the tests at Edwards and tests by others as applied to damage from sonic boom of low magnitudes (in order of 2 psf) was made. The findings resulting therefrom are presented below:

1. Damage to properly designed and constructed houses from low magnitude sonic booms is extremely unlikely.

2. Damage should not occur to structure elements such as glass windows from racking motions caused by low magnitude sonic booms.

3. Further data is needed on in situ strengths and modes of failure of structure elements in order to determine the most likely cause of damage.

Generalized DAF Spectrum (Chapter X)

A generalized DAF spectrum was derived for use in predicting the response of a structure element when only the nominal overpressure and the type of aircraft are known. The findings are as follows:

1. A generalized DAF spectrum was obtained by studying the asymptotic behavior of DAF spectra computed from digitized free field signature data.

2. When the nominal pressure signature of a sonic boom is known, the generalized DAF spectrum can be used to predict the nominal response of a known structure element.

3. The magnitudes of the generalized DAF spectrum for different durations (Figure 10-1) were:

Duration of Boom in Seconds	Range of Natural Frequencies in cps	Generalized DAF Magnitude
0.5	0.8 to 50	2.0
0.4	1.1 to 50	2.0
0.3	1.5 to 50	2.0
0.2	2.1 to 50	2.0
0.1	4.4 to 50	2.15

4. If a DAF spectrum is desired that is more detailed than the generalized DAF spectrum, and if the free field signature parameters (P_1, P_2, T_1, T_2) have been measured, a DAF spectrum can be computed from the wave model as described in Chapter VI.

Damage Complaint Investigations (Chapter XI)

To provide a fairly reliable basis for determining the extent of glass damage caused by the test program, a survey was made of all glass windows and doors in buildings and structures at Edwards. Provisions were also made to have an engineering investigator inspect each complaint received from Edwards and the adjacent communities. The findings resulting from analyses made of the survey data, complaint investigations and test flight data are presented below:

1. The rate of valid glass damage in Edwards AFB buildings, all of which had been condition surveyed prior to the test program, was 0.127 panes damaged per million boom-pane exposures or 27 percent of the rate for build-

ings in communities adjacent to Edwards which were not condition surveyed prior to test missions.

2. During Phase I, the 110,390 glass panes in structures at Edwards were subjected to more booms from test missions than were the 605,000 glass panes in the adjacent communities; however, the aircraft while over Edwards were flying straight courses and then made turns at supersonic speeds over adjacent communities. Some focusing of the boom overpressure (or super booms) may therefore have been produced with peak overpressures greatly exceeding those produced on the Base.

3. During Phase I, 90 percent of the incidents of valid glass damage (engineering investigator determined damage could have been caused by sonic boom) were attributable to B-58 missions. The ramaining 10 percent were apparently due to F-104 missions.

4. The valid glass damage rate per mission during Phase I was 8.8 times the rate during Phase II when aircraft generally flew straight courses while at supersonic speeds.

5. The number of complaints received decreased from 61 during Phase I to eleven during Phase II. This large decrease in number of complaints can be attributed to two factors: a) the B-58 aircraft made turns and other maneuvers at supersonic speeds over several communities adjacent to Edwards AFB during Phase I, and b) during Phase II the XB-70 flew supersonically on a relatively straight course over a few of the cities adjacent to Edwards.

6. For all incidents of damage recorded during Phases I and II, 60.5 percent were for glass damage.

7. Fifty-eight percent of all incidents of damage received during Phases I and II were listed as valid. Of these valid incidents, 80 percent were for glass, 5.5 percent for plaster or stucco, 0.0 percent for structural, and 14.5 percent for bric-a-brac or other fallen object damage.

8. Glass damage was repaired or the broken glass removed for 55 percent of the glass damage incidents before the engineering investigator could investigate the alleged damage and hence, the validity of all glass damage could not be definitely established.

9. Damaged glass panes ranged in size from 1.3 square feet to 82.5 square feet. 2.7, 43.2, 43.2, and 10.9 percent of the incidents of damage occurred in the 0-2, 2-9, 9-40 and over 40 square feet size groups respectively.

10. No sonic boom damage was observed in the test structures prior to or after the test flights. There were minor shrinkage cracks in the test structures prior to start of test flights. However, no discernible extension or widening of these cracks was observed although observations were made and recorded daily.

11. As the condition of the glass panes at Edwards AFB was determined prior to the Test Program, the number of damaged panes caused by booms from test missions should be a reliable indicator of valid glass damage to be expected from future level supersonic flights generating sonic boom peak overpressures of 2 to 3 psf. The rate was one damaged pane per 7.9 million boom-pane exposures.

12. A large percentage (from 51 to 84 percent) of future valid incidents of damage from sonic boom should be for glass.

PROJECT ORGANIZATION

The work described in this report was performed under the general direction of the National Sonic Boom Evaluation Office, United States Air Force. The JABARD project group was composed of R. L. Sharpe, Project Manager; Dr. J. A. Blume, Senior Technical Consultant to the group; L. A. Lee, Project Field Manager; G. Kost, Senior Research Engineer; J. Proulx, Statistical-Research Engineer; K. F. Schopp, Head, Computer Support Services; R. E. Monroe, Research Engineer; R. F. Runge, Research Engineer - Damage Investigations; and W. W. Powers, Liaison and Photography.

Major subcontractors supplied the following services:

AETRON Division of Aerojet General Corporation - instrumentation
engineers and technicians for operating instrumentation during
Phase II.

The Boeing Company, Airplane Division - furnished pressure micro-
phone systems on exteriors of E-1 and E-2, and personnel to
install and operate instrumentation - Phase II.

Lockheed California Company - furnished pressure microphone systems
for measuring and recording boom signatures under NASA supervision,
and personnel to install and operate equipment - Phase II.

Datacraft, Inc. - furnished instrumentation for House L-2, and
personnel to install and operate systems - Phase I. Furnished high-
frequency accelerometer systems for Houses E-1 and E-2 - Phases I
and II. Dr. J. H. Wiggins was a technical consultant during Phase I.

PRESENTATION OF REPORT

A summary of the major findings was presented in Chapter I. This
chapter presented a brief description of the test program and test struc-
tures, the methods of analysis used, and a summary of all findings resulting
from the work. The following chapters will present, in order, construction
of the test structures, description of instrumentation and procedures followed
in recording and reducing data, analysis of free field signatures, effects of
five field signature parameters on response spectra or Dynamic Amplification
Factors (DAF), test structure plate response, test structure racking re-
sponse, structure damage, generalized DAF spectrum, and damage complaint
investigations. A bibliography and glossary of terms then follow. The
report terminates with appendices containing details of the structural and
statistical principles utilized, instrumentation details, calibration pro-
cedures, aircraft mission logs for Phases I and II, typical instrumentation
log, summary of free field signature data, a typical analog tape log and
derivations of certain formulae.

III. TEST STRUCTURES

The test facilities at Edwards Air Force Base consisted of two test house structures located south of the main runway and a bowling alley located about two miles northwest of the test house area. In addition, a test house in Lancaster was leased for Phase I testing. The types of test house structures to be constructed and instrumented were selected after review of many different house plans. Two houses were selected to be built on the Base, a two-story house (National Homes Model 8603), and a one-story house (Model 9855). These two models have been mass produced and constructed in the midwest, and a survey of the midwest area indicated that these homes were typical of contemporary midwestern construction.

Model 8603 is a two-story home with four bedrooms, two and one-half baths, living room, dining room, kitchen and family room with a total living area of 1,905 square feet. Model 9855 is a one-story home with three bedrooms, two baths, living room and kitchen-dining-family room with a total living area of 1,205 square feet.

The structures were built on an expedited schedule. Authorization to proceed with procurement was received on 18 April 1966. Contract documents were then prepared, competitive bids taken, and notice to proceed with construction of two houses, one Model 8603 and one Model 9855 at Edwards AFB was issued on 24 April 1966. Figure 3-1a shows the Plot Plan for the two structures at Edwards.

A two-story house, identical to the two-story house at Edwards, was built and leased in Lancaster, California. Authorization to proceed was issued on 18 April 1966, a lease was signed on 30 April, and construction started 1 May 1966. Figure 3-1b shows the location of the test structure in Lancaster.

Blume representatives monitored and inspected the construction of test structures at Edwards Air Force Base and Lancaster. The basic construction materials are listed in Table 3-1. The construction of the houses at Edwards AFB included the required extensions of sewer, water and butane gas services, construction of concrete driveways and sidewalks, and other minor work necessary for installation and operation of test equipment. All test house construction was completed on 1 June 1965. Construction schedules for the three structures are listed in Table 3-2. Photographs of the one-story house, E-1, and the two-story house, E-2 at various stages of construction are shown in

Figures 3-2 through 3-4. Figure 3-5 shows the completed house at Lancaster, L-2. All houses were furnished and equipped with appliances, furniture, drapes, rugs, dishes, etc. The test houses were constructed in accordance with the drawings in Figures 3-7 through 3-15.

In addition to the three test houses, the Bowling Alley on the Base was selected as a structure with a representative long-span roof. Instruments were installed to measure and record the response of the roof structure and the building frame to sonic boom. The Bowling Alley (E-3) is shown in Figure 3-6. The structural frame is composed of three steel rigid frames plus column-beam framing for the north wall. The roof and exterior walls are fluted steel decking. Details of the framing are shown in Figure 3-16.

The instrumentation of the test structures is discussed in the following chapter.

TABLE 3-1

CONSTRUCTION MATERIALS
HOUSES E-1, E-2, and L-2

Mud Sills	Pressure Treated Foundation Grade Redwood
Floor Joists	Douglas Fir Construction Grade
Sub Floor	5/8" Plyscore Plywood
Trusses	2" x 4" "Gangnail" Wood Trusses
Wallboard	1/2" U.S. Gypsum
Studding	Standard and Better Douglas Fir
Roof Sheathing	1" x 6" Standard and Better Douglas Fir
Glass	Double Strength Libby-Owens-Ford and Pittsburg Plate Glass
Insulation	3-1/2" Owens-Corning Fiberglass with Aluminum Foil One Face
Roof Shingles	Asphalt 235#, U.S. Gypsum
All Concrete	Local Aggregate 5 Sacks of Cement per Yard
Siding	Ship-lap Redwood

TABLE 3-2

ACTUAL CONSTRUCTION SCHEDULES

	House E-1	House E-2	House L-2
	1966	1966	1966
Notice to Proceed	24 April	24 April	1 May
Foundation Concrete Placed	April	26 April	3 May
Floor Framing Started	1	27 April	7 May
Rough Plumbing Started	27 April	28 April	7 May
Brick Work Completed	2 May	3 May	10 May
Windows Installed	3 May	3 May	13 May
Completed Roofing	5 May	6 May	13 May
Siding Completed	6 May	6 May	14 May
Wall Board Completed	8 May	9 May	15 May
Cabinets Installed	11 May	11 May	16 May
Doors, Trim, Finish Hardware	12 May	12 May	16 May
Tile Work Completed	15 May	15 May	22 May
Utilities Connected	17 May	17 May	23 May
Finished Plumbing	18 May	18 May	25 May
Concrete Drive, Walks	20 May	21 May	21 May
Preliminary Final Inspection	26 May	26 May	28 May
Final Acceptance	1 June	1 June	1 June

MAGNETIC NORTH

STREET

YUCCA DRIVE

HOSPITAL

SAGE ST.

MODEL 9855, E-1

MODEL 8603, E-2

CENTER ST.

FAA RADAR
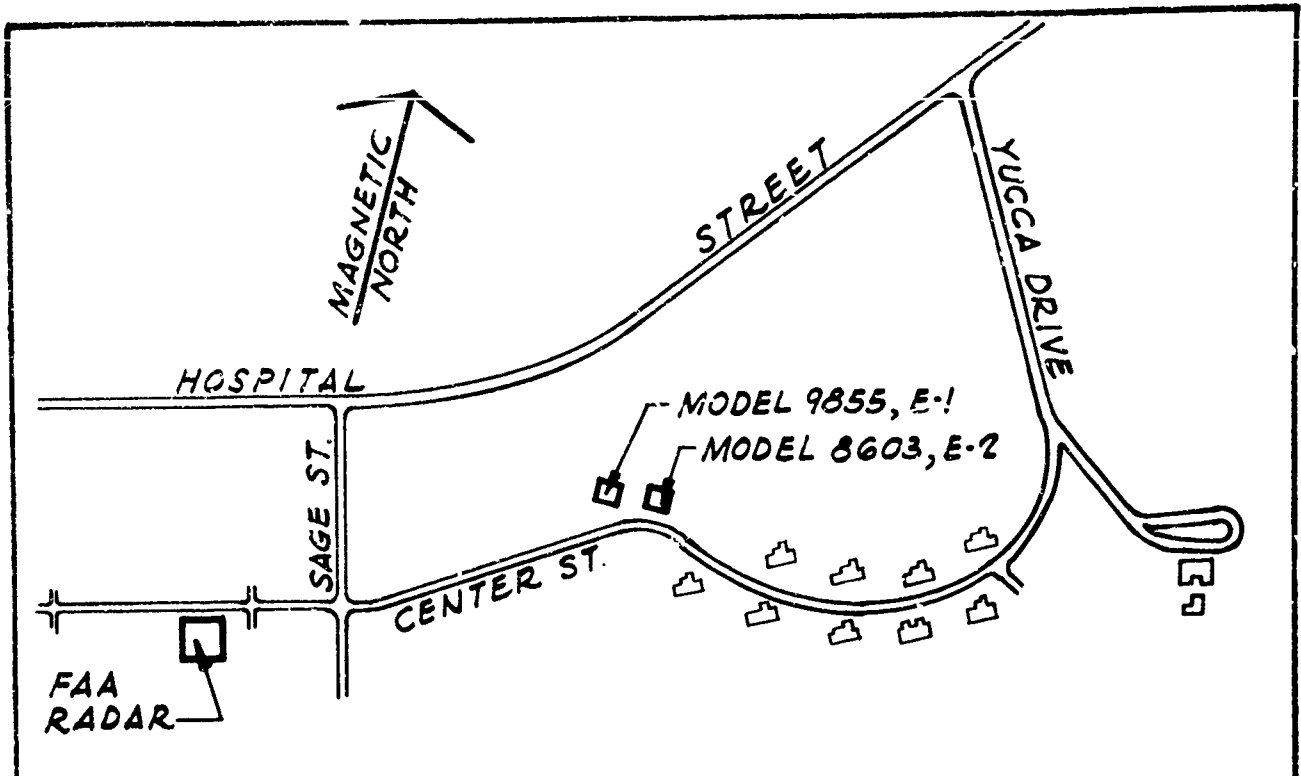
PLOT PLAN FOR STRUCTURES E-1 & E-2

SCALE: 0'   500'   1000'

FIGURE 3-1a

MAGNETIC NORTH

AVENUE J

10TH STREET

J-5

MODEL 8603, L-2
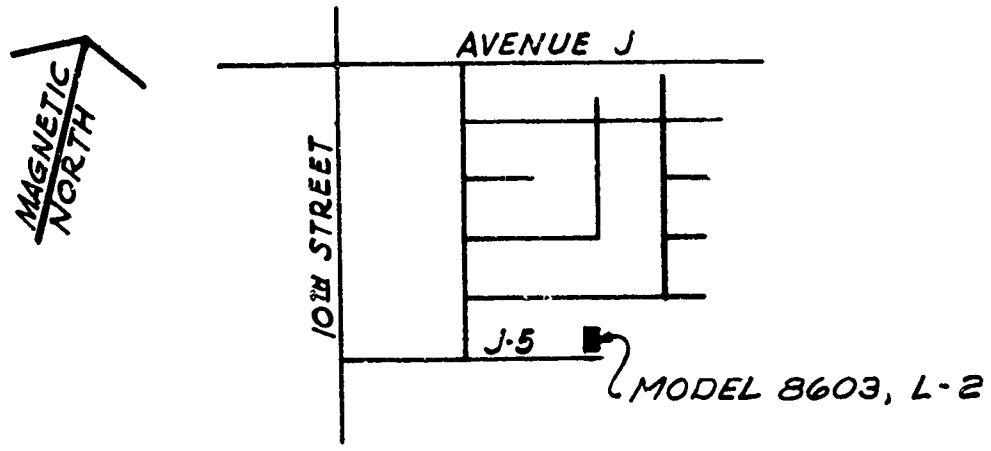
PLOT PLAN FOR STRUCTURE L-2
NO SCALE

FIGURE 3-1b

PLOT PLANS FOR STRUCTURES E-1, E-2 & L-2

FIG. 3-1

3.5

FIGURE 3-2

TWO-STORY HOUSE E-2   START OF WALL FRAMING

FIGURE 3-3

TWO-STORY HOUSE E-2   START OF ROOFING

FIGURE 3-4

TEST HOUSES E-1 AND E-2
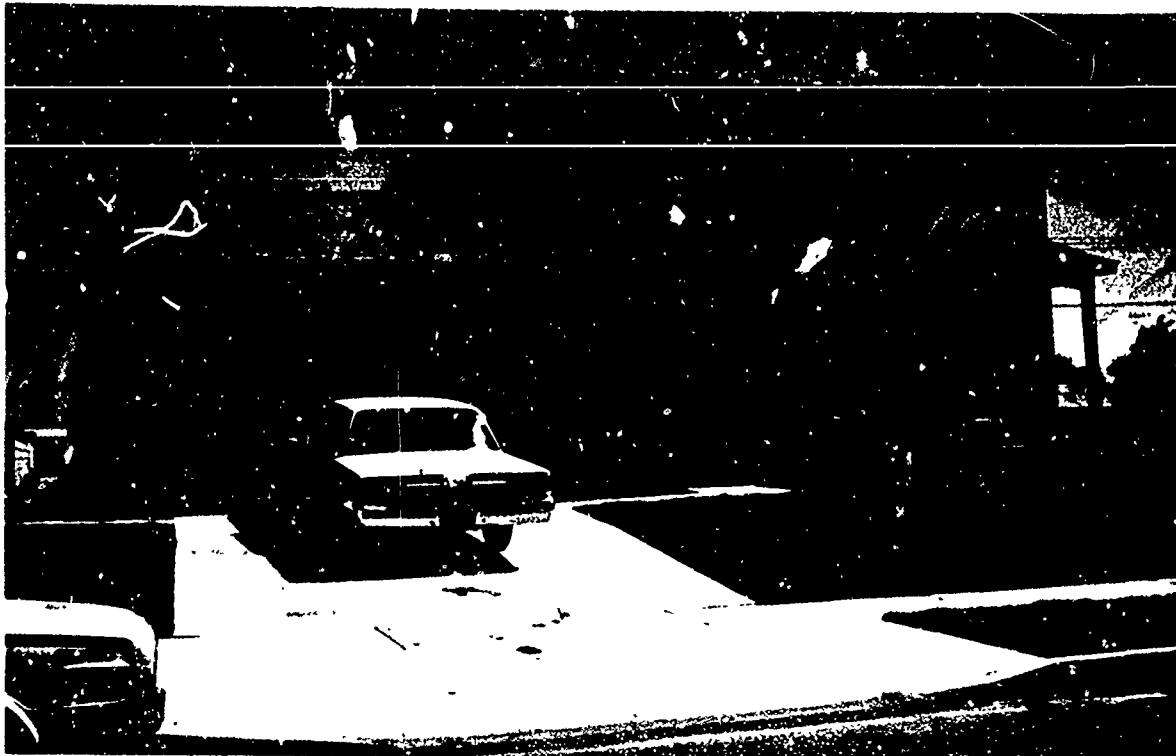
FIGURE 3-5

TWO-STORY HOUSE L-2
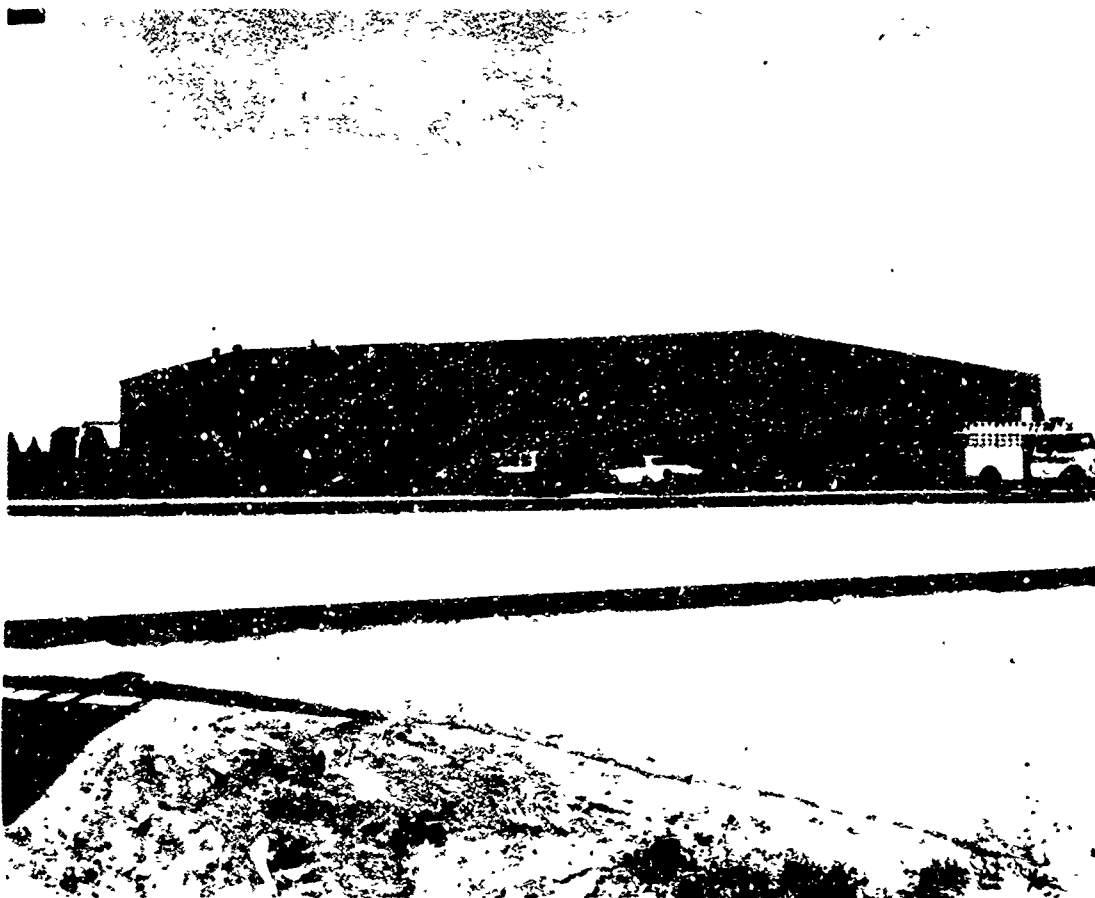
FIGURE 3-6

BOWLING ALLEY E-3, EDWARDS AFB

3.8
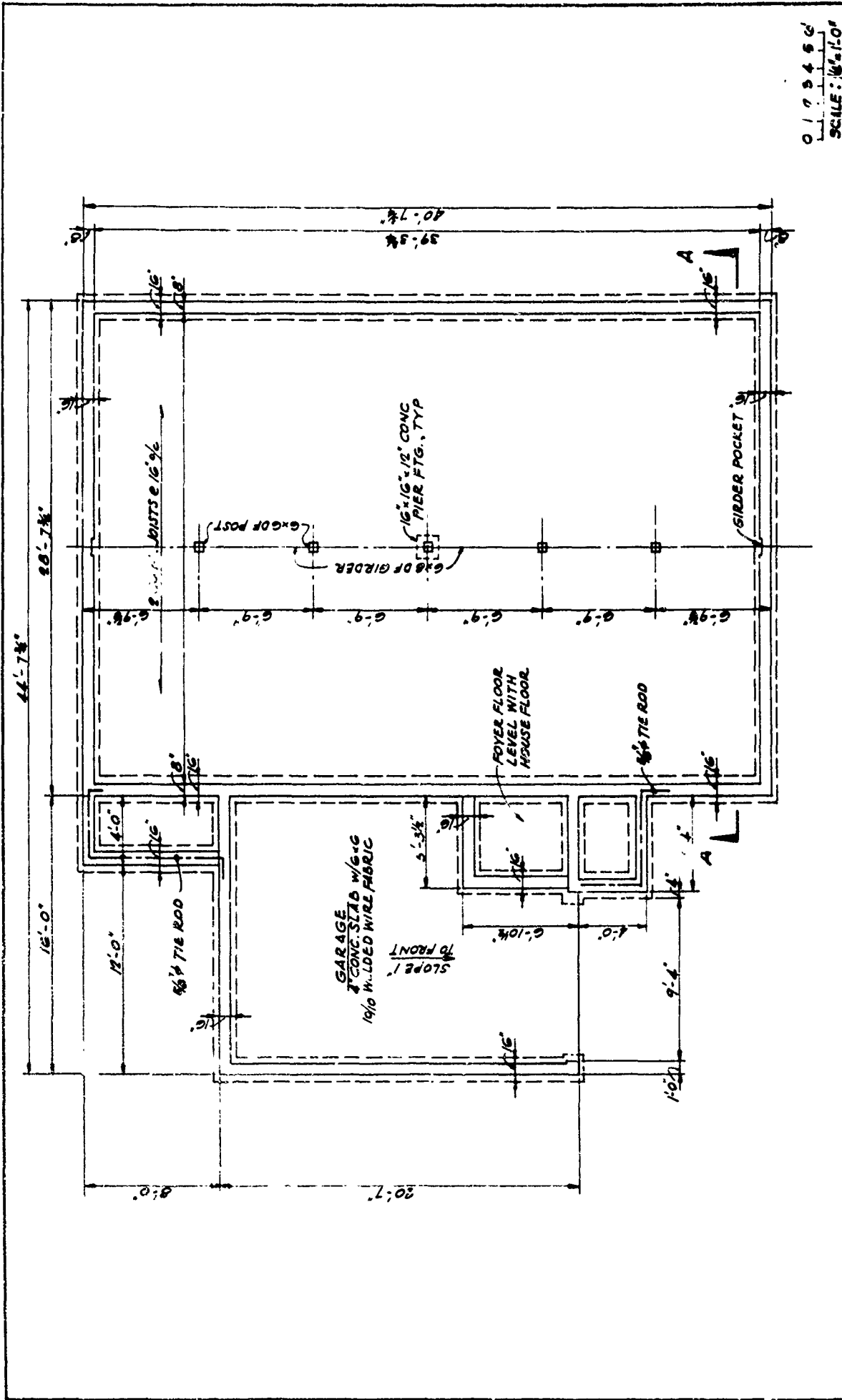
MODEL 9855 (E-1) FOUNDATION PLAN

FIG.
3-7

SCALE: ¼"=1'-0"
0 1 2 3 4 5 6'

FIG.
3-7

3.9

MODEL 9855 (E-1) FLOOR PLAN

BEDROOM 1

BATH
BATH

BEDROOM

BEDROOM

FAMILY
DINING
&
KITCHEN

LIVING ROOM

STOR.

GARAGE

SCALE : ¼"=1'-0"
0 1 2 3 4 5 6'

FIG.
3-8

FIG.
3-8

3.10

SOUTH ELEVATION
SCALE: ⅛"=1'-0"

NORTH ELEVATION
SCALE: ⅛"=1'-0"

EAST ELEVATION
SCALE: ⅛"=1'-0"

WEST ELEVATION
SCALE: ⅛"=1'-0"

HORIZONTAL SIDING

CLG. LINE
FLOOR LINE
7'-6"
10½ MIN.

MODEL 9855 (E-1) ELEVATIONS

0 2 4 6 8 10 12'
SCALE: 1/16"=1'-0"

0 1 2 3 4 5 6'
SCALE: ⅛"=1'-0"

FIG.
3-9

FIG
3-9

3.11
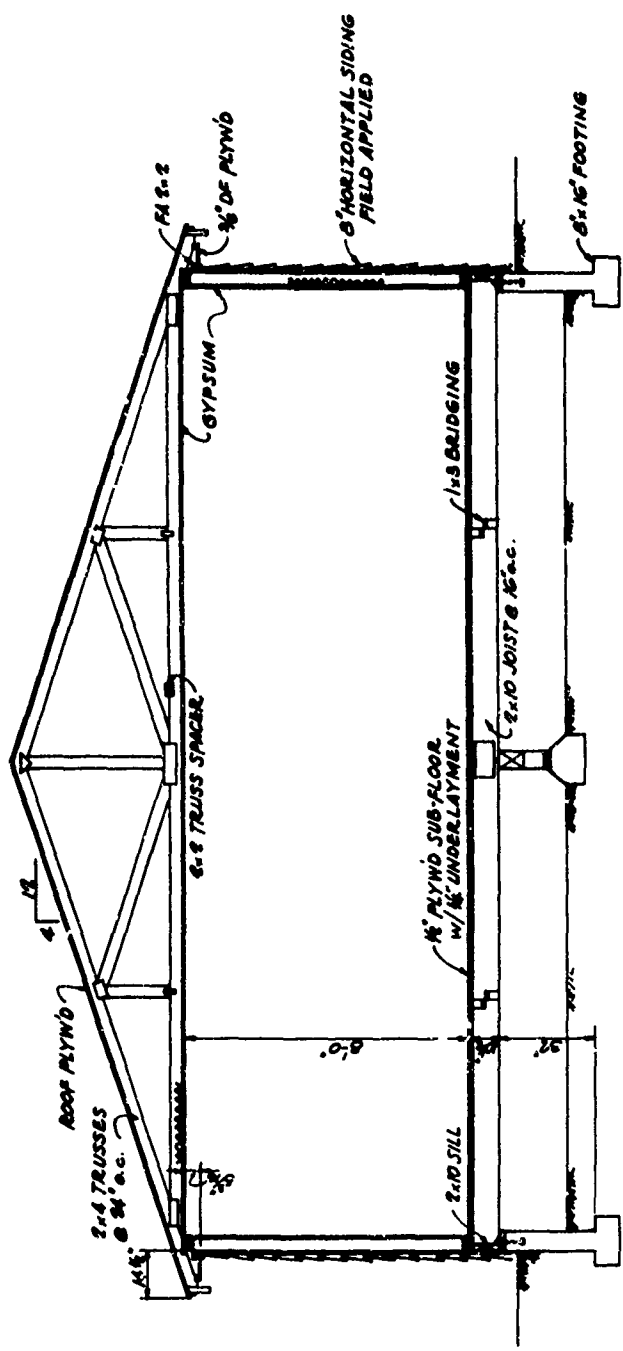
SECTION A-A

MODEL 9855 (E-1) TYPICAL CROSS SECTION

FIG.
3-10

FIG.
3-10

0 1 2 3 4'
SCALE: 3/8"=1'.0"

2x4 TRUSSES
@ 24" o.c.

ROOF PLYW'D

4x8 TRUSS SPACER

FA 2.2

3/8" OF PLYW'D

GYPSUM

6" HORIZONTAL SIDING
FIELD APPLIED

1x3 BRIDGING

2x10 JOIST @ 16" o.c.

1/2" PLYW'D SUB-FLOOR
W/1/4" UNDERLAYMENT

2x10 SILL

6"x16" FOOTING

6'-0"

3.12
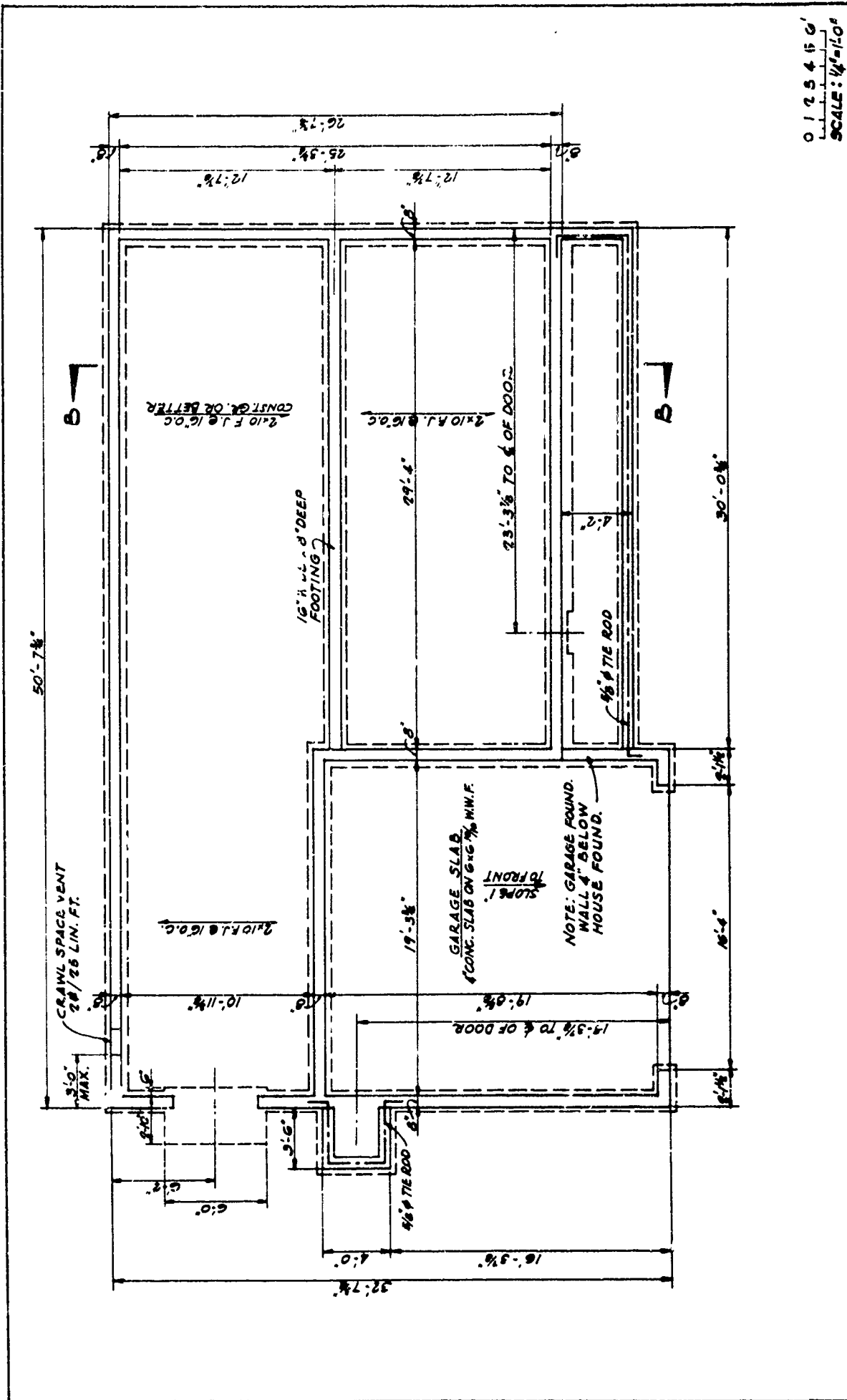
MODEL 8603 (E-2) FOUNDATION PLAN

FIG.
3-11

SCALE: ¼"=1'-0"
0 1 2 3 4 5 6'

FIG.
3-11

3.13
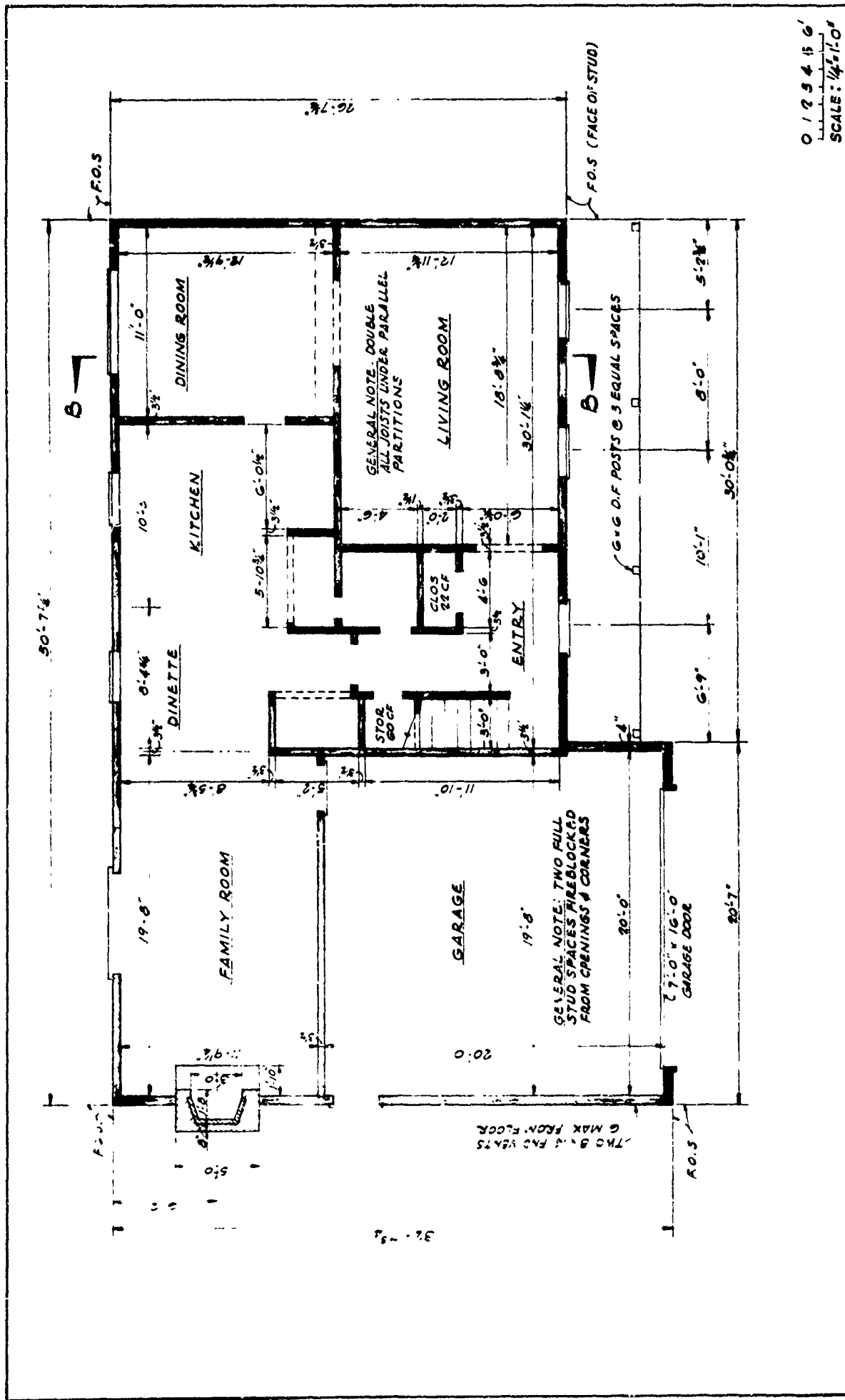
MODEL 8603 (E-2) FIRST FLOOR PLAN

FIG.
3-12

0 1 2 3 4 5 6'
SCALE: ¼"=1'-0"

FIG
3-12

3.14

MODEL 8603 (E-2) SECOND FLOOR PLAN

FIG.
3-13
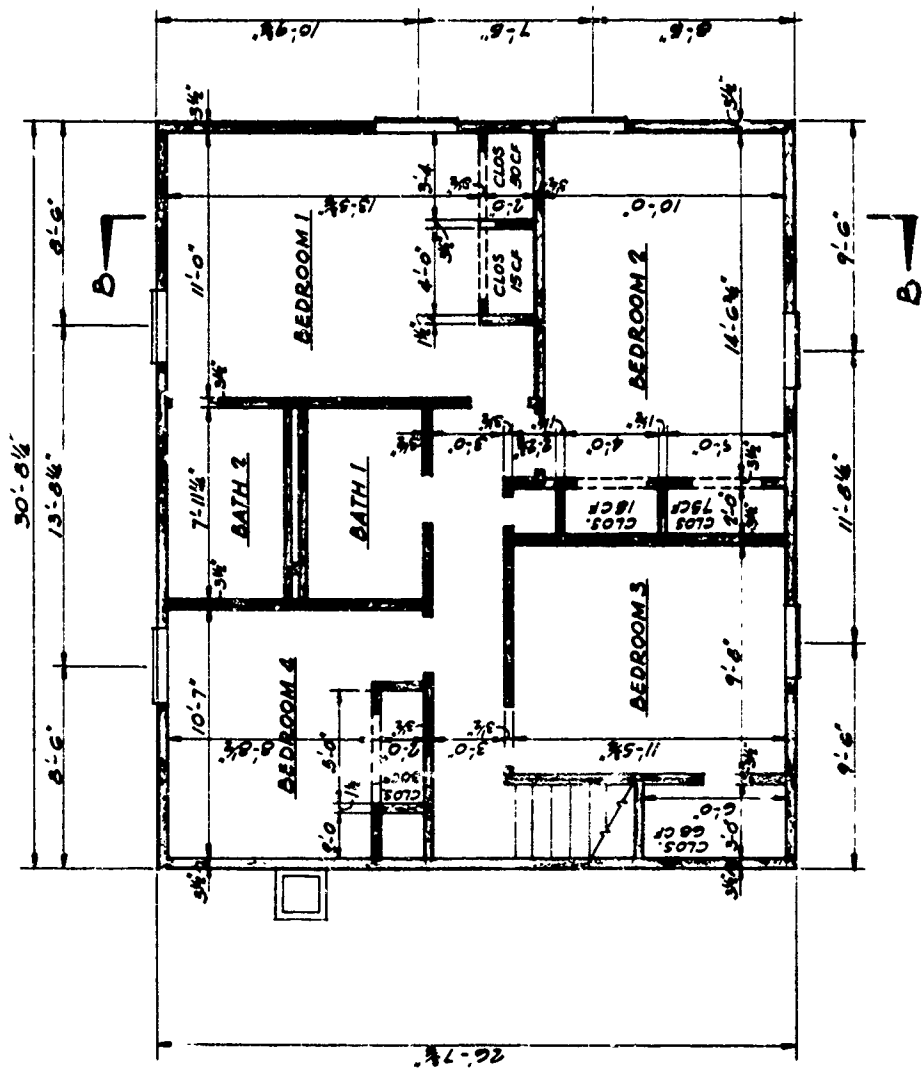
0 1 2 3 4 5 6'
SCALE: 1/4"=1'-0"

FIG.
3-13

3.15
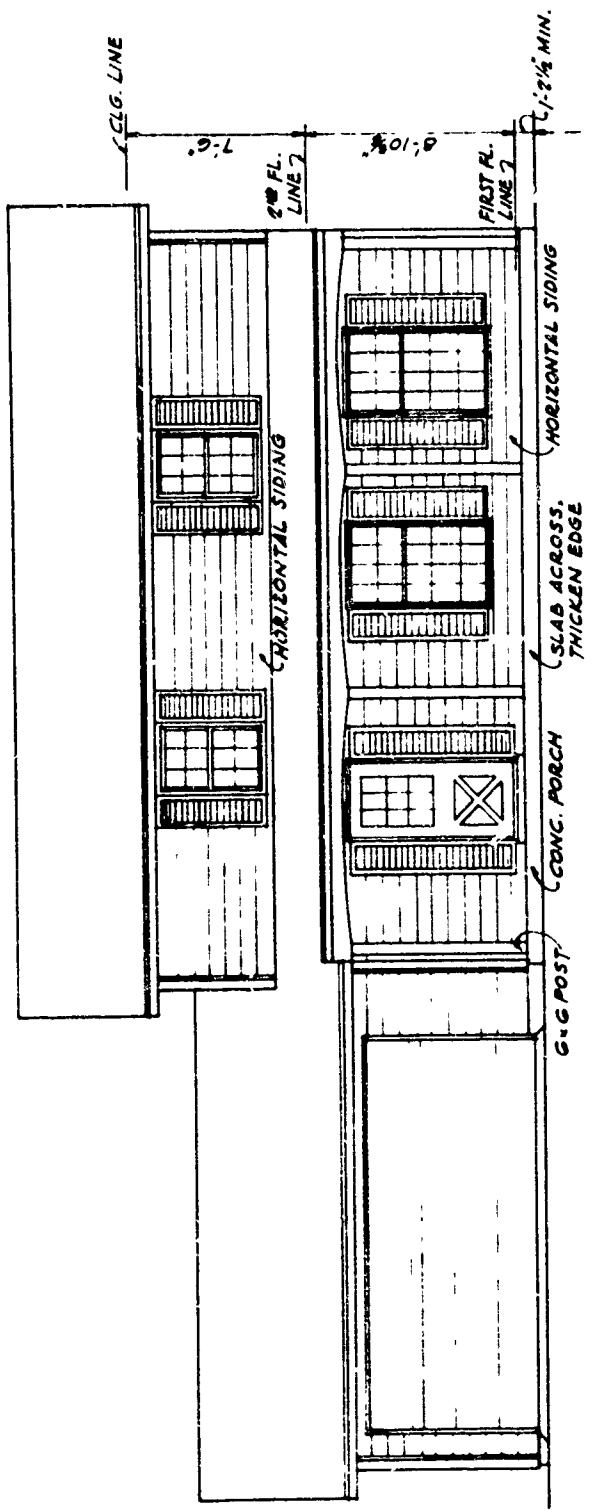
SOUTH ELEVATION
SCALE 1/8"=1'-0"
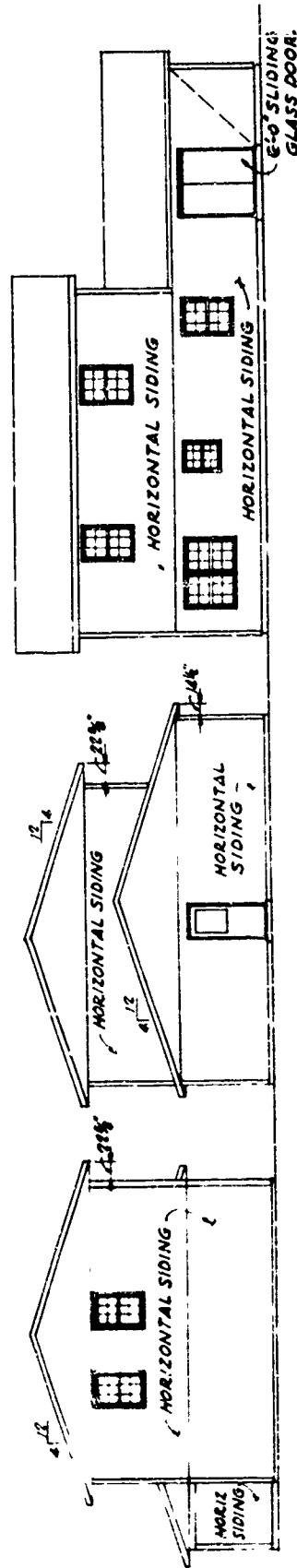
NORTH ELEVATION
SCALE 1/8"=1'-0"

WEST ELEVATION
SCALE 1/8"=1'-0"
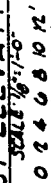
EAST ELEVATION
SCALE 1/8"=1'-0"

MODEL 8603 (E-2) ELEVATIONS

GENERAL NOTE: 1×4 DF
DIAGONAL LET-IN BRACE
@ CORNERS.

FIG.
3-14

SECTION B-B

MODEL 8603 (E-2) TYPICAL CROSS SECTION

FIG.
3-15

SCALE: 3/16"=1'-0"
0 1 2 3 4'

GANG NAIL COMPONENTS PRE FAB
TRUSSES. DESIGN & CALCULATIONS
WILL BE SUBMITTED PRIOR TO
ERECTION

ASPHALT COMP SHINGLES
ON 1-15# FELT OVER 3/8 O.F.
EXTERIOR PLYWOOD
SHEATHING

2×4 TRUSSES @ 24" O.C.

ROOF PLY I'D

2×2 TRUSS SPACER

2×2 CONT. INSULATION STOP

2×6 R.D. W FASCIA CONT.
2" SCREENED VENT CONT.
3/8 EXT OF PLYWD SOFFIT

GYPSUM

INSULATION

WOOD DROPSIDING
ON 15# FELT UNDER.
FIELD APPLIED

T & G OF BEAM

6×6 OF
POSTS

HORIZONTAL
SIDING

1/2" PLYWD SUBFLOOR
W/1/4" UNDERLAYMENT

2×10 JOISTS @ 16" O.C.

2×4 BEARING WALL

1×3 BRIDGING

2×10 SILL

2-2×6 SILLS
CONT T & B

2×4 CO WD SILL W/ 1/2 DB
7" N CONC @ G-5 O.C. MAX TYP.

GRADE

6" MIN.

FIG
3-15

3.17

Structural steel rigid frames at Col. lines B, C & D

Metal siding

SECTION A-A

25'

118'

PLAN

25'   25'   25'

Ⓐ   Ⓑ   Ⓒ   Ⓓ

NORTH

BOWLING ALLEY, E-3

FIG. 3-16

The test facilities at Edwards Air Force Base were comprised of two test house structures; a one-story house, E-1, and a two-story house, E-2; and a third test structure, a Bowling Alley, E-3, which was located about two miles northwest of the test house area (Figure 4-1). In addition a test house structure, L-2, was leased in Lancaster for Phase I testing. The construction of the test houses has been covered in the previous chapter. Free field sonic boom signatures were recorded by six microphones located in a cruciform array 100 feet north of house E-2 (Figure 4-2).

Three basic types of measuring instruments (transducers) were installed; microphones, accelerometers, and strain gages. Microphones were used to measure overpressures at ground level near the instrumented structures (free field signatures) and to measure exterior and interior overpressures on structure elements (loading signatures). Accelerometers and strain gages were used to measure the response of the structures and selected structure elements. Each instrument was selected to be compatible with the characteristics (frequency response and size) of the structure element on which it was mounted.

The signals generated by these transducers when subjected to sonic booms were recorded on analog magnetic tape by precision tape recorders. The recordings were reviewed shortly after each mission and minor modifications were made in the instrumentation when required. The quality of recordings and recoverability of data recorded during Phase II were extremely high. Practically all data were recoverable and over 90 percent of the records were of excellent quality.

DATA RECORDING

During Phase I, structural data were recorded in the four test structures, E-1, E-2, E-3 and L-2. All instrumentation except high frequency accelerometers was furnished, installed and operated in E-1, E-2 and E-3 by NASA. High frequency accelerometers in E-1 and E-2, and all instruments in L-2 were furnished, installed and operated by Datacraft, Inc., under subcontract to John A. Blume and Associates Research Division (JABARD).

The arrangement of the instrumentation was modified for Phase II of the program to increase the effectiveness of the information obtained. The most important changes were the addition of loading microphones on the outside of houses E-1 and E-2 and additional audio microphones inside E-1 and E-2. During Phase I, the boom intensities and structural reactions at the Lancaster house, L-2, were often masked by natural phenomena due to the large lateral displacement of the aircraft and generally prevailing windy conditions. Therefore, measurements were not recorded at L-2 after Phase I because of the minimal information obtained.

AETRON Division, Aerojet-General Corporation, under subcontract to JABARD, operated instrumentation during Phase II in test structures E-1, E-2 and E-3. Equipment was checked out and necessary adjustments were made for Phase II operation during the last two weeks in October. Some of the transducers were rearranged in E-1 and E-2 to meet Phase II requirements of other participants. Four additional microphone systems and two displacement transducers in E-2 and two additional microphone systems in E-1 were furnished and installed. AETRON installed recording and signal conditioning equipment in a designated room at the Bowling Alley, connected it to transducers previously installed by NASA and then checked out and operated the ten transducer systems.

The Boeing Company, Airplane Division, under subcontract to JABARD, furnished, installed and operated twelve microphone systems located on the exteriors of E-1 and E-2 to measure boom pressure loadings on these two structures during Phase II. Recording, signal conditioning, and direct write equipment were installed in the garage of E-2. Power for equipment was available in E-1 and E-2 from power panels separate from those used for supplying power for lights, receptacles, and air conditioning in the two structures.

Lockheed California Company, under subcontract to JABARD, furnished, installed, and operated 18 free field pressure microphone systems that were located on the dry lake bed east of the test houses, Figure 4-1. These instruments were installed to meet the requirements of NASA and ESSA.

Final reports describing work done by AETRON and Boeing are on file with the National Sonic Boom Evaluation Office. AETRON's report is entitled "Final Report, Subcontract BR-AFSBR-III", and Boeing's report is

entitled "Test Support to Sonic Boom Program, (Sub) Contract BR-AFSBR-110".

Tables B-1 to B-4 in Appendix B present listings of the locations of the instrumentation with their specifications, and Figures B-1 to B-7 present plan and elevation sketches of the test structures showing locations of transducers for Phase II. Table B-5 lists the equipment used in the various instrumentation systems, and Table B-6 lists the transducer frequency response and accuracy.

A number of precautions were taken to minimize thermal drift in equipment subject to temperature changes. In test structures E-1, E-2 and E-3, power to all equipment was kept on continually so that temperature gradients in the equipment could stabilize. Racks were generally enclosed so that the temperature of the air immediately surrounding the equipment did not change too rapidly in case of a sudden change in ambien‑ temperature. Power was also left on to minimize thermal shocks which tend to shorten component life. Instruments were calibrated according to the procedures outlined under Instrument Calibration Procedures, Appendix C.

CEC Model No. VR-3300 magnetic tape recorders were used for all instrumentation except the Boeing microphone system. This system utilized an Ampex CP-100 machine. Fourteen-track machines were used in and near the structures and seven-track machines on the large microphone arrays. Tape speed was 30 ips with FM recording. Center frequency was 54.0 kcps with an information frequency of 0-10 kcps ± 0.5 dB. The full-scale signal to noise ratio (RMS signal/RMS noise) was 43 dB. Harmonic distortion was 1.5%.

A time code was recorded on one channel of each analog magnetic tape. During Phase I and up to November 21, 1967 of Phase II, the time code was standard IRIG Format "B", Figure 4-3. During Phase II on November 21, 1967, a mission identification system was incorporated into the time code to provide positive mission identification on each analog tape. With this identification system, it was possible to insert mission numbers and aircraft designations into the IRIG "B" time code. The resultant time code (Figure 4-4) consisted of a normal time code for seconds, minutes, hours, and days; followed by the number after the dash of the mission number; then units, tens, and hundreds of the portion of the mission number before the dash; followed by a blank; then units, tens, and hundreds of the aircraft designation; and the remaining three positions not assigned.

4.3

Start and stop times for accurately digitizing analog data were based on manual reading of direct-write oscillograph records. Nominal boom times were recorded from a time code translator located in test structure E-2 as a check on the values read from the oscillographs. Manual readout to the nearest second was required for booms. Noise recordings of a typical aircraft flyby included three minutes of uninterrupted aircraft noise with 75 seconds recorded before and after 9 aircraft passed overhead. Notation of start and stop times for box records was provided by JABARD personnel. "Recorders On" signals were the responsibility of NASA and Edwards AFB control.

When "Recorders On" signals were heard at the test structures, the tape recorders were turned on by hand; and as previously mentioned, the digitizing start and stop times were based on manual reading of the oscillograph records. It was felt that these two hand operations could be eliminated if a signal were automatically generated a short time before the boom occurred at the test structures. This signal could then be used to start the tape recorders and digitizing automatically. In order to generate this signal, a microphone was located along the flight track about 00 feet northeast of E-2. This microphone functioned well and generated the signal as expected.

DATA REDUCTION AND DISSEMINATION

The JABARD Data Reduction and Dissemination Group (DR&D) during Phase II were responsible for performing certain preliminary data reduction; assembling, card punching and processing free field cruciform microphone data; card punching and processing mission logs and instrument location logs; digitizing free field and structure response data; duplicating certain analog tape records; and disseminating summaries of the data as directed to appropriate participants.

NASA was responsible for providing values of positive overpressures, rise time, boom duration and waveform as shown by the sample waveforms in Figure 4-5. These values were measured from oscillographic records of the free field cruciform array microphones. The data were supplied for inclusion into the data printout scheme setup and implemented by DR and D as soon as possible after missions were flown. NASA also reduced data from the radar plots for all missions and furnished DR and D a summary together with copies of the radar plots.

4.4

The data furnished to DR and D was logged daily and all information was punched on a series of six data cards so that they could be processed by computer and printed output furnished to participants. The information contained on each card and the arrangement of the data for Phase II is as follows:

1. <u>Mission Log</u>

    a. Date
    b. Mission
    c. Aircraft
    d. Altitude, 1000 ft., MSL*
    e. Mach number (or speed kph for subsonic aircraft)*
    f. EPR (take-off or landing)*
    g. Heading*
    h. Offset from track, left or right*
    i. Observed boom time, or time overhead for subsonic aircraft, ZULU*
    j. Remarks
    k. Card type identification number (1)

    *Over test structure E-2

2. <u>Digitization Log - Data</u>

    a. Data
    b. Mission
    c. Aircraft
    d. Digitizing start time
    e. Digitizing stop time
    f. Location
    g. Card type identification number (2)

3. <u>Instrument Location Log</u>

    a. Date
    b. Channel
    c. House number and instrument designation
    d. Instrument type
    e. Location
    f. Location number (0 = inoperative, 1 = 1st position, 2 = 2nd position, etc.
    g. Card type identification number (3)

4. Channel Calibration Log

   a. Mission
   b. Channel
   c. House number and instrument designation
   d. Pre-calibrations
   e. Post-calibrations
   f. Run attenuation and gain setting
   g. Remarks
   h. Digitization sample rate, sps
   i. Digitization filter cutoff
   j. Card type identification number (4)

5 Digitization Log - Calibrations

   a. Date
   b. Channel
   c. House number and instrument designation
   d. Calibration type (pre or post)
   e. Digitizing start and stop times
   f. Digitization sample rate, sps
   g. Digitization filter cutoff, cps
   h. Card type identification number (5)

6. Summary of Cruciform Data

   a. Mission
   b. Channel
   c. House number and instrument designation
   d. Wave form type code number for pressure mikes, see Figure 4-5
   e. Peak amplitudes in psf
   f. Rise time, seconds
   g. Period or duration of N-wave in seconds
   h. Wave angle, degrees
      Wave angle is the angle between the pressure wave front and
      the ground as determined from the cruciform array
   i. Wave ground speed, ft/sec
   j. Card identification number (6)

     The Mission Log in chronological order for Phase I is given as Table D-1,
Appendix D. The Phase II Mission Log in order of mission numbers is given in
Table D-2. The Instrument Location Log for a typical day, 15 November 1966,
is given as Appendix E. A copy of the summary of Cruciform Data is presented
in Appendix F. Table F-1 is the data for Phase I, EAFB; F-2 is for Phase I,
Lancaster; and F-3 is for Phase II, EAFB. The data are arranged in order by
mission number to facilitate their use with the Mission Log. A description
of the N-wave and its characteristics are given in Figure 4-5. Cards 2, 1 and

5 were primarily for use during digitizing of the analog data.

In addition to the data punched on the series of six data cards, an Analog Tape Log and a Digital Tape Log were prepared containing the following information:

1. Analog Tape Log

    The purpose of this log was to record the information contained on each analog tape. There is one master copy of each log plus one copy of the appropriate log is filed with each analog tape. The log for each tape is as follows: (Numbers in parenthesis refer to data card numbers.)

    a. Heading card, containing analog tape number, date, tape recorder number, and total number of missions
    b. Channel locations (Card 3)
    c. Pre-calibration digitization start-stop times (Card 5)
    d. Mission identification (Card 1)
    e. Mission digitization start-stop times (Card 2)
    f. Channel calibrations (Card 4)
    g. Post calibration digitization start-stop times (Card 5)

    A sample of the Analog Tape Log for a typical day and tape recorder is given in Appendix G.

2. Digital Tape Log

    The analog tape records all channel data, whereas the digital tape contains only selected channels. The digital tape log is similar to the analog tape log, but contains the necessary identification for only those channels that have been digitized.

The free field cruciform array analog tapes were digitized using the facilities available at Edwards AFB. The analog to digital conversion (A/D) equipment at Edwards AFB was capable of digitizing six channels of data at a sampling rate of 5000 samples per second per channel. The computer facilities consisted of an IBM 7094/44 direct coupled system. The raw digital cruciform tapes were in multiplexed form and a computer program was developed in order to provide a check of the digital data and to arrange the data in a readily usable form. This program de-multiplexed and arranged the data serially by mission and channel, evaluated the sinusoidal calibrations by a curve

4.7

fitting and averaging process, edited the digital data so that the final
output was one second of data, converted the pressure data to pounds per
square foot, located positive and negative peaks and computed the time
interval between them, and stored identification information on the tape.
A brief description of the format of the cruciform digital tapes is given
below:

1. Sampling rate - 5000 samples/second/channel
2. Number of words per record - 920
3. Number of bits per word - 24
4. Bit density - 556 B.P.I.

Structural analog data for the test flights were converted to digital
form to facilitate processing on a digital computer. Digitizing rates for
the structural data are given in the following table:

DIGITIZATION   UIREMENTS

Instrument	Tape Recorder Number	Digitization Rate SPS	Filter Cutoff CPS
Low Frequency Accelerometers	TR-2	8000	
Low Frequency Accelerometers	TR-4	8000	
Low Frequency Accelerometers	TR-5	8000	
Loading Microphones	TR-2	8000	
Loading Microphones	TR-4	1600	
Loading Microphones	TR-5	8000	
Loading Microphones Channels 801-807	TR-8	8000	
Loading Microphones Channels 808-812	TR-8	1600	
Strain Gages	TR-2	1600	
Strain Gages	TR-5	1600	
Displacement Gages	TR-4	1600	

Cruciform Array

Loading Microphones	TR-6	5000	1350

NOTES:

1) For tape recorders 2, 4, 5 and 8, the time code (tape channel 14) is
    digitized as a data channel and the sampling rate is 8000 sps.

4.8

Data Retrieval

All analog digital tapes have been numbered and cataloged and will be stored under controlled temperature and humidity conditions. Through the use of analog ᵧital tape logs described in the previous section, a detailed record has been kept of the data recorded on each tape. This record includes instrument locations, calibrations, mission logs, and digitization start and stop times. Data cards for all logs, mission log, cruciform summary, etc., are also readily available.

Phase I tapes have been indexed and are presently being stored in a controlled temperature and humidity atmosphere.

The following is a summary of the location of data taken during the Edwards AFB Phase II test program:

John A. Blume & Associates Research Division
612 Howard Street
San Francisco, California   94105

1. For tape recorders 2, 4, 5, and 8:

   a. Analog tapes,
   b. oscillographic recordings,
   c. analog tape logs,
   d. original calibration data she·   ɪd
   e. digital tapes and accompanyiʳ   ᴊmentation.

2. For tape recorder 6:

   a. Copies of analog tapes,
   b. oscillographic recordings for XB-70 missions,
   c. raw digital tapes, and
   d. final digital tapes and accompanying documentation.

3. Master copies of:

   a. Mission Log,
   b. Summary of Cruciform Data,
   c. Instrument Location Log, and
   d. Analog Tape Logs for tape recorders 1, 2, 3, 4, 5, 6, and 8.

4. Data card decks for:

    a. Mission Log,
    b. Digitization Log - Data,
    c. Instrument Location Log,
    d. Channel Calibration Log,
    e. Digitization Log - Calibrations,
    f. Summary of Cruciform Data, and
    g. Analog Tape Logs for tape recorders 1, 2, 3, 4, 5, 6, and 8.

5. Copies of Radar Plots.

Stanford Research Institute
333 Ravenswood Avenue
Menlo Park, California

1. For tape recorders 1 and 3:

    a. Analog tapes,
    b. oscillographic recordings,
    c. analog tape logs, and
    d. original calibration data sheets.

2. For tape recorder 6:

    a. Copies of original digital tapes and accompanying documentation.

NASA, Langley Research Center
Langley Station
Hampton, Virginia

1. For tape recorder 6:

    a. Original analog tapes,
    b. original calibration data sheets,
    c. oscillographic recordings, and
    d. original cruciform summary data sheets.
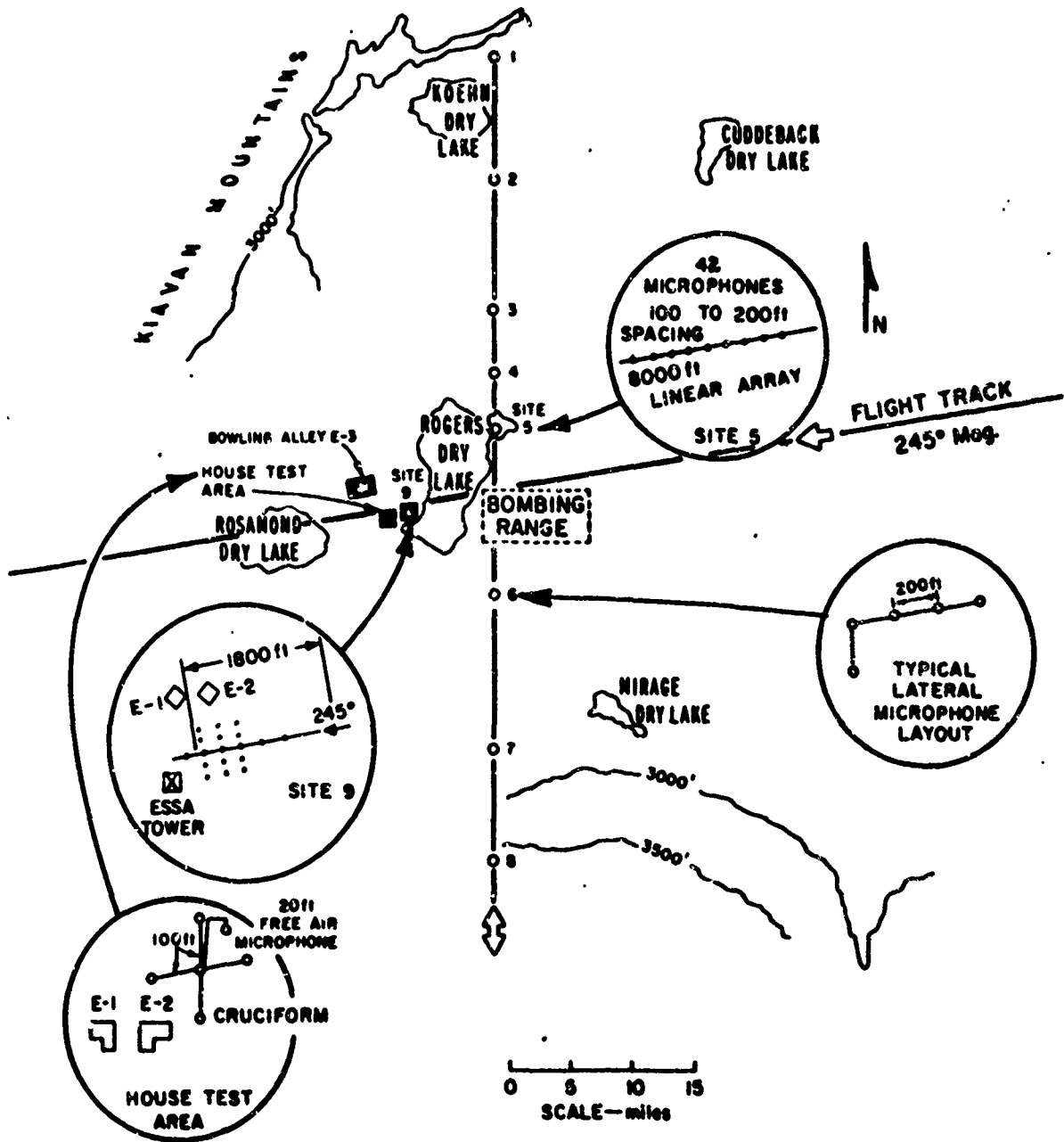
FIG. 4-1 SCHEMATIC SHOWING TEST AREA, SONIC BOOM MEASUREMENT STATION
DEPLOYMENT, AND AIRCRAFT FLIGHT TRACK AND HEADING
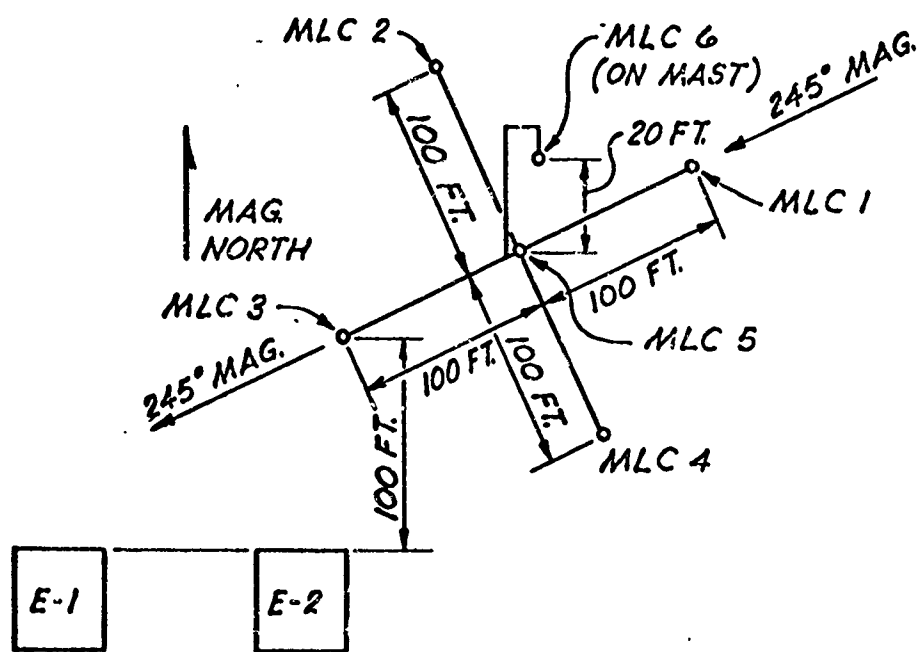
Fig. 4-2 FREE FIELD MICROPHONES

(CRUCIFORM ARRAY)

IRIG STANDARD TIME CODE - FORMAT "B"

TIME FRAME 1 SECOND

INDEX COUNT (.01 SECONDS)

TYPICAL MODULATED CARRIER
RECOMMENDED FREQUENCY 1000 CPS
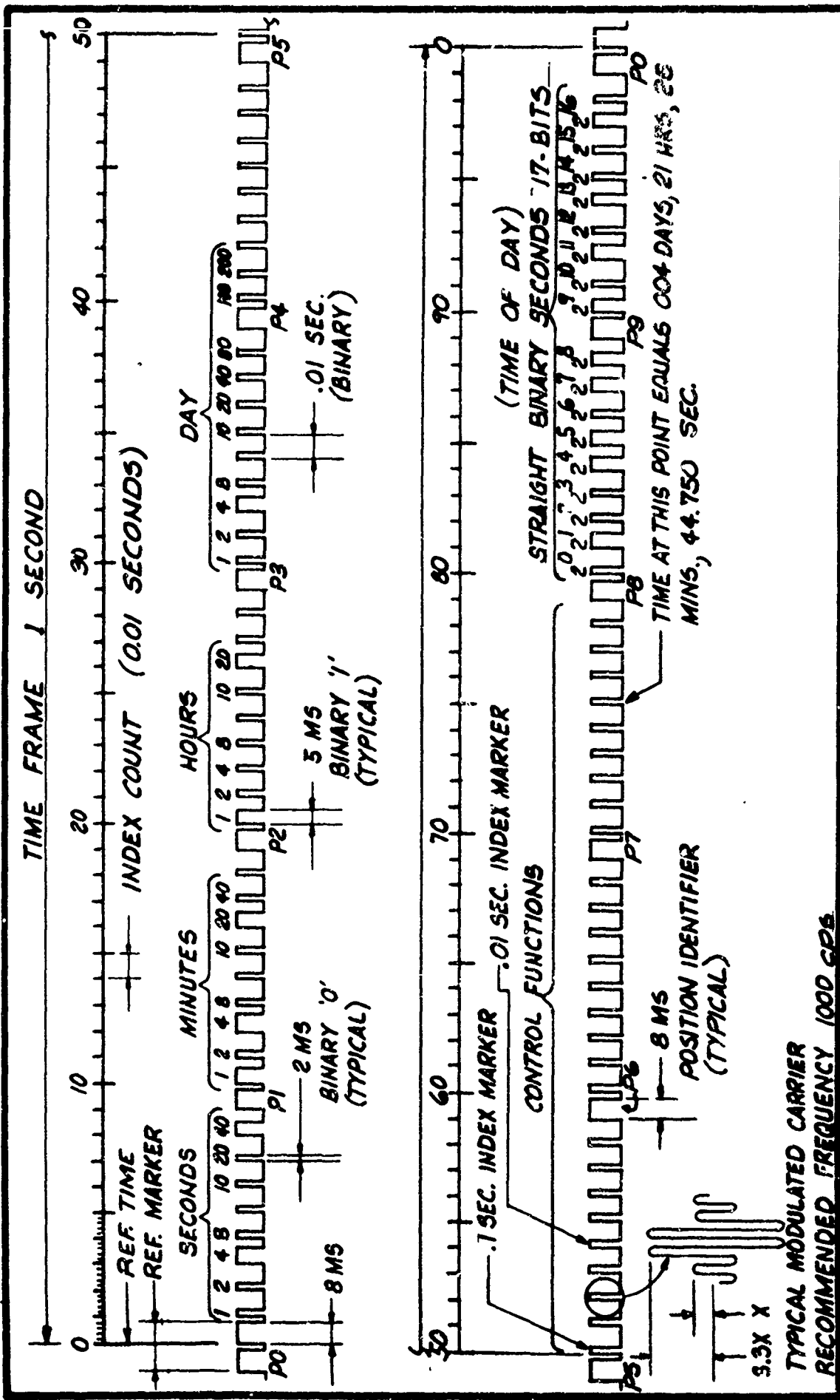
FIG. 4.3
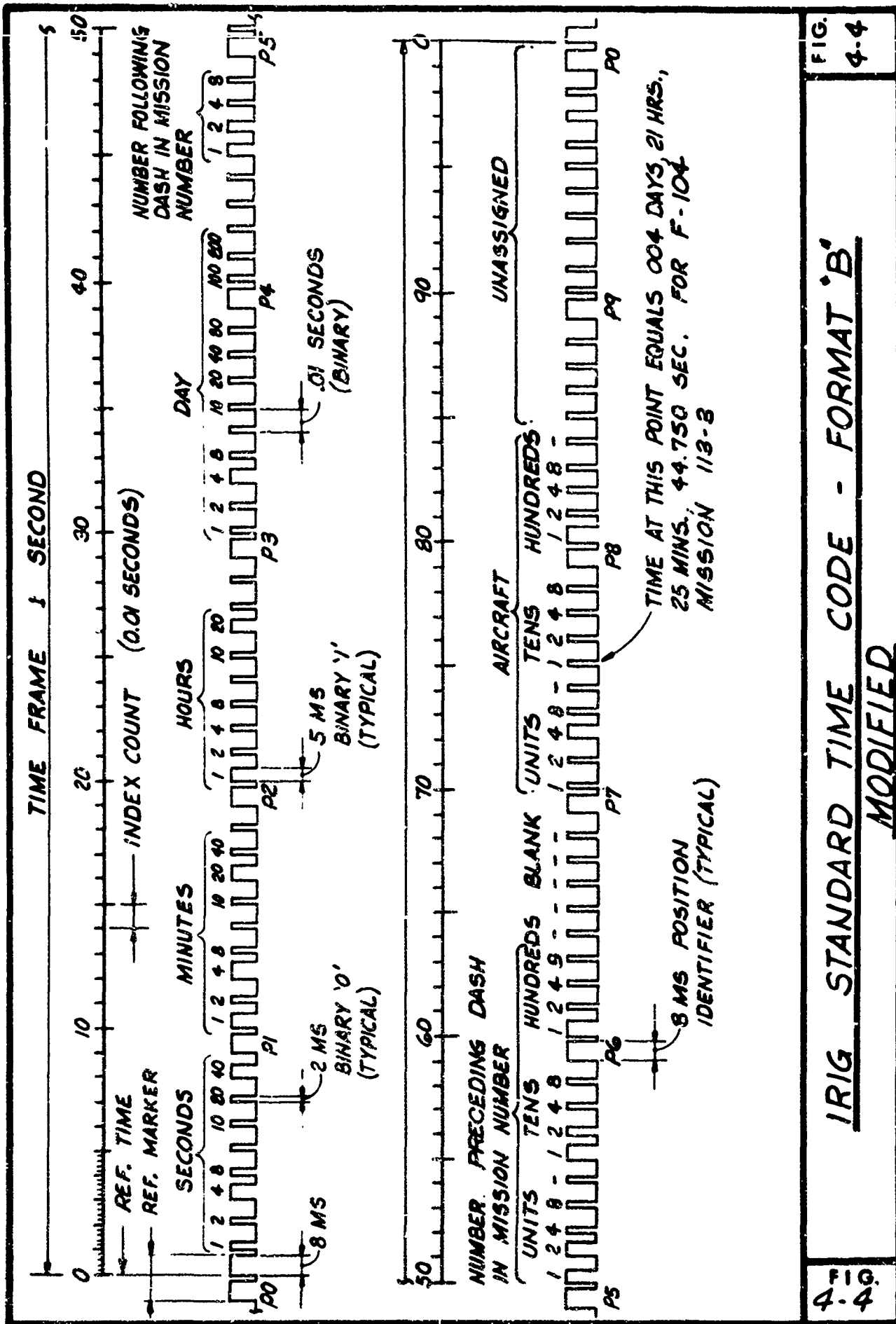
IRIG STANDARD TIME CODE - FORMAT 'B' MODIFIED

FIG. 4.4

4.14
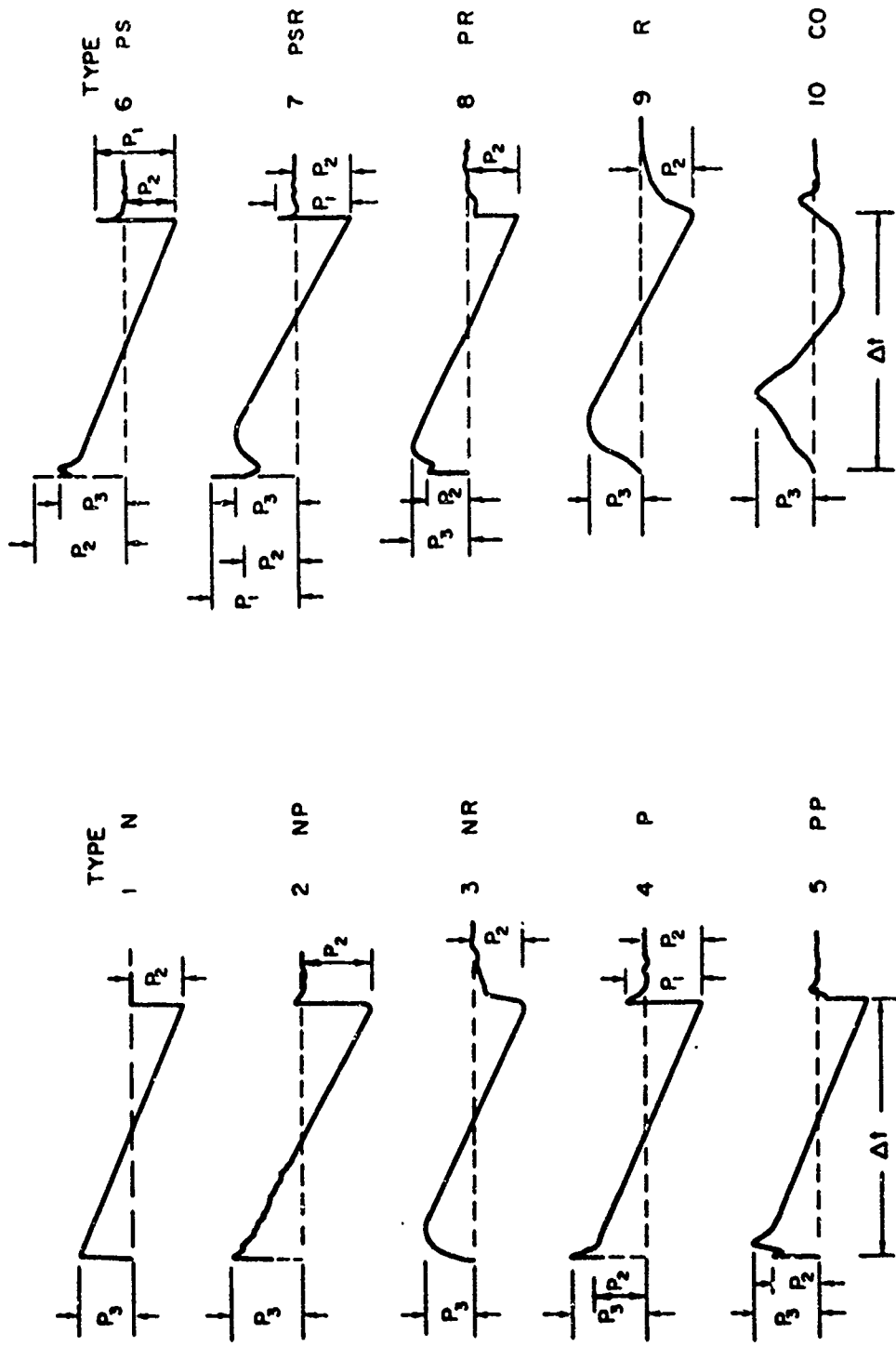
FIG. 4-5 SONIC BOOM WAVEFORM CATEGORIES

4.15

V. ANALYSIS OF FREE FIELD SIGNATURE PARAMETERS

There were three objectives in the analysis of free field signature parameters. First, it was of interest to find if the channels were statistically equal or if the measured values of a parameter were independent of the channel on which it was measured and recorded. The immediate consequence of this study was to answer the question: Is it possible to use only one channel instead of five channels in recording free field signatures? Secondly, tests of equality of means were performed on free field signature parameters and on the Dynamic Amplification Factors (DAF) computed from free field signatures in order to determine which parameters most influenced the DAF. The results of these tests were needed in establishing a criterion for random sampling of missions in further studies. Thirdly, to determine the number of samples for structure response studies, a complete statistical description (mean, standard deviation and coefficient of variation) of the parameters was needed.

In the statistical analysis of free field signatures, each sonic boom mission was defined as a random phenomenon. The parameters of the free field signature (overpressures, duration and rise time) were defined as random variables. The measured values obtained from oscillographic prints of the signatures were defined as observations of random variables. The data used in the analyses were measured by five microphones arranged in a cruciform array located near structure E-2 for comparable missions of XB-70/B-58/F-104 aircraft (flights flown within a few minutes of each other). A channel as defined for the study of free field signature parameters, consisted of a measuring instrument (microphone), the signal conditioning and recording system, an oscillographic print of the record and the manual measurement of the parameter from this print.

An analysis of variance was the statistical test from which it was possible to obtain simultaneously the results for the equality of channels and the equality of means for each parameter and a complete statistical description of each parameter. With this test it was assumed that the channels and the missions were chosen at random. Random sampling meant that each item had an equal probability of being chosen. It was reasonable to assume that the channels in the E-2 cruciform array were selected at random from a number of channels used to measure and record free field sig-

natures in this experiment. It was also reasonable to assume that the missions were selected from a large number of possible missions with different combinations of altitude, offset, speed and weight of the aircraft which would create similar signatures. In he analysis of variance[14,15] the hypothesis that the effects (channel and mission) were not present was tested against the alternate hypothesis that the effects were present. When the result of a test showed that an effect was present, a factor was calculated to determine which missions or channels were different. The hypotheses were tested at different confidence levels to make sure that the results were not influenced by lower decimal values of the data. The hypotheses were tested in this chapter at the 95 percent confidence level.

The free field signature parameters studied were: Peak positive overpressure (P_1), the absolute value of peak negative overpressure (P_2), the rise time (T_1), the time from start of boom to the negative peak (T_2), and the ratio of the absolute value of peak negative overpressure to peak positive overpressure (P_2/P_1).

The tests for channel effects of free field signature parameters produced the following results. There is a channel effect in P_2 for the XB-70 and B-58 missions and in the ratio P_2/P_1 for the XB-70 missions. Similar results have been found using a different test[29]. The difference in channels in each case was found between channels 605 and 607. This did not mean that the data from those channels should have been rejected, but that the coefficient of variation within each mission was composed of a coefficient of variation due to the boom and of a coefficient of variation due to the instruments. It was observed that, in most cases, the coefficient of variation of the data was primarily influenced by the coefficient of variation of the boom. The channel effect could be explained. As noted previously, a channel as used for the free field signature parameter study consisted of a measuring instrument (microphone), a signal conditioning and recording system, an oscillographic print of the record and a manual measurement from the print. The microphones used for free field signature measurement were modified to extend the low frequency response to 0.02 cps. The channel effect in P_2 for the XB-70 missions was large enough to affect the ratio P_2/P_1, but was not large enough for the B-58 missions to affect the same ratio. Also the channel effect in P_2 was not present for the F-104 missions. As the average frequency $(1/T_2)$ of P_2 for XB-70 missions was

5.2

3.64 cps, for B-58 missions 6.1 cps, and for F-104 missions 12.8 cps. It
could be inferred that the channel effect increased as the frequency re-
sponse decreased below the normal lower limit of the microphone. It could
also be inferred that one channel would have been sufficient to measure
free field signature parameters when the measured response frequency was
within the normal range of the microphone. Based on microphones used and
data recorded, it was concluded that to adequately measure the free field
signature parameters more than one microphone was needed for XB-70 and B-58
missions, but only one was needed for F-104 missions.

The tests of equality of free field signature parameters for different
missions produced the following results. The magnitude of peak positive
overpressure (P_1) and of the absolute value of peak negative overpressure
(P_2) decreased as the altitude and/or lateral offset of the aircraft in-
creased, as can be determined from Tables 5-1, 5-2, and 5-3. The averages
of the parameters were compared using the factors at the bottom of the
table. These factors indicated when two averages were different at the 95%
confidence level. For example, in Table 5-1, the average positive over-
pressure (P_1) of mission 5-2 was equal to 1.20 psf and of mission 10-1 to
2.41 psf. The difference between the two averages was 1.21 and was greater
than 0.3, the factor at the bottom of the table. Therefore, the average P_1
of mission 10-1 was greater than the average P_1 of mission 5-2 at the 95%
confidence level. The ratio of the absolute value of negative overpressure
to positive overpressure (P_2/P_1) decreased as the offset of the aircraft
increased. This result was evident only for the XB-70 missions as illus-
trated in Figure 5-1. There was only a small difference in the averages of
rise time (T_1) and time from start of boom to negative peak (T_2) recorded
for overhead and offset missions for each type of aircraft. This result
can be determined from Tables 5-1, 5-2, and 5-3.

The coefficients of variation of the free field signature parameters
calculated for all missions listed in Tables 5-1, 5-2, and 5-3 were:

	Coefficient of Variation of				
Aircraft	P_1	P_2	T_1	T_2	P_2/P_1
XB-70	20%	31%	54%	10%	17%
B-58	35%	25%	64%	6%	14%
F-104	20%	18%	45%	10%	10%

The number of missions needed for a comparative study of predicted and measured response was a function of the coefficient of variation of the data. From the above table it was evident that the number of missions needed would be different depending on which coefficient of variation was used. It was therefore necessary to know which of the free field signature parameters studied most influenced the DAF computed from free field signatures. Thus an analysis of the variance test was performed on maximum DAF's computed from free field signatures to study again the channel effect and the mission effect. The natural frequencies of the DAFs studied were, for the XB-70 missions 2.66, 3.23 and 3.93 cps, and for the B-58 missions 3.93, 4.78 and 5.81 cps. These natural frequencies were chosen as they were in the range of maximum DAF values.

There were no channel effects found in computed DAFs . Even if P_2 and the ratio P_2/P_1 affected the forcing function used to determine the DAF, the impulse response function and the damping (2%) were sufficient to eliminate the channel effect found in P_2 and P_2/P_1. Therefore, the data from a single channel would have been adequate to evaluate the DAF computed from free field signatures.

The results of the tests of equality of maximum DAFs for different missions indicated the following. The magnitudes of the maximum DAFs for each aircraft were different and occurred at different natural frequencies. In comparing the difference in DAF magnitude with the difference in free field signature parameters, it was found that the magnitude of the DAF decreased as the ratio P_2/P_1 decreased for XB-70 missions; Figure 5-2. It was found that the natural frequency at which the maximum DAF occurred decreased as T_2 increased for the XB-70 missions, as shown in Figure 5-3. The effect of T_2 was also evident in a visual comparison between DAF envelopes for eight XB-70 missions, eight B-58 missions and five F-104 missions in Figure 5-4. From this figure it was evident that duration of sonic boom affected the range of structure natural frequencies over which maximum dynamic amplification occurred. Since boom duration increased with aircraft size, sonic booms from large aircraft such as the XB-70 and the future SST will affect a greater range of structure elements than sonic booms from smaller aircraft such as the B-58 and the F-104. Previous studies[18] have indicated that rise time also affects the magnitude of the DAF. However, with the data recorded, this effect could not be verified. It was therefore concluded that the ratio P_2/P_1 caused the major effect

on the magnitude of the DAF and that the number of missions needed in further studies of structure response should be determined from the statistical description of the ratio P_2/P_1.

The number of missions needed to study the response of structure elements was obtained from statistical sampling techniques.[16] The sample size varied according to the degree of precision desired in the results and the confidence level of the conclusions about the results. The following table demonstrates this process.

Degree of Precision in Results in %	Confidence Level in %	Number of Missions Needed		
		XB-70	B-58	F-104
10	95	11	8	4
15	95	5	4	2
20	95	3	2	1
10	90	8	6	3
15	90	4		2
20	90	2	2	1

The degree of precision in the results meant that the results obtained from the analyses of the sampled missions would be within 10% (or 15% or 20%) of the results which would have been obtained if all missions had been analysed. The probability that the results were within such a percentage was given by the confidence level. The degree of precision in the results and the confidence level were chosen according to the pertinence of the study.

SUMMARY OF FINDINGS

The free field signature parameters were analysed to determine if the channels were statistically equal or if the measured values of a parameter were independent of the channel on which it was recorded; to determine which parameters most influenced the Dynamic Amplification Factor (DAF); and to determine the number of samples necessary for studies of structure response data. The analytical techniques were such that the findings are stated with

a 95 percent confidence level; that is, there is a 95 percent probability that the findings are correct. Following are the findings resulting from these analyses:

1. For the XB-70 missions the peak negative overpressure, P_2, and the ratio of the absolute value of peak negative overpressure to peak positive overpressure, P_2/P_1, were not independent of the channel on which they were recorded. All other parameters studied (positive overpressure, P_1, rise time, T_1, and the time from start of boom to negative peak, T_2) were independent of the channels.

2. For the B-58 missions P_2 was not independent of the channel on which it was recorded. All other parameters studied (P_1, T_1, T_2, and P_2/P_1) were independent of the channels.

3. For the F-104 missions all parameters (P_1, P_2, T_1, T_2, and P_2/P_1) were independent of the channels on which they were recorded. A single channel would have been adequate to measure free field signatures.

4. The magnitude of P_1 and of the absolute value of P_2 decreased as the lateral offset and/or altitude of the aircraft increased.

5. The ratio P_2/P_1 decreased as the offset of the aircraft increased for XB-70 missions.

6. There was little difference between rise times (T_1) of overhead and offset missions for each type of aircraft.

7. There was little difference between times from start of boom to negative peak (T_2) of overhead and offset missions for each type of aircraft.

8. The Dynamic Amplification Factors (DAF) computed from free field signatures were independent of the channel the signatures were recorded on. Therefore, a single microphone would have been sufficient to evaluate DAFs.

9. The magnitude of the maximum DAF decreased as the ratio P_2/P_1 decreased.

10. The natural frequency at which the maximum DAF occurred was a function of the time from start of boom to negative peak T_2. As T_2 increased, the maximum DAF occurred at a lower natural frequency.

5.6

11. Sonic booms from large aricraft such as the XB-70 and the future SST will affect a greater range of structure elements than will sonic booms from smaller aircraft such as the B-58 and the F-104.

12. The number of missions needed in the study of the response of structure elements varied depending on the degree of precision in the results and on the confidence level.

TABLE 5-1

SUMMARY OF FREE FIELD SIGNATURE PARAMETERS

AIRCRAFT XB-70

Mission	Altitude Feet	Mach	Offset Feet	Average P_1 psf	Average P_2 psf	Average P_2/P_1	Average T_1 $\times 10^{-3}$ sec	Average T_2 $\times 10^{-1}$ sec
1-1	37,200	1.46	L10,300	2.91	2.61	0.90	3.6	2.30
2-1	37,300	1.48	L37,600	2.55	1.45	0.58	6.2	2.37
3-2	37,600	1.50	L 900	2.47	2.46	0.99	4.7	2.34
4-2	38,600	1.50	0	2.49	2.22	0.89	5.2	2.32
5-2	59,100	2.49	R12,900	1.20	0.82	0.69	4.9	2.83
6-2	50,000	2.50	R67,900	1.78	1.01	0.57	5.9	2.84
7-3	60,300	2.50	R71,300	1.32	0.83	0.63	4.8	2.64
8-3	60,000	2.50	R68,200	1.39	0.90	0.65	10.8	2.69
9-1	59,400	2.51	R32,100	2.09	1.23	0.59	3.7	2.74
10-1	59,700	2.46	L13,300	2.41	1.66	0.69	4.3	2.63
11-3	59,400	2.50	0	2.09	1.58	0.76	4.6	2.78
12-2	60,300	2.50	L 200	2.19	1.71	0.78	4.9	2.90
13-2	60,200	1.80	R 6,400	2.00	1.64	0.81	7.9	2.87
14-1	59,700	1.80	R 200	2.11	1.71	0.81	9.3	3.11
15-1	60,600	1.80	R 9,500	2.18	1.81	0.83	4.8	2.96
16-2	59,700	1.80	R 700	2.29	1.84	0.80	5.0	2.99
113-2	60,300	1.80	L 100	2.20	1.85	0.84	4.8	3.13
				0.30	0.19	0.07	6.0	0.02

Two parameters are different when the difference
in their averages is equal to or greater than

5.8

TABLE 5-2

SUMMARY OF FREE FIELD SIGNATURE PARAMETERS

AIRCRAFT B-58

Mission	Altitude Feet	Mach	Offset Feet	Average P_1 psf	Average P_2 psf	Average P_2/P_1	Average T_1 ×10⁻³ sec	Average T_2^{-1} ×10⁻¹ sec
1-3	32,400	1.4	L 7,200	3.08	2.37	0.77	5.0	1.65
2-3	33,000	1.5	L 7,500	2.32	2.26	0.98	11.7	1.53
3-1	32,400	1.5	R 7,800	2.55	1.85	0.72	4.9	1.53
4-1	32,000	1.5	R 1,900	2.25	2.01	0.89	15.8	1.49
5-1	36,300	1.65	R63,300	0.68	0.64	0.94	13.0	1.73
6-1	35,500	1.65	R40,400	1.31	1.15	0.88	16.2	1.57
7-1	35,800	1.62	R38,700	1.75	1.25	0.71	5.3	1.47
8-1	35,500	1.65	L 3,300	2.39	2.27	0.95	5.5	1.64
9-2	40,400	1.65	R 1,700	2.71	1.79	0.71	3.1	1.74
10-2	32,400	1.32	L 6,000	3.27	2.60	0.80	13.2	1.85
11-2	40,200	1.65	R 800	1.86	1.80	0.97	4.8	1.71
12-1	39,200	1.65	L 2,100	2.39	1.90	0.79	5.3	1.72
13-1	35,900	1.65	L 2,500	2.21	1.84	0.83	4.9	1.59
14-2	38,800	1.53	R 4,200	2.64	1.85	0.70	4.1	1.56
15-2	39,600	1.65	0	2.34	2.04	0.87	4.3	1.63
16-1	39,700	1.65	R 3,000	2.25	2.09	0.94	5.1	1.70
113-1	39,100	1.65	L 700	2.61	1.97	0.76	4.0	1.64
Two parameters are different when the difference in their averages is equal to or greater than				1.37	0.18	0.14	5.2	0.01

TABLE 5-3

SUMMARY OF FREE FIELD SIGNATURE PARAMETERS

AIRCRAFT F-104

Mission	Altitude Feet	Mach	Offset Feet	Average P_1 psf	Average P_2 psf	Average P_2/P_1	Average $T_1 \times 10^{-3}$ sec	Average $T_2 \times 10^{-1}$ sec
1-4	18,600	1.30	R 2,200	3.24	2.75	0.87	2.5	0.81
2-4	17,600	1.30	—	3.51	2.79	0.80	1.9	0.79
3-4	17,800	1.30	L 2,300	2.36	2.36	1.00	4.4	0.77
9-3	21,100	1.14	R 2,000	1.54	1.50	0.97	7.4	0.85
11-1	20,800	1.40	L 1,500	2.01	2.03	1.01	4.5	0.73
12-3	22,030	1.42	R 6,700	2.10	1.96	0.97	5.2	0.76
13-3	20,000	1.40	R 3,400	2.01	1.92	0.96	5.3	0.74
14-3	21,400	1.30	R 1,400	2.10	2.15	1.07	3.6	0.86
15-3	20,200	1.40	R 200	2.31	2.09	0.91	3.8	0.73
16-3	20,600	1.40	R 5,000	2.10	1.85	0.92	2.7	0.76
113-3	20,600	1.40	R 1,200	1.95	1.89	0.98	4.5	0.78

Two parameters are different when the difference   0.43   0.14   0.13   4.0   0.19
in their averages is equal to or greater than

5.10

TABLE 5-4

SUMMARY OF DAFs COMPUTED FROM FREE FIELD SIGNATURES

AIRCRAFT XB-70

Mission	Altitude Feet	Mach	Offset Feet	Average DAF @ 2.66 cps	Average DAF @ 3.23 cps	Average DAF @ 3.93 cps
3-2	37,600	1.50	L 900	1.64	1.95	2.03
4-2	38,600	1.50	0	1.52	1.81	1.83
5-2	59,100	2.49	R12,900	1.52	1.50	1.34
7-3	60,300	2.50	R71,300	1.35	1.43	1.29
8-3	60,000	2.50	R68,200	1.48	1.55	1.44
9-1	59,400	2.51	R32,100	1.55	1.66	1.51
10-1	59,700	2.46	L13,300	1.68	1.83	1.65
11-3	59,400	2.50	0	1.68	1.79	1.53
12-2	60,300	2.50	L 200	1.76	1.79	1.52
13-2	60,200	1.80	R 6,400	1.80	1.82	1.50
15-1	60,600	1.80	R 9,500	1.84	1.80	1.47
16-2	59,700	1.80	R 700	1.86	1.82	1.50
113-2	60,300	1.80	L 100	1.87	1.74	1.43
				0.16	0.17	0.15

Two DAFs are different (for the same frequency) when
the difference in their averages is greater than or
equal to

TABLE 5-5

SUMMARY OF DAFs COMPUTED FROM FREE FIELD SIGNATURES

AIRCRAFT B-58

Mission	Altitude Feet	Mach	Offset Feet	Average DAF @ 3.93 cps	Average DAF @ 4.78 cps	Average DAF @ 5.81 cps
3-1	32,400	1.5	R 7,800	1.32	1.60	1.73
4-1	32,000	1.5	R 1,900	1.53	1.86	2.02
5-1	36,300	1.65	R63,300	1.99	2.16	1.96
8-1	35,500	1.65	L 3,300	1.63	1.87	1.84
9-2	40,400	1.65	R 1,700	1.51	1.68	1.54
10-2	32,400	1.32	L 6,000	1.80	1.95	1.76
11-2	40,200	1.65	R 800	1.87	2.10	1.99
12-1	39,200	1.65	L 2,100	1.58	1.76	1.63
13-1	35,900	1.65	L 2,500	1.47	1.73	1.77
15-2	39,600	1.65	0	.59	1.84	1.85
16-1	39,700	1.65	R 3,000	1.74	1.97	1.89
13-1	39,100	1.65	L 700	1.48	1.69	1.66
				0.10	0.12	0.12

Two DAFs are different (for the same frequency) when
the difference in their averages is greater than or
equal to
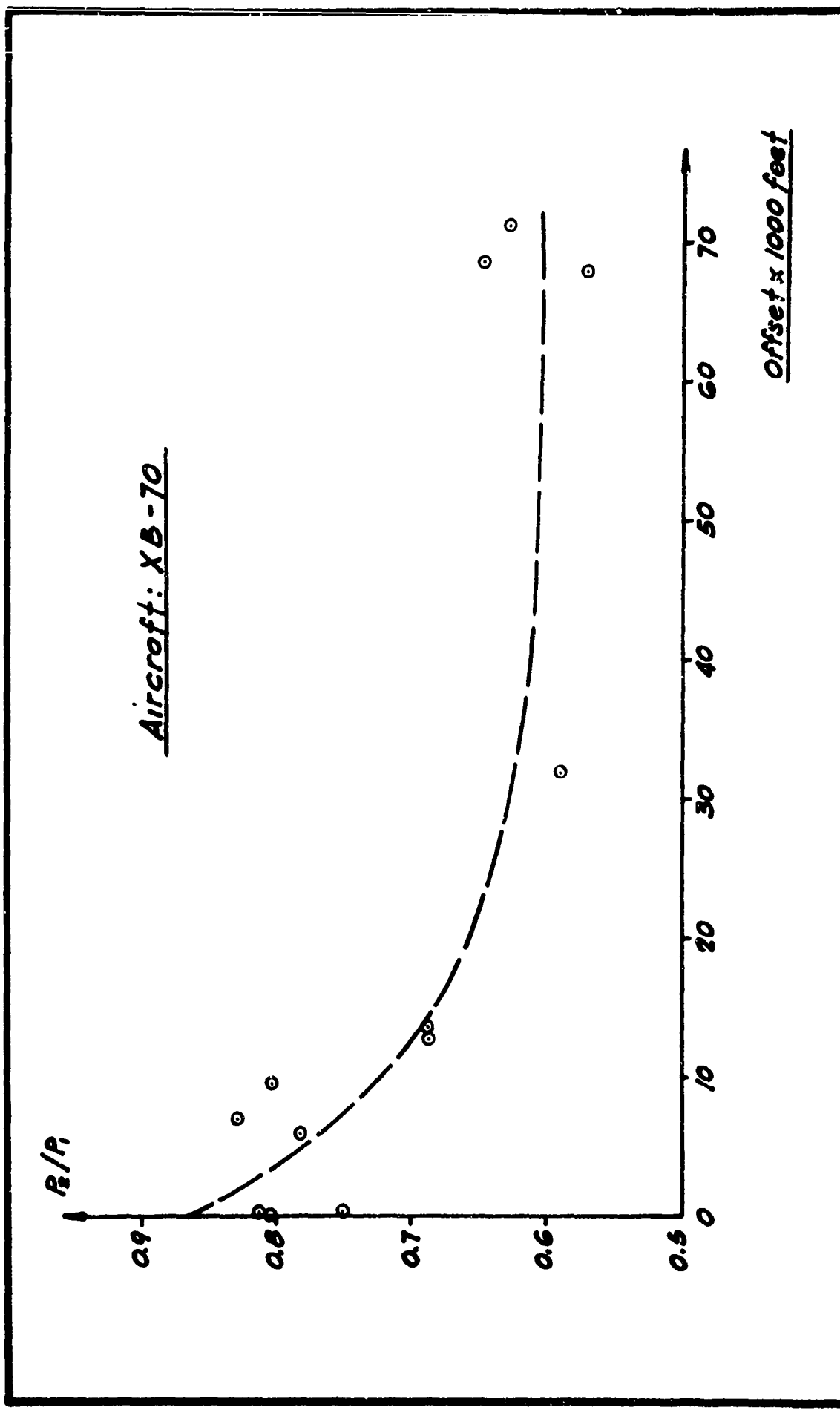
Aircraft: XB-70

RATIO R_2/R_1 vs. OFFSET

Offset × 1000 feet

R_2/R_1

FIG. 15-1

FIG. 5-1

5.13

MAXIMUM DAF vs. P_3/P_1

Maximum DAF

Aircraft: XB-70

Missions
3-2
4-2
10-1
11-3
12-2
15-1
16-2
13-2

P_3/P_1 $\left(\dfrac{\text{Absolute negative overpressure}}{\text{Positive overpressure}}\right)$
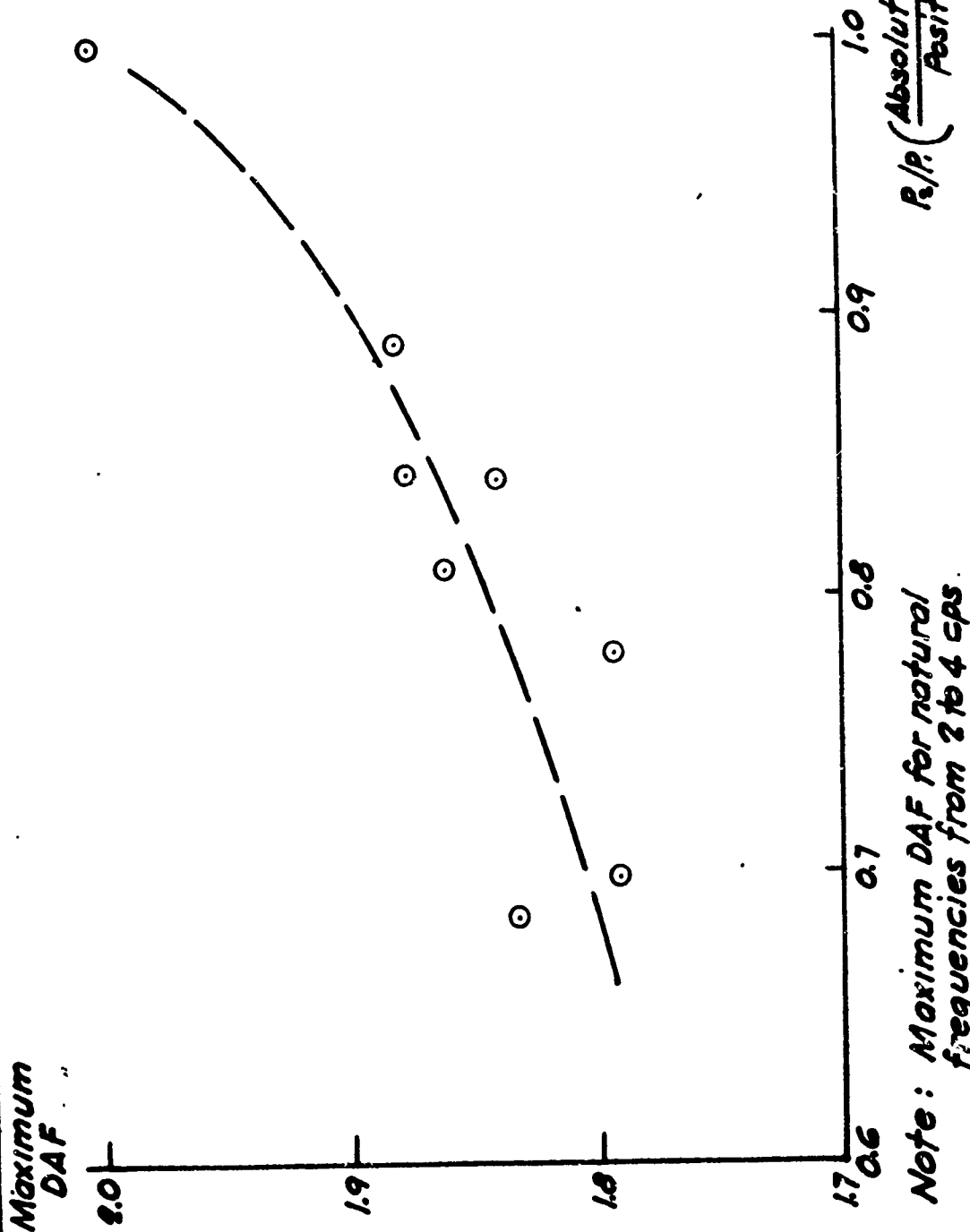
Note: Maximum DAF for natural frequencies from 2 to 4 cps.

FIG.
5·2

FIG.
5·2

NATURAL FREQUENCY OF MAXIMUM DAF vs. T_2

Aircraft: XB-70

Missions
3-2
4-2
10-1
11-3
12-2
15-1
16-2
113-2

T_2 (Time from start of boom to negative peak)

$T_2 \times 10^{-1}$ sec.

Maximum frequency at which maximum DAF occurs, cps

FIG. 5-3

5.15

TYPICAL SIGNATURES

PRESSURE — PEAK PRESSURE

F-104

B-58

XB-70

DURATION — TIME

DYNAMIC AMPLIFICATION FACTOR (DAF)

NATURAL FREQUENCY C.P.S.
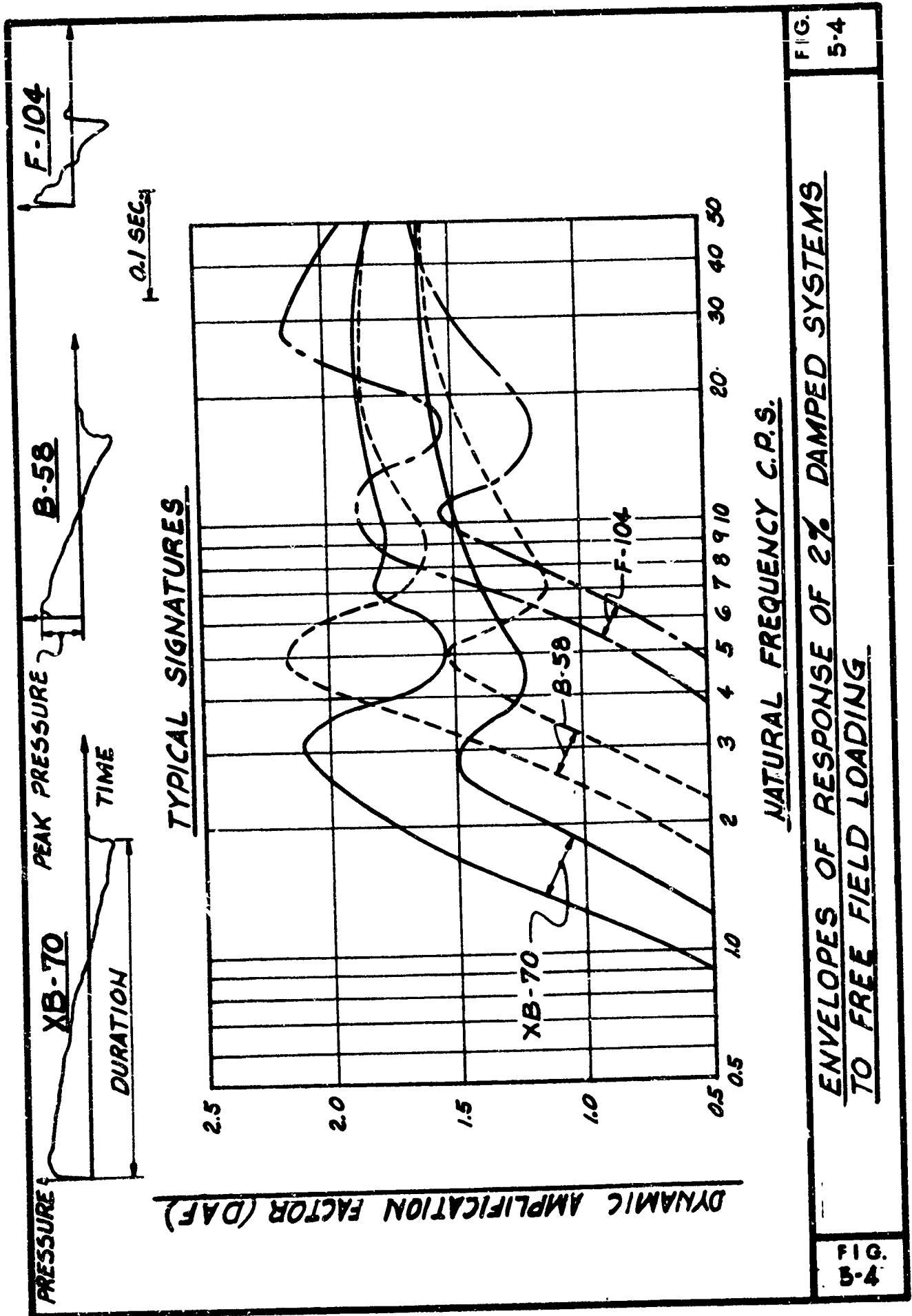
ENVELOPES OF RESPONSE OF 2% DAMPED SYSTEMS
TO FREE FIELD LOADING

FIG. 5-4

5.16

VI. EFFECTS OF FREE FIELD SIGNATURE PARAMETERS
ON DYNAMIC AMPLIFICATION FACTORS

There were two objectives in making the study of the effects of free field signature parameters on DAF spectra. First, it was of interest to derive a wave model from free field signature parameters (over-pressures, rise time, duration) that could be used to make an accurate evaluation of the DAF and thereby eliminate the lengthy and costly process of digitizing free field signatures that is presently needed to compute the DAF. Secondly, to gain a greater insight on the probable magnitude of the DAF for large lateral offsets of an aircraft, the effects of values of free field signature parameters beyond the range of the data recorded by the E-2 cruciform microphone array on the DAF were analysed using the wave model.

To fulfill the first objective, the derivation of a wave model, it was assumed that for purposes of calculating DAF a free field signature could be completely described by the parameters; peak positive overpressure (P_1), rise time (T_1), peak negative overpressure (P_2), and time from start of boom to negative peak (T_2). The total duration of the signature (τ) was assumed to be equal to T_2 plus T_1. Linearity was assumed between peak overpressure points, as illustrated in Figure 6-1. The averages of P_2/P_1, T_1 and T_2 were computed for eight XB-70 missions, eight B-58 missions and five F-104 missions. They were:

Aircraft	P_2/P_1 *	$T_1 \times 10^{-3}$ sec	$T_2 \times 10^{-1}$ sec
XB-70	0.773	5.15	2.88
B-58	0.852	5.63	1.67
F-104	0.966	4.66	0.75

*absolute value

These average values were used in computing DAF spectra from the wave model. Two different methods of comparison were used to see if the DAF spectra calculated from the wave model were representative of the spectra computed from digitized free field signatures. A visual comparison of the spectra in Figures 6-2, 6-3, and 6-4 showed that the DAF spectra of the wave model were generally within the envelopes of the DAF spectra obtained from digitized free field signatures of the same missions. Then to mathematically substantiate the visual comparisons, a "goodness of fit" (chi-square)[14] test was per-

formed. In this statistical test the average values of the DAF spectra computed from digitized free field signatures were compared with the values of the wave model DAF spectra at twenty-one different natural frequencies between 1 and 50 cps. The results of the test showed the fit is good at the 95% confidence level for all three types of aircraft. These results are illustrated in the following tabulation of values of the test statistic computed from the data and the chi-square value. The test statistic must be smaller than chi-square value to conclude that the fit is good at the 95% confidence level.

Aircraft	Test Statistic	Chi-Square Value @ 95% C. L.
XB-70	0.07	31.4
B-58	0.05	31.4
F-104	0.57	31.4

The small values of the test statistic were due to the small difference between the average values of the DAF spectra computed from digitized free field signatures and the values of the DAF spectra computed from the wave model. A value greater than 31.4 would have indicated that there was no fit at all. It was therefore concluded that a free field signature wave model described by P_1, P_2, T_1 and T_2 could be used to accurately evaluate the DAF computed from digitized free field signatures. It was further concluded that, for future work with free field signatures, knowledge of the values of P_1, P_2, T_1 and T_2 would be sufficient for obtaining DAF spectra that would be representative of those obtained directly from free field signatures. The digitization of free field signatures could therefore be eliminated.

The wave model was then used to fulfill the second objective of this study which was to investigate the effects of values of free field signature parameters beyond the range of the data recorded by the E-2 cruciform array on the DAF spectra. First, different values of P_1, P_2, T_1, T_2 were used to confirm that the ratio of the absolute value of peak negative overpressure to peak positive overpressure (P_2/P_1) influenced the magnitude of maximum DAF. The same input values were then used to study the influence of T_1 on the magnitude of the DAF and finally to obtain DAF spectra for values of T_2 larger than those measured and recorded by the E-2 cruciform microphone array.

It was found that as the ratio P_2/P_1 increased the magnitude of the maximum

6.2

DAF increased. This result was derived for natural frequencies of 4 to 7 cps, and a wave duration of 0.2 sec. as indicated in Figure 6-5. Similar results were found in Chapter V for the XB-70 missions. It was also found that, for the XB-70 missions, the ratio P_2/P_1 decreased with increasing lateral offset of the aircraft. It was therefore evident that one effect of increasing lateral offset was to cause a corresponding decrease in the magnitude of the maximum DAF.

In previous studies[32] it was found that T_1 increased with increasing lateral offset, and that the two limiting shapes of a free field signature could be an N wave with zero rise time, and a sinusoidal pulse, Figure 6-6. The effect of T_1 on the DAF was therefore studied within these limits. To generalize the findings, the ratio of rise time to duration (T_1/τ) was used in the study instead of the value of T_1. The results were plotted in Figure 6-7. It was found that as the ratio T_1/τ increased, the magnitude of the maximum DAF increased. For this study a wave duration of 0.2 sec. and a ratio P_2/P_1 equal to 1 were used and the values of maximum DAF were computed for natural frequencies of 4 to 7 cps. Therefore it was concluded that increasing the lateral offset of an aircraft increased the maximum DAF values. The total influence of lateral offset on the magnitude of the DAF could not be determined. There were insufficient recorded data to definitely indicate which of the two ratios, P_2/P_1 or T_1/τ, was predominant. Analyses of more data recorded at large lateral distances from the flight track are needed.

Throughout this study the DAF spectra were computed with a damping coefficient of 2%. The effect of different damping coefficients was studied for different wave durations. The results plotted in Figure 6-8 were computed for a wave duration of 0.3 sec. with a rise time equal to 2% of the wave duration and a ratio P_2/P_1 equal to 1. The DAF values plotted were calculated for a natural frequency of 3 cps. It was found that the magnitude of the DAF decreased as the damping coefficient increased.

It was assumed that free field signatures for aircraft larger than the XB-70 would be similar in shape. By using the wave model DAF spectra were then computed for durations of 0.4 and 0.5 sec. and different combinations of ratio T_1/τ and P_2/P_1 as illustrated in Figures 6-9 and 6-10. As found in Chapter V, durations of 0.4 and 0.5 sec. increased the range of structure natural frequencies over which maximum dynamic amplification occurred.

SUMMARY OF FINDINGS

The objectives of this chapter were first, to derive a wave model in order to eliminate the digitization of free field signatures presently needed to compute DAF spectra and second, to study the change in magnitude of the maximum DAF for different large lateral offsets of an aircraft. The data used in the analyses were measured during Phase II by five microphones arranged in a cruciform array located near structure E-2 for the comparable missions of XB-70/B-58/F-104 aircraft (flights flown within a few minutes of each other). The following findings resulted from these studies:

1. The DAF spectra obtained using a wave model described by free field signature parameters P_1, P_2, T_1 and T_2 were equal at the 95 percent confidence level to the DAF spectra obtained from digitized free field signatures.

2. Using the derived wave model it was found that:

   a. the magnitude of the maximum DAF decreased as the ratio P_2/P_1 decreased,

   b. the magnitude of the maximum DAF increased as the ratio T_1/τ increased, and

   c. the magnitude of the maximum DAF decreased as the damping coefficient increased.

3. In the analysis of the effects of lateral offset of aircraft, the ratio P_2/P_1 in the recorded free field signatures caused the predominent effect on DAF. The recorded signatures showed little change in rise times (T_1) or in durations (τ) for overhead and offset missions for each type of aircraft. Therefore the influence of lateral offset on DAF spectra was limited to the effect of the ratio P_2/P_1.

IDEALIZED SONIC BOOM PRESSURE WAVE MODEL

FIG.
6-1

6.5
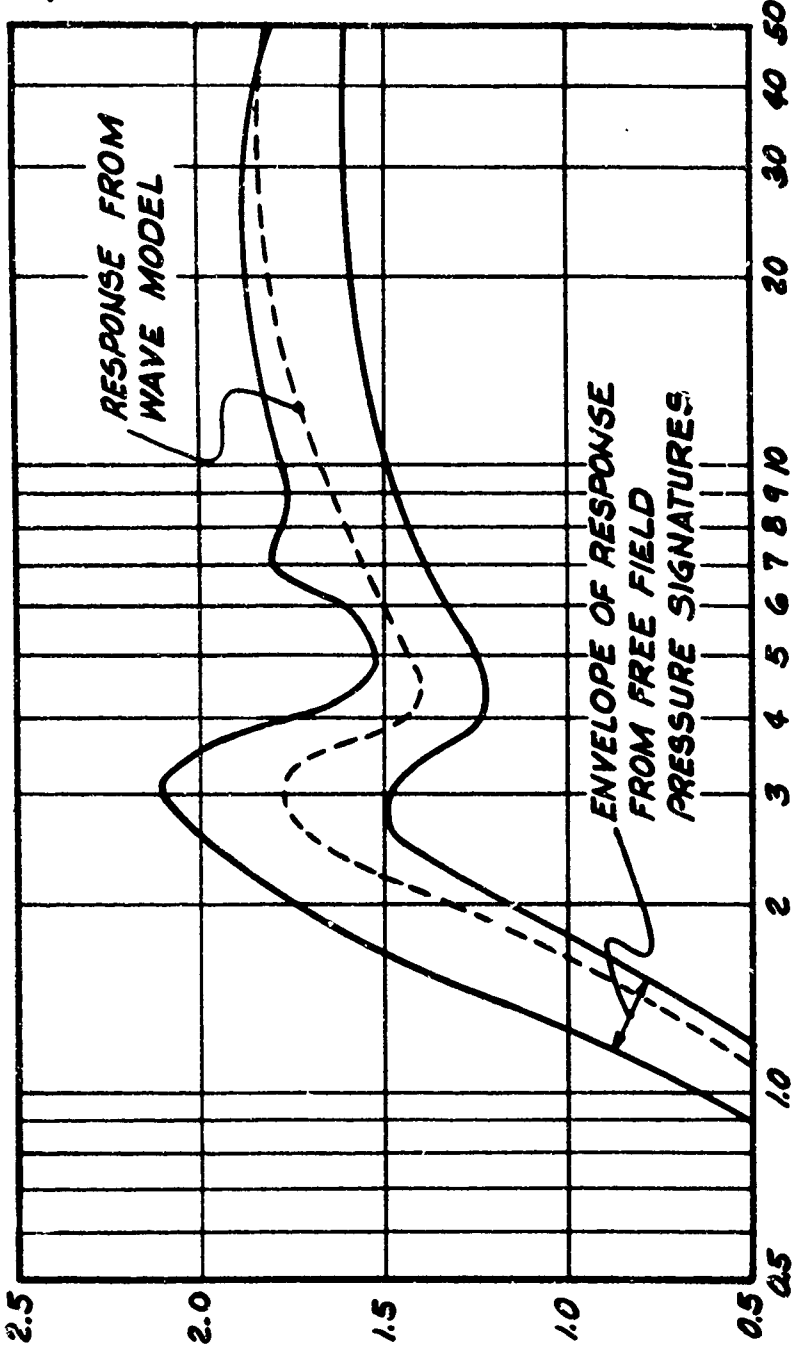
MISSIONS

5 - 2
10 - 1
11 - 8
12 - 2
13 - 2
15 - 1
16 - 2
113 - 2

RESPONSE FROM WAVE MODEL

ENVELOPE OF RESPONSE FROM FREE FIELD PRESSURE SIGNATURES.

NATURAL FREQUENCY C.P.S.

DYNAMIC AMPLIFICATION FACTOR (DAF)

RESPONSE OF 2% DAMPED SYSTEMS TO FREE FIELD LOADING

XB-70 OVERHEAD FLIGHTS

FIG. 6-2
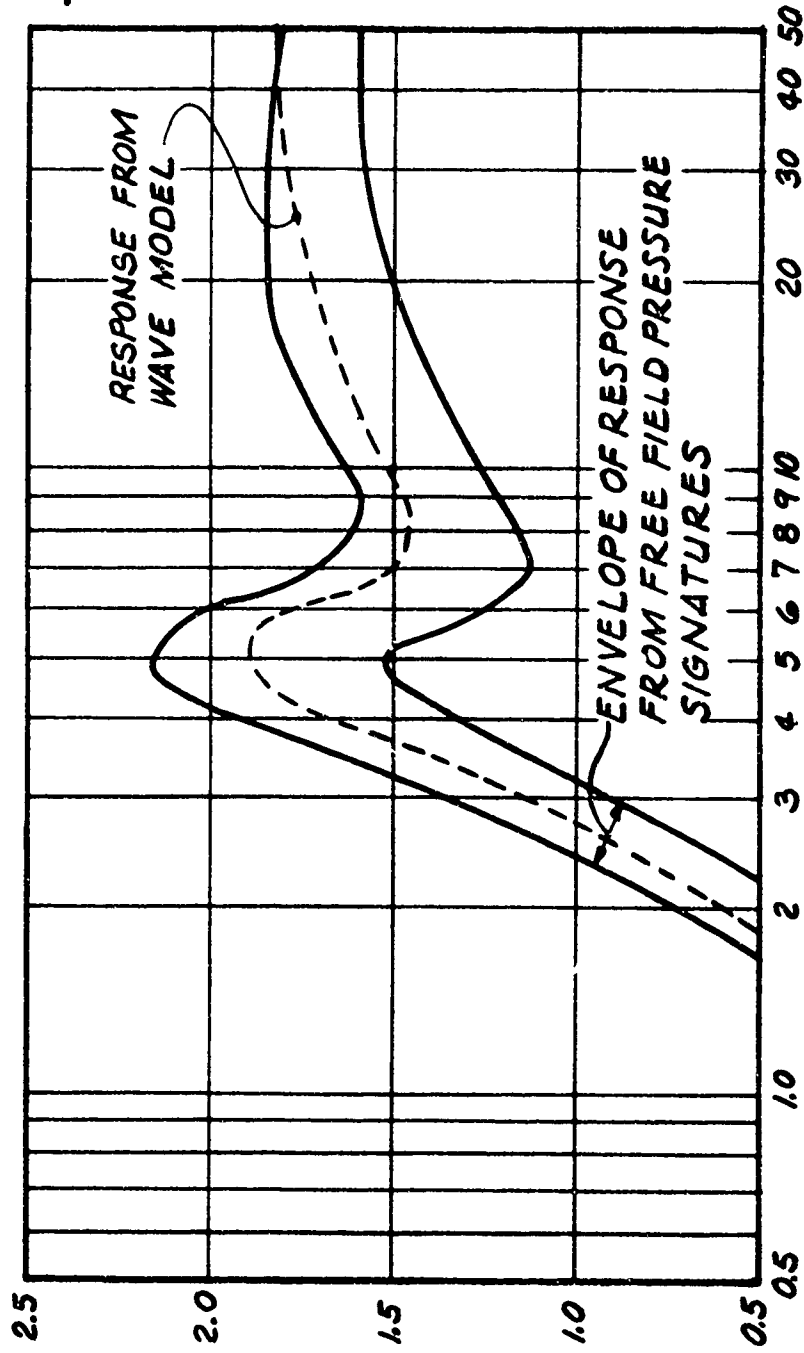
FIG. 6-2

6.6

RESPONSE OF 2% DAMPED SYSTEMS TO FREE FIELD LOADING

B-58 OVERHEAD FLIGHTS
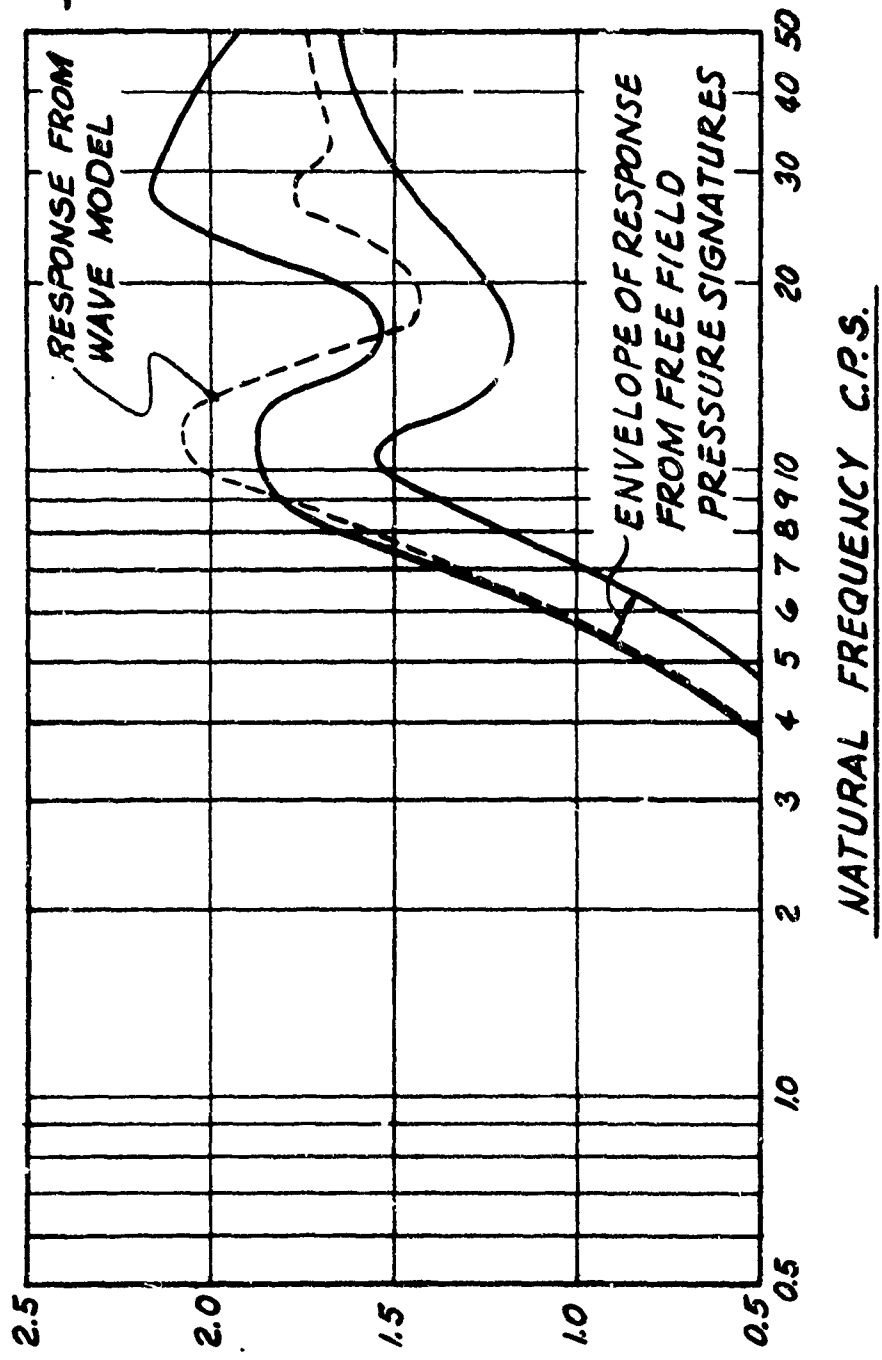
MISSIONS

11 - 1	
12 - 3	
13 - 3	
15 - 3	
113 - 3	

RESPONSE FROM WAVE MODEL

ENVELOPE OF RESPONSE FROM FREE FIELD PRESSURE SIGNATURES

NATURAL FREQUENCY C.P.S.

DYNAMIC AMPLIFICATION FACTOR (DAF)

RESPONSE OF 2% DAMPED SYSTEMS TO FREE FIELD LOADING — F-104 OVERHEAD FLIGHTS

FIG. 6·4

FIG. 6·4

6.8

Wave duration 0.2 sec.
Rise time: 2% of duration
Damping 2%

Maximum DAF

P_2/P_1

0.2   0.4   0.6   0.8   1.0

1.2   1.4   1.6   1.8   2.0

NOTE: Maximum DAF for natural frequencies of 4 to 7 cps.
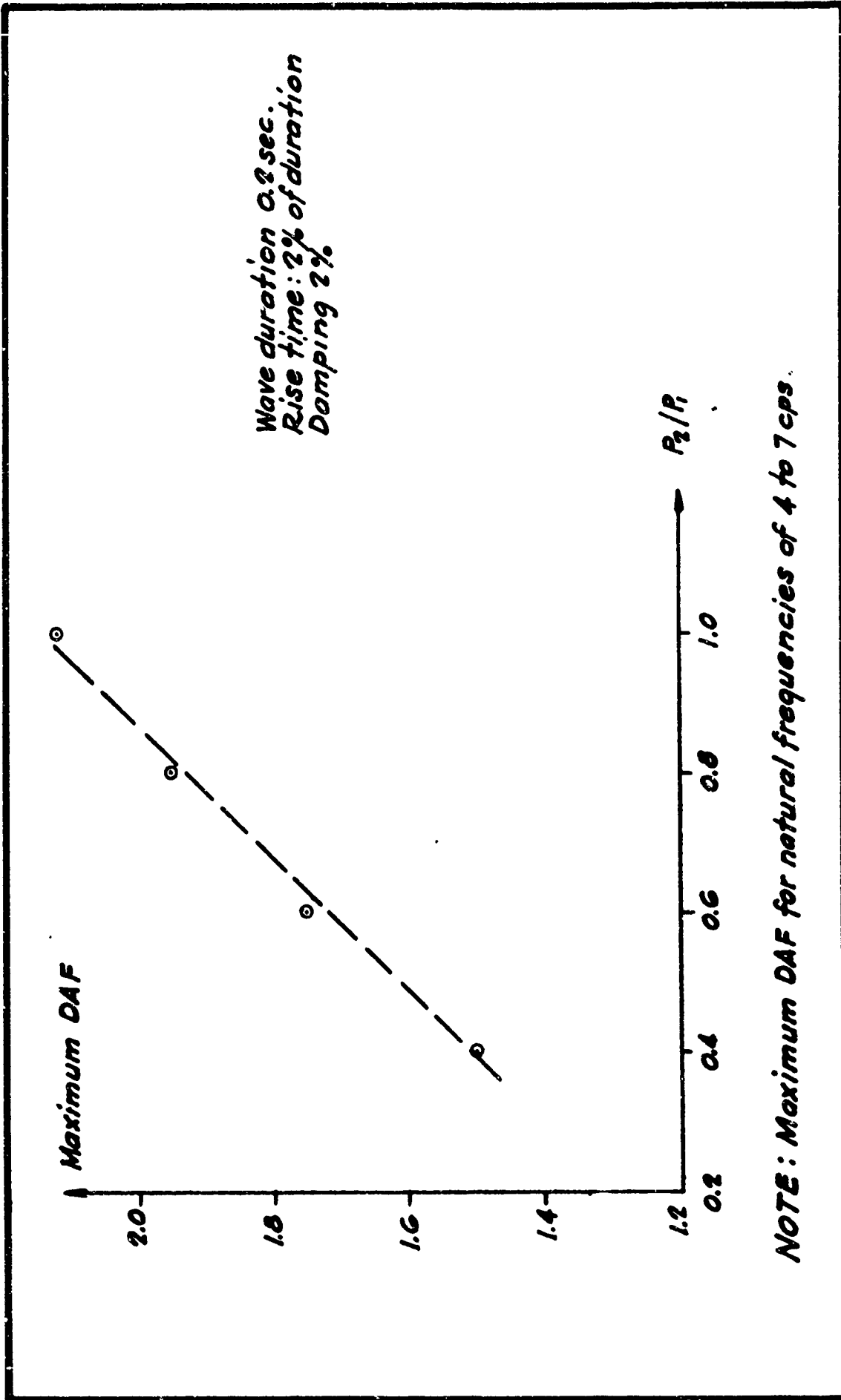
MAXIMUM DAF vs. RATIO P_2/P_1

FIG.
6-5

FIG.
6-5

6.9
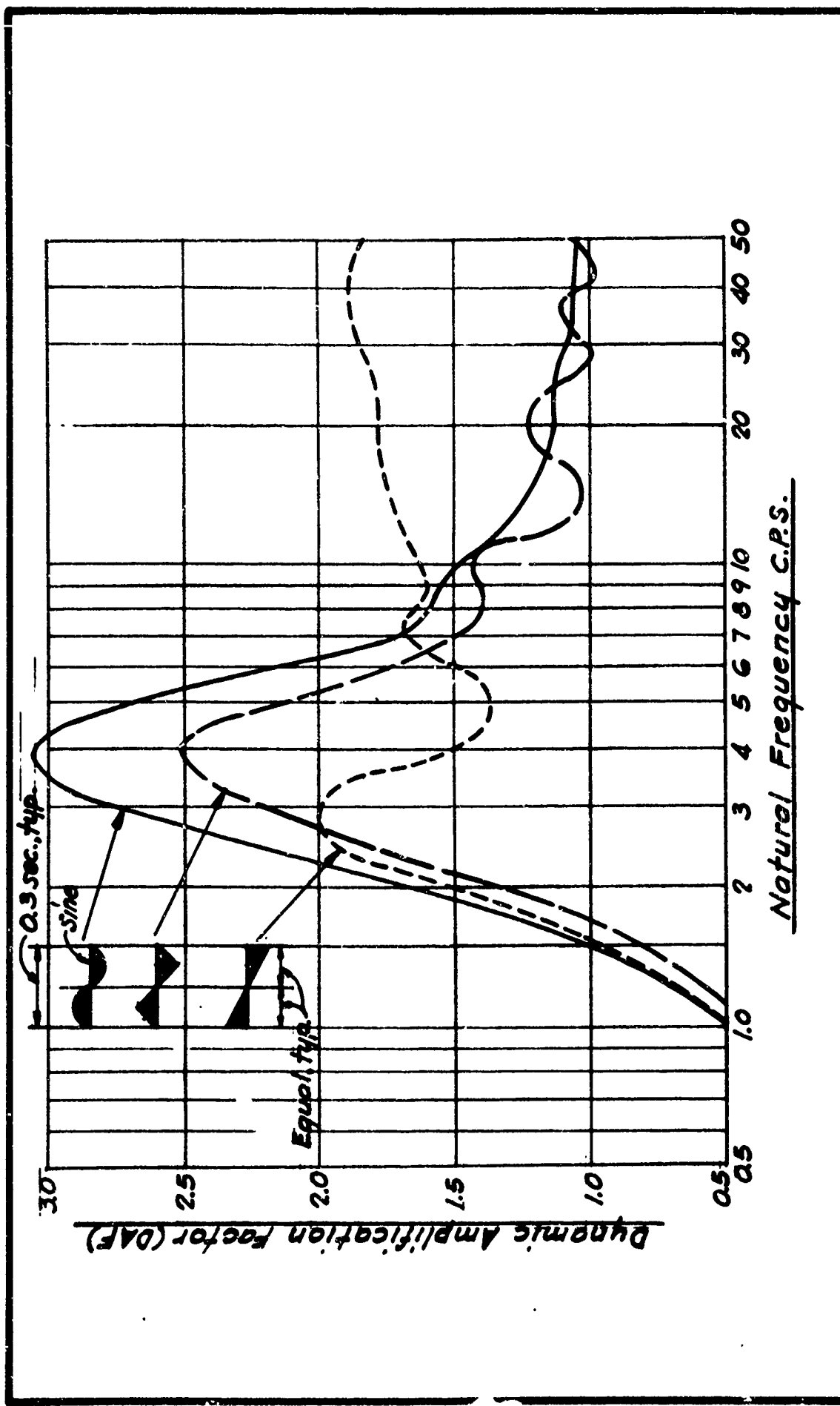
RESPONSE OF 2% DAMPED SYSTEMS
EFFECT OF LOADING PULSE SHAPE
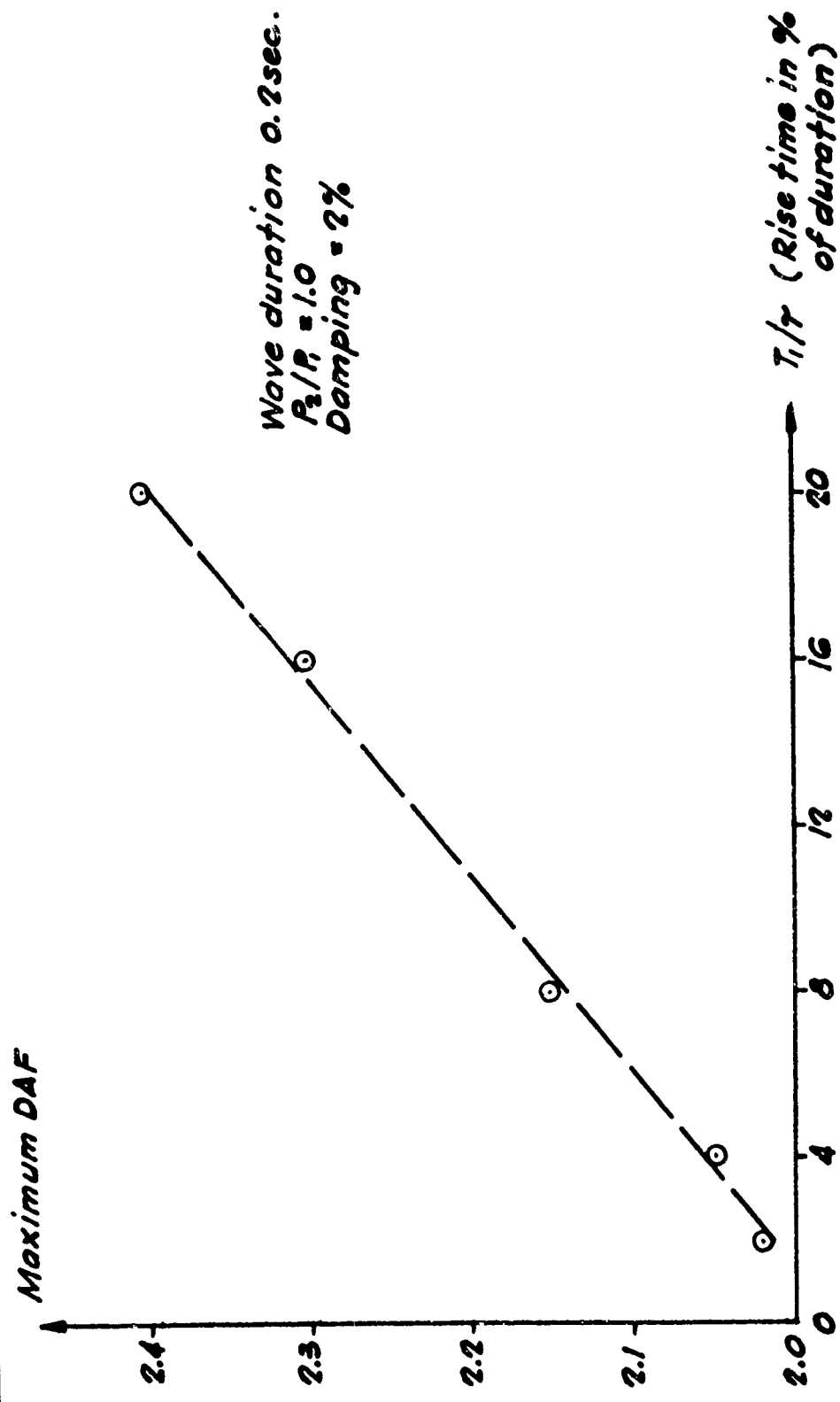
FIG. 6·6

Wave duration 0.2 sec.
$P_2/P_1 = 1.0$
Damping = 2%

Maximum DAF

T_1/r (Rise time in % of duration)

NOTE: Maximum DAF for natural frequencies of 4 to 7 cps.

MAXIMUM DAF vs. T_1/r

FIG. 6-7

6.11

Wave duration 0.3 sec.
Rise time 2% of duration
$P_2/P_1 = 1.0$

Maximum DAF

Damping in % of critical

NOTE: Maximum DAF for natural frequency of 3 cps
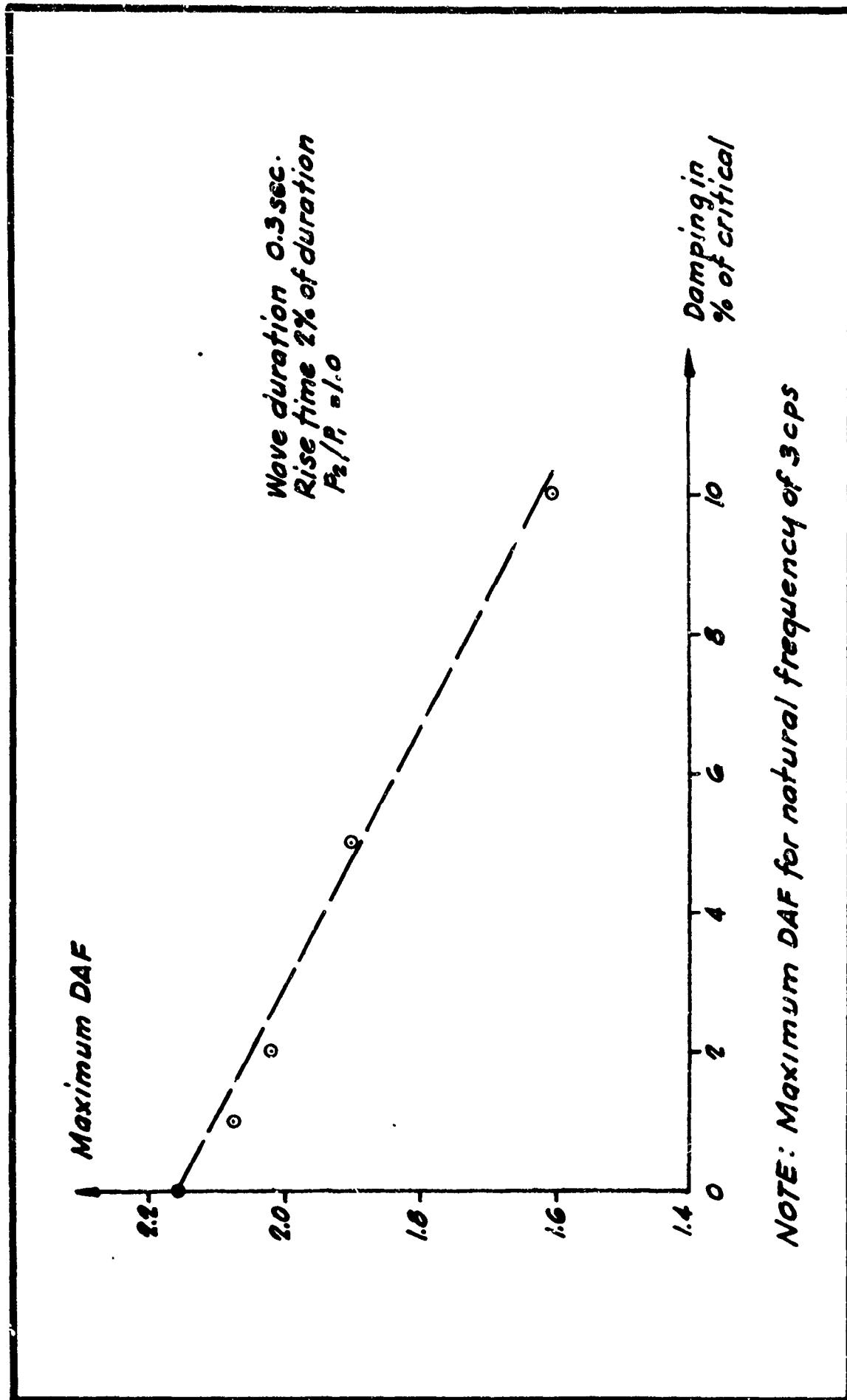
MAXIMUM DAF vs. DAMPING

FIG. 6-8
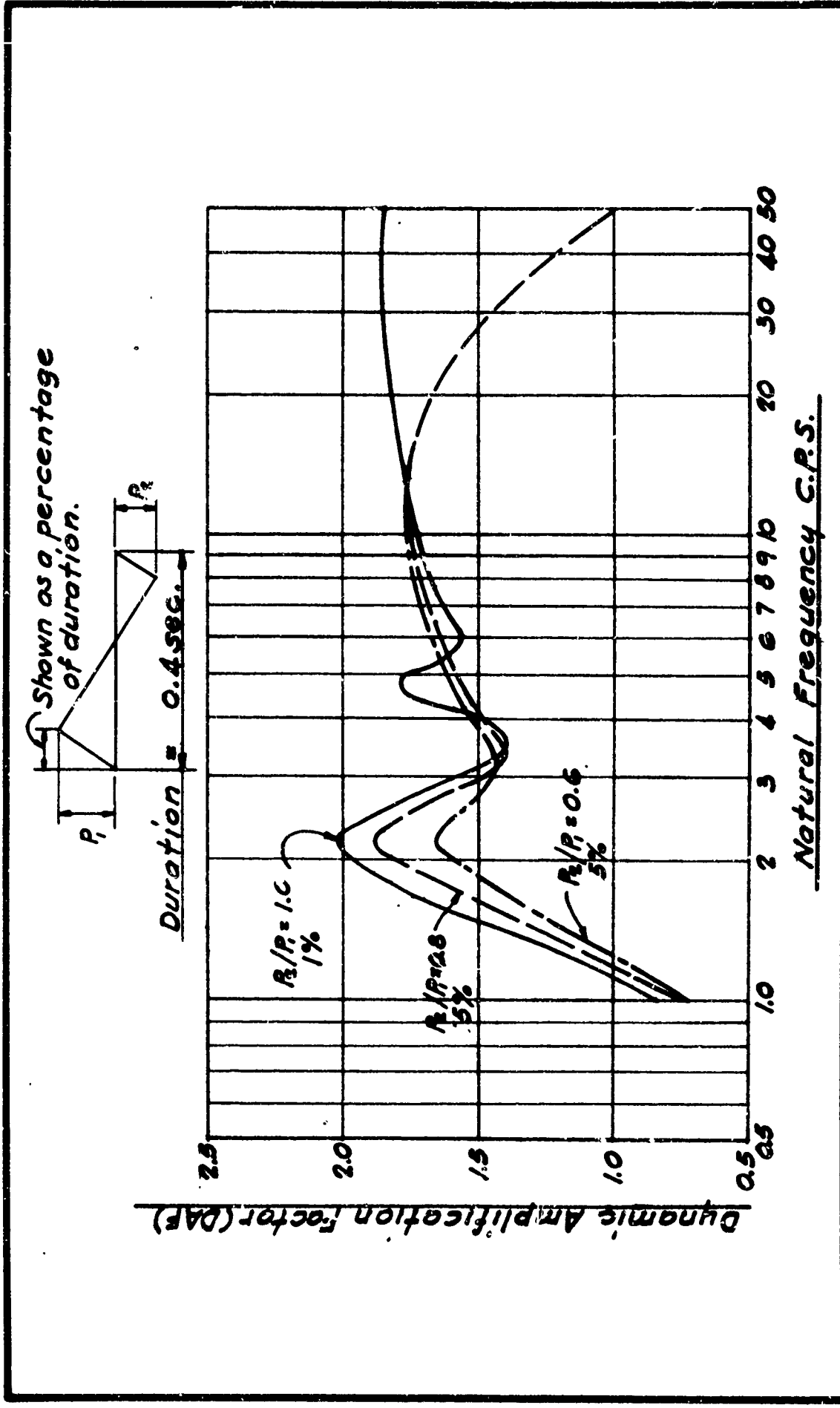
FIG. 6-8

6.12

RESPONSE OF 2% DAMPED SYSTEMS
COMBINED EFFECTS OF RISE TIME AND RATIO R/P
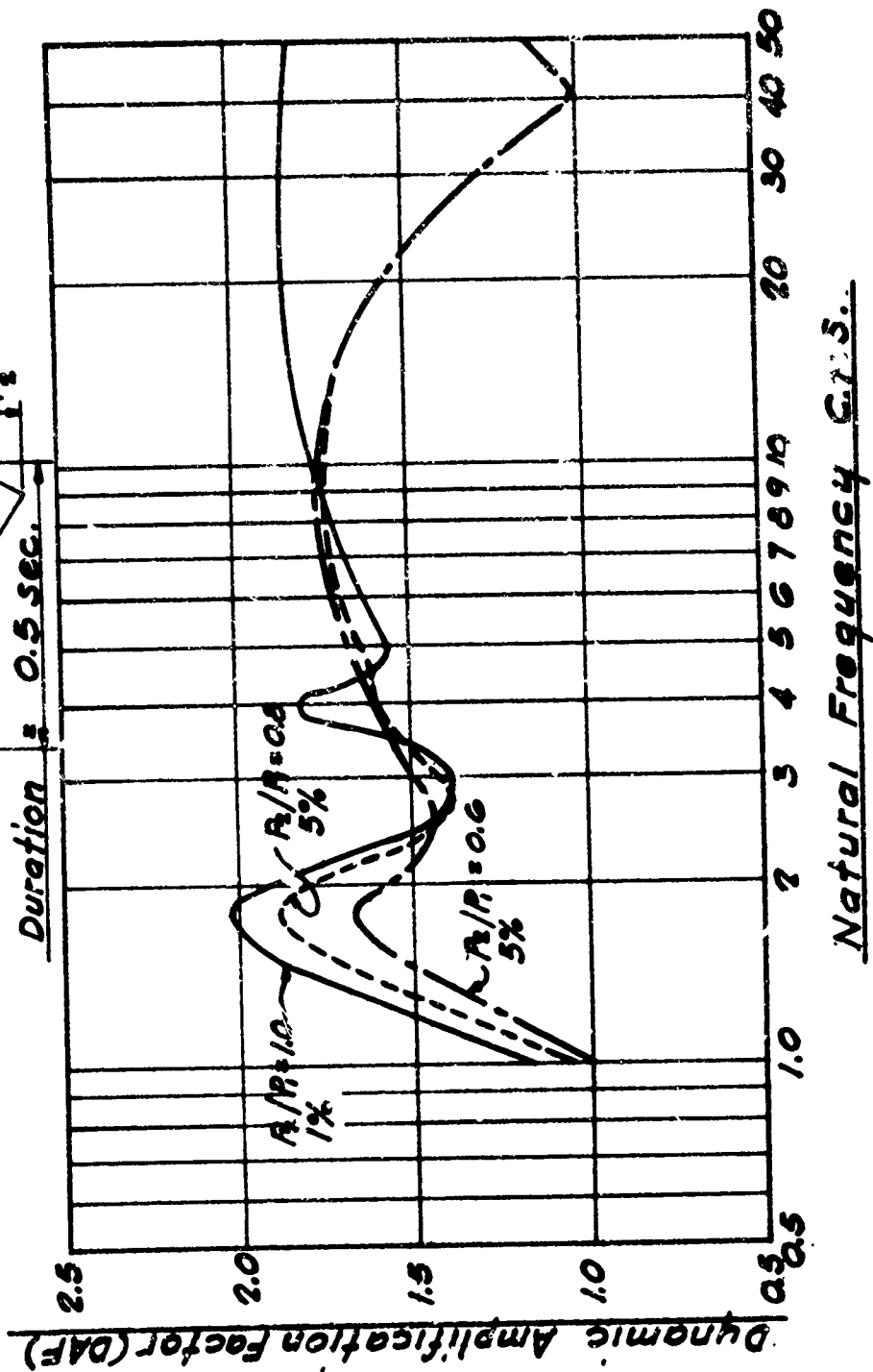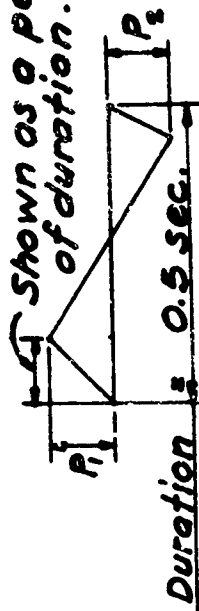
FIG.
6.9

FIG.
6.9

RESPONSE OF 2% DAMPED SYSTEMS
COMBINED EFFECTS OF RISE TIME AND RATIO P_r/P_s.

FIG. 6-10

VII. ANALYSIS OF STRUCTURAL RESPONSE DATA - PLATE RESPONSE

The analysis of structural response data was divided into two sections: plate response and racking response. Plate response was defined as the lateral deformation of individual structure elements and was primarily of a bending mode. Racking response was defined as the deformation of the structure as a whole and was primarily of a shearing mode. The analysis of the plate response data is covered in this chapter and racking response will be discussed in the following chapter. This chapter is divided into three sections: A) Wall Plate Response in Test Houses E-1 and E-2; B) Window Plate Response in Test House E-1; and C) Response of the Roof Frame of the Bowling Alley, E-3.

A. WALL PLATE RESPONSE IN TEST HOUSES E-1 AND E-2

The analysis of the wall plate response in Test Houses E-1 and E-2 considered three typical walls: the east wall of bedroom number one in House E-2 (BRI-1); the east wall of the dining room in House E-2 (DR-2); and the north wall of bedroom number one in House E-2 (BRI-2). Predicted displacements were computed and compared with measured displacements for the three walls. Predicted displacements were computed using two sources of loading data: peak overpressures and DAF spectra obtained from free-field signatures and peak overpressures and DAF spectra obtained from net pressure signatures. The effects on plate response of flight track offset, Mach number and aircraft vector were also investigated. In addition, the results of the Phase II tests were compared with those from previous tests.

INSTRUMENTATION

Accelerometers were installed on the east wall of BRI-1, the east wall of DR-2, and the north wall of BRI-2 to determine the plate response of typical walls in the test houses. These accelerometers were mounted at mid-height of the center stud of each wall. In addition to the accelerometers, pressure microphones were installed on the inside and outside of these walls so that the actual loading or net pressure on the walls could be determined. The locations of these instruments are shown in Figure 7-1; their characteristics are listed in Appendix B.

NOTE: All figures and tables are placed at the end of this chapter. For the altitude, Mach number, offset, etc., of aircraft missions used in this chapter, see Tables 5-1, 5-2, and 5-3.

TEST RESULTS - MEASURED DISPLACEMENTS

The analog magnetic tape recordings of the accelerometer data were con-
verted to digital form as discussed in Chapter IV. The digital records were
then numerically integrated twice to obtain displacements. Peak displacements
determined for the BRI-I, DR-2, and BRI-2 walls are listed in Tables 7-I,
7-3, and 7-5, respectively, under the heading of Measured Displacements. Dis-
placements were calculated for comparable XB-70, B-58, and F-104 overhead
missions (flights flown within a few minutes of each other) for all three of
the walls, and for XB-70 flights of different Mach number and offset for the
BRI-I and DR-2 walls.

Acceleration and corresponding displacement records for the DR-2 wall
for typical missions of XB-70, B-58, and F-104 aircraft are shown in Figures
7-2 through 7-7. Similar displacement records for Phase I are shown in
Figure 7-8. Note that the displacements obtained during Phases I and II were
of similar magnitude for similar overpressures.

Displacements of DR-2 for typical missions of XB-70, B-58, and F-104
aircraft were superimposed on the actual or net loading signatures on the
wall, Figures 7-9, 7-10, and 7-11. (Net pressure was the outside pressure
minus the inside pressure, and was the actual pressure on the wall). Note that
the pattern of displacements corresponded closely to the shape of the net
pressure signature.

The effects on structural response of the offset of the aircraft flight
track was determined from plots of displacement versus offset for XB-70
missions for BRI-I and DR-2, Figures 7-12 and 7-13. There was an indication
that response decreased with an increase in offset.

The curves in Figures 7-12 and 7-13 indicated that plate response de-
creased slightly with an increase in Mach number. The average peak plate dis-
placement of DR-2 for overhead XB-70 missions at Mach 1.8 was 0.316 inches
and for those at Mach 2.5 was 0.283 inches, which was a decrease in response
of about 10 percent. The free field cruciform microphone microphone data
indicated that the average wave angle (angle between wave front and ground)
was 43° for these XB-70 missions at Mach 1.8 and 28° for those at Mach 2.5.

The effect of aircraft vector (angle between aircraft flight track and
structure element) on plate response was studied by comparing the measured
displacements for overhead flights for DR-2 and BRI-2. The DR-2 wall was
subjected to a vector that was nearly head-on (flight track nearly perpendicu-
lar to wall surface) and the BRI-2 wall was subjected to a vector that was

7.2

nearly side-on (flight track nearly parallel to wall surface). For over-
head missions of the XB-70, B-58, and F-104, the average displacements of
DR-2 were 0.0317, 0.0318, and 0.0223 inches respectively; and of BRI-2
were 0.0152, 0.0165, 0.0115 inches respectively. Thus, the displacements
due to a side-on vector were approximately fifty percent of the displace-
ments due to a head-on vector. Similar results were also found at White
Sands.[3]

PREDICTED DISPLACEMENTS

The predicted plate displacements for the three walls in the test houses
were computed using methods explained in Appendix A and Equation A-3:

$$\Delta = \frac{P}{K} \, DAF = \Delta_{static} \, DAF \qquad (A-3)$$

where
Δ = Predicted dynamic displacement,

P = Total load on the element,

K = Element stiffness, and

DAF = Dynamic amplification factor

In the following discussion, the methods used to determine the variables, P,
K, and DAF are briefly summarized.

The first variable considered was the stiffness, K, of the wall plates.
Three methods to determine the stiffness of the walls are presented here for
the east wall of DR-2. It was assumed that the instrumented stud acted as a
simple beam and spanned between the top and bottom plates.

The first method used to calculate the stiffness of the DR wall of E-2
was an approximate approach discussed in Reference 4. The stiffness was given
as:

$$K = 76.8 \, \frac{EI}{L^3} \qquad (7-1)$$

where
I = Moment of inertia of 2 x 4 stud = 6.45 in^4,

E = Elastic modulus of wood = 1.76 x 10^6 lb/in^2, and

L = Length of stud = 7.5 ft.

Substituting these values,

$$K = 1200 \, lb/in.$$

A second approach to the calculation of the stiffness was outlined in
Reference 5, and K was computed from:

$$T = 2\pi \sqrt{\frac{mK_{1m}}{K}} \qquad (7-2)$$

which can be rewritten as:

$$K = \frac{mK_{lm}4\pi^2}{T^2} \qquad (7-3)$$

where:

T = Natural period of the first mode of vibration of the structural element and was determined to be approximately 0.05 sec. from actual tests of the wall and from the integrated accelerometer records,

m = Mass of the wall tributary to the stud = 1.23 lb-sec^2/ft. and

K_{lm} = Load-mass transformation factor which relates the simple beam (stud) to the lumped mass single degree of freedom system and is equal to 0.78.

Substituting these actual values,

K = 1250 lb/in.

Using a third approach, the total predicted displacement was obtained from Equation A-4, Appendix A, for the special case of a simply supported beam with a uniform mass and load[5]. The displacement was given by:

$$\Delta(x) = \frac{4q}{m\pi} \sum^n \frac{1}{n\omega_n^2} (DAF)_n \sin \frac{n\pi x}{L} \qquad (7-4)$$

where

n = 1, 3, 5 . . . . and indicates the various mode shapes,

x = Distance from support to point of interest,

q = Load in lb/ft on the element,

m = mass of the element, and

$$\omega_n = \frac{n^2\pi^2}{L^2} \sqrt{\frac{EI}{m}} \qquad (7-5)$$

Note that since n appears in the denominator higher modes were relatively unimportant. Taking n = 1, this equation was rewritten as:

$$\Delta(x) = \frac{4qL^4}{\pi^5 EI} (DAF) (\sin \frac{\pi x}{L}) \qquad (7-6)$$

Letting x = L/2 and noting that the total load on the element P = qL,

$$\Delta = \frac{4PL^3}{\pi^5 EI} (DAF) \qquad (7-7)$$

or

$$\Delta = \frac{P}{K} \times DAF$$

where
$$K = \frac{\pi^5 EI}{4} = 76.5 \, EI \qquad\qquad (7-8)$$

which gives the same result as previously determined.

In a similar manner the stiffnesses of BRI-1 and BRI-2 were determined. The following values of stiffness were used in the computation of the predicted displacements: BRI-1, K = 1930 lb/in; DR-2, K = 1200 lb/in; and BRI-2, K = 1200 lb/in.

It should be noted that in the computation of the stiffness as outlined by the first method, the moment of inertia, I, was taken as that of the stud only. The amount of contribution of the interior and exterior wall surfaces to the stiffness of the assembly was unknown and could only be estimated. It was reasonable to assume that there is no contribution from the loose fitting, lapped exterior siding for small displacements. If it were assumed that the gypsum board and the stud were adequately connected, and that $E_{wood} = 1.77 \times 10^6$ lb/in^2 and $E_{gypsum} = 4.42 \times 10^4$ lb/in^2 (Reference 2), then the moment of inertia of the assembly (7.18 in^4) was about ten percent higher than the value for the stud alone (6.45 in^4). The actual value of I was probably somewhere between these two values. The moment of inertia of the stud alone was used in this analysis, and the use of the higher value would not appreciably effect the results.

Once the stiffness, K, was established, it was necessary to determine P and the DAF. The total load, P, on the stud was assumed to be a uniform load acting on the entire length of the stud. For a load of 1 psf, the load on each wall was determined as:

$$P = (1.0 \text{ lb/ft}^2)(\frac{16}{12} \text{ ft}) \, (7.5 \text{ ft}) = 10 \text{ lb}.$$

The static displacement was evaluated for a 1 psf load. For BRI-1,

$$\Delta_{static} = 5.2 \times 10^{-3} \text{ in/psf}$$

and for DR-2,

$$\Delta_{static} = 8.4 \times 10^{-3} \text{ in/psf}.$$

The above two walls, BRI-1 and DR-2, were both subjected to head-on vectors whereas the BRI-2 wall was subjected to a side-on vector. Previous tests at White Sands[3] indicated that the plate displacement due to a side-on vector is approximately 50 percent of the displacement due to a head-on vector. Therefore, the predicted displacements for BRI-2 were multiplied by a factor of 0.50. The static displacement for a one psf load for BRI-2 was then

$$\Delta_{static} = 4.2 \times 10^{-3} \text{ in/psf}.$$

7.5

With the above unit values for Δ_{static}, it was possible to compute Δ_{static} for the actual boom pressure, and the predicted displacement was Δ_{static} times the appropriate DAF.

It was assumed in computing the predicted displacements that the wall studs acted as simple beams with a span equal to the distance from the bottom plate to top plate. The displacements of the supports were negligible. For example, results of studies of ground motion caused by sonic booms[31] during Phase II indicated that the maximum ground velocity caused by a sonic boom of approximately 2 psf was less than one percent of the peak velocity of the DR-2 wall. Studies of racking response data (Chapter VIII) indicated that the peak racking displacement of the roof line of E-1 was less than 10 percent of the peak displacement of the BRI-I wall. Therefore the displacement of the supports of the wall studs were not utilized in determining the predicted displacements.

The predicted displacements were computed for two different cases of loading. The first case considered was the net pressure loading, which was the outside pressure minus the inside pressure. The load P was determined from the peak net pressure and the DAF spectrum was obtained from the net pressure signature. Outside, inside, and net pressure signatures for the DR-2 wall for typical missions of XB-70, B-58 and F-104 aircraft were compared, Figures 7-14, 7-15, and 7-16. DAF spectra determined from net pressure signatures for DR-2 for typical missions are given in Figure 7-17. Note that the net pressure signatures were slightly distorted N-waves with the negative pulse being somewhat extended, and that this extension only slightly affected the DAF in the frequency range of these walls.

The second case considered was the free field pressure loading. The load P was determined from the average peak positive overpressure from the five free field cruciform microphones, and the DAF used was the average DAF obtained from the free field pressure signatures. (Envelopes of DAF curves from free field signatures have been presented in Figure 5-4.)

A third case considered was the exterior loading. For this case, the load P could be determined from the peak exterior pressures on the wall and the DAF obtained from the exterior loading signatures. DAF spectra for exterior loading for the DR-2 wall for typical missions are given in Figure 7-18. Comparison of the DAF spectra from exterior loading, Figure 7-18, with those from free field signatures, Figure 5-4, and those from net pressure loading, Figure 7-17, indicated that for the frequency range of 10-40 cps, all three

7.6

spectra were approximately equal. For this reason, it was decided that a detailed analysis of exterior loading was not warranted, so the study was concentrated on net and free field loading.

Predicted displacements based on free field and net pressure signatures were listed in Tables 7-1 through 7-4 for the east wall of BRI-1 and the east wall of DR-2. Predicted displacements based on free field pressure signatures only were listed in Table 7-5 for the north wall of BRI-2. Values in these tables were computed as previously indicated. The static displacements for a 1 psf load were multiplied by the appropriate values of overpressure and DAF to obtain the predicted displacements. For example, for XB-70 mission 13-2 (Table 7-1), the predicted displacement for BRI-1 was:

$$\Delta = (5.2 \times 10^{-3} \text{ in/psf}) \ (2.00 \text{ psf}) \ (1.79) = 0.0186 \text{ in.}$$

COMPARISON OF PREDICTED AND MEASURED DISPLACEMENTS

Predicted displacements were plotted versus measured displacements for the BRI-1, DR-2, and BRI-2 walls in Figures 7-19 through 7-25. Predicted displacements based on free field signature data versus measured displacements for comparable overhead missions of XB-70, B-58, and F-104 aircraft for the three walls were plotted in Figures 7-19, 7-22, and 7-25. Predicted displacements based on free field signature data values versus measured displacements for XB-70 missions at different offsets and Mach numbers were plotted in Figures 7-20 and 7-23 for the BRI-1 and DR-2 walls respectively. Figures 7-21 and 7-24 show predicted displacements based on net pressure signature data versus measured displacements for the BRI-1 and DR-2 walls.

It was observed from these figures that measured response or displacement compared closely with predicted response based on both free field and net pressure signature data for overhead and offset flights and for flights of different Mach number. The ratios of the predicted displacement to the measured displacement were computed and listed in Tables 7-1 through 7-5. The average of the ratios for each aircraft are also given. For the case of the predicted displacements computed from free field signature data, the over-all average ratios of predicted to measured displacement were equal to 1.03, 1.05, and 1.00 at the 95 percent confidence level for the BRI-1, DR-2, and BRI-2 walls respectively. For predicted displacements computed from net overpressure data, the average ratios of predicted to measured displacement were equal to 1.00 at the 95 percent confidence level for both the BRI-1 and DR-2 walls. These

7.7

values, summarized in Table 7-6, were based on the use of a "t-test". The degree of precision in these results and the probability that the results have this degree of precision were summarized in the table on page 5.5.

SUMMARY OF FINDINGS

This section presented the results of the analysis of the wall plate response of three typical walls in test houses E-I and E-2. The walls considered were the east wall of bedroom number one in house E-I (BRI-I), the east wall of the dining room in house E-2 (DR-2), and the north wall of bedroom number one in house E-2 (BRI-2). Predicted displacements were computed and compared with measured displacements for the three walls. Predicted displacements were computed based on peak overpressure and DAF spectra calculated from free field signatures, and on peak overpressures and DAF spectra calculated from net pressure signatures. The effects of flight track offset, Mach number and aircraft vector on plate response were investigated. In addition, the results of the Phase II tests were compared with those from previous tests. The following summary of findings resulted from these analyses:

1. Peak plate displacements of three typical walls in the two test houses were less than 0.034 inches for sonic boom overpressures of approximately 2 psf. Results from Phase I were of similar magnitude.

2. The DAF spectra curves determined from the free field, exterior and net pressure loading signatures were in significant agreement for structure element natural frequencies from 10 to 40 cps.

3. There was an indication that plate response may decrease with an increase in offset for flights of the same altitude and Mach number.

4. Plate response decreased slightly with an increase in Mach number for flights of the same altitude and offset. An increase in Mach number from 1.8 to 2.5 for overhead flights of the XB-70 caused a decrease in plate response of approximately 10 percent.

5. Peak displacements of a wall subjected to nearly side-on vectors (flight track nearly parallel to the wall surface) were fifty percent of the displacements of an equivalent wall subjected to nearly head-on vectors (flight track nearly perpendicular to the wall surface). Similar results were also found at White Sands.[3]

7.8

6. Measured displacements of three typical walls compared very well with predicted displacements based on either free field or net pressure signature data. For predicted displacements computed using free field data, the average ratios of predicted to measured displacements were equal to 1.03, 1.05, and 1.00 at the 95 percent confidence level for the BRI-1, DR-2, and BRI-2 walls respectively. For predicted displacements computed using net pressure data, the average ratios of predicted to measured displacements were equal to 1.00 at the 95 percent confidence level for both the BRI-1 and DR-2 walls. These findings applied to comparable overhead missions of XB-70, B-58, and F-104 aircraft (flights flown within a few minutes of each other), and to XB-70 missions with different offset and Mach number.

7. Plate response could be adequately predicted using peak over-pressures and DAF spectra calculated from free field signatures.

The following section, Part B, presents the results of the analysis of the window plate response data.

B. WINDOW PLATE RESPONSE IN TEST HOUSE E-1

This section presents the results of the analysis of the response of one large window in test house E-1. The window considered was installed in lieu of the large garage door in the test house. The window was larger (nominal 8'-6" by 6'-6") than that normally found in houses and somewhat thinner (0.25") than glass installed for this size of opening. The window was subjected to sonic booms on a trailing vector for all flights. Predicted displacements based on peak overpressures and DAF spectra calculated from free field signatures were computed and compared with the measured displacements.

INSTRUMENTATION

The window was instrumented with a centrally located strain gage, SG-3. In addition, microphone ML5 was placed inside the garage and ML6 outside the garage to measure the local pressure signatures. The instruments were in these locations for approximately sixty percent of the XB-70/B-58/F-104 missions. A schematic of the test set-up is shown in Figure 7-26.

TEST RESULTS - MEASURED DISPLACEMENTS

The natural frequencies, p, of the E-I window were given by:[8]

$$p = \pi^2 \sqrt{\frac{D}{M}} \left(\frac{m^2}{L^2} + \frac{n^2}{b^2} \right)$$ (7-9)

corresponding to a deflected shape

$$w = A \sin \frac{m\pi x}{L} \sin \frac{n\pi y}{b}$$ (7-10)

where

w = displacement to the surface

D = window stiffness = $\frac{Et^3}{12(1-v^2)}$ = 14,000 inch-pounds

E = modulus of elasticity = 10×10^6 pounds/square inch

t = window thickness = 0.25 inch

v = Poisson's ration = 0.24

b = dimension of the window in the vertical direction = 80.5 inches

L = dimension of window in the horizontal direction = 104.5 inches

M = mass per unit area = 3.28 pounds/square foot

n = number of half waves in the y direction

m = number of half waves in the x direction

The period, T, was

$$T = \frac{2\pi}{p}$$ (7-11)

Values of T corresponding to several mode shapes are given in Figure 7-27.

Strain displacements at the center of the window and the corresponding pressure signatures for three typical missions are shown in Figures 7-28, 7-29, and 7-30. It was evident from the strain records that the window response to the sonic booms caused by the F-104, B-58, and XB-70 was primarily in the first mode. The second symmetrical mode, which corresponded to two vertical nodal lines at the third point of the window, was also prese. (Figure 7-27). Values for the periods of the window for these two modes were found from the strain records to be 0.177 and 0.043 seconds which agreed quite closely with the calculated values of 0.170 and 0.043 seconds (assuming simply supported edges). The non-symmetrical modes corresponding to a nodal line through the center of the window could not be measured by the strain gage. If the boom overpressure were applied uniformly over the entire window, these mode shapes would not be excited. The amplitude of the

7.10

second symmetrical mode strain was never more than ± 20 percent of the first
mode strain which meant that the corresponding displacement amplitude was 2.2
percent of the first mode displacement.

The recorded strains were converted to displacements as follows:
For flexural deformation of the window, the strain in the "x" direction was

$$\epsilon_x = -z \frac{\partial^2 w}{\partial x^2} \qquad (7-12)$$

where

z = distance from the middle surface of the window in a
    direction perpendicular to the plane of the window.

If the deflected shape of the window is taken as:

$$w = A \sin \frac{\pi x}{L} \sin \frac{\pi y}{b} \qquad (7-13)$$

which corresponds to the first mode response of the window to uniformly applied
pressure, the strain at the exterior surface at the middle of the window
(x = L/2, y = b/2, z = t/2), is

$$\epsilon_x = A\frac{t}{2} \left(\frac{\pi}{L}\right)^2 \qquad (7-14)$$

Thus the peak displacement, A, was determined from the known strain values
obtained from SG-3, as

$$A = \frac{2L^2}{\pi^2 t} \epsilon_x \qquad (7-15)$$

Substituting actual values:

$$A = 8900 \ \epsilon_x \qquad (7-16)$$

Peak measured displacements for overhead and offset XB-70, B-58, and
F-104 missions (including different Mach numbers) for the E-I garage window
are summarized in Table 7-7. Note that the response due to the B-58 was
greater than the response due to either the XB-70 or F-104. This was expected,
since the DAF spectra from B-58 signatures peaked at about 5 cps (Figure 5-4)
and the frequency of the fundamental mode of vibration of this window was
approximately 5.7 cps.

PREDICTED DISPLACEMENTS

In order to compute the predicted displacements utilizing equation A-3
($\Delta = \Delta_{static} \times DAF$) and free field signature data, certain factors that could
affect a large flexible window on a trailing vector were investigated. The

relationship of DAF spectra obtained from free field signatures to DAF spectra obtained from the net (outside minus inside) pressure signatures was evaluated. The relationship of the free field overpressure signatures to the net pressure loading was examined. The investigation of the latter relationship was covered in two parts: outside overpressure versus free field overpressure; and net overpressure versus outside overpressure.

Relationship of DAF Spectra Computed from Net Overpressure and Free Field Signatures:

DAF spectra calculated from net pressure signatures on the E-I window were plotted in Figures 7-31, 7-32, and 7-33. It was observed that for the XB-70 and F-104 missions the DAF spectra curves in the range of the second mode vibration (23.2 cps) were higher than for first mode (5.9 cps). However, for the B-58 the DAF curve was higher for the first mode for one case.

Comparisons of the DAF spectra determined from free field, outside and net overpressure signatures for typical missions were made in Figures 7-34 through 7-42. From these figures, it was apparent that in general no appreciable error would be introduced by substituting the DAF spectra from free field signatures for the DAF spectra from net overpressure signatures.

Relationship Between Outside Overpressure and Free Field Overpressure:

The relationship between outside overpressure, P_o, and free field overpressure, P_f, for a trailing vector depends on many factors: altitude, offset and Mach number for a given mission; orientation and geometry of the structure, etc. A detailed analysis of these factors and the development of a deterministic model based on theoretical considerations and/or empirical relationships was beyond the scope of this study. However, theoretical approaches to this problem have been discussed by Wiggins[25] and Zumwalt[26].

Since the outside overpressure was caused by a trailing vector of the sonic boom, no reflected waves were superimposed on the original N-wave. It was reasonable to assume that the ratio P_o/P_f is always less than 1.0 for a trailing vector. A study of the overpressure signatures at test house E-I indicated that in all cases the outside overpressure measured by ML6 was less than the free field signatures.

From the observed data, it was determined that the average ratios of P_o/P_f for XB-70, B-58, and F-104 missions were 0.80, 0.80, and 0.62 respectively, with extreme values less than 17, 24, and 26 percent of the average values.

7.12

A summary of the average ratios of P_o/P_f is shown in Table 7-6. The overall average of the ratio P_o/P_f was 0.76 and distribution of the pressure ratios are presented in Figure 7-43.

Relationship Between Net Overpressure and Outside Overpressure:

The relationship between the free field overpressure and outside overpressure was determined from the experimental data in the preceding section. It was next necessary to determine the relationship between the outside overpressure and the net (outside minus inside) overpressure, so that the net pressure P_n, could be related to the free field overpressure.

Examination of the data indicated that the average ratios of P_n/P_o for XB-70, B-58, and F-104 missions were 0.51, 0.57 and 0.63 respectively, with extreme values less than 40, 25, and 16 percent of the average values. A summary of these ratios is shown in Table 7-8. The overall average ratio P_n/P_o for all missions was 0.57 and the distributions of the pressure ratios are presented in Figure 7-43.

The rise in overpressure within the structure was due to two effects: permeability, or the passage of the pressure waves through openings in the structure; and transmissibility, or increase in overpressure due to an inside volume change produced by the displacement of the structural elements enclosing the volume. In the case of the garage, it was believed, but not proven, that the permeability was not as significant as the transmissibility because the garage structure was sealed against flow of air. Pieces of carpet were placed on the bottom of the doors to reduce leakage and all doors were closed during the test missions.

It was shown in tests conducted by Andrews Associates in Oklahoma City[27] that overpressures within a structure were directly proportional to the displacements of the roof of the structure. In these tests, the inside pressure fluctuations had the same relative magnitude and frequency as the roof deflections when the roof was excited by a harmonic disturbing force.

An analysis was made based on the assumption that the overpressure within the garage could be related to the displacement of the window since the garage was relatively air-tight and since the window was much more flexible than the enclosing walls and roof. It was also assumed that pressure times volume was a constant inside the garage. The inside overpressure due to the displacement of the plate glass window was then determined to be: (Refer to Appendix H for derivation)

$$P_i = P_o \frac{P_a B}{P_a B + \frac{\pi^2 v}{4LB}} \qquad (7-17)$$

where

$$B = \frac{16L^4 (DAF)}{D\pi^6 (1 + \frac{L}{b})^2} \qquad (7-18)$$

V = enclosed volume

L = length of window

b = height of window

t = window thickness

v = Poisson's ratio

P_a = atmospheric pressure

P_i = inside overpressure

P_o = outside overpressure

DAF = Dynamic Amplification Factor

D = window stiffness = $\dfrac{Et^3}{12(1-v^2)}$

E = modulus of elasticity

Substituting actual values, $P_i = 0.20 \, P_o$. The net pressure was then $P_n = P_o - P_i = P_o - 0.20 \, P_o = 0.80 \, P_o$. This ratio was considerably higher than the ratio determined from the recorded data ($P_n/P_o = 0.57$). The difference between the calculated ratio of P_n/P_o and the experimentally determined ratio indicated that the prior assumptions were not entirely correct. An approximate analysis was then made that included the effect of the displacement of the garage walls and roof.

A ratio of P_n/P_o more nearly equal to the ratio obtained from the experimental data was obtained when the measured displacements of the E-1 window (Table 7-7) were compared with the measured displacements of BRI-1 wall (Table 7-1); it was determined that $\Delta_{wall}/ \Delta_{window} \approx 0.1$. The stiffnesses and orientation of the BRI-1 wall were then compared with those of the garage wall. The relationship was expressed as:

$$\Delta_{garage\ wall} \approx C_1 C_2 C_3 \ \Delta_{BRI-1\ wall}$$

where

C_1 = Ratio of stiffnesses = (1930/1200)

C_2 = Factor to account for fact that garage walls were subjected to a side-on or trailing vector ≈ 0.5

C_3 = Ratio of moment of inertia of stud and gypsum board as a unit to moment of inertia of stud alone ≈ 1.1.

7.14

Refer to Part A of this chapter for explanation of these values. Substituting,

$$\Delta_{\text{garage wall}} \approx 0.9 \; \Delta_{\text{BRI-I wall}} \approx 1.0 \; \Delta_{\text{BRI-I wall}}$$

From the analysis in Appendix H, it was determined that the inside pressure, P_I, was proportional to the change in volume, V', of the inside of the garage or $P_I \propto V'$. It was assumed that the volume change was in turn proportional to the peak displacement times the gross area of each element, and that the stiffness of the walls was approximately equal to the stiffness of the roof. Therefore, it was evident that

$$\frac{V_1}{V_2} = \frac{\Delta_1 \, A_1}{\Delta_1 \, A_1 + \Delta_2 \, A_2}$$

or

$$V_2 = V_1 \left(1 + \frac{\Delta_2 \, A_2}{\Delta_1 \, A_1} \right)$$

where

V_1 = Volume change due to window displacement

V_2 = Volume change due to wall and roof displacement

Δ_2 / Δ_1 = Ratio of wall to window displacement as previously described in ≈ 0.1

A_2 = Area of walls and roof ≈ 671 sq. ft.

A_1 = Area of window ≈ 58 sq. ft.

Substituting these values,

$$V_2 \approx 2.2 \; V_1$$

and

$$P_I \approx 0.2 \, (2.2) \; P_o = 0.44 \; P_o$$

or

$$P_n = P_o - P_I \approx 0.56 \; P_o$$

which was approximately equal to the value previously determined from the recorded data (0.57). It was assumed in this approximate analysis that the displacement c all the elements were in phase; that is, all of the elements deflect in, for example, at the same time.

While the previous analysis was admittedly approximate, it did illustr the fact that the inside pressure was related to the displacement of the structure elements. A detailed theoretical analysis taking into accoun the distribution of the pressure around the structure and the actual stiffnesses of the different elements should yield similar results and should

indicate an aircraft effect (different ratios of P_n/P_o for different air-craft).

One apparent contradiction to the hypothesis that the inside pressure was due primarily to the transmissibility of the structure was that an examination of the strain records and the pressure records indicated that these two curves had different characteristic shapes. However, it may be that all of the structure elements are in phase initially and produce the N-type inside pressure wave and then become out of phase. No data was available to prove or disprove this.

Relationship Between Free Field and Net Pressures:

The ratio of the net pressure to the free field overpressure based on the recorded data was determined from $P_n/P_f = (P_o/P_f)(P_n/P_o)$ and the average values were 0.42, 0.46, and 0.40 for the XB-70, B-58, and F-104 respectively. The overall average value for all aircraft, $P_n/P_f = 0.43$ was used in the computation of the predicted displacements.

Computation of Predicted Displacements:

The predicted displacements were computed from methods explained in Appendix A and Equation A-3: $\Delta = \Delta_{static}$ DAF

Assuming a uniform load, simply supported edges, and considering only the first mode, the static displacement was computed from formula[28]:

$$\Delta_{static} = \frac{16 P_n L^4}{D\pi^6 \left[1 + (\frac{L}{b})^2\right]^2} \qquad (7-19)$$

where L, D, and b are as previously defined, and Pn was the net pressure acting on the window. For a net load of 1 psf, and substituting actual values:

$$\Delta_{static} = 0.13 \text{ in/psf.}$$

Predicted displacements of overhead and offset XB-70/B-58/F-104 flights (including different Mach numbers) were listed in Table 7-7.

COMPARISON OF PREDICTED AND MEASURED DISPLACEMENTS

Predicted displacements were plotted versus measured displacements for the E-1 garage window in Figure 7-44. The ratios of predicted to measured displacements were computed and are listed in Table 7-7. It was observed from this graph and table that the measured and predicted values compare well for the E-1 window for the XB-70, B-58, and F-104 missions. By the use

of a t-test it was determined that the average ratio of the predicted to measured displacement was equal to 1.05 at the 95 percent confidence level. The degree of precision in these results and the probability that the results have this degree of precision were summarized in the table on page 5.5.

Even though it was determined earlier that the second symmetrical mode displacement was only 2.2 percent of the first mode displacement for the window, a minor error was introduced into the determination of the window displacement by neglecting the second mode response of the window since the strain is magnified nine times for equal modal displacement amplitudes. Also, it was possible for the second mode strain to be in or out of phase with the first mode causing a net addition or subtraction to the first mode strain on the oscillograph trace. Thus the relatively small second mode displacement could introduce a ± 20% error in the determination of peak strain of the window. This could be the cause of much of the scatter in the comparison of predicted and actual displacements shown in Figure 7-44. Another possible source of error in the computation of predicted displacements was the fact that the small displacement theory was used. Similar computations using large displacement theory should result in smaller predicted displacements.

SUMMARY OF FINDINGS

This section presented the results of analyses of the response of the large window in the garage of house E-1. The following findings resulted from these analyses:

1. Measured displacements compared well with predicted displacements computed from free field data when the free field overpressure data were reduced by an appropriate factor to account for transmissibility, geometry, and orientation of the structure. For the E-1 window it was determined that the average ratio of the predicted measured displacement was equal to 1.05 at the 95 percent confidence level for XB-70, B-58, and F-104 missions.

2. Large glass windows such as the one in E-1 garage respond to a sonic boom loading primarily in the fundamental mode of vibration. A minor excitation of the second symmetrical mode also occurs.

3. For the E-1 garage window, the maximum stress determined from the strain data for the missions investigated was 790 psi. The corresponding theoretical predicted stress was 980 psi.

7.17

4. Greater response of the E-I window was measured for B-58 missions than for XB-70 and F-104 missions. This was expected since the DAF spectra curves obtained from B-58 signature data peaked at about 5 cps and the frequency of the fundamental mode of vibration of this window was approximately 5.7 cps.

5. Window plate response could be adequately predicted using peak over-pressure and DAF spectra calculated from free field signatures. For windows located on the trailing vector side of the structure, the free field data must be reduced by an appropriate factor to account for orientation and geometry of the structure.

The following section, Part C, presents the results of the analysis of the Bowling Alley roof frame response data.

C. RESPONSE OF THE ROOF FRAME OF THE BOWLING ALLEY, E-3

The Bowling Alley, E-3, was located approximately two miles north of test houses E-I and E-2. The building was 144' by 75' in plan with steel frames spanning approximately 118 feet and located at 25 ft. centers. The steel deck roof was supported by purlins at 5 ft. centers. This discussion presents the results of the analysis of the response to sonic boom loading of one of the long span roof frames.

INSTRUMENTATION

Strain gages, an accelerometer, and pressure microphones were installed on the steel frame. Strain gages (SIL and S2L) were located on the bottom flange at mid-span and at one quarter-span point. An accelerometer (A5V) was mounted on the bottom flange at mid-span to measure vertical accelerations. In addition, pressure microphones (M4 and M2) were located above and below the roof deck at midspan to determine the actual or net loading on the roof struc-ture. The locations of these instruments are given in Appendix B. Free field data was not available at the Bowling Alley and the nearest instruments for measuring free field overpressures were located at the test houses.

TEST RESULTS

Peak strains in the bottom flange at midspan of the frame for several SB-70, B-58, and F-104 missions are listed in Table 7-9. The maximum stress

In the bottom flange was approximately 450 psi. Peak vertical displacements of the center of the building frame for XB-70 mission 12-2 and B-58 mission 12-1 were 0.19" and 0.11" respectively.

Overpressure records for typical XB-70, B-58, and F-104 missions are shown in Figures 7-45 through 7-50. These figures show the outside overpressure (M4), inside overpressure (M2), and net overpressure (outside minus inside). Note that the net pressure signatures were different from the typical free field signatures.

DAF spectra determined from these net overpressure signatures are shown in Figures 7-51, 7-52, and 7-53. Since the shape of the net overpressure signatures were different from those of the free field signatures, the corresponding DAF spectra were different.

In the previous sections on wall and window plate response, the measured displacements were compared with predicted displacements computed from equation A-3, Appendix A: $\Delta = (P/K) \cdot DAF$. For the case of the walls and windows, the stiffness, K, was readily determined. However, for the Bowling Alley, the quantities $P \cdot DAF$ based on free field and net overpressure data were compared. The calculated stiffnesses of the steel frame were based on numerous assumptions of connection rigidity and other factors, many of which were uncertain due to looseness of some connecting bolts, etc.

As previously mentioned, the displacements, Δ, of the center of the frame were computed from

$$\Delta = \frac{P}{K} DAF$$

where
P = Total net load on the girder

DAF = Dynamic amplification factor obtained from the net pressure signature

K = Frame stiffness

which can be rewritten
$$K = \frac{P \cdot DAF}{\Delta}$$

Since the displacement Δ was proportional to the strain ε for each aircraft,

$$\frac{P \cdot DAF}{\varepsilon} = \text{Constant} = C$$

where P was taken as the peak pressure on the roof. This should, of course, be true for all aircraft and the average values of C obtained for the XB-70, B-58, and F-104 missions should be equal. Actual and average values of C for the three aircraft are listed in Table 7-9. By the use of a t-test, it was found that the average values for all three aircraft were equal at the 95% confidence level.

7.19

The quantity C was also computed for the free field signature data, where P was the average free field peak overpressure at test house E-2 and DAF was an average value from DAF spectra for the free field signatures at E-2. These values are listed in Table 7-10. The average values of C obtained from the free field data were not equal for the three aircraft, and also were not equal to the values obtained from the net overpressure data. The ratio of C based on free field signature data to C based on net overpressure data for each aircraft were compared (which was the same as comparing P·DAF). The predicted displacements using free field signature data would have been an average of 1.26, 2.03, and 1.91 times the predicted displacements based on net overpressure data for XB-70, B-58, and F-104 missions respectively. Inherent in this conclusion was the assumption that the free field signatures at the Bowling Alley were the same as the test houses.

SUMMARY OF FINDINGS

This section presented the results of the analyses of the response of a roof frame of the Bowling Alley, E-3, to sonic boom loading. The following findings resulted from these analyses:

1. The maximum stress due to sonic boom loading in the bottom flange of the building frame at mid-span was approximately 450 psi.

2. Peak vertical displacements of the center of the building frame for XB-70 mission 12-2 and B-58 mission 12-1 were 0.19" and 0.11" respectively. Free field peak overpressures near E-2 for these missions were 2.19 psf and 2.39 psf respectively.

3. The shape of net overpressure signatures on the roof of the Bowling Alley measurably differed from those for typical free field N-waves.

4. DAF spectra determined from net overpressure signatures differed from spectra determined from typical free field N-waves.

TABLE 7-1

MEASURED RESPONSE VS PREDICTED RESPONSE

BASED ON FREE FIELD SIGNATURES

EAST WALL BR-1, E-1 (CHANNEL 202)

Aircraft	Misson	Altitude K ft	Mach	Offset K ft	Average Pressure P psf	DAF	Predicted Displacement ΔP inches	Measured Displacement ΔM inches	ΔP/ΔM	Average ΔP/ΔM
XB-70	13-2	60.2	1.8	6.4	2.00	1.79	0.0186	0.0208	0.89	0.99
	15-1	60.6	1.8	5.5	2.18	1.75	0.0198	0.0187	1.06	
	16-2	59.7	1.8	3.7	2.29	1.76	0.0210	0.0211	1.00	
	113-2	60.3	1.8	0.1	2.20	1.75	0.0200	0.0198	1.01	
XB-70	12-2	60.3	2.5	0.2	2.19	1.72	0.0194	0.0179	1.08	1.08
XB-70	7-3	60.3	2.5	71.3	1.32	1.67	0.0114	0.0094	1.22	1.22
	8-3	60.0	2.5	68.2	1.39	1.79	0.0128	0.0108	1.18	
	9-1	59.4	2.5	32.1	2.09	1.67	0.0180	0.0144	1.25	
B-58	8-1	35.5	1.65	3.3	2.39	1.65	0.0203	0.0205	0.99	1.02
	12-1	39.2	1.65	2.1	2.40	1.60	0.0200	0.0194	1.03	
	13-1	35.9	1.65	2.5	2.21	1.62	0.0187	0.0193	0.97	
	15-2	39.6	1.65	0.0	2.34	1.66	0.0201	0.0188	1.07	
	16-1	39.7	1.65	3.0	2.25	1.64	0.0192	0.0184	1.04	
	113-1	39.1	1.65	0.7	2.61	1.64	0.0221	0.0216	1.02	
F-104	12-3	22.0	1.4	6.7	2.02	1.28	0.0135	0.0127	1.06	1.09
	13-3	20.0	1.4	3.4	2.01	1.25	0.0132	0.0129	1.02	
	15-3	20.2	1.4	0.2	2.31	1.35	0.0162	0.0131	1.24	
	113-3	20.6	1.4	1.2	1.95	1.34	0.0132	0.0136	1.03	

TABLE 7-2

MEASURED RESPONSE VS PREDICTED RESPONSE
BASED ON NET PRESSURE SIGNATURES
EAST WALL BR-1, E-1 (CHANNEL 202)

Aircraft	Mission	Altitude K ft	Mach	Offset K ft	Average Pressure P psf	DAF	Predicted Displacement ΔP Inches	Measured Displacement ΔM Inches	$\frac{\Delta P}{\Delta M}$	Average $\frac{\Delta P}{\Delta M}$
XB-70	13-2	60.2	1.8	6.4	2.30	1.50	0.0179	0.0208	0.86	0.89
	15-1	60.6	1.8	9.5	2.32	1.41	0.0169	0.0187	0.91	
B-58	13-1	35.9	1.65	2.5	2.18	1.50	0.0170	0.0193	0.88	0.95
	113-1	39.1	1.65	0.7	3.06	1.31	0.0221	0.0216	1.02	
F-104	13-3	20.0	1.4	3.4	2.00	1.18	0.0123	0.0129	0.96	0.97
	15-3	20.2	1.4	0.2	2.00	1.18	0.0123	0.0131	0.94	
	113-3	20.6	1.4	1.2	2.34	1.10	0.0133	0.0132	1.00	

7.22

TABLE 7-3

MEASURED RESPONSE VS PREDICTED RESPONSE

BASED ON FREE FIELD SIGNATURES

EAST WALL DR, E-2 (CHANNEL 404)

Aircraft	Mission	Altitude K ft	Mach	Offset K ft	Average Pressure P psf	DAF	Predicted Displacement ΔP Inches	Measured Displacement ΔM Inches	ΔP/ΔM	Average ΔP/ΔM
XB-70	13-2	60.2	1.8	6.4	2.00	1.79	0.0300	0.0298	1.00	1.01
	15-1	60.6	1.8	9.5	2.18	1.76	0.0320	0.0313	1.02	
	16-2	59.7	1.8	0.7	2.29	1.79	0.0342	0.0339	1.01	
XB-70	12-2	60.5	2.5	0.2	2.19	1.75	0.0318	0.0277	1.14	1.13
	11-3	59.4	2.5	0.0	2.09	1.77	0.0306	0.0280	1.05	
	10-1	59.7	2.46	13.3	2.41	1.69	0.0340	0.0293	1.16	
XB-70	7-3	60.3	2.5	71.3	1.32	1.72	0.0169	0.0152	1.24	1.14
	8-3	60.0	2.5	68.2	1.39	1.82	0.0212	0.0192	1.10	
	9-1	59.4	2.5	32.1	2.09	1.72	0.0298	0.0272	1.09	
B-58	13-1	35.9	1.65	.5	2.21	1.67	0.0310	0.0311	1.00	1.01
	15-2	39.6	1.65	0.0	2.34	1.70	0.0332	0.0323	1.03	
	16-1	39.7	1.65	3.0	2.25	1.68	0.0316	0.0320	0.99	
F-104	13-3	20.0	1.4	3.4	2.01	1.46	0.0246	0.0215	1.15	1.14
	15-3	20.2	1.4	0.2	2.31	1.35	0.0261	0.0231	1.13	

TABLE 7-4

MEASURED RESPONSE VS PREDICTED RESPONSE

BASED ON NET PRESSURE SIGNATURES

EAST WALL CR, E-2 (CHANNEL 404)

Aircraft	Mission	Altitude K ft	Mach	Offset K ft	Average Pressure P psf	DAF	Predicted Displacement ΔP inches	Measured Displacement ΔM inches	$\frac{\Delta P}{\Delta M}$	Average $\frac{\Delta P}{\Delta M}$
XB-70	13-2	60.2	1.8	6.4	2.50	1.66	0.0346	0.0298	1.16	1.08
	15-1	60.6	1.8	9.5	2.55	1.62	0.0345	0.0313	1.10	
	16-2	59.7	1.8	0.7	2.45	1.62	0.0332	0.0339	0.98	
B-58	13-1	35.9	1.65	2.5	2.50	1.55	0.0324	0.0311	1.04	1.09
	15-2	39.6	1.65	0.0	2.71	1.72	0.0390	0.0323	1.21	
	16-1	39.7	1.65	3.0	2.82	1.49	0.0351	0.0320	1.10	
F-104	13-3	20.0	1.4	3.4	2.35	1.40	0.0275	0.0215	1.28	1.26
	15-3	20.2	1.4	0.2	2.30	1.46	0.0282	0.0231	1.22	
	16-3	20.6	1.4	5.0	2.32	1.50	0.0290	0.0228	1.27	

TABLE 7-5

MEASURED RESPONSE VS PREDICTED RESPONSE

BASED ON FREE FIELD SIGNATURES

NORTH WALL BR-1, E-2 (CHANNEL 406)

Aircraft	Mission	Altitude K ft	Mach	Offset K ft	Average Pressure P psf	DAF	Predicted Displacement ΔP inches	Measured Displacement ΔM inches	$\frac{\Delta P}{\Delta M}$	Average $\frac{\Delta P}{\Delta M}$
XB-70	13-2	60.2	1.8	6.4	2.00	1.79	0.00150	0.0142	1.06	1.07
	15-1	60.6	1.8	9.5	2.18	1.78	0.00164	0.0152	1.08	
	16-2	59.7	1.8	0.7	2.29	1.79	0.00172	0.0161	1.06	
B-58	13-1	35.9	1.65	2.5	2.21	1.70	0.00158	0.0122	1.30	1.02
	15-2	39.6	1.65	0.0	2.34	1.72	0.00169	0.0195	0.86	
	16-1	39.7	1.65	3.0	2.25	1.71	0.00160	0.0178	0.90	
F-104	13-3	20.0	1.4	3.4	2.01	1.77	0.00148	0.0118	1.25	1.25
	15-3	20.2	1.4	0.2	2.31	1.44	0.00140	0.0111	1.26	

7.25

TABLE 7-6

MEASURED RESPONSE AND PREDICTED RESPONSE

TRUE VALUES OF THE RATIO OF PREDICTED

TO MEASURED DISPLACEMENT AT 95% CONFIDENCE LEVEL

Wall	House	Pressure Signature	$\dfrac{\text{Predicted Displacement}}{\text{Measured Displacement}}$
BR-1	E-1	Free Field	1.03
DR	E-2	Free Field	1.05
BR-1	E-2	Free Field	1.00
BR-1	E-1	Net	1.00
DR	E-2	Net	1.00

TABLE 7-7
MEASURED RESPONSE VS PREDICTED RESPONSE
BASED ON FREE FIELD SIGNATURES
E-i GARAGE WINDOW

Aircraft	Mission	Average Pressure P_f	DAF	Predicted Displacement ΔP	Measured Displacement ΔM	$\dfrac{\Delta P}{\Delta M}$
		psf		inches	inches	
XB-70	4-2	2.64	1.30	0.198	0.152	1.30
	5-2	1.20	1.42	0.098	0.058	1.69
	8-3	1.38	1.42	0.112	0.065	1.72
	11-3	2.09	1.45	0.174	0.107	1.63
	12-2	2.19	1.40	0.i77	0.157	1.13
	16-2	2.30	1.50	0.198	0.153	1.29
	113-2	2.20	1.54	0.196	0.218	0.90
B-58	3-1	2.52	1.72	0.250	0.194	1.29
	4-1	2.11	2.02	0.246	0.246	1.00
	5-1	0.68	1.95	0.077	0.068	1.13
	8-1	2.40	1.85	0.254	0.290	0.87
	!1-2	1.86	1.92	0.206	0.204	1.02
	12-1	2.63	1.65	0.250	0.253	0.99
	16-1	2.60	1.90	0.285	0.244	1.17
	113-1	2.49	1.70	0.243	0.250	0.97
F-104	3-4	2.36	0.88	0.120	0.182	0.66
	12-3	2.02	0.91	0.105	0.094	1.i2
	113-3	1.95	1.00	0.131	0.112	1.17

TABLE 7-8

PEAK PRESSURE RELATIONSHIPS FOR E-1 WINDOW

Mission	P_f psf	P_o psf	P_n psf	$\dfrac{P_o}{P_f}$	$\dfrac{P_n}{P_o}$	$\dfrac{P_n}{P_f}$
			F-104			
3-4	2.36	1.56	0.90	.66	.58	.38
11-1	2.01	1.56	1.14	.78	.73	.57
12-3	2.02	1.02	0.60	.50	.59	.30
14-3	1.95	1.10	0.75	.56	.68	.38
16-3	2.05	1.00	0.57	.49	.57	.28
113-3	1.95	1.44	0.90	.74	.63	.46
Average				.62	.63	.40
			B-58			
3-1	2.52	1.68	0.78	.67	.47	.31
4-1	2.11	2.04	1.20	.99	.59	.57
5-1	0.68	0.60	0.50	.88	.90	.44
6-1	1.30	1.28	0.68	.99	.53	.52
8-1	2.40	2.10	1.48	.88	.71	.62
11-2	1.86	1.68	0.96	.91	.57	.52
12-1	2.49	1.68	1.14	.68	.68	.46
14-2	2.63	1.87	0.98	.71	.53	.37
16-1	2.30	1.40	0.90	.61	.64	.39
113-1	2.61	1.89	0.96	.73	.51	.37
Average				.80	.57	.46
			XB-70			
4-2	2.64	2.64	1.04	.77	.51	.39
5-2	1.20	1.20	0.30	.80	.31	.25
6-2	1.85	1.85	0.90	.76	.64	.49
8-3	1.38	1.38	0.35	.73	.35	.25
11-3	2.09	2.09	1.08	.93	.57	.52
12-2	2.19	2.19	1.11	.80	.60	.51
14-1	2.20	2.20	1.00	.77	.59	.46
16-2	2.30	2.30	0.99	.76	.56	.44
113-2	2.20	2.20	1.00	.87	.52	.45
Average				.80	.51	.42
Average for All Missions				.76	.57	.43

TABLE 7-9

BOWLING ALLEY

NET PRESSURE RESPONSE DATA

Aircraft	Mission	Strain ϵ	Net Pressure P	Net DAF	$C = \dfrac{P \cdot DAF}{\epsilon}$	C_{ave}
		μ in/in	psf			
XB-70	2-1	4.9	0.69	1.30	0.183	0.189
	9-1	12.2	1.63	1.60	0.214	
	12-2	14.9	1.99	1.48	0.198	
	13-2	12.2	2.06	1.07	0.182	
	113-2	13.9	2.25	1.04	0.168	
B-58	2-3	12.2	2.52	0.72	0.149	0.174
	9-2	9.8	1.67	0.90	0.153	
	12-1	10.6	2.05	0.98	0.190	
	13-1	12.2	1.62	1.50	0.199	
	113-1	10.6	1.69	1.12	0.179	
F-104	2-4	4.9	1.06	0.95	0.205	0.210
	9-3	4.9	0.96	1.05	0.206	
	12-3	5.3	1.99	0.61	0.229	
	13-3	6.1	1.71	0.82	0.229	
	113-3	4.0	1.28	0.56	0.179	

7.29

TABLE 7-10

BOWLING ALLEY

FREE FIELD RESPONSE DATA

Aircraft	Mission	Strain ε	Free Field Pressure @ E-2 P	Free Field DAF	$C=\dfrac{P \cdot DAF}{\varepsilon}$	C_{ave}
		μ in/in	psf			
XB-70	9-1	12.2	2.09	1.37	0.232	0.238
	12-2	14.9	2.19	1.47	0.216	
	13-2	12.2	2.00	1.55	0.255	
	113-2	13.9	2.20	1.57	0.247	
B-58	9-2	9.8	2.71	1.42	0.391	0.354
	12-1	10.6	2.39	1.51	0.340	
	13-1	12.2	2.21	1.65	0.300	
	113-1	10.6	2.61	1.56	0.383	
F-104	9-3	4.9	1.54	1.22	0.384	0.401
	12-3	5.3	2.10	1.02	0.404	
	13-3	6.1	2.01	1.01	0.335	
	113-3	4.0	1.95	0.91	0.485	

ACCELEROMETER MID-HEIGHT CTR. STUD, CHANNEL 206

ACCELEROMETER MID-HEIGHT CTR. STUD, CHANNEL 806

ACCELEROMETER A-11 MID-HT. CNTR. STUD CHANNEL 404

PRESSURE MICROPHONE ML-17 CNTR. WALL CHANNEL 807

PRESSURE MICROPHONE ML-4 CNTR. ROOM CHANNEL 410

PRESSURE MICROPHONE ML-12 OPPOSITE A-11 CHANNEL 812

PRESSURE MICROPHONE ML-2, 6'-2" ABOVE FLR. CHANNEL 402

BR1

DR.

E-2

ACCELEROMETER A-11 MID-HEIGHT CNTR. STUD CHANNEL 202

PRESSURE MICROPHONE ML-3 NEXT TO A-11 CHANNEL 204

PRESSURE MICROPHONE ML-2 MID-HT. WALL CHANNEL 804

BR1

E-1

PARTIAL PLANS
NO SCALE

INSTRUMENT LOCATIONS
PLATE RESPONSE BR1-E-1, DR-E-2 & BR1-E-2
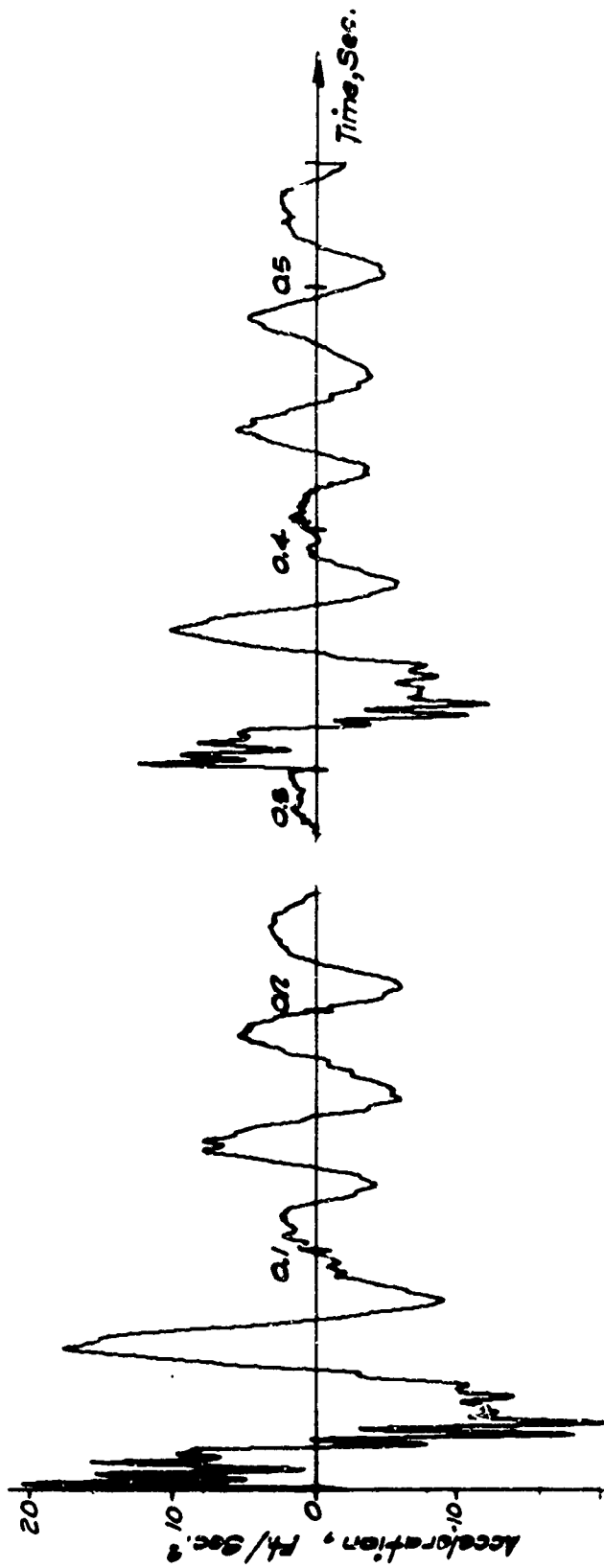
FIG. 7-1

FIG. 7-1

7.31

PLATE ACCELERATION
EAST WALL DINING ROOM E-2
(CHANNEL 404)

XB-70 Msn. 16-2
Average free field positive overpressure
= 2.29 p.s.f.

FIG.
7-2

B-58 Msn. 16-1

Average free-field positive overpressure = 2.25 psi-f.
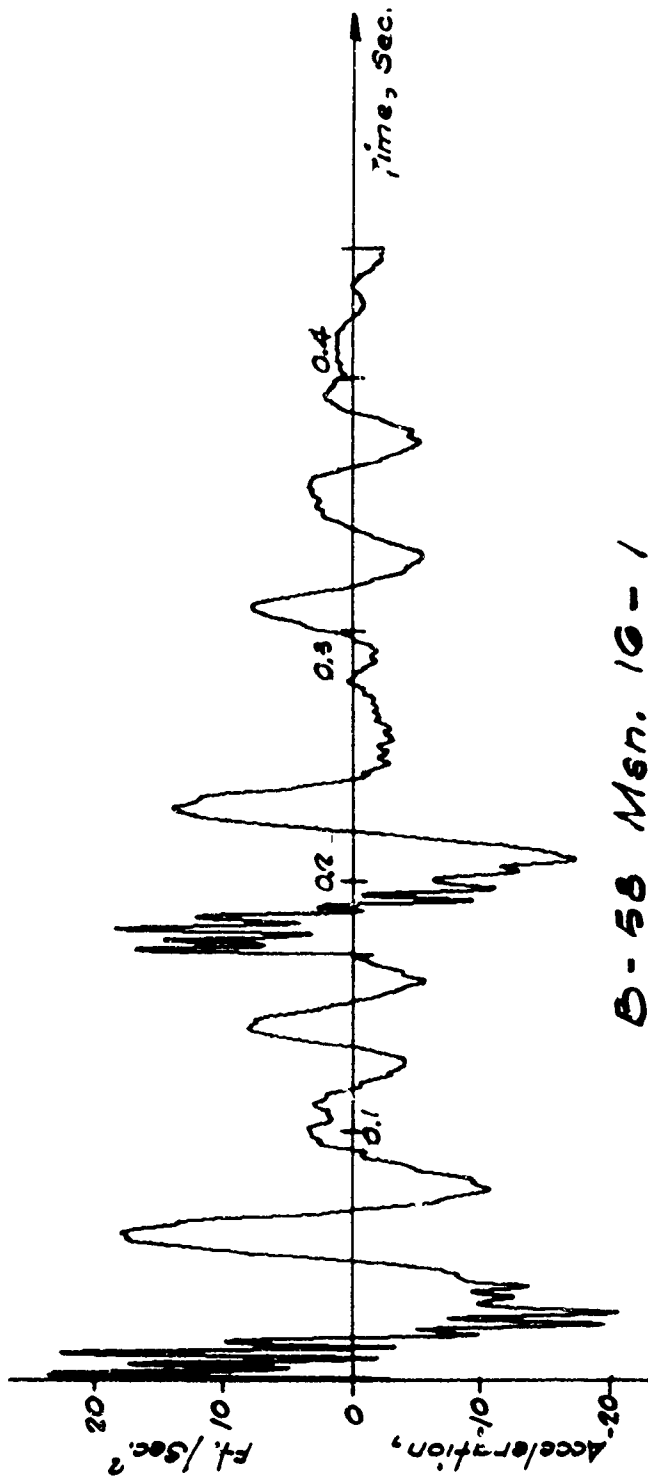
PLATE ACCELERATION
EAST WALL DINING ROOM E-2
(CHANNEL 404)

FIG. 7-3

FIG 7-3

7.33

PLATE ACCELERATION
EAST WALL DINING ROOM E-2
(CHANNEL 404)

F-104 Msn. IG-3
Average free field positive overpressure = 2.02 p.s.f.

FIG 7-4

FIG. 7-4

7.34

XB-70 Msn. 16-2
Average free field positive overpressure
= 2.24 p.s.f.

PLATE DISPLACEMENT
EAST WALL DINING ROOM E-2
(CHANNEL 404)

FIG.
7-5

FIG.
7-5

PLATE DISPLACEMENT
EAST WALL DINING ROOM E-2
(CHANNEL 404)

B-58   Msn. 16-1
Average free field positive overpressure
= 2.25 p.s.i.

FIG.
7-6

FIG.
7-6

F-104 Man. 16 - 5
Average free field positive over pressure = 2.02 p.s.f.

PLATE DISPLACEMENT
EAST WALL DINING ROOM E-2
(CHANNEL 464)

FIG.
7-7

FIG.
7-7

7.37

PLATE DISPLACEMENTS

PHASE I FLIGHTS

MSN	A/C	ALT	MACH	FREE FIELD PRESSURE, psf
14	F-104	35.6K	1.70	1.19
13	XB-70	52.9K	1.81	2.52
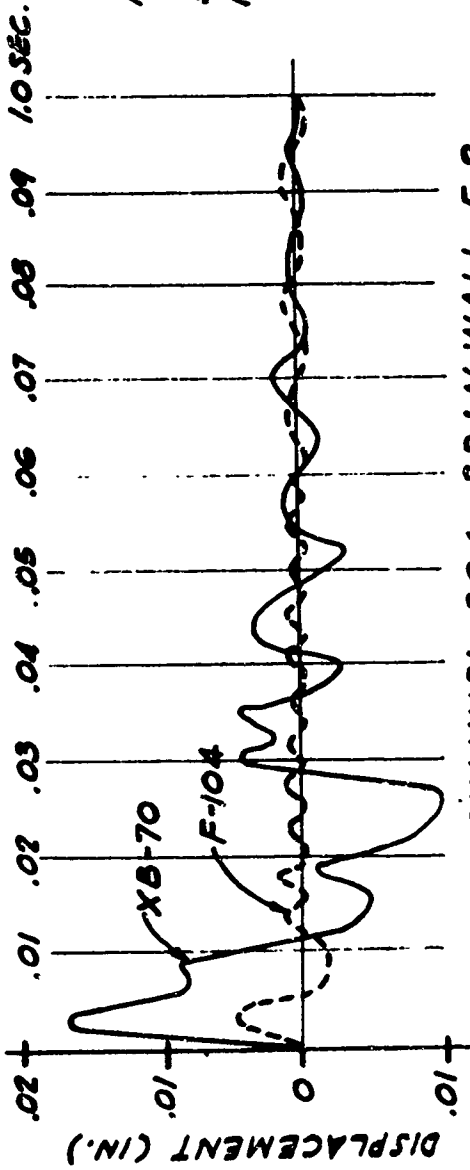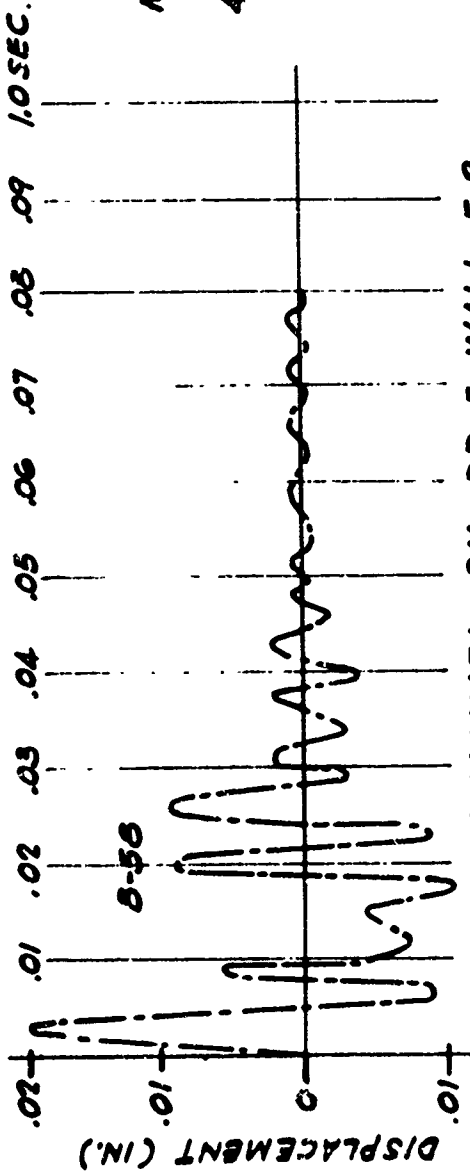
CHANNEL 304 - BR. IN. WALL, E-2

PHASE I FLIGHTS

MSN	A/C	ALT	MACH	FREE FIELD PRESSURE, psf
46B	B-58	43.7K	1.65	1.65
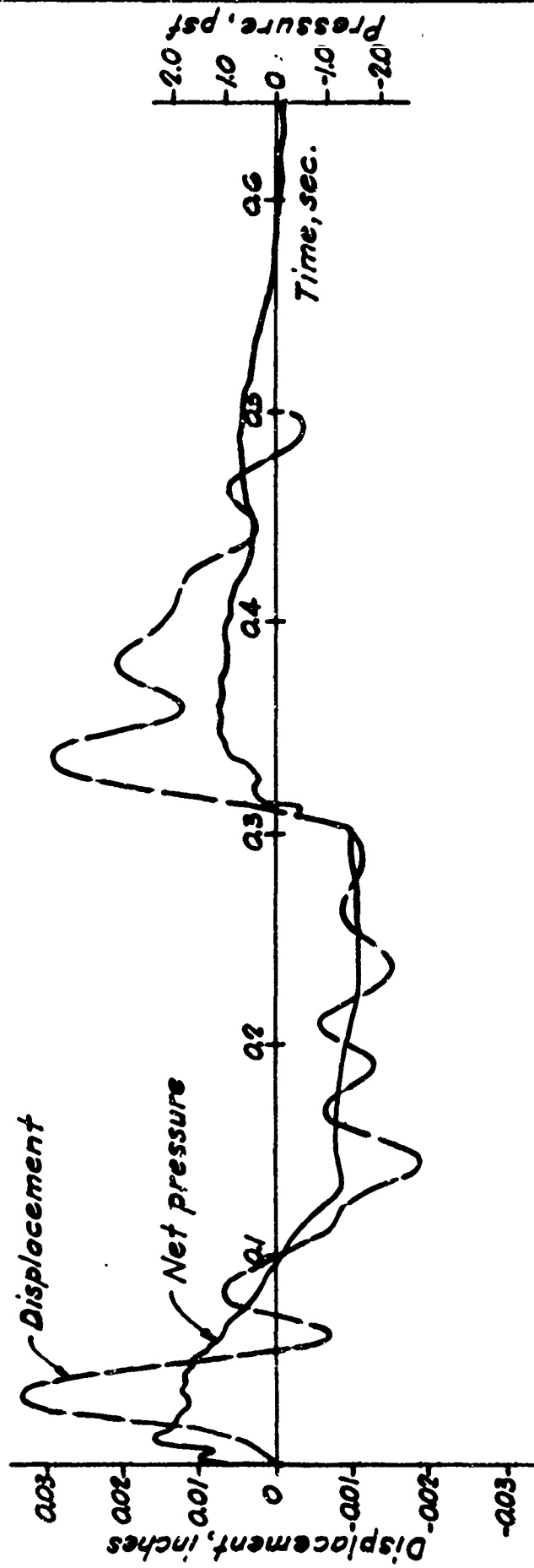
CHANNEL 311 - DR. E. WALL, E-2

FIG. 7-8

7.38

PLATE DISPLACEMENT AND PRESSURE SIGNATURE
EAST WALL DINING ROOM E-2

XB-70 Msn 16-2

FIG.
7-9

7.39

PLATE DISPLACEMENT AND PRESSURE SIGNATURE
EAST WALL DINING ROOM E-2

B-58 Msn. 16-1

FIG. 7-10

FIG. 7-10

7.40

PLATE DISPLACEMENT AND PRESSURE SIGNATURE
EAST WALL DINING ROOM E-2
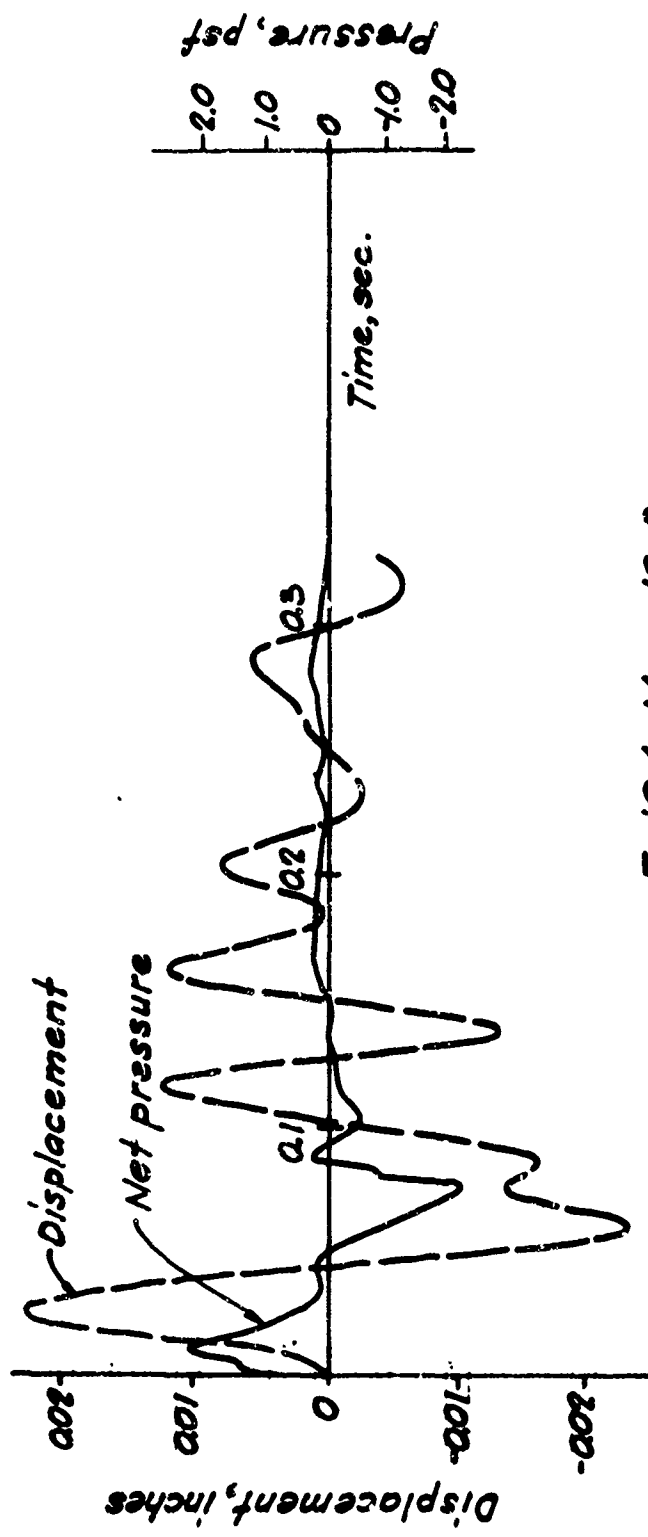
F-104 Msn. 16-3

FIG.
7-11
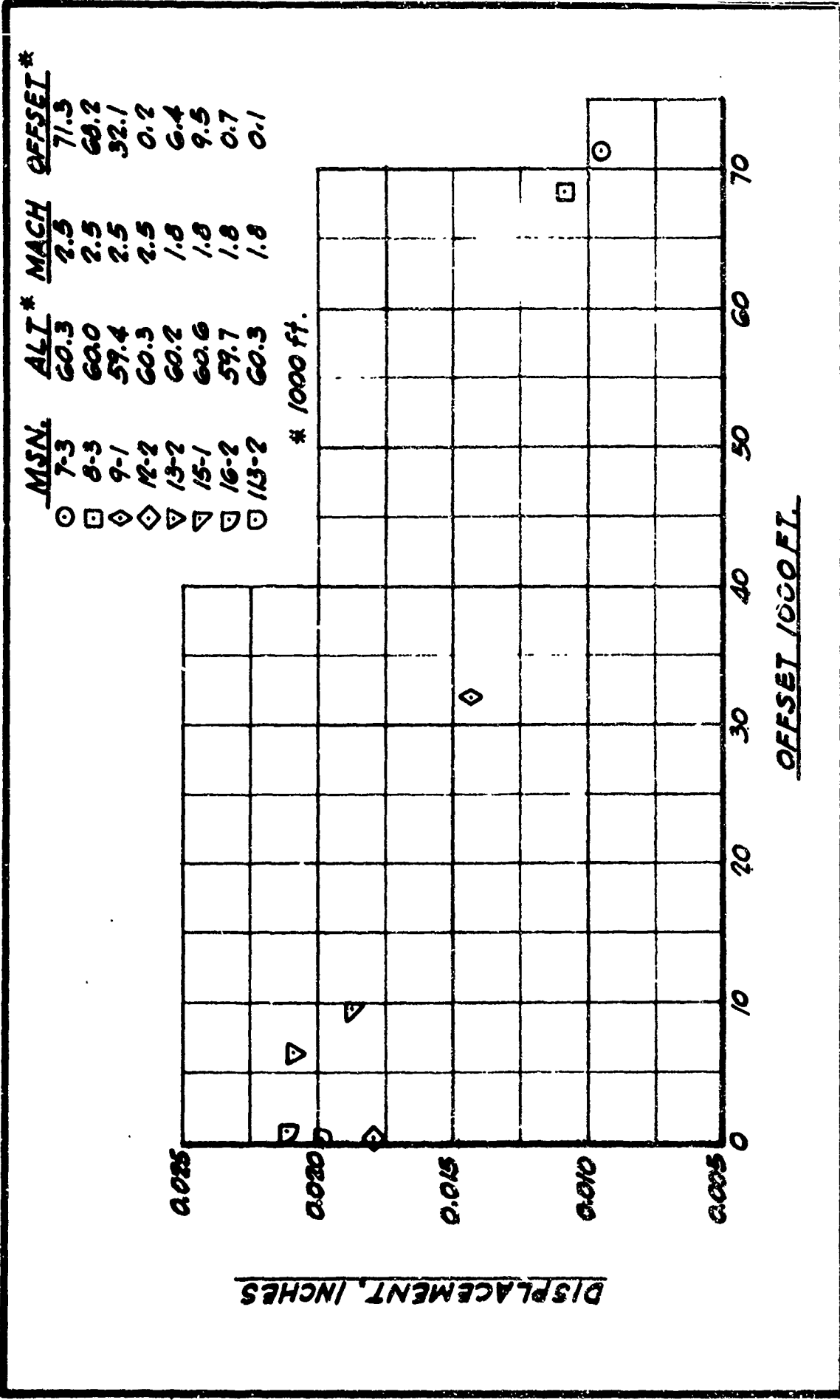
FIG.
7-11

FIG.
7-12

MSN	ALT*	MACH	OFFSET*
⊙ 7-3	60.3	2.5	71.3
⊡ 8-3	60.0	2.5	60.2
◇ 9-1	59.4	2.5	32.1
◇ 12-2	60.3	2.5	0.2
▽ 13-2	60.2	1.8	6.4
▽ 15-1	60.6	1.8	9.5
▽ 16-2	59.7	1.8	0.7
⊡ 13-2	60.3	1.8	0.1

* 1000 ft.

OFFSET 1000 FT.

DISPLACEMENT, INCHES

RESPONSE vs. OFFSET
XB-70 - BR'L. HOUSE E-1

FIG.
7-12

7.42

RESPONSE vs. OFFSET
XB-70 ~ DR, HOUSE E-2

OFFSET 1000 FT

DISPLACEMENT INCHES

MSN.	ALT.*	MACH	OFFSET*
⊙ 7-3	60.3	2.5	71.3
☐ 8-3	60.0	2.5	68.2
◇ 9-1	59.4	2.5	32.1
▷ 10-1	59.7	2.46	13.3
▽ 11-3	59.4	2.5	0
▽ 12-2	60.3	2.5	0.2
▷ 13-2	60.2	1.8	6.4
◇ 15-1	60.6	1.8	9.5
◇ 16-2	59.7	1.8	0.7

* 1000 ft

FIG.
7-13

PRESSURE SIGNATURES
E. WALL DINING ROOM, E-2

XB-70 Msn. 16-2

FIG.
7-14

7.44
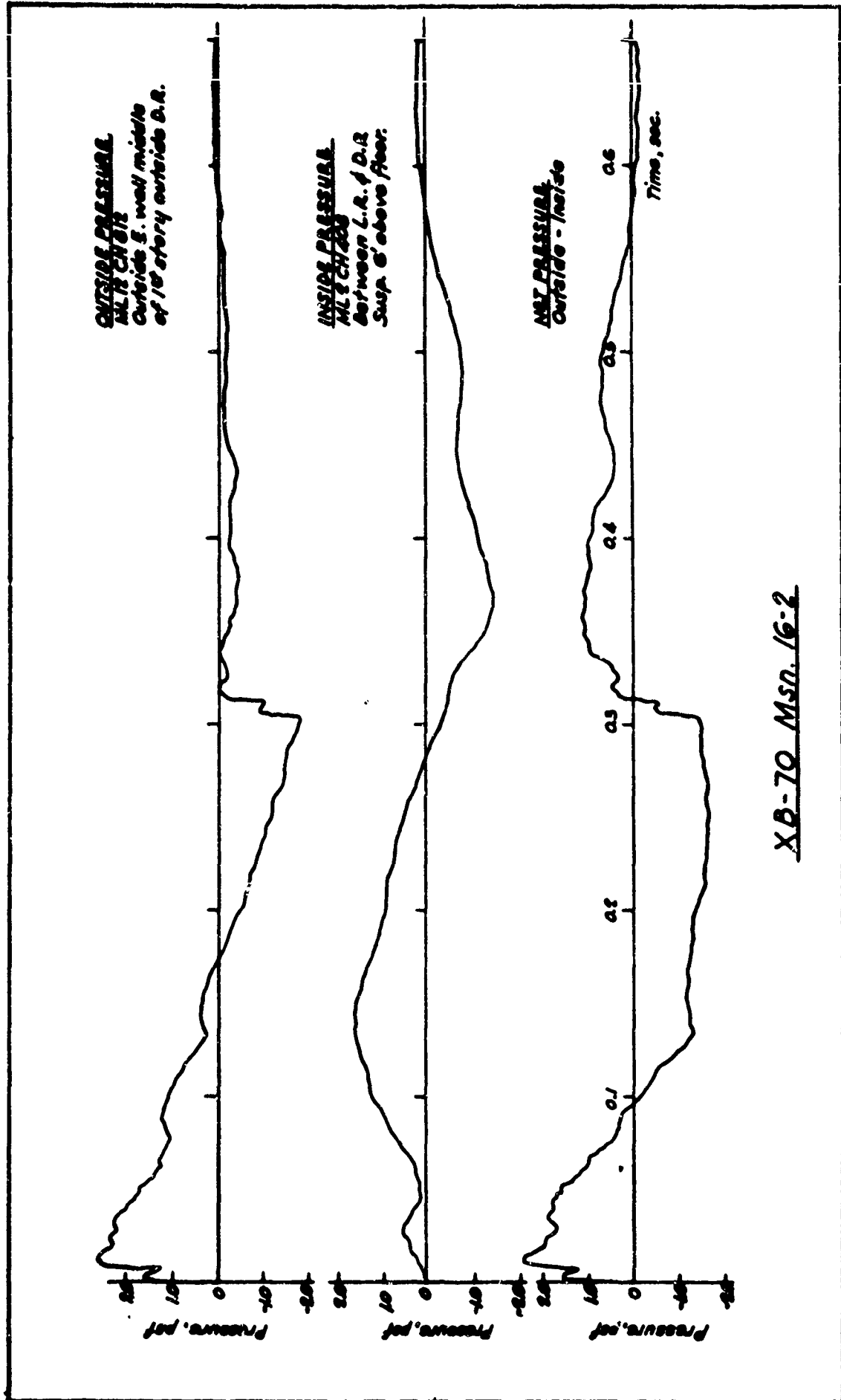
OUTSIDE PRESSURE
ML12 CH 812
Outside E. wall middle
of 1st story outside D.R.
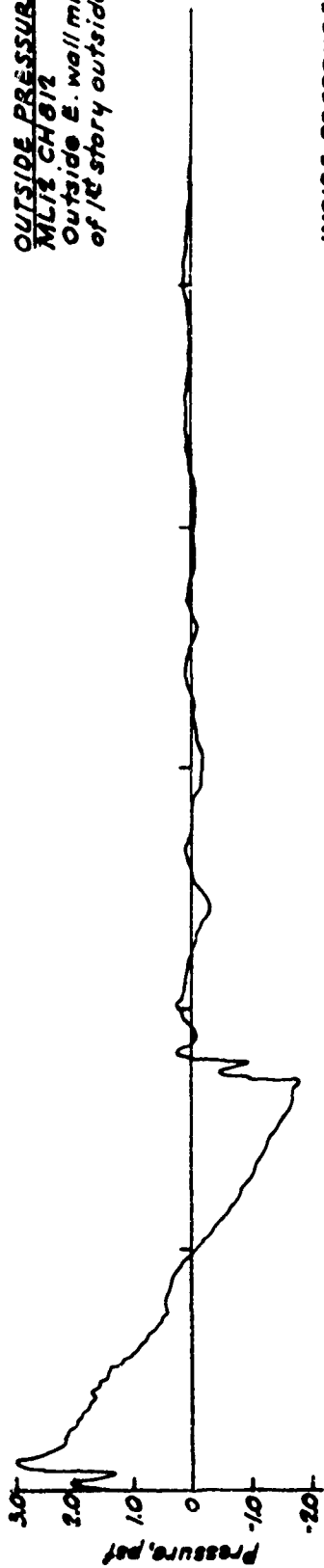
INSIDE PRESSURE
ML2 CH 408
Between L.R. / D.R.
Susp. G above floor.
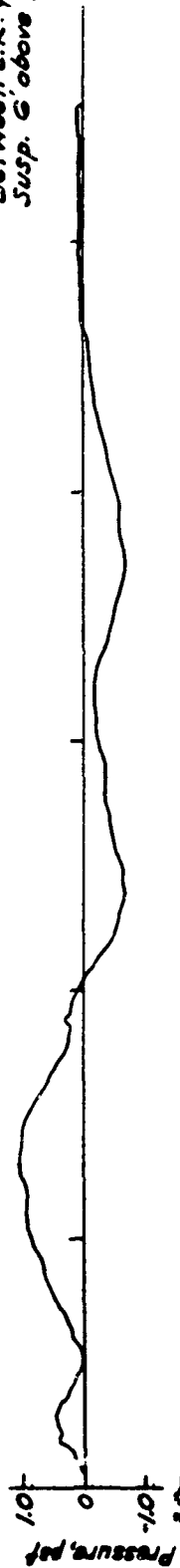
NET PRESSURE
Outside - Inside
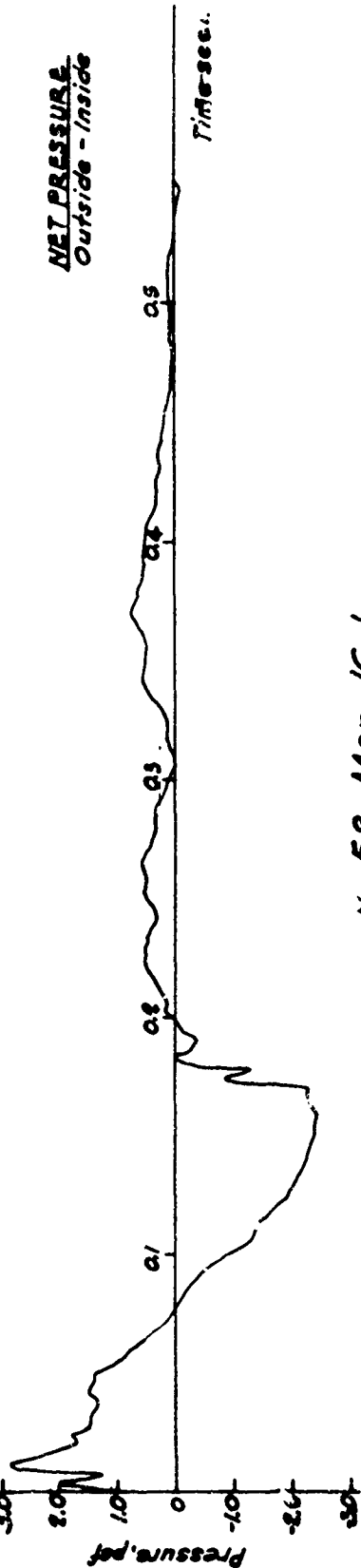
B-58 Msn. 16-1

PRESSURE SIGNATURES
E. WALL DINING ROOM, E-2

FIG.
7-15

7.45

OUTSIDE PRESSURE
MLR CH 512
outside E. wall middle
of 1st story outside D.R.

INSIDE PRESSURE
MLR CH 508
between L.R. & D.R.
Susp. 6' above floor.

NET PRESSURE
Outside - Inside

E-104 Msn. 16-3

PRESSURE SIGNATURES
E. WALL DINING ROOM, E-2

FIG
7-16

FIG.
7-16

Net Pressure = Outside pressure − Inside pressure
Outside pressure from channel 812, microphone on exterior
East wall, Dining Room
Inside pressure from channel 408, microphone between Living
Room and Dining Room, suspended 6' above floor.
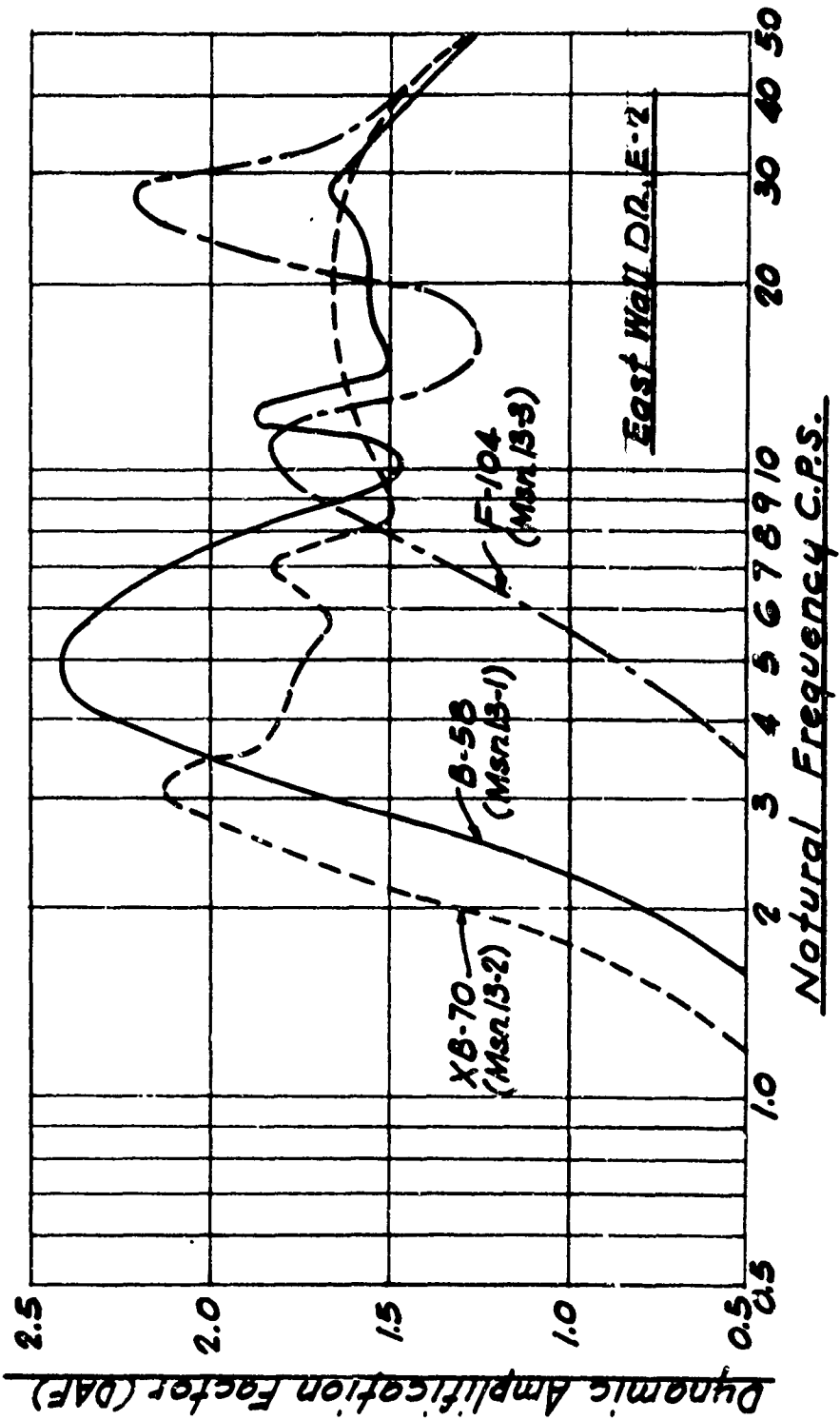
RESPONSE OF 2% DAMPED SYSTEMS TO NET LOADING, HOUSE E-2
EAST WALL DR.

East Wall DR, E-2

E-104 (Msn.13-8)

B-58 (Msn.13-1)

XB-70 (Msn.13-2)

Natural Frequency C.P.S.

Dynamic Amplification Factor (DAF)
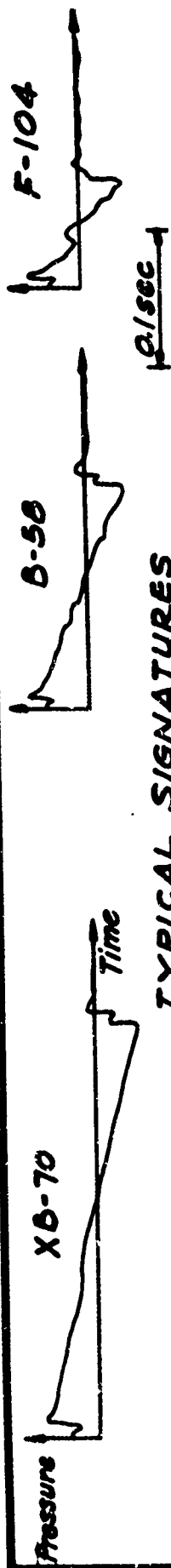
FIG. 7-17

TYPICAL SIGNATURES
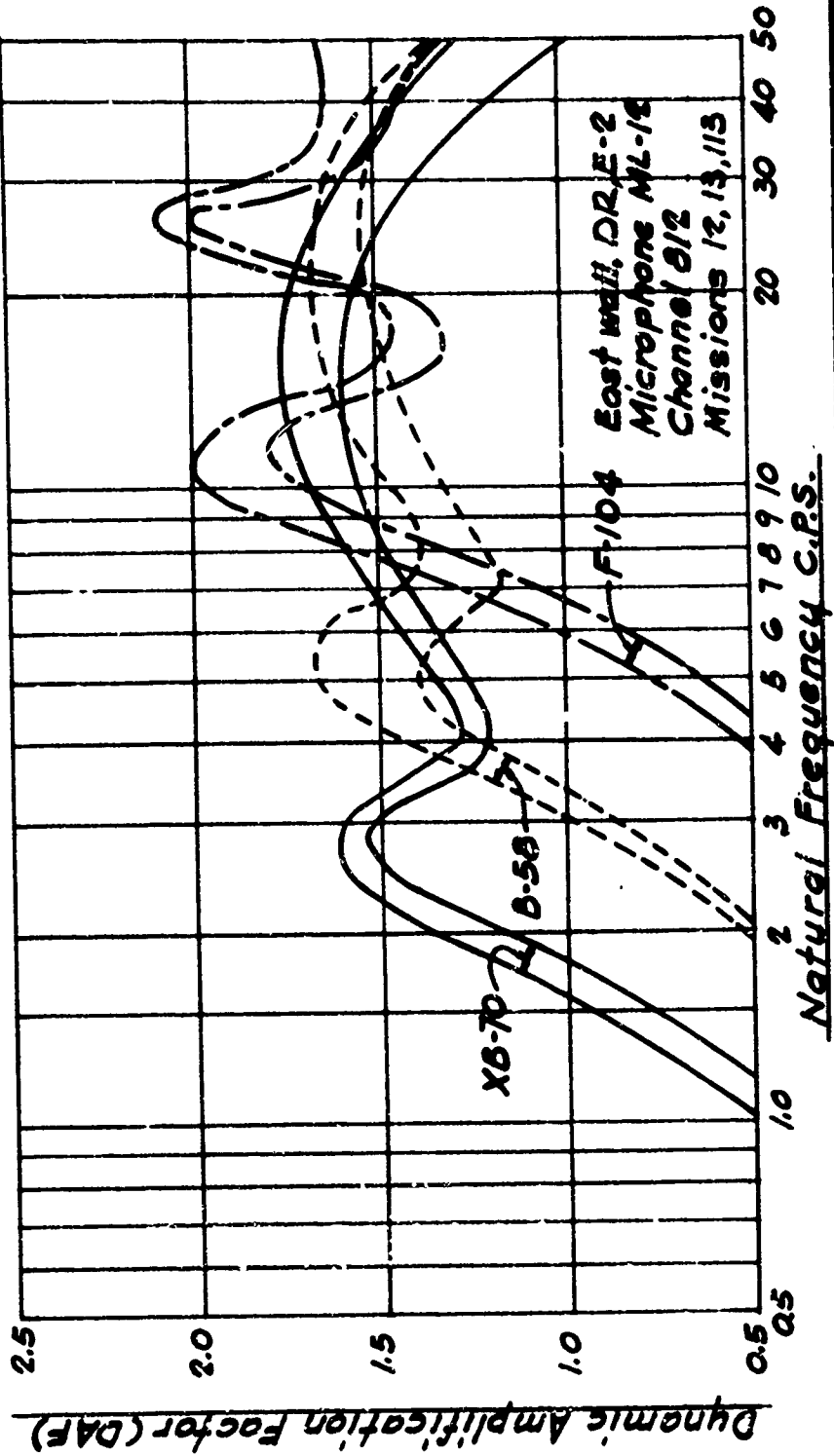
ENVELOPES OF RESPONSE OF 2% DAMPED   EAST WALL
SYSTEMS TO EXTERIOR WALL LOADING   DR. E-2

FIG.
7-18

7.48

AIRCRAFT SYMBOL

AIRCRAFT	SYMBOL
XB-70	⊙
B-58	▽
F-104	☐

(All overhead missions)

MEASURED RESPONSE vs. PREDICTED RESPONSE
BASED ON FREE FIELD SIGNATURES   EAST WALL BRI, HOUSE E-1

FIG. 7-19

XB-70 ONLY

NOMINAL VALUES

SYMBOL	ALT*	MACH	OFFSET*
◇	60	2.5	70
▣	60	2.5	0
◉	60	1.8	0

* 1000 ft.

MEASURED RESPONSE vs. PREDICTED RESPONSE
BASED ON FREE FIELD SIGNATURES, EAST WALL BR1, HOUSE E-1

PREDICTED RESPONSE DISPLACEMENT, INCHES

MEASURED RESPONSE DISPLACEMENT, INCHES

FIG. 7-20

7.50

MEASURED RESPONSE vs. PREDICTED RESPONSE
EAST WALL BRI, HOUSE E-1
BASED ON NET SIGNATURES

FIG.
7-21

7.51

MEASURED RESPONSE vs. PREDICTED RESPONSE BASED ON FREE FIELD SIGNATURES, EAST WALL DR, HOUSE E-2

FIG. 7-22

7.52

XB-70 ONLY

NOMINAL VALUES

SYMBOL	ALT.*	MACH	OFFSET
◇	60	2.5	70
◇	60	2.5	32
□	60	2.5	0
⊙	60	1.8	0

* 1000 ft.

MEASURED RESPONSE, DISPLACEMENT, INCHES

PREDICTED RESPONSE, DISPLACEMENT, INCHES

MEASURED RESPONSE vs. PREDICTED RESPONSE
BASED ON FREE FIELD SIGNATURES, EAST WALL DR., HOUSE E-2.

FIG. 7-23

7.53

AIRCRAFT SYMBOL

XB-70 ⊙
B-58 ▽
F-104 ▣
(All overhead missions)

MEASURED RESPONSE, DISPLACEMENT, INCHES

DISPLACEMENT, INCHES
PREDICTED RESPONSE

MEASURED RESPONSE vs. PREDICTED RESPONSE
BASED ON NET SIGNATURES, EAST WALL DR., HOUSE E-2

FIG. 7-24
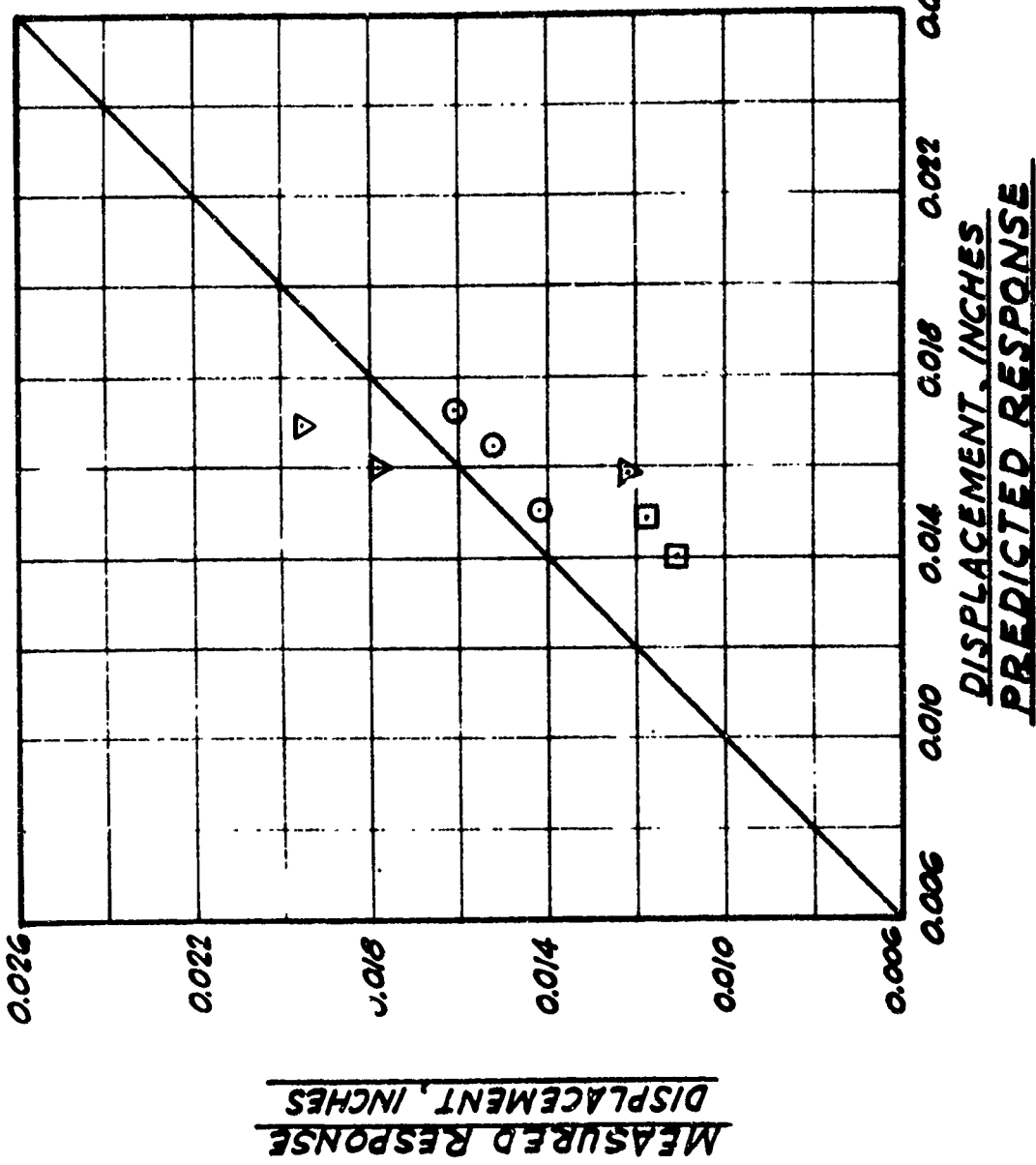
FIG. 7-24

7.54

MEASURED RESPONSE vs. PREDICTED RESPONSE
BASED ON FREE FIELD SIGNATURES, NORTH WALL BR1, HOUSE E:2

FIG. 7-25

INSTRUMENT LOCATION
GARAGE WINDOW - HOUSE E-1
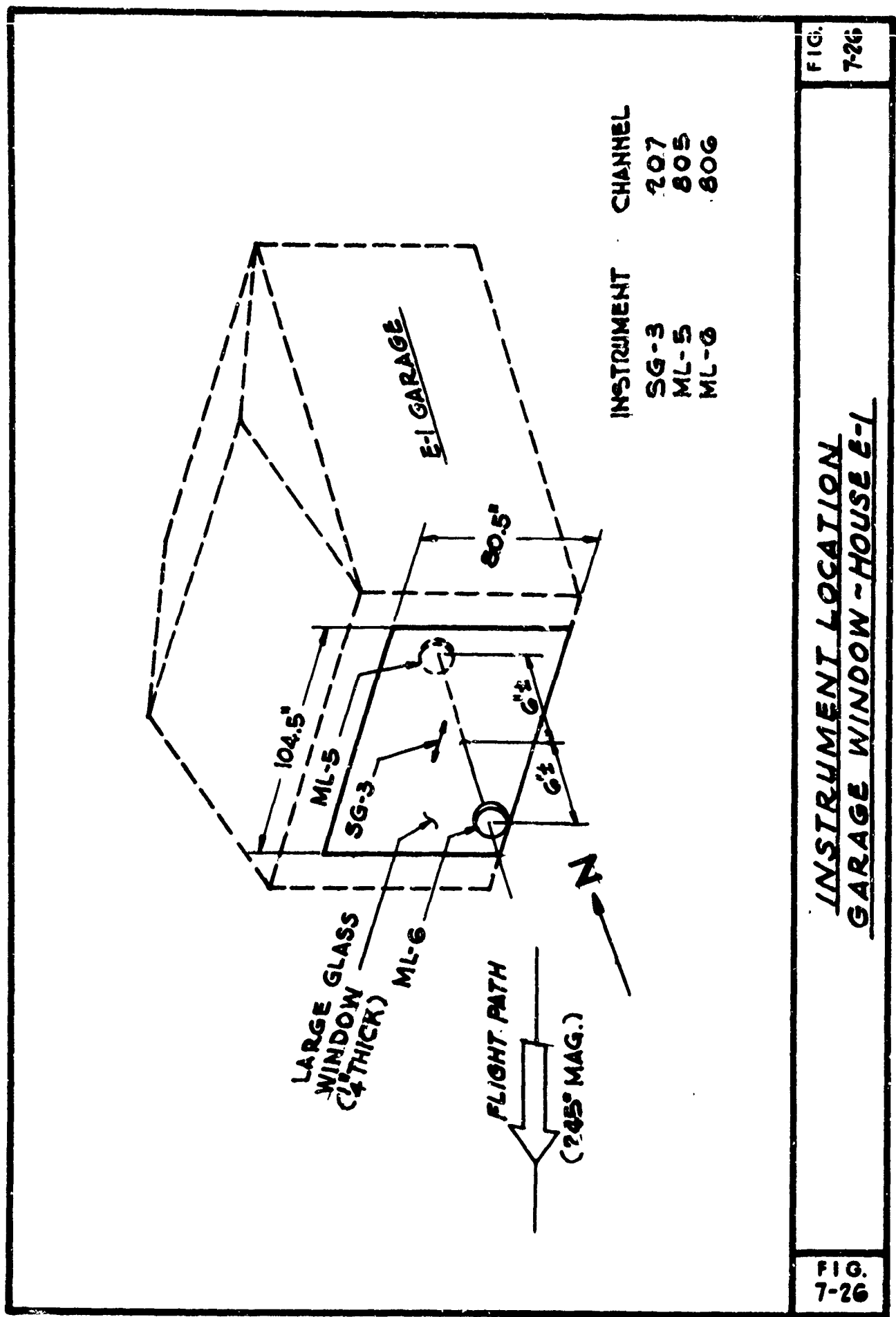
INSTRUMENT	CHANNEL
SG-3	207
ML-5	805
ML-6	806

E-1 GARAGE

80.5"

104.5"

ML-5

SG-3

6"

6"

LARGE GLASS
WINDOW
(¼" THICK)   ML-6

N

FLIGHT PATH

(245° MAG.)

FIG.
7-26

FIG.
7-26

7.56

SYMMETRICAL MODES   NON-SYMMETRICAL MODES

n=1
m=1
T= 0.170 sec.

Nodal Line
n=1
m=2
T= 0.124 sec.

Nodal Lines
n=1
m=3
T= 0.043 sec.

Nodal Line
n=2
m=1
T= .104 sec.
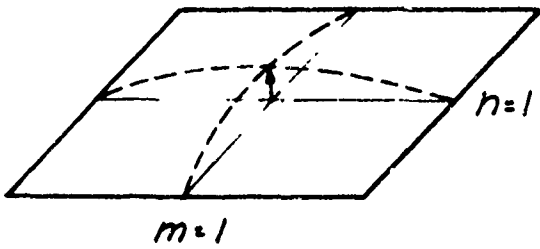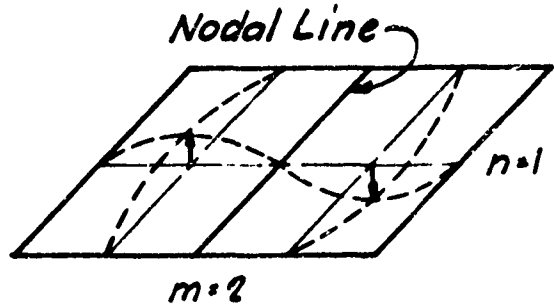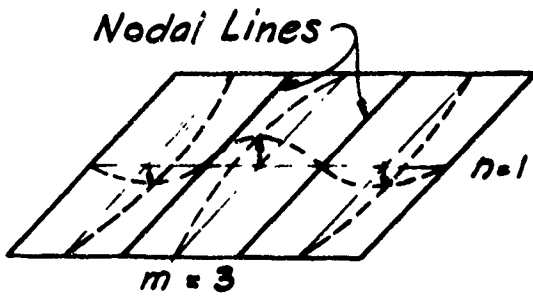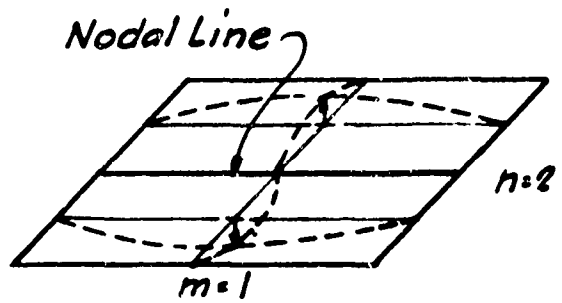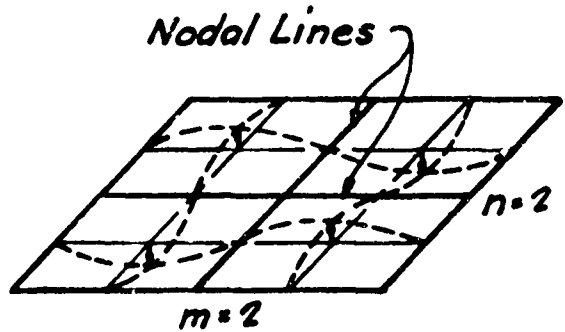
Nodal Lines
n=2
m=2
T= .085 sec.

NATURAL PERIODS AND CORRESPONDING
MODE SHAPES FOR E-1 WINDOW

FIG.
7-27

XB-70 MSN. 1i-3
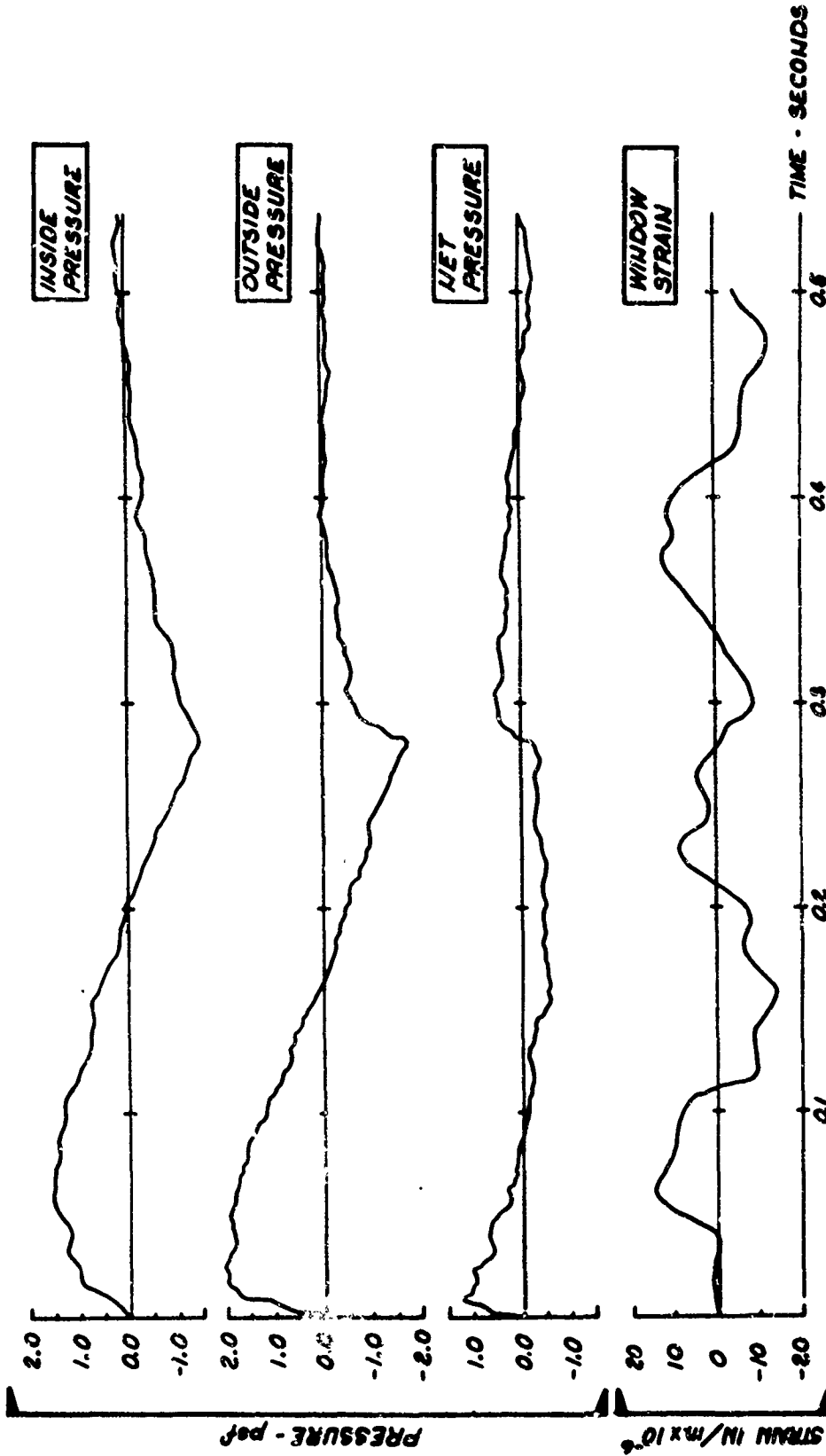
INSIDE PRESSURE

OUTSIDE PRESSURE

JET PRESSURE

WINDOW STRAIN

PRESSURE SIGNATURES
ON LARGE GLASS WINDOW HOUSE E-1

TIME - SECONDS

PRESSURE - psf

STRAIN IN/IN x 10⁻⁶

FIG.
7-28

7.58

PRESSURE SIGNATURES
ON LARGE GLASS WINDOW HOUSE E-1

FIG. 7-29

B-58 MSN. 11-2

7.59

F-104 MSN. 11-1

INSIDE PRESSURE

OUTSIDE PRESSURE

NET PRESSURE

WINDOW STRAIN

PRESSURE SIGNATURES
ON LARGE GLASS WINDOW HOUSE E-1

TIME - SECONDS

PRESSURE - psf

STRAIN IN/in x 10⁻⁶

7.60

MISSIONS
16 - 2
11 - 3
5 - 2
8 - 3
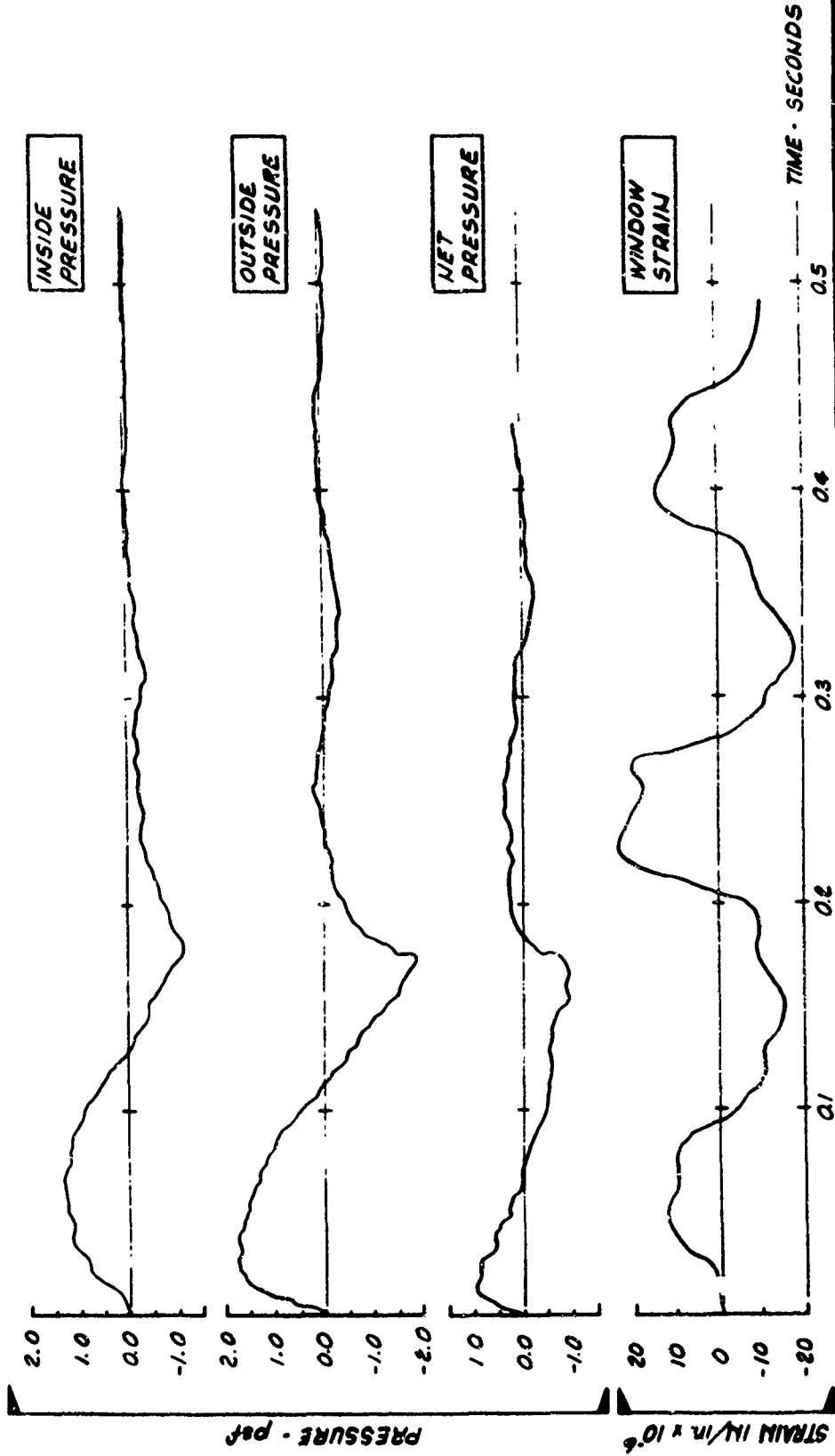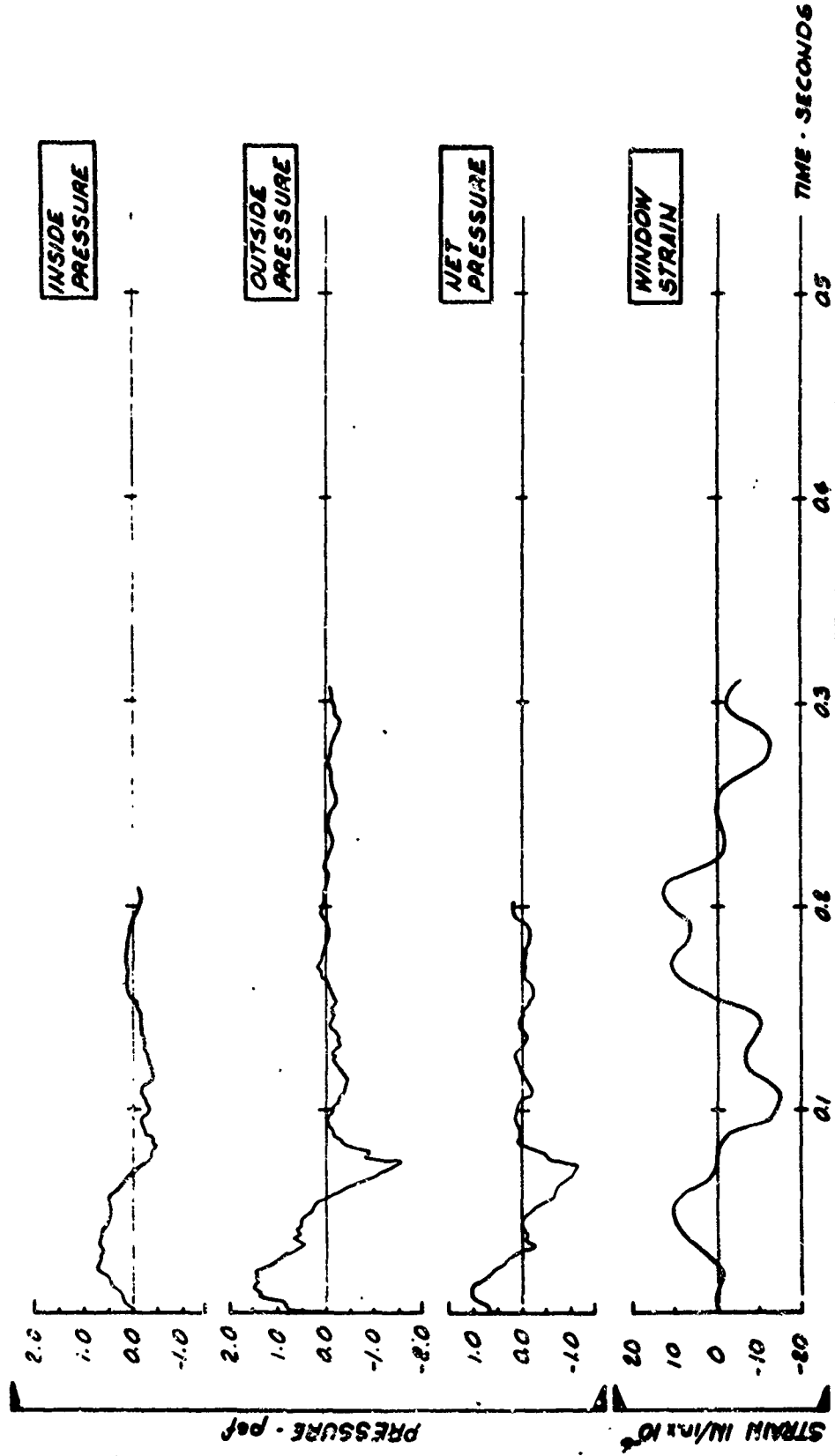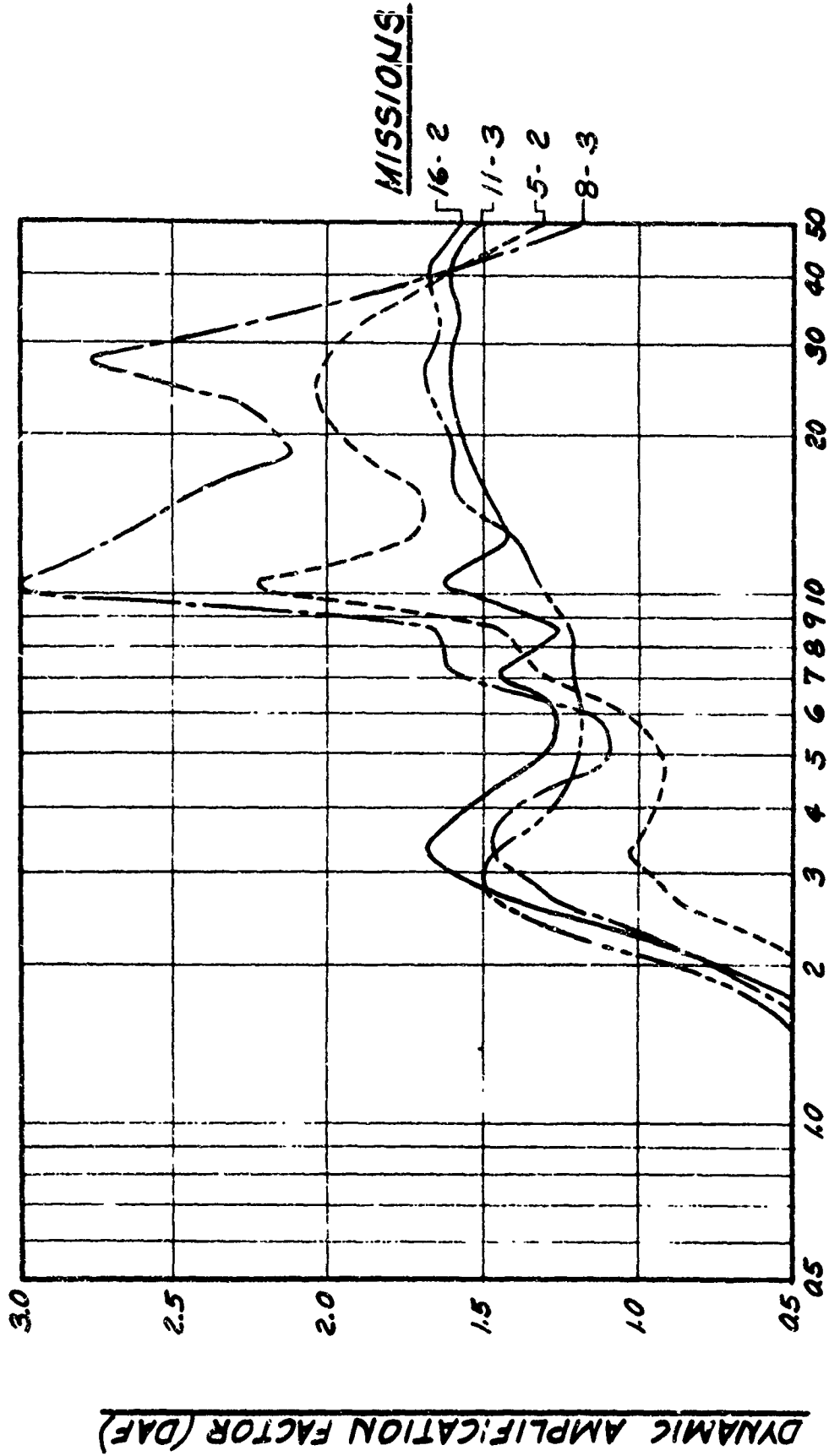
NATURAL FREQUENCY C.P.S.

DYNAMIC AMPLIFICATION FACTOR (DAF)

RESPONSE OF 2% DAMPED SYSTEMS TO NET PRESSURE LOADING
LARGE GLASS WINDOW, HOUSE E-1 ~ XB-70

FIG.
7-31

FIG.
7-31

7.61
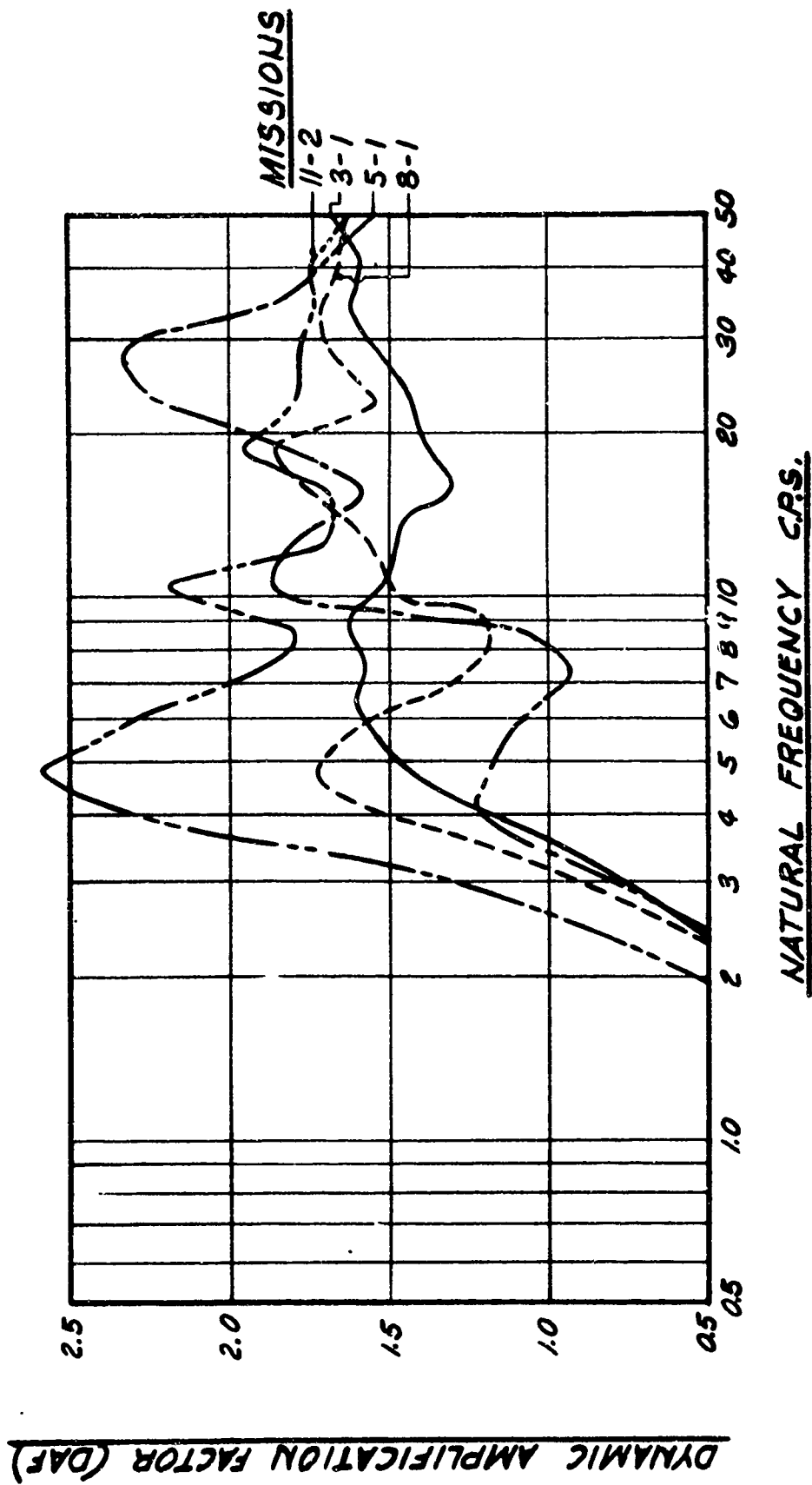
RESPONSE OF 2% DAMPED SYSTEMS TO NET PRESSURE LOADING LARGE GLASS WINDOW, HOUSE E-1 ~ B-58

FIG.
7-32
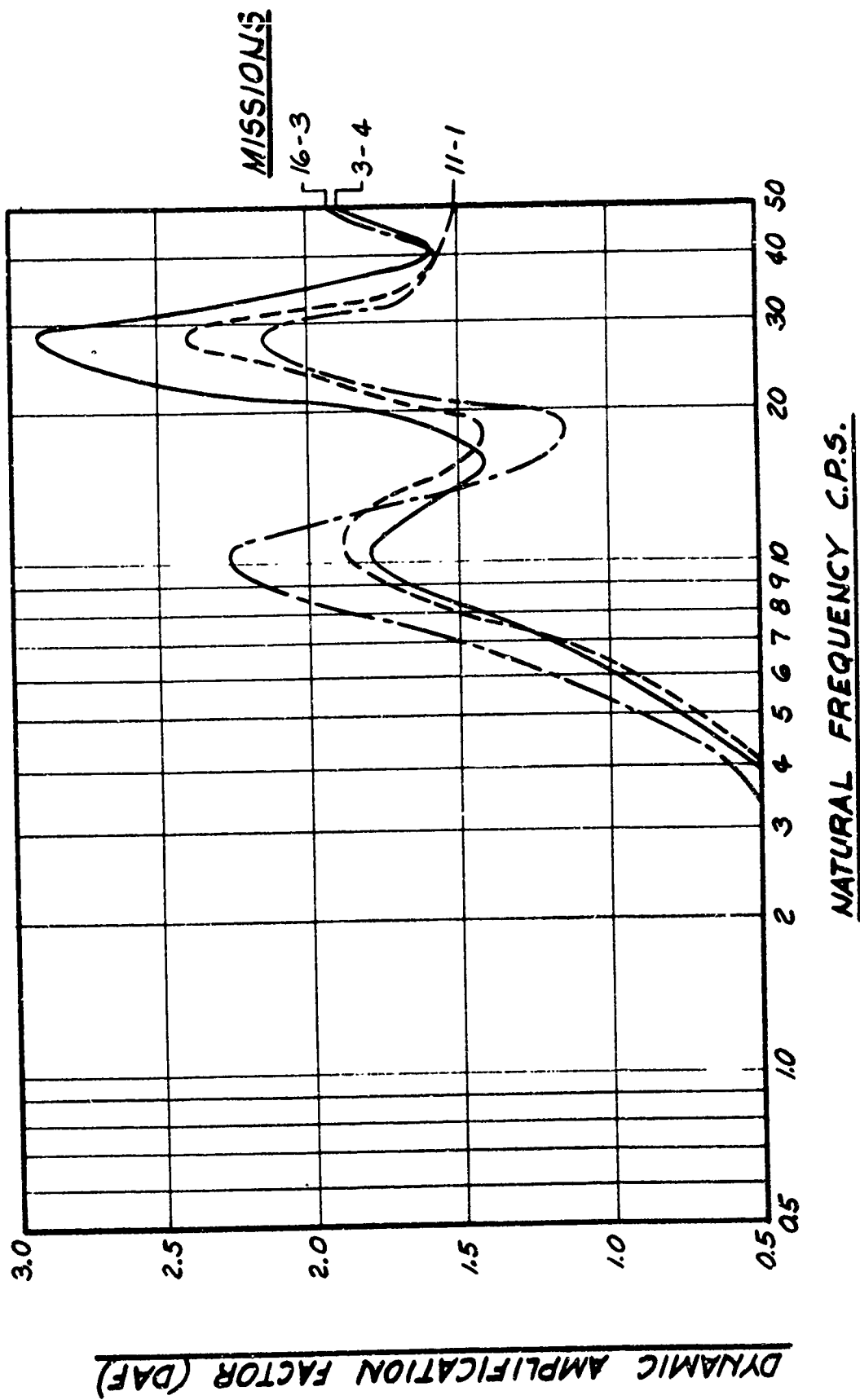
RESPONSE OF 2% DAMPED SYSTEMS TO NET PRESSURE LOADING
LARGE GLASS WINDOW, HOUSE E-1 ~ F-104

FIG. 7-33

7.63

COMPARISON OF DAF FOR FREE FIELD, OUTSIDE & NET
PRESSURES. XB-70 MISSION 11-3
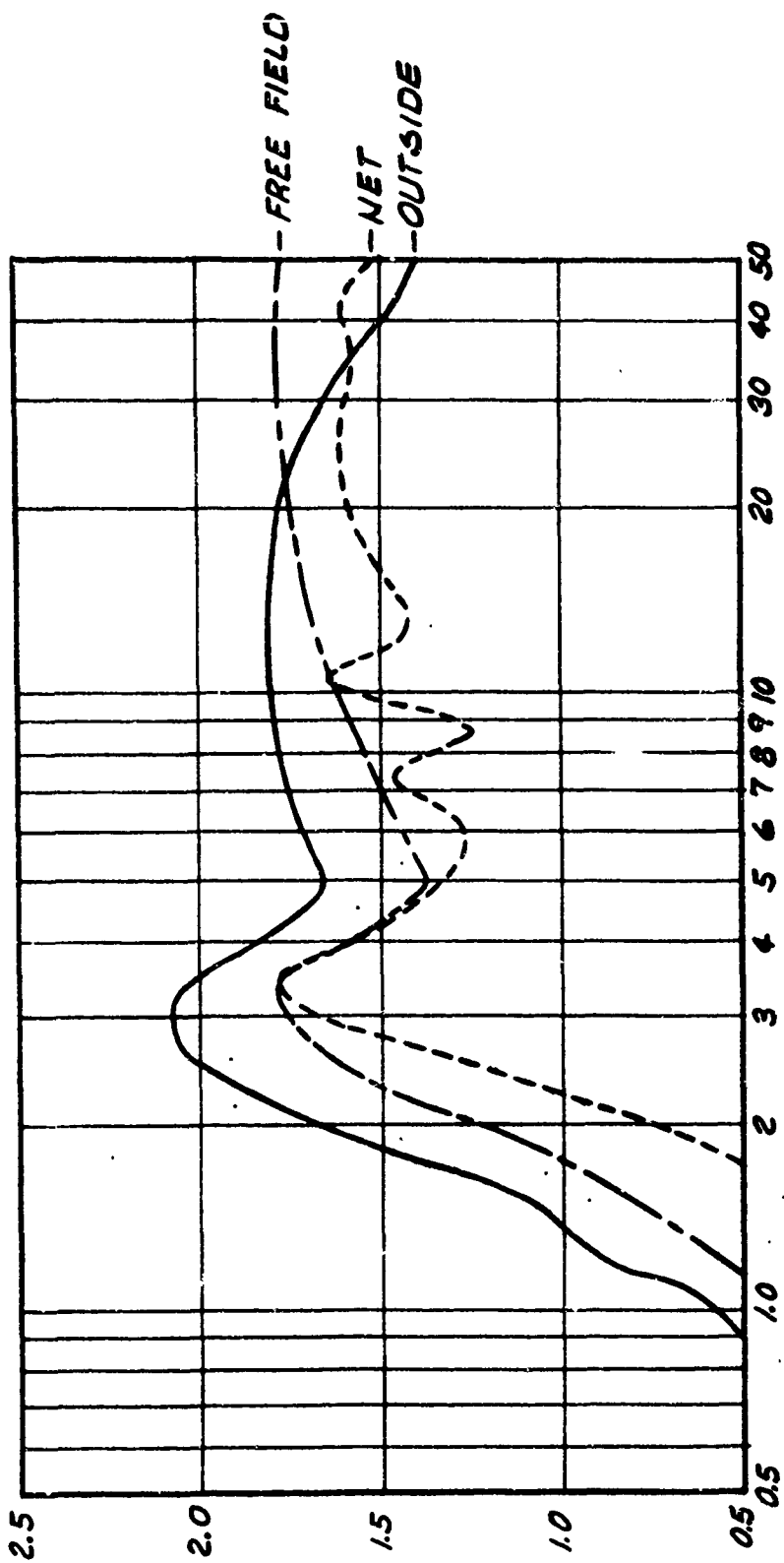
FIG.
7-34
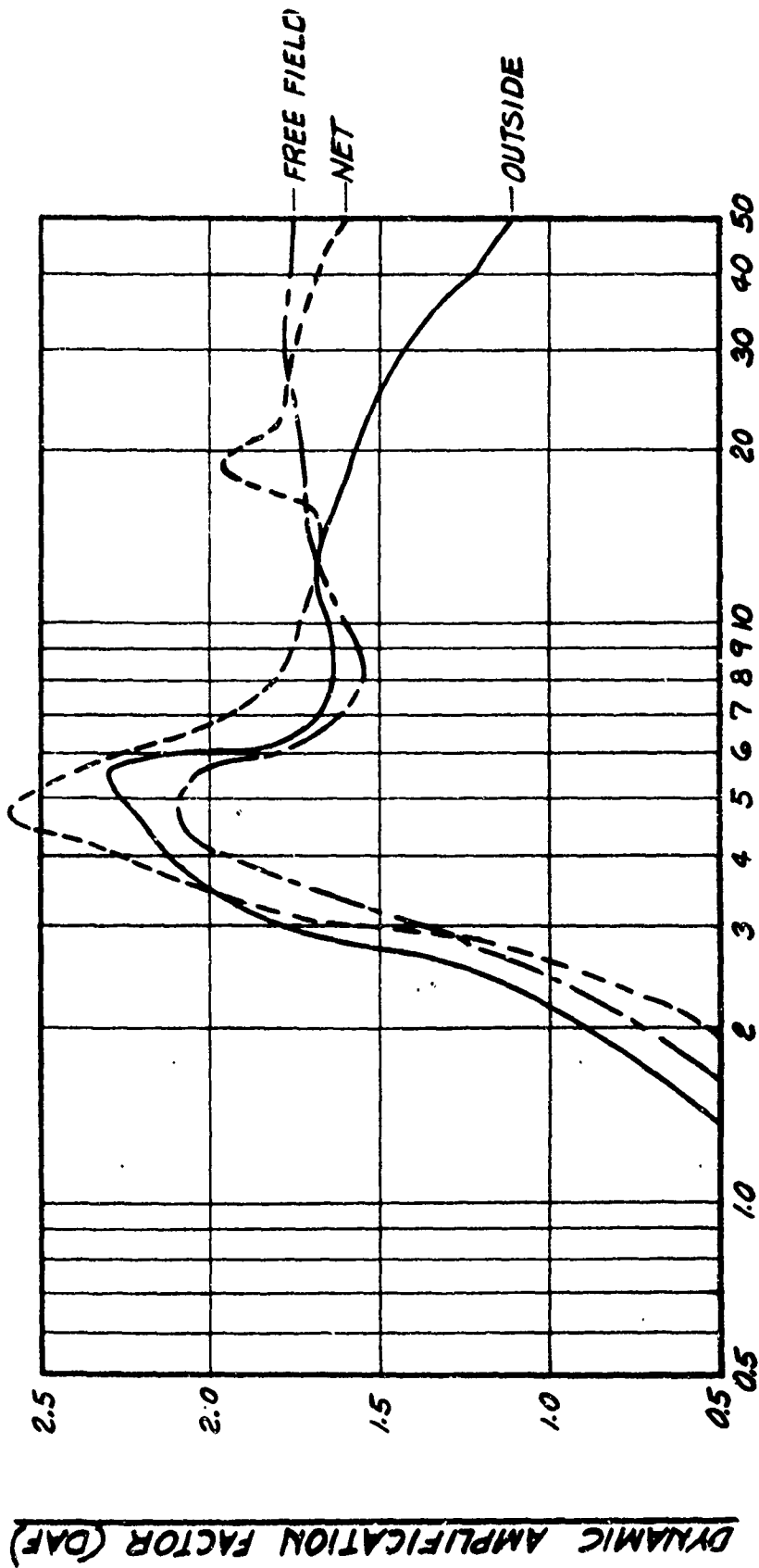
COMPARISON OF DAF FOR FREE FIELD, OUTSIDE & NET
PRESSURES   B-58, MISSION 11-2

FIG.
7-35

NATURAL FREQUENCY C.P.S.

DYNAMIC AMPLIFICATION FACTOR (DAF)
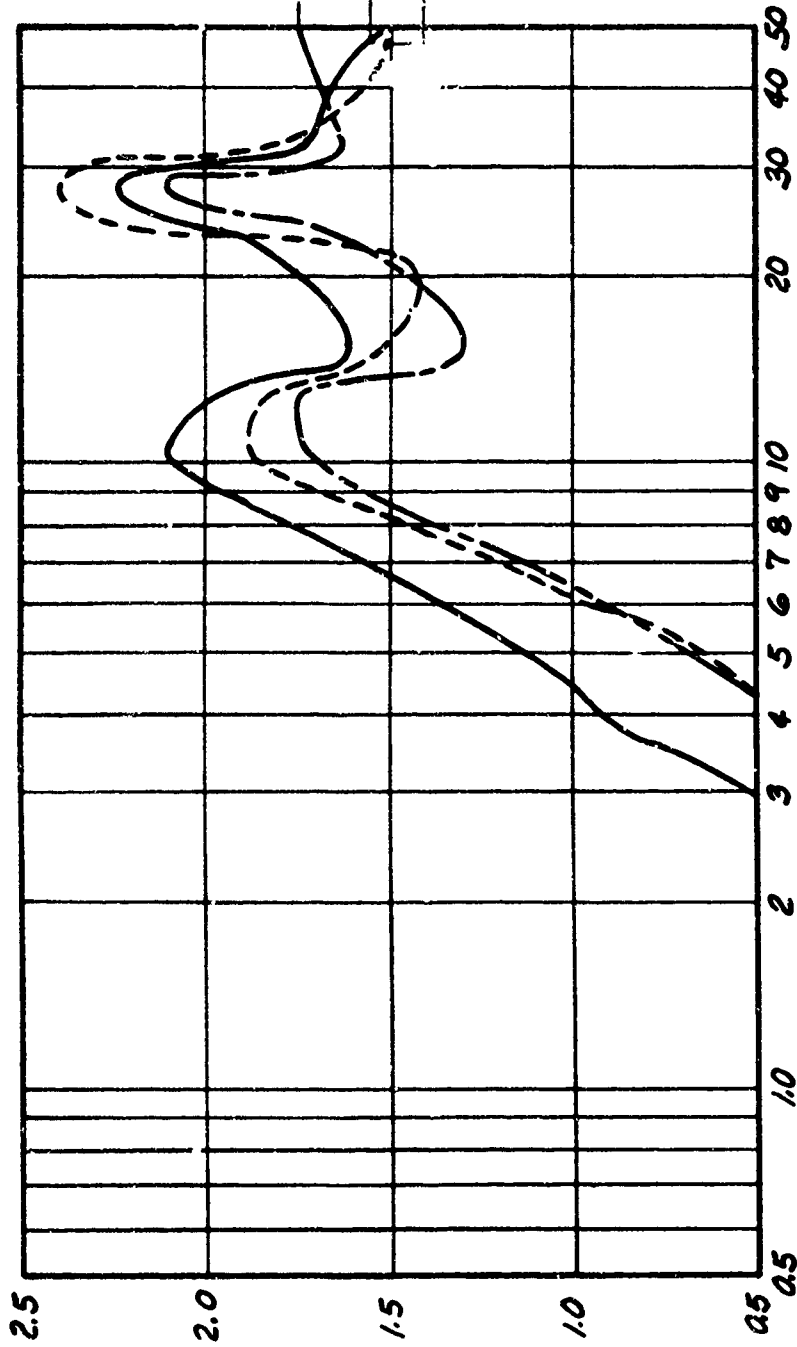
COMPARISON OF DAF FOR FREE FIELD, OUTSIDE, & NET PRESSURES

F-104, MISSION 11-1

FIG.
7-36

FIG.
7-36

7.66

COMPARISON OF DAF FOR FREE FIELD AND NET PRESSURES
XB-70 MISSION δ-3

FIG. 7-37

7.67
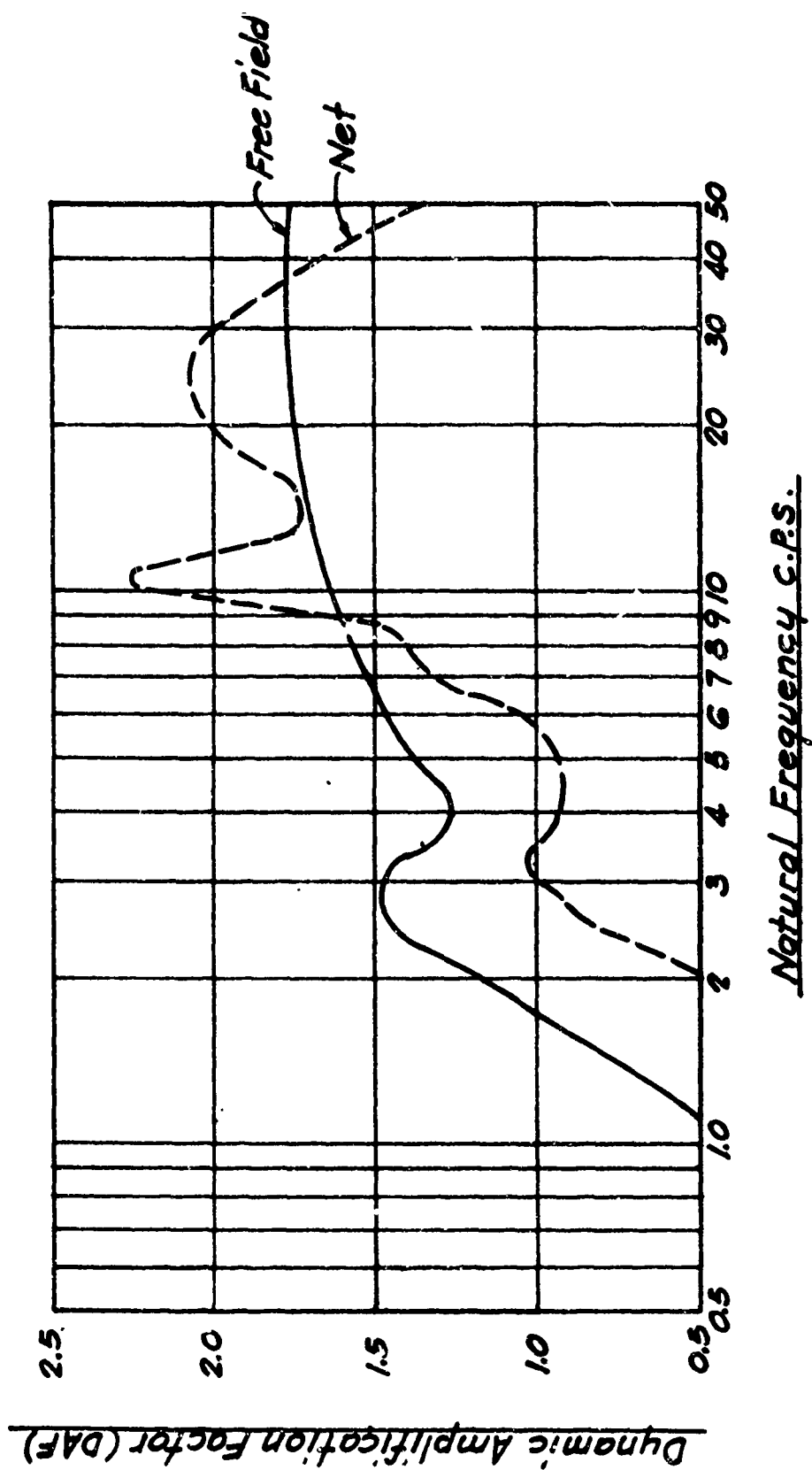
COMPARISON OF DAF FOR FREE FIELD AND NET PRESSURES
XB-70 MISSION 5-2

FIG. 7-38
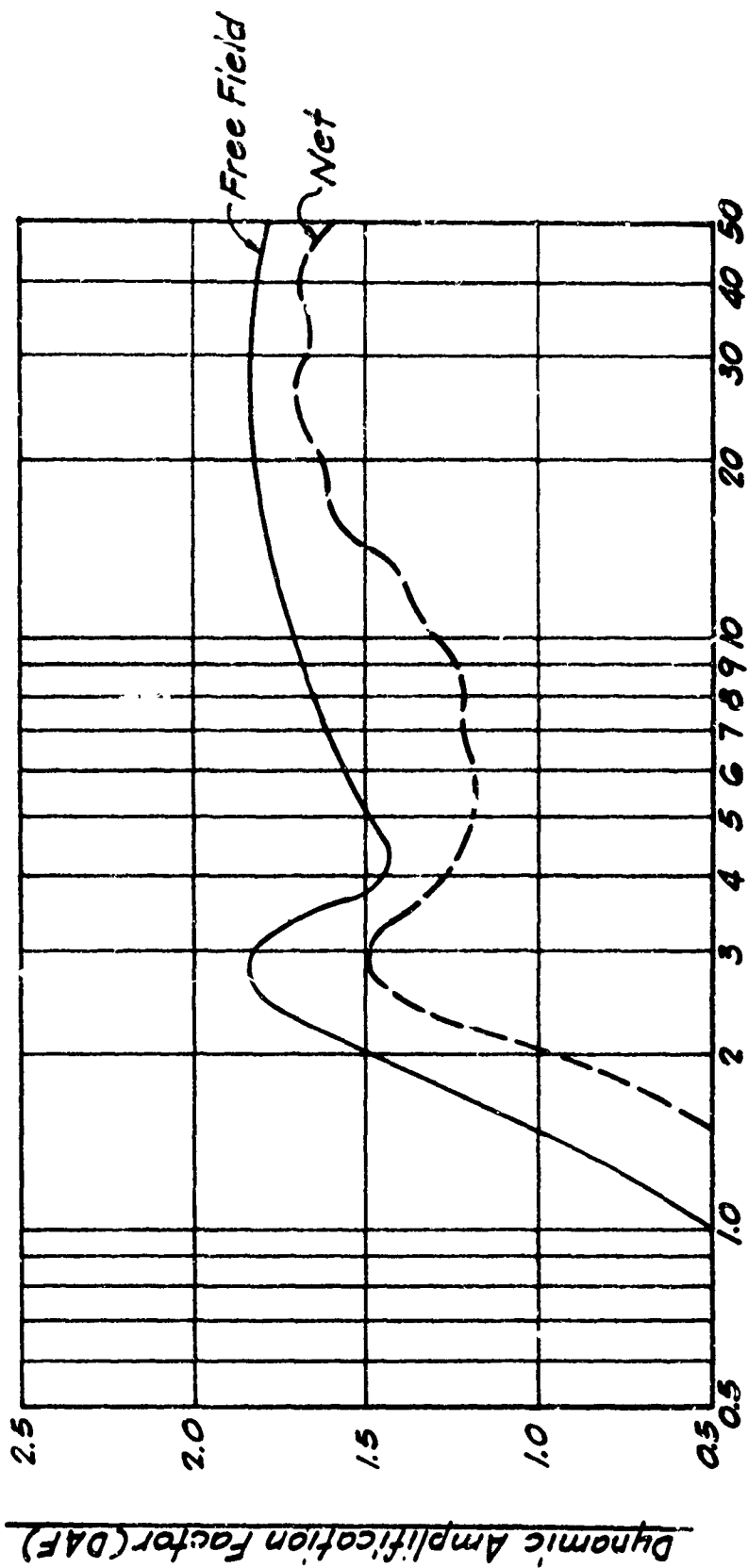
COMPARISON OF DAF FOR FREE FIELD AND NET PRESSURES

XB-70 MISSION 16-2

FIG.
7-39
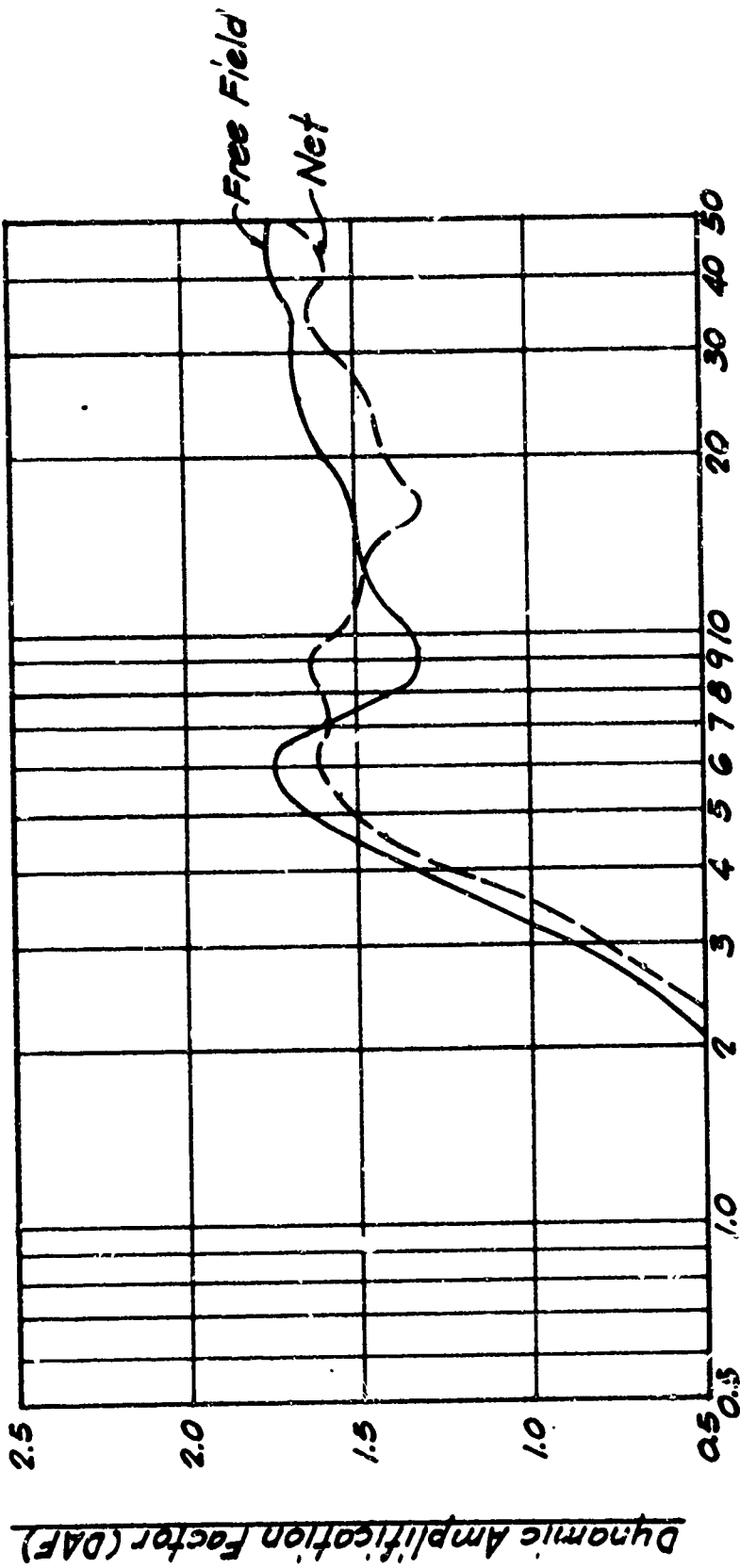
7.69

COMPARISON OF DAF FOR FREE FIELD AND NET PRESSURES
B-58 MISSION 3-1

FIG.
7-40

7.70
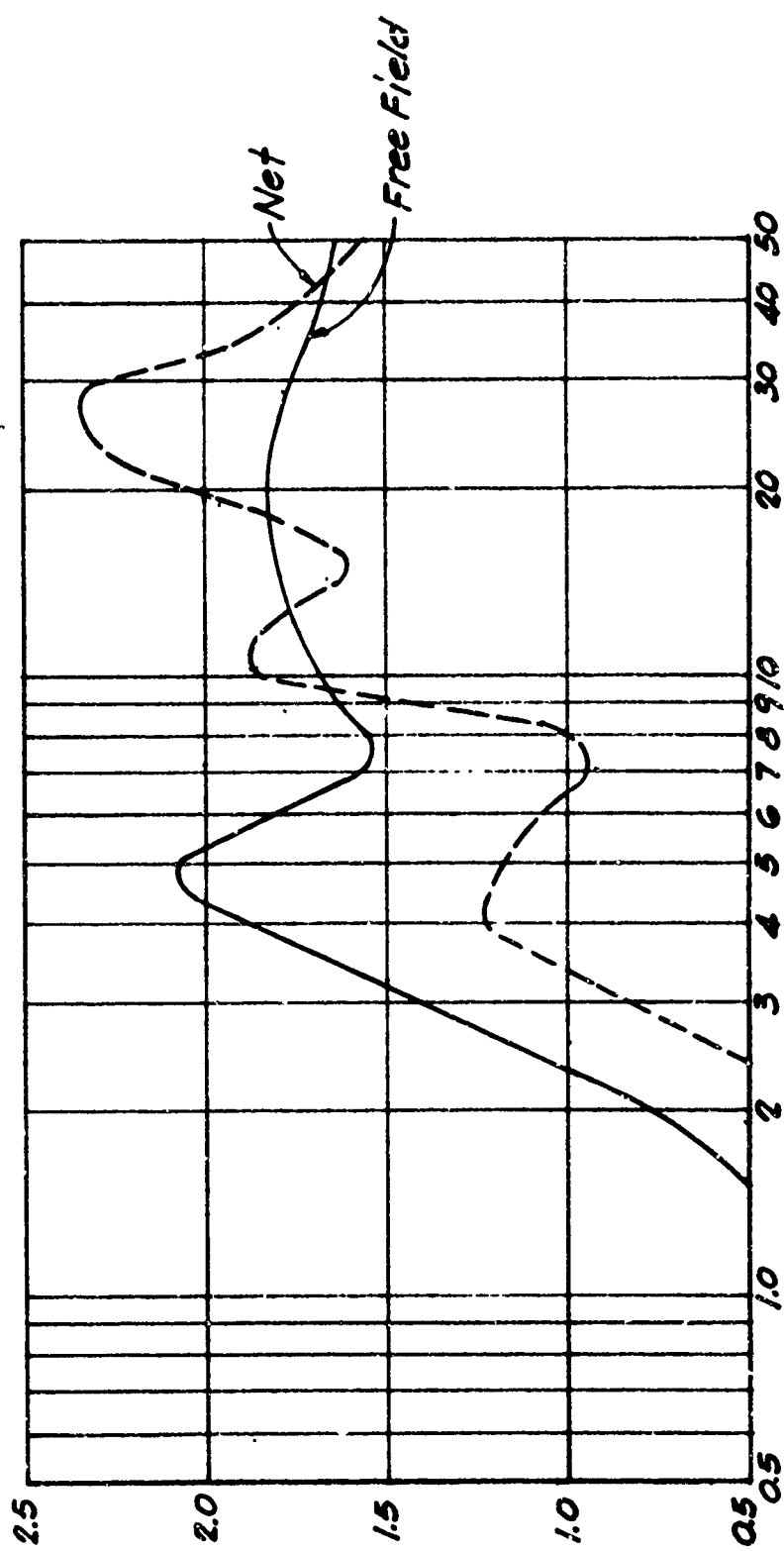
COMPARISON OF DAF FOR FREE FIELD AND NET PRESSURES

B-58   MISSION 5-1

FIG.
7-41

7.71

Free Field
Net

Natural Frequency C.P.S.

Dynamic Amplification Factor (DAF)
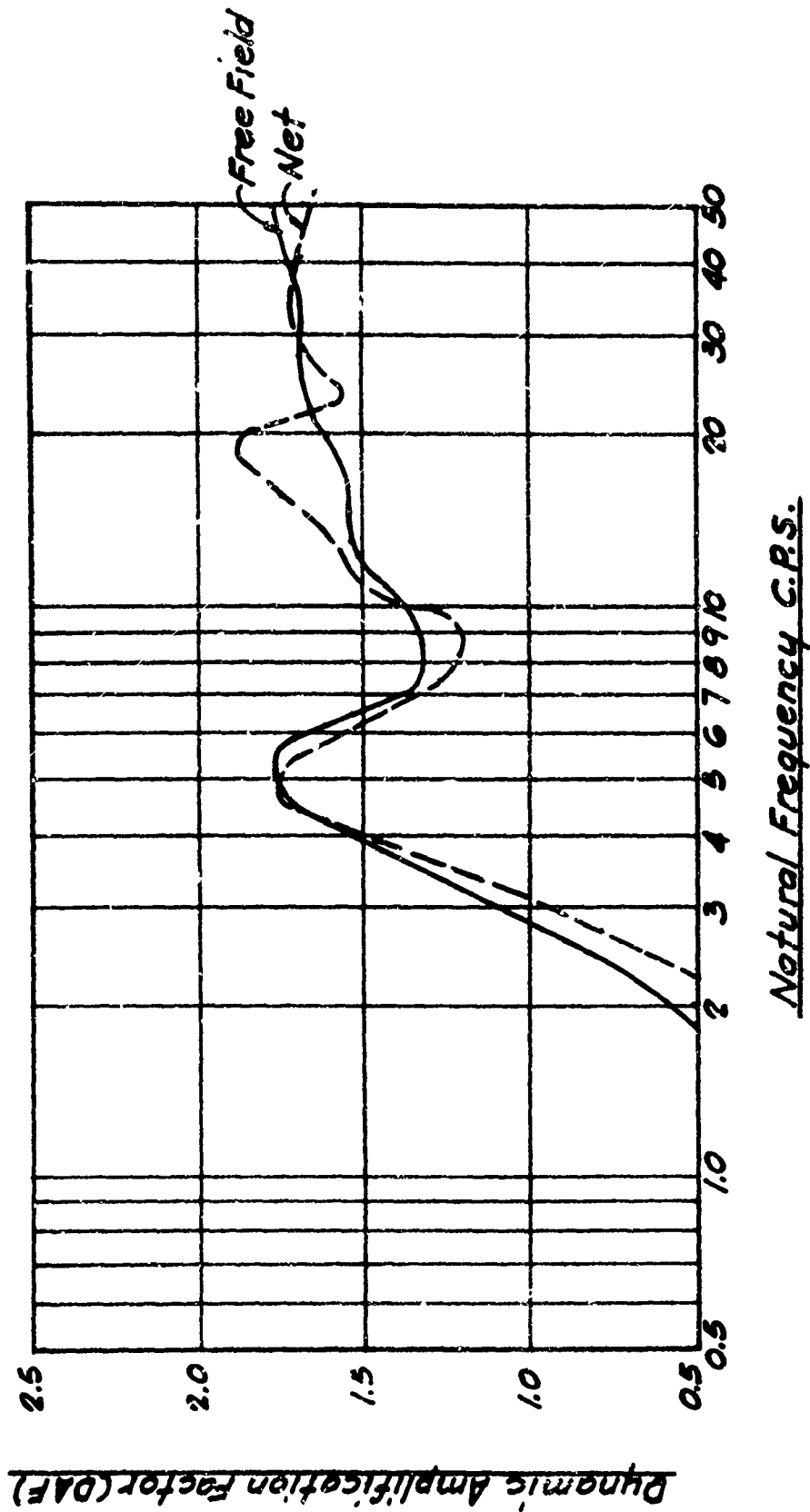
COMPARISON OF DAF FOR FREE FIELD AND NET PRESSURES
B-58 MISSION B-1

FIG. 7-42

7.72

PEAK PRESSURE RELATIONSHIP FOR E-1 WINDOW

FIG.
7-43

7.73

LEGEND
⊙ F-104
▣ B-58
▣ XB-70
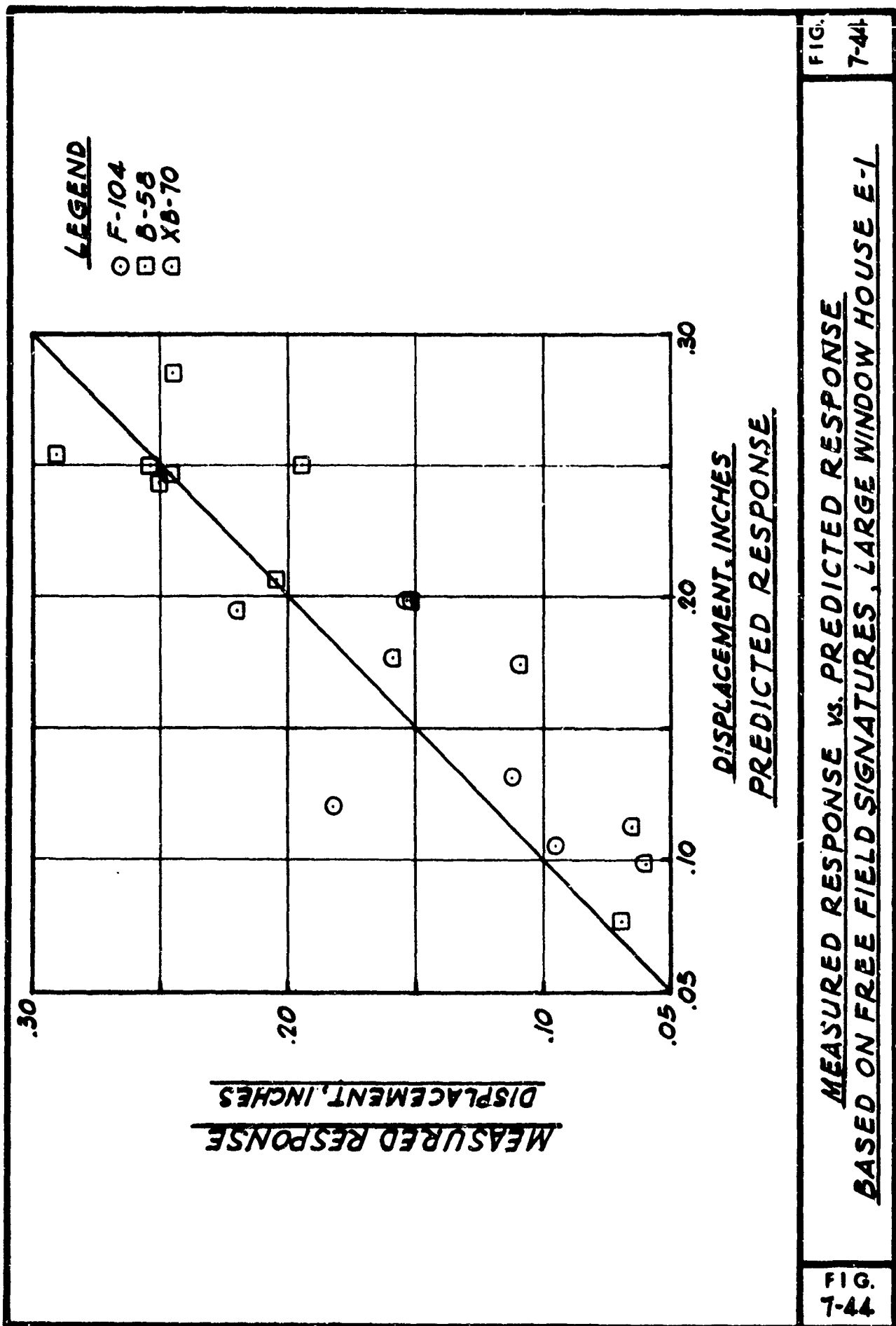
MEASURED RESPONSE vs. PREDICTED RESPONSE
BASED ON FREE FIELD SIGNATURES, LARGE WINDOW HOUSE E-1
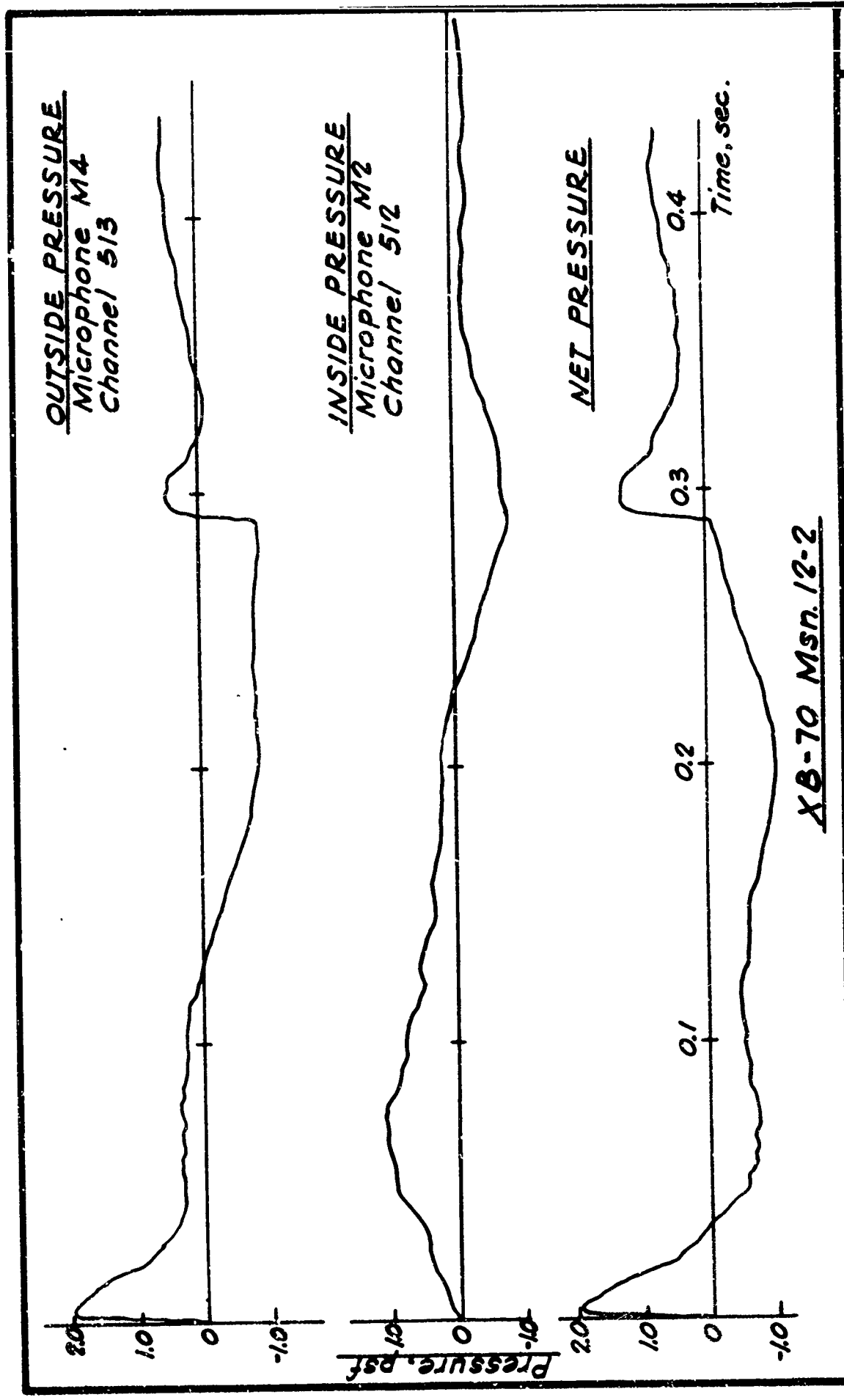
DISPLACEMENT, INCHES
PREDICTED RESPONSE

MEASURED RESPONSE
DISPLACEMENT, INCHES

FIG.
7-44

7.74

OUTSIDE PRESSURE
Microphone M4
Channel 513

INSIDE PRESSURE
Microphone M2
Channel 512

NET PRESSURE

Time, sec.

XB-70 Msn. 12-2

PRESSURE SIGNATURES
BOWLING ALLEY ROOF

Pressure, psf

7.75

FIG.
7-45

FIG.
7-45

2

OUTSIDE PRESSURE
Microphone M4
Channel 513

INSIDE PRESSURE
Microphone M2
Channel 512

NET PRESSURE

Time, sec.
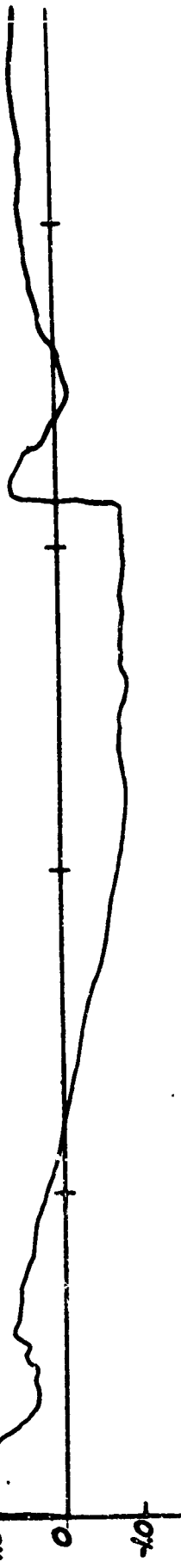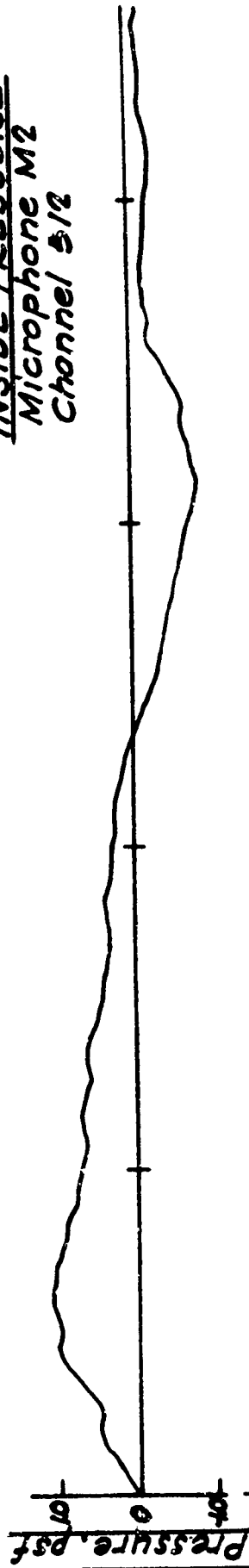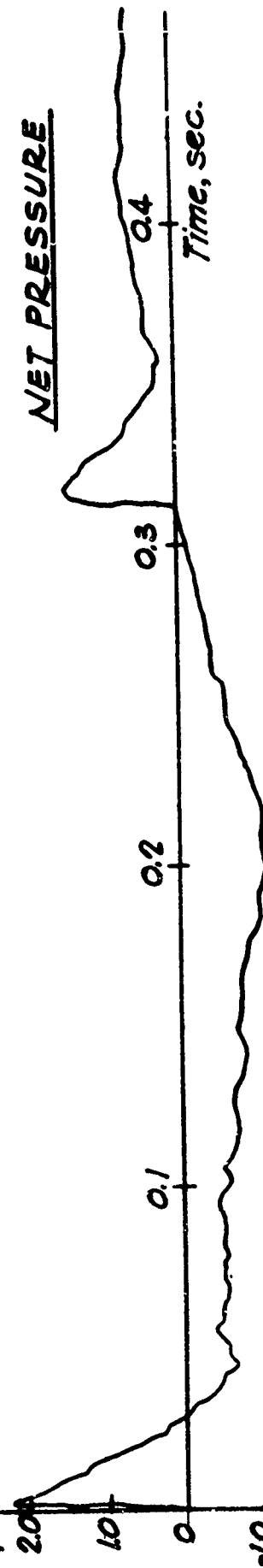
Pressure, psf

XB-70 Msn. 113-2

PRESSURE SIGNATURES
BOWLING ALLEY ROOF

FIG.
7-46

FIG.
7-46

7.76

PRESSURE SIGNATURES
BOWLING ALLEY ROOF

B-58 Msn. 12-1

OUTSIDE PRESSURE
Microphone M4
Channel 513

INSIDE PRESSURE
Microphone M2
Channel 512

NET PRESSURE

Pressure, psf

Time, sec.
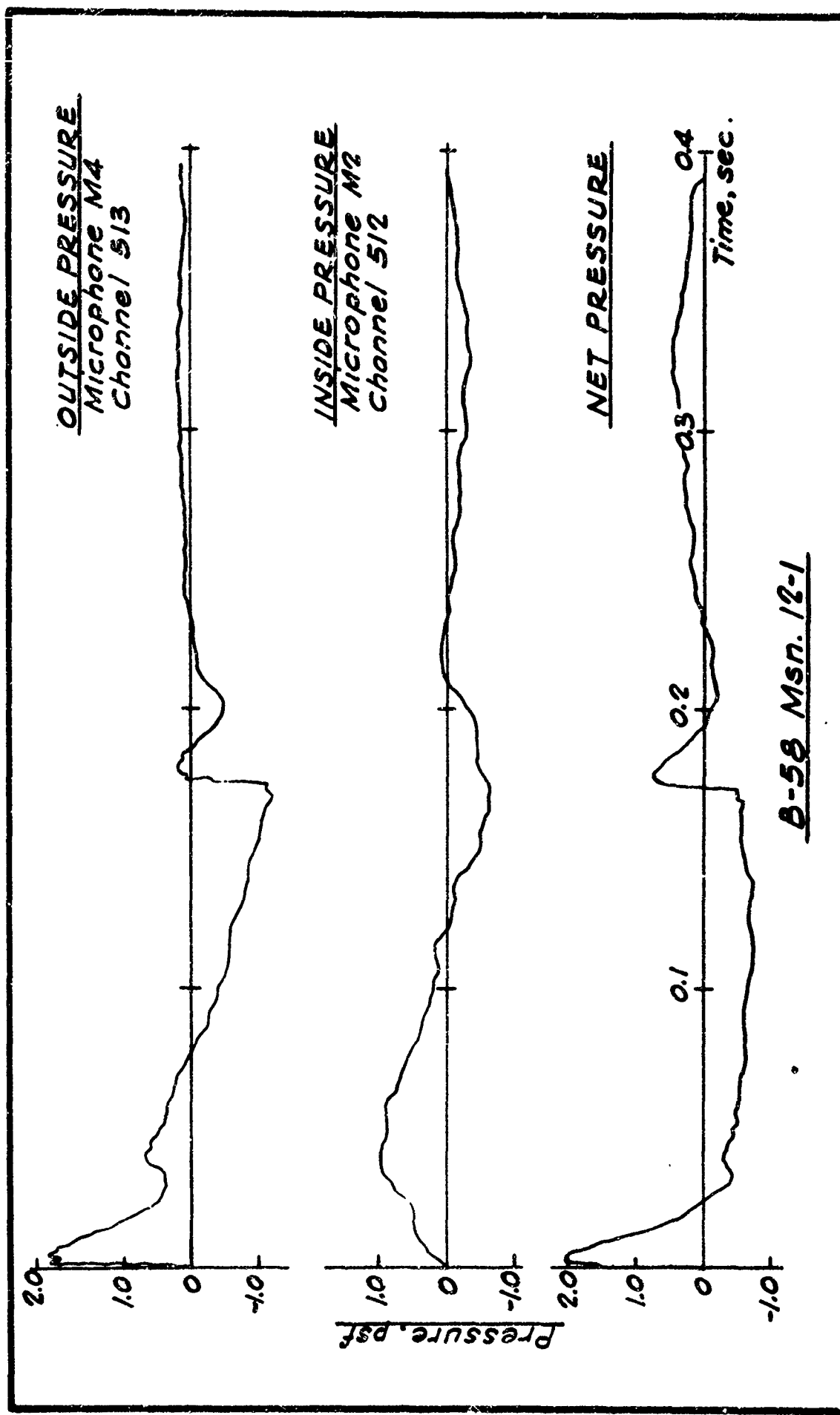
FIG.
7-47

OUTSIDE PRESSURE
Microphone M4
Channel 513
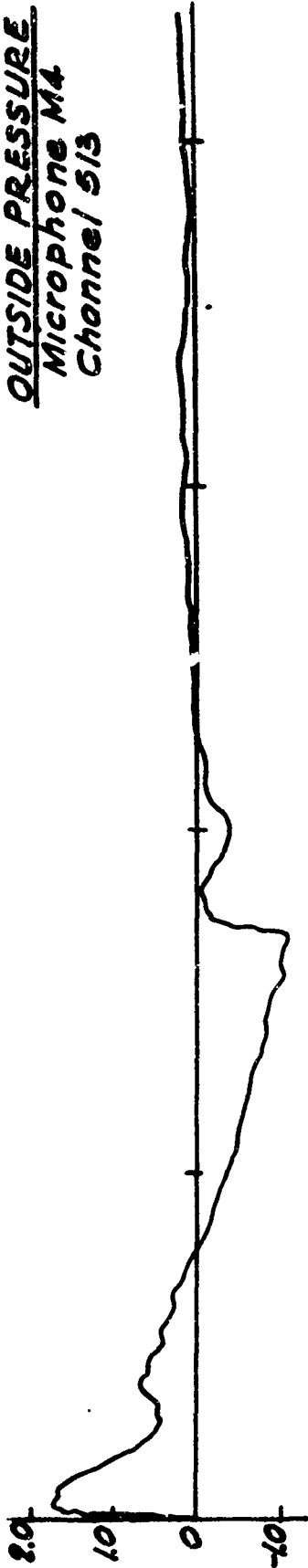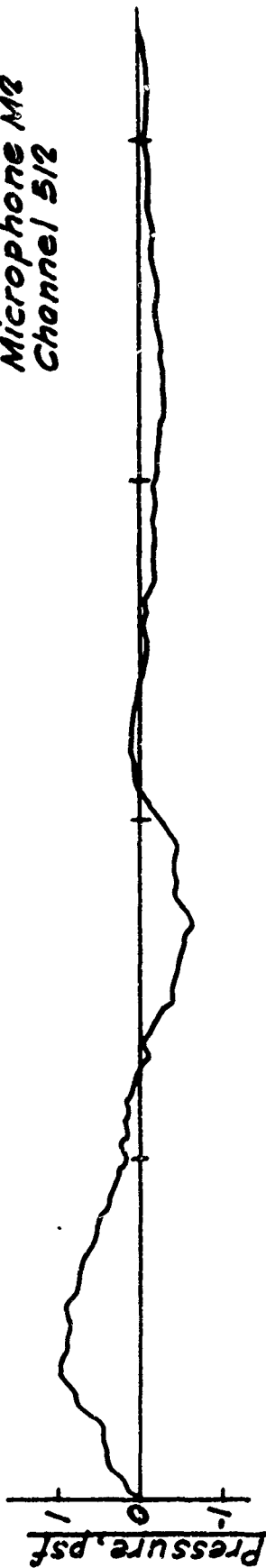
INSIDE PRESSURE
Microphone M2
Channel 512

NET PRESSURE

Time, sec.

Pressure, psf

B-58 Msn. 113-1

PRESSURE SIGNATURES
BOWLING ALLEY ROOF

FIG.
7-48

7.78

OUTSIDE PRESSURE
Microphone M4
Channel 513
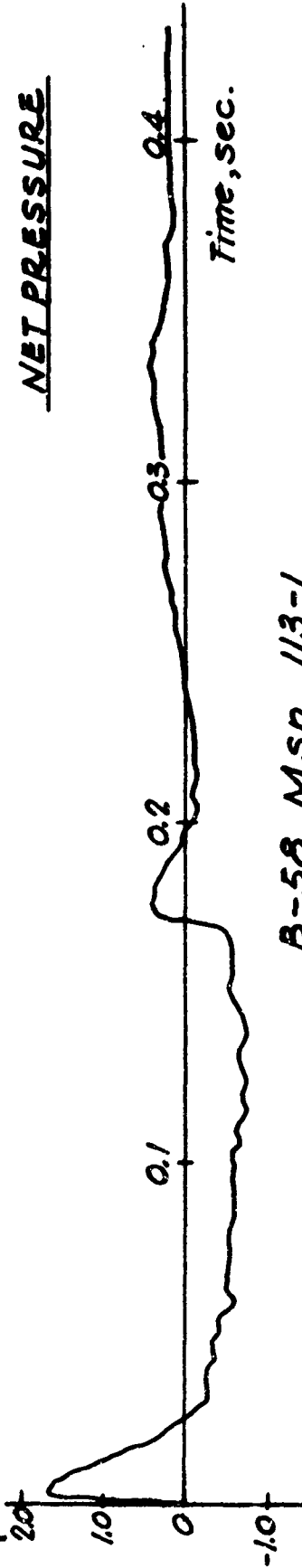
INSIDE PRESSURE
Microphone M2
Channel 512
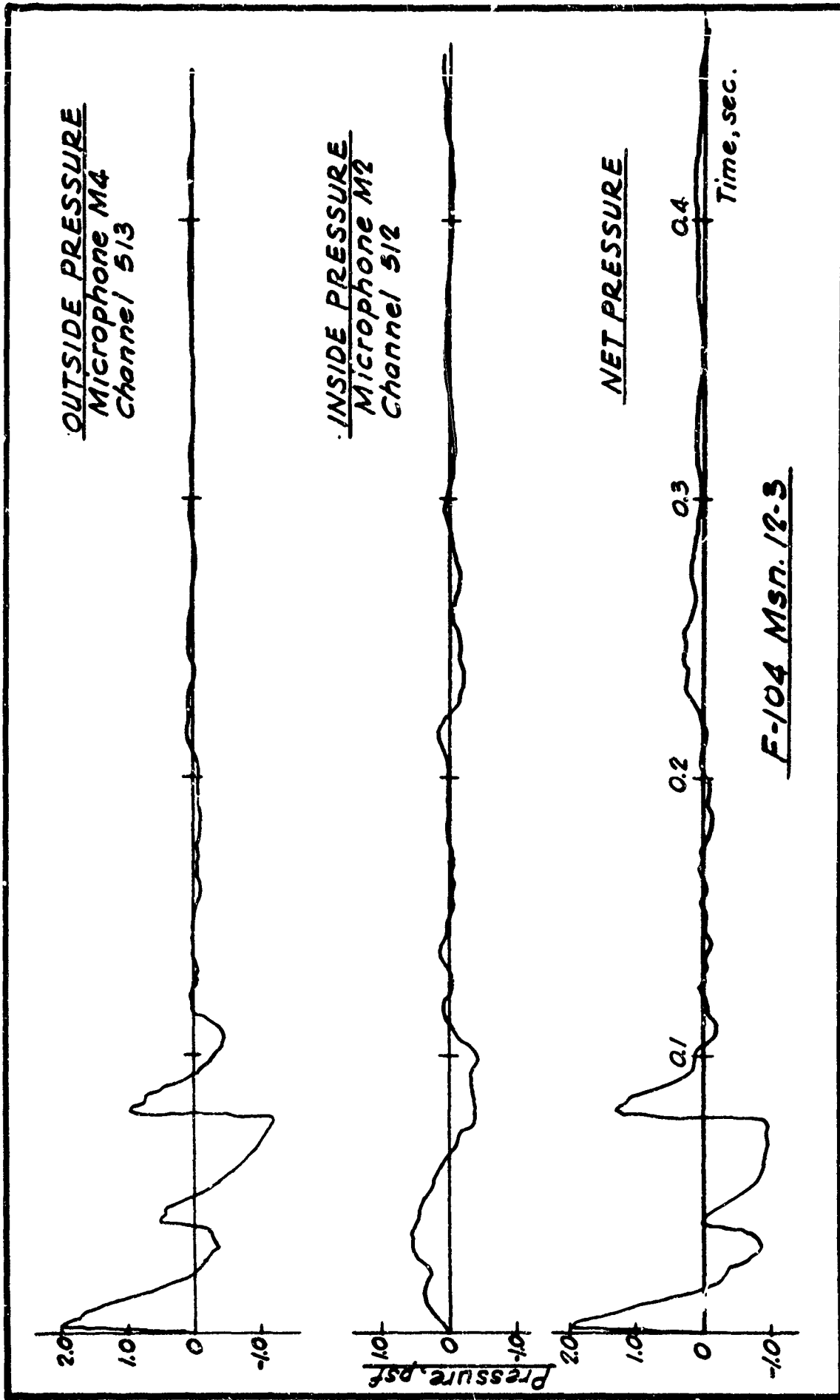
NET PRESSURE

F-104 Msn. 12-3

PRESSURE SIGNATURES
BOWLING ALLEY ROOF

FIG.
7-49

OUTSIDE PRESSURE
Microphone M4
Channel 513
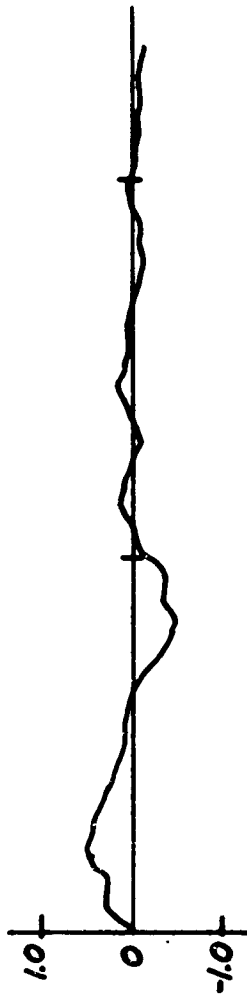
INSIDE PRESSURE
Microphone M2
Channel 512

NET PRESSURE

PRESSURE SIGNATURES
BOWLING ALLEY ROOF

F-104 Msn. 113-3

Time, sec.

Pressure, psf

FIG.
7-50
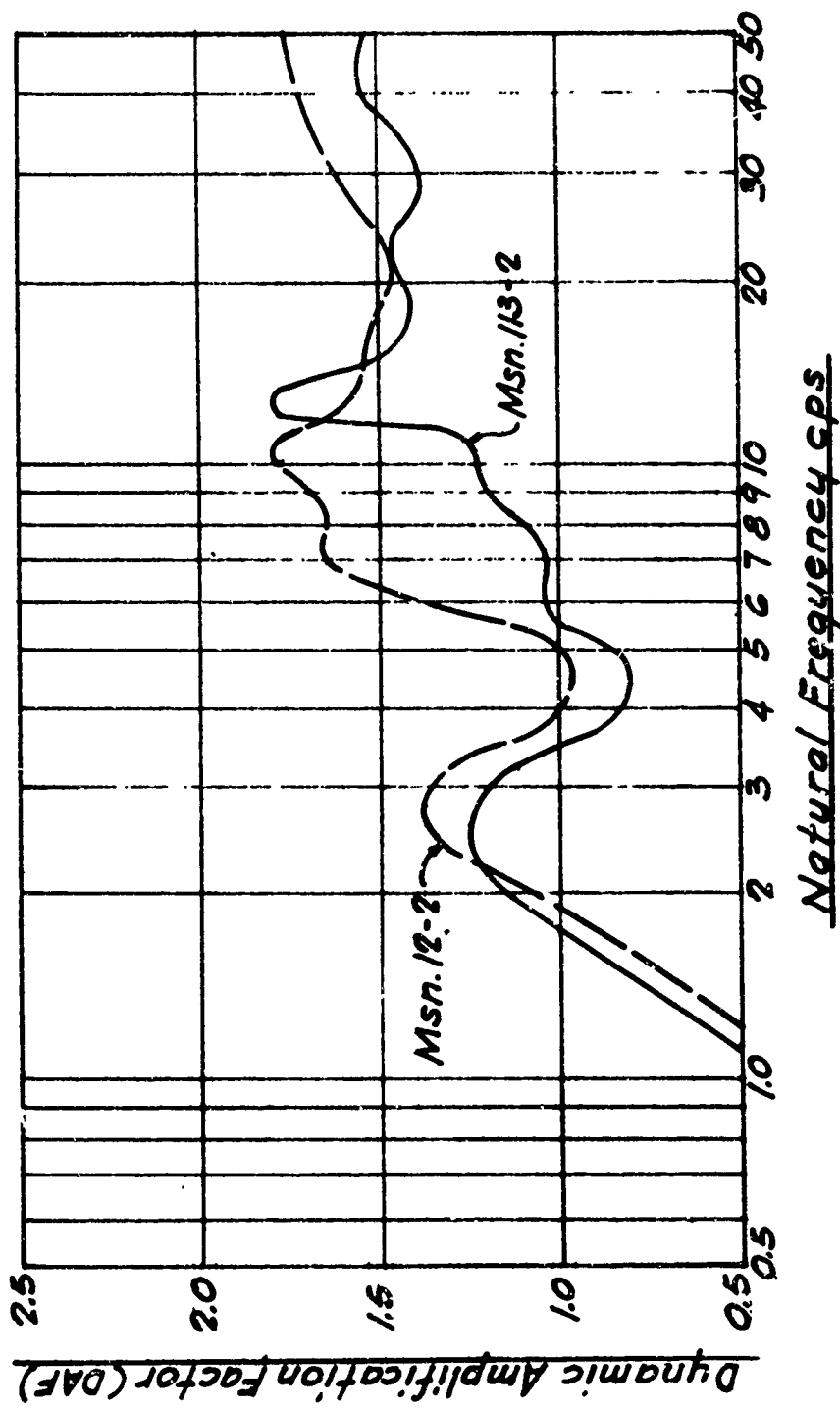
RESPONSE OF 2% DAMPED SYSTEMS TO NET PRESSURE LOADING
BOWLING ALLEY ROOF ~ XB-70

FIG. 7-51

7.81
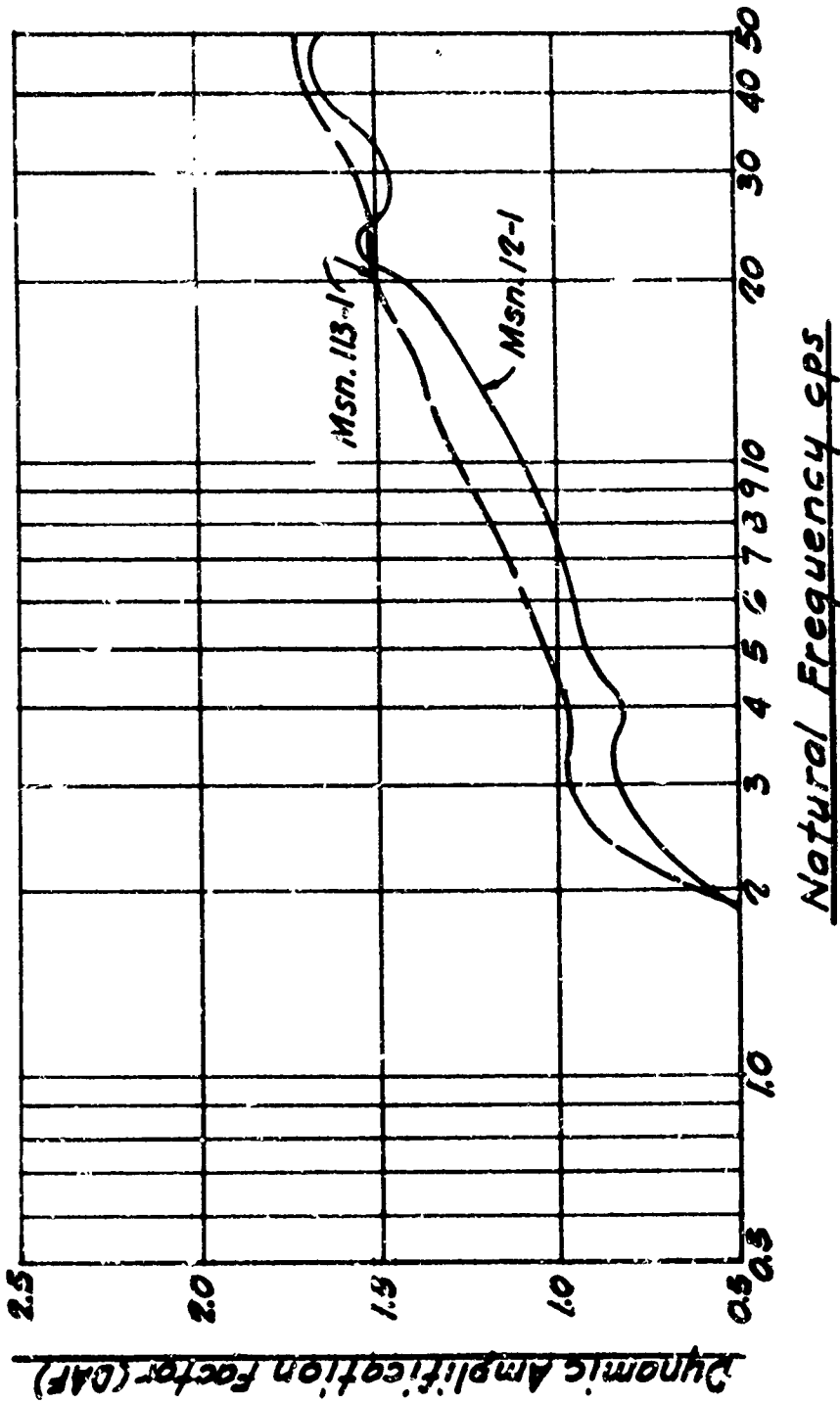
RESPONSE OF 2% DAMPED SYSTEMS TO NET PRESSURE LOADING
BOWLING ALLEY ROOF ~ B-58

FIG.
7-52

FIG.
7-52

7.82
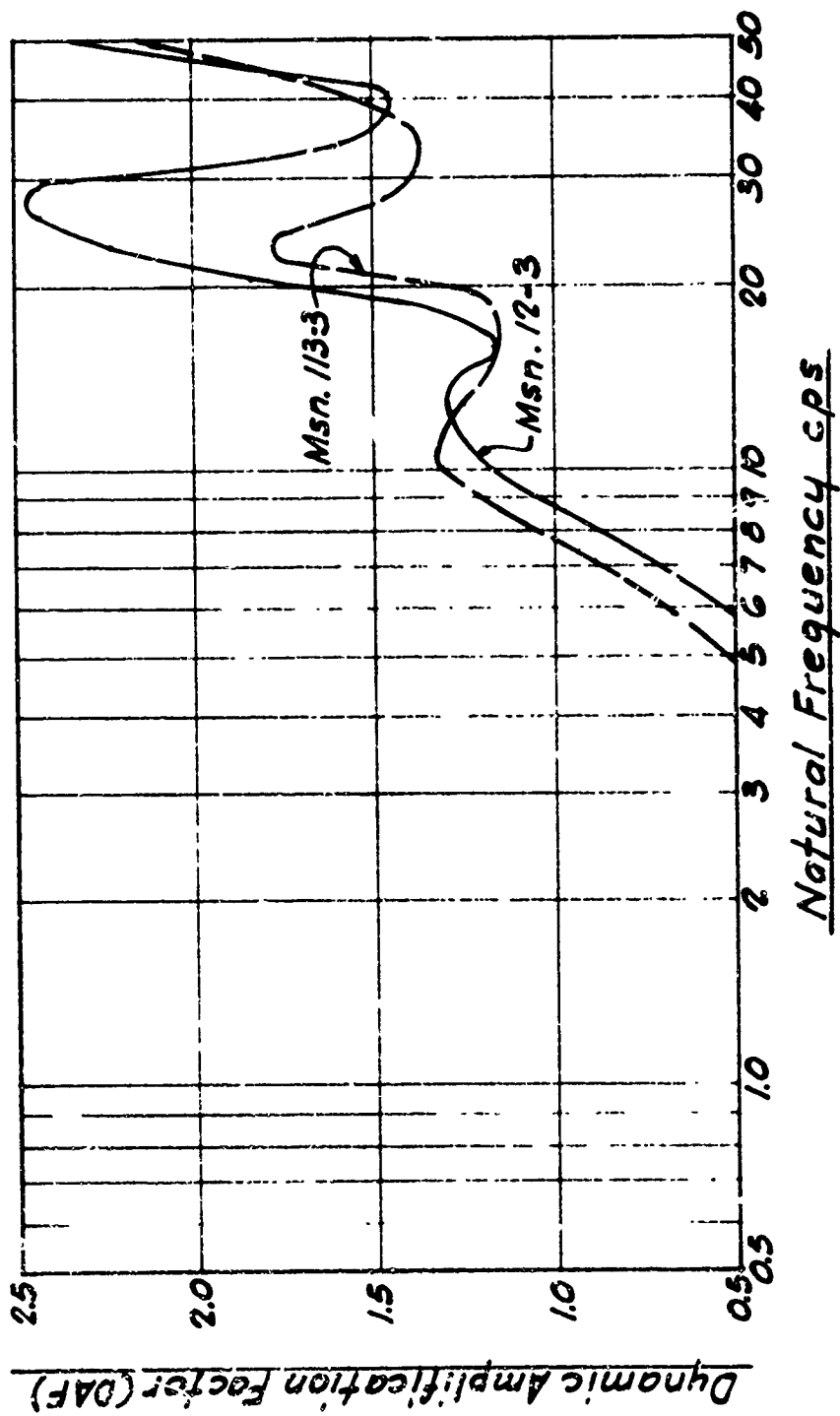
RESPONSE OF 2% DAMPED SYSTEMS TO NET PRESSURE LOADING
BOWLING ALLEY ROOF ~ F-104

FIG. 7-53

FIG. 7-53

7.83

VIII. ANALYSIS OF STRUCTURAL RESPONSE DATA - RACKING RESPONSE

The previous chapter discussed the analysis of plate response data.
Plate response was the lateral deformation of individual structure elements
and was primarily of a bending mode. Racking response, the deformation of
the structure as a whole and primarily of a shearing mode, is discussed in
this chapter. The analysis of the racking response data was divided into
two sections: A) Test Houses E-1 and E-2, and B) Bowling Alley E-3.

A. TEST HOUSES E-1 AND E-2

This section presents the results of the analysis of the racking response
of Test Houses E-1 and E-2. Predicted response based on free field peak over-
pressures and DAF computed from free field signatures was compared with mea-
sured response for the north-south and east-west racking motions of E-1. The
reasons and justification for using free field data have been discussed in
Chapter II. The racking response of House E-1 was analysed in detail and the
racking response of E-2 was investigated in lesser detail and compared with
E-1. The aircraft flight track was oriented such that it was possible to
study racking response due to aircraft vectors that were nearly head-on (east-
west racking) and side-on (north-south racking). In addition, the results of
the Phase II tests were compared with the results from the Phase I[19,20] and
White Sands[2] tests.

INSTRUMENTATION

Accelerometers were installed at the northeast corners of Test Houses
E-1 and E-2 to determine the racking response. These accelerometers were in-
stalled at the roof lines of Houses E-1 and E-2 and at the second story floor
line of House E-2. The locations of these instruments are shown in Figure 8-1.
In addition, pressure microphones were installed in and around the two houses
so that the actual and net pressure loading on the houses could be determined.
The locations of the pressure microphones are shown in Appendix B.

Note: All figures and tables are placed at the end of this chapter. For the
altitudes, Mach number, offset, etc., of aircraft flight missions used in this
chapter, see Tables 5-1, 5-2, and 5-3.

TEST RESULTS - MEASURED DISPLACEMENTS

Peak racking accelerations were of low magnitude (on the order of 0.1g). Table 8-1 lists peak accelerations at the roof lines of the northeast corners of Houses E-1 and E-2 for typical overhead missions of XB-70, B-58 and F-104 aircraft. These peak accelerations were of the same order of magnitude as those obtained in the Phase I tests[19,20]. Figures 8-2, 8-3 and 8-4 show acceleration-time records for east-west racking of the northeast corner of House E-1 for typical overhead XB-70, B-58 and F-104 missions.

The analog magnetic tape recordings of the accelerometer data were converted to digital form as discussed in Chapter IV. The digitized records were then numerically integrated twice to obtain displacements. Peak displacements obtained from the numerical integration process for typical overhead XB-70, B-58 and F-104 missions are listed in Table 8-2. The displacement-time records shown in Figures 8-5, 8-6 and 8-7 were typical for east-west racking of House E-1 for overhead XB-70/B-58/F-104 missions during Phase II. North-south racking displacements for the roof line of E-2 for XB-70, B-58 and F-104 missions during Phase I are shown in Figure 8-8. Note that these displacements were of the same order of magnitude (less than 0.005 in.) as the Phase II data. North-south and east-west displacements for the roof line of House E-2 were combined and are shown in Figure 8-9. In this figure, one half cycle (inside peak to outside peak) represents a time interval of about 0.07 seconds.

A comparison of the racking displacements of E-1 and E-2 listed in Table 8-2 and the racking displacements obtained during the White Sands tests[2] indicated that Phase II and White Sands racking displacements were of similar magnitude for structures of similar construction and for similar overpressures.

Note that the racking displacements due to F-104 and B-58 missions were generally larger than those due to the XB-70 and that the displacements due to F-104 missions were usually larger than those caused by B-58 missions, Table 8-2. Several factors caused this trend in response: signature duration, Mach number, and building length, all of which affect the net pressure signatures on the houses. Pressure signatures for the east wall and west wall and net pressure on the structure for typical east to west overhead XB-70/B-58/F-104 missions are shown in Figures 8-10, 8-11, and 8-12. For the missions shown, the time lags between the start of the boom on the east wall and on the west wall (building length divided by the speed of the aircraft) were 0.027, 0.031 and 0.033 seconds for the XB-70, B-58 and F-104 respectively.

Examination of the net pressure pulses indicated why the response was greater for the B-58 and F-104 missions. For these two aircraft, the net pressure signature was a distorted N-wave. However, the XB-70 net pressure signature was greatly changed from an N-wave and was reduced to two very short pulses separated by approximately 0.24 sec. This net pressure signature produced smaller displacements, as would be expected.

It is therefore reasonable to expect that the future SST, with a faster speed and pressure signature of longer duration, will produce racking displacements of a typical house that will be of similar order of magnitude, or probably smaller, than those produced by the XB-70. However, the magnitude of displacements was very small for all aircraft for the low overpressure levels encountered and were far below the minimum required to cause damage.

PREDICTED DISPLACEMENTS

Predicted racking displacements were computed for the north-south and east-west directions of Test House E-1 using methods explained in Append. A and Equation (A-3):

$$\Delta = \frac{P}{K} \times DAF$$

where
- Δ = Peak dynamic racking displacement
- P = Total racking load on the house
- K = Structure stiffness
- DAF = Dynamic amplification factor as determined from free field signatures

The following is a brief summary of methods used to determine P, K, and DAF.

The total racking load, P, was taken as the average free field peak overpressure from the five cruciform microphones times the effective building surface area. The effective surface area was taken as the area of the vertical surfaces (walls) normal to the direction of racking. The effective areas for racking in the N-S and E-W directions were 159 sq. ft. and 103 sq. ft. respectively. The total load, P, for a free field overpressure of one psf was then P_{ns} = 159 lb. and P_{ew} = 103 lb.

For the small displacements involved, the stiffness K was difficult to accurately calculate utilizing normal values of material properties. Therefore, the stiffness was calculated by approximate methods. The following is an outline of two different methods used to determine the stiffness of House E-1:

8.3

The first method used, which depended in part on recorded test data, was
to determine the stiffness, K, from[8]:

$$T = 2\pi\sqrt{\frac{W}{Kg}} \qquad (8-1)$$

which can be written as:

$$K = \frac{4\pi^2 W}{T^2 g} \qquad (8-2)$$

where W = Weight of roof, ceiling and upper one third of all walls = 18,900 lb.,
and   T = Natural period as determined from integrated accelerometer records.

$$(T_{ns} = 0.062 \text{ sec.}, T_{ew} = 0.083 \text{ sec.})$$

Substituting these values:

$$K_{ns} = 5.0 \times 10^5 \text{ lb/in}$$

$$K_{ew} = 2.8 \times 10^5 \text{ lb/in}$$

The second method of determining the racking stiffness of House E-1 was
the conventional approach which utilized normal values of material properties.
The equation for the deformation of a shear wall due to a shearing load applied
at the top of the wall is[24]:

$$\Delta = \frac{1.2 \, hV}{AG} \qquad (8-3)$$

where Δ = Displacement at top of wall

h = Height of wall = 7.5 ft

V = Shear force applied at top of wall

A = Shear area = wall length times thickness

G = Shearing modulus = 0.4 E = 0.4 (44,200 lb/in^2)

= 17,600 lb/in^2.   (Ref.2)

This equation was rewritten as:

$$V = \frac{AG\Delta}{1.2h} \qquad (8-4)$$

For Δ = 1, V = K = Stiffness, and

$$K = \frac{AG}{1.2h} \qquad (8-5)$$

For Test House E-1, it was determined that there were 229 and 178 lineal
feet (gross length minus width of openings) in the N-S and E-W directions re-
spectively, of wood stud wall with 0.5" thick gypsum board on one face. There-

fore A_{ns} = (229 ft) (0.5 in) (12 in/ft) - 1,374 in^2

A_{ew} = (178 ft) (0.5 in) (12 in/ft) = 1,068 in^2

Substituting the actual values of A, G, and h, the N-S and E-W racking stiffnesses as determined by this second approach were:

K_{ns} = 2.23 x 10^5 lb/in

K_{ew} = 1.72 x 10^5 lb/in

Note that these values were lower than those computed by the first approach. Similar results (where computed displacements, which are inversely proportional to stiffnesses, were greater than those experimentally determined for small deformations) have been observed by others[21]. For this reason, and the fact that the results from the first method depended in part on recorded test data (natural period) and that the weight, W, of the structure could be accurately estimated, the results from the first method were used as being more accurate. Therefore, the values determined by the first method (K_{ns} = 5.0 x 10^5 lb/in and K_{ew} = 2.8 x 10^5 lb/in) were used in the computation of the predicted displacements.

In order to facilitate the computation of predicted displacements, the load, P, and stiffness, K, were combined to determine the unit racking displacement (P/K) for the northeast corner of House E-1 for a sonic boom overpressure of one psf. The unit racking displacements were:

Δ_{ns} = P_{ns}/K_{ns} = 0.00032 in/psf

Δ_{ew} = P_{ew}/K_{ew} = 0.00036 in/psf

Predicted displacements were determined by multiplying these unit racking displacements by the average free field peak overpressure and corresponding DAF from spectra determined from the free field signatures. Predicted racking displacements for House E-1 are summarized in Table 8-3 for typical overhead XB-70, B-58, and F-104 missions.

COMPARISON OF PREDICTED AND MEASURED DISPLACEMENTS

The predicted displacements were plotted versus measured displacements in Figure 8-13. In this figure the 45° diagonal line indicated a one to one ratio of predicted to measured response. The predicted displacements were in good agreement with the measured displacements even though there was some scatter in the measured displacements. For both the east-west and north-south racking of House E-1, it was determined by the use of a statistical t-test that the average

8.5

ratio of predicted displacements (using free field data) to the measured displacements was equal to 1.0 at the 95 percent confidence level. The degree of precision of results and the probability that the results have this degree of precision were summarized in the table on page 5.5.

It was concluded from the comparison of the predicted and measured racking response that the free field peak overpressures and DAF spectra calculated from the free field signatures provide a good method for approximating the actual loading conditions and therefore racking response can be predicted using free field data. This conclusion applies to both "head-on" (aircraft flight track perpendicular to wall surface) and "side-on" (aircraft flight track parallel to wall surface) vectors, since for all practical purposes, the east-west racking is the result of a head-on vector and the north-south racking of a side-on vector.

SUMMARY OF FINDINGS

This section summarized the analysis of the racking response of test houses E-1 and E-2. Predicted response using free field peak overpressures and DAF spectra computed from free field signatures was compared with measured racking response in the north-south and east-west directions of E-1. The aircraft flight track was oriented such that it was possible to study racking response due to aircraft vectors that were nearly head-on (east-west racking) and side-on (north-south racking). The results of the Phase II tests were also compared with those from Phase I[19,20] and White Sands[2] tests. The following findings resulted from these analyses:

1. Racking displacements at the roof line of the northeast corners of test houses E-1 and E-2 were extremely small (less than 0.0018" for E-1 and less than 0.005" for E-2) for sonic booms on the order of 2 psf overpressure.

2. Racking displacements of E-1 and E-2 recorded during Phases I and II were of similar magnitudes for similar overpressures.

3. The racking displacements of E-1 and E-2 recorded during Phase II were of magnitude similar to displacements obtained at White Sands[2] for structures of similar construction and for similar overpressures.

4. Racking displacements predicted from free field peak overpressures and DAF spectra calculated from free field pressure signatures were in good agreement with measured displacements. For both the east-west and north-south

8.6

racking of house E-1, the average ratio of the predicted to measured displacement was equal to 1.0 at the 95 percent confidence level for comparable XB-70, B-58, and F-104 missions. These findings applied to both head-on and side-on vectors.

5. Racking response could be adequately predicted by using peak overpressure and DAF spectra calculated from free field signatures.

6. The future SST, for peak overpressures of about 2 psf, should produce racking displacements of typical houses that will be of similar magnitude, or possibly smaller, than those caused by the XB-70 missions. These racking displacements should be negligible and far below those required for damage.

The implications of these findings as related to structure element damage are discussed in Chapter IX. The following section discusses the racking response of the Bowling Alley.

B. BOWLING ALLEY E-3

This section briefly summarizes the analysis of the racking response of the Bowling Alley E-3.

INSTRUMENTATION

In order to study the racking response of the Bowling Alley, accelerometers were installed near the tops of the steel columns as shown in Appendix B.

TEST RESULTS - MEASURED DISPLACEMENTS

The analog magnetic tape recordings of the accelerometer data were converted to digital form as discussed in Chapter IV and then numerically integrated twice to obtain displacements. Peak displacements for typical missions of XB-70, B-58, and F-104 aircraft are listed in Table 8-4. The displacements were of extremely low magnitude (all less than 0.0041 inches). As free field signatures were not measured near the Bowling Alley, a comparison could not be made of displacements predicted from free field versus measured displacements. The magnitude of the racking displacements were so small (ie s than the ma.imum measured for E-2) that there was no damage.

TABLE 8-1

RACKING ACCELERATIONS AT ROOF LINE

NORTHEAST CORNER OF TEST STRUCTURES E-1 AND E-2

House	Racking Direction	Aircraft	Mission	Average Free Field Pressure	Peak Acceleration[1]	
				psf	ft/sec^2	g's
E-1	E-W	XB-70	13-2	2.00	-2.92	-0.091
			15-1	2.18	-2.51	-0.078
			16-2	2.29	-3.74	-0.116
		B-58	13-1	2.21	-3.80	-0.118
			15-2	2.34	+3.66	+0.114
			16-1	2.25	-3.82	-0.118
		F-104	13-3	2.01	-3.81	-0.118
			15-3	2.31	+4.74	-0.146
			16-3	2.02	-3.94	-0.122
E-1	N-S	XB-70	13-2	2.00	-4.26	-0.132
			15-1	2.18	-3.24	-0.100
			16-2	2.29	-4.21	-0.131
		B-58	13-1	2.21	-5.05	-0.157
			15-2	2.34	-4.02	-0.125
			16-1	2.25	-3.61	-0.112
		F-104	13-3	2.01	-6.01	-0.186
			15-3	2.31	+5.02	+0.156
			16-3	2.02	-3.17	-0.095
E-2	E-W	XB-70	13-2	2.00	-2.71	-0.084
		B-58	13-1	2.21	-2.56	-0.079
		F-104	13-3	2.01	-8.67	-0.268
E-2	N-S	XB-70	13-2	2.00	-3.65	-0.113
		B-58	13-1	2.21	+2.91	+0.090
		F-104	13-3	2.01	+3.29	+0.102

1) Minus sign indicates acceleration toward house.

   Plus sign indicates acceleration away from house.

TABLE 8-2

RACKING DISPLACEMENTS AT ROOF LINE

NORTHEAST CORNER OF TEST STRUCTURES E-1 AND E-2

House	Racking Direction	Aircraft	Mission	Average Free Field Pressure	Racking Displacement[1]	Normalized Racking Displacement
				psf	inch	in/psf
E-1	E-W	XB-70	13-2	2.00	+0.00129	0.00065
			15-1	2.18	+0.00112	0.00051
			16-2	2.29	+0.00112	0.00049
		B-58	13-1	2.21	-0.00156	0.00071
			15-2	2.34	-0.00120	0.00051
			16-1	2.25	-0.00157	0.00070
		F-104	13-3	2.01	+0.00177	0.00088
			15-3	2.31	+0.00156	0.00068
			16-3	2.02	+0.00168	0.00083
E-1	N-S	XB-70	13-2	2.00	-0.00142	0.00071
			15-1	2.18	-0.00094	0.00043
			16-2	2.29	-0.00077	0.00034
		B-58	13-1	2.21	+0.00148	0.00067
			15-2	2.34	+0.00099	0.00043
			16-1	2.25	+0.00077	0.00034
		F-104	13-3	2.01	+0.00177	0.00088
			15-3	2.31	+0.00137	0.00059
			16-3	2.02	+0.00162	0.00080
E-2	E-W	XB-70	13-2	2.00	-0.00309	0.00155
		B-58	13-1	2.21	+0.00421	0.00190
		F-104	13-3	2.01	+0.00379	0.00188
E-2	N-S	XB-70	13-2	2.00	+0.00310	0.00155
		B-58	13-1	2.2	+0.00298	0.00135
		F-104	13-3	2.01	-0.00491	0.00245

1) Minus sign indicates displacement toward house.

Plus sign indicates displacement away from house.

8.9

TABLE 8-3

PREDICTED RACKING DISPLACEMENTS

HOUSE E-1

Direction	Aircraft	Mission	Measured Displacement ΔM	Free Field Pressure	Free Field DAF	Predicted Displacement ΔP	$\frac{\Delta P}{\Delta M}$
			Inches	psf		Inches	
E-W	XB-70	13-2	0.00129	2.00	1.74	0.00125	0.97
		15-1	0.00112	2.18	1.68	0.00132	1.18
		16-2	0.00112	2.29	1.70	0.00140	1.24
	B-58	13-1	0.00156	2.21	1.54	0.00123	0.79
		15-2	0.00120	2.34	1.55	0.00130	1.08
		16-1	0.00157	2.25	1.54	0.00124	0.79
	F-104	13-3	0.00177	2.01	1.70	0.00123	0.70
		15-3	0.00156	2.31	1.76	0.00130	0.84
N-S	XB-70	13-2	0.00142	2.00	1.77	0.00113	0.80
		15-1	0.00094	2.18	1.70	0.00118	1.26
		16-2	0.00077	2.29	1.72	0.00126	1.64
	B-58	13-1	0.00148	2.21	1.62	0.00114	0.77
		15-2	0.00099	2.34	1.58	0.00118	1.19
		16-1	0.00077	2.25	1.58	0.00114	1.48
	F-104	13-3	0.00177	2.01	1.49	0.00096	0.54
		15.3	0.00137	2.31	1.65	0.00122	0.89

8.10

TABLE 8-4

BOWLING ALLEY RACKING DISPLACEMENTS

AT TOP OF SOUTHEAST CORNER COLUMN

IN EAST-WEST DIRECTION

Aircraft	Mission	Peak Acceleration[1] ft/sec^2	Peak Displacement[1] Inches
XB-70	12-2	-0.631	-0.00308
	113-2	-0.604	0.00406
B-58	12-1	0.903	-0.00354
	113-1	-0.564	-0.00341
F-104	12-3	0.682	-0.00134
	113-3	-0.412	-0.00087

1) Minus sign indicates acceleration or displacement in eastern direction.

N-S ACCELEROMETERS
ROOF LINE, CHNL #01
2ND FLOOR LINE, CHNL 405

E-W ACCELEROMETER
AT ROOF LINE,
CHNL. 201

N-S ACCELEROMETER
AT ROOF LINE,
CHNL. 203

E-W ACCELEROMETERS
ROOF LINE, CHNL. +03
2ND FLOOR LINE, CHNL.
407.

E-2
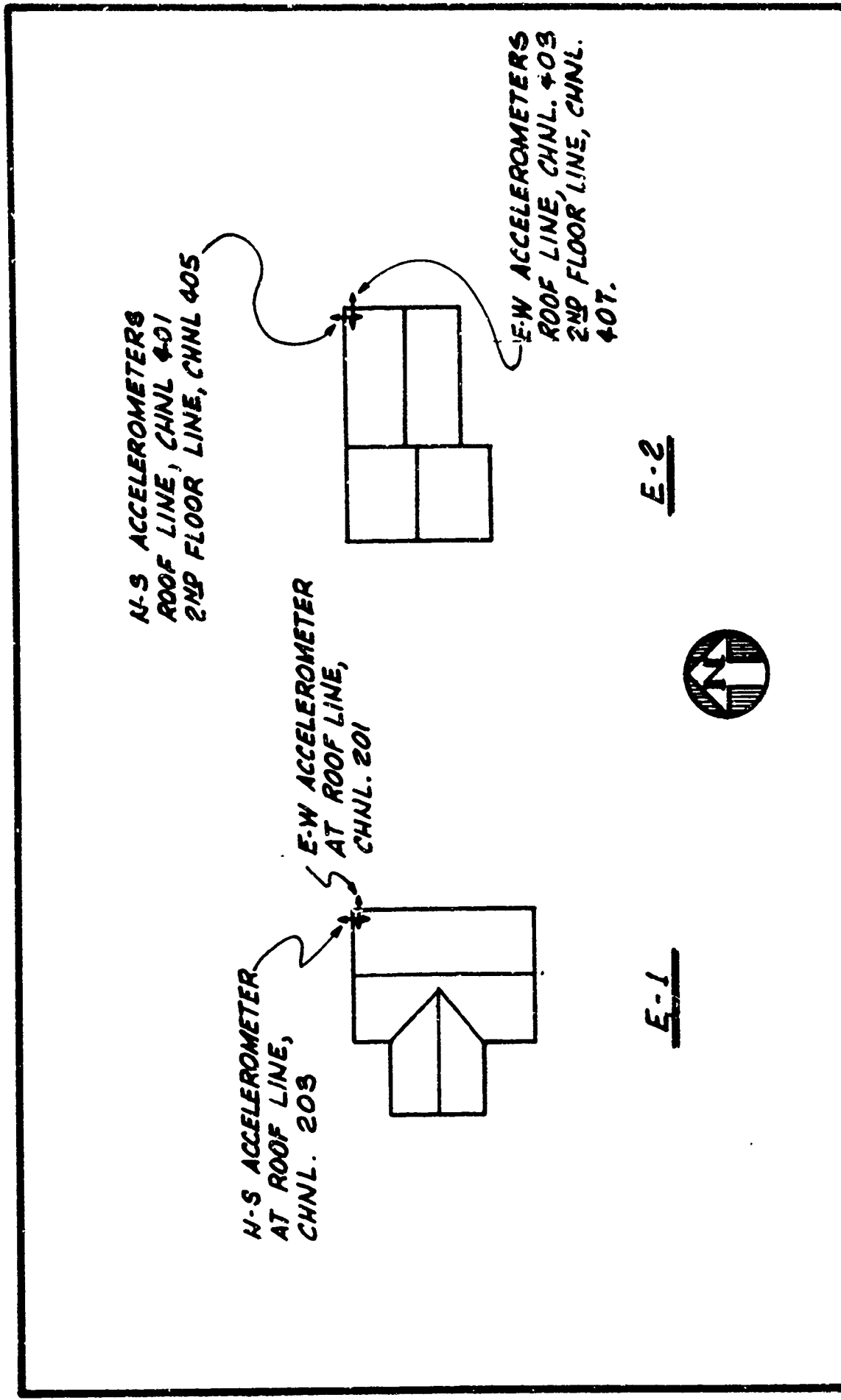
E-1

RACKING ACCELEROMETER LOCATION
TEST HOUSES E-1 & E-2

FIG.
8-1
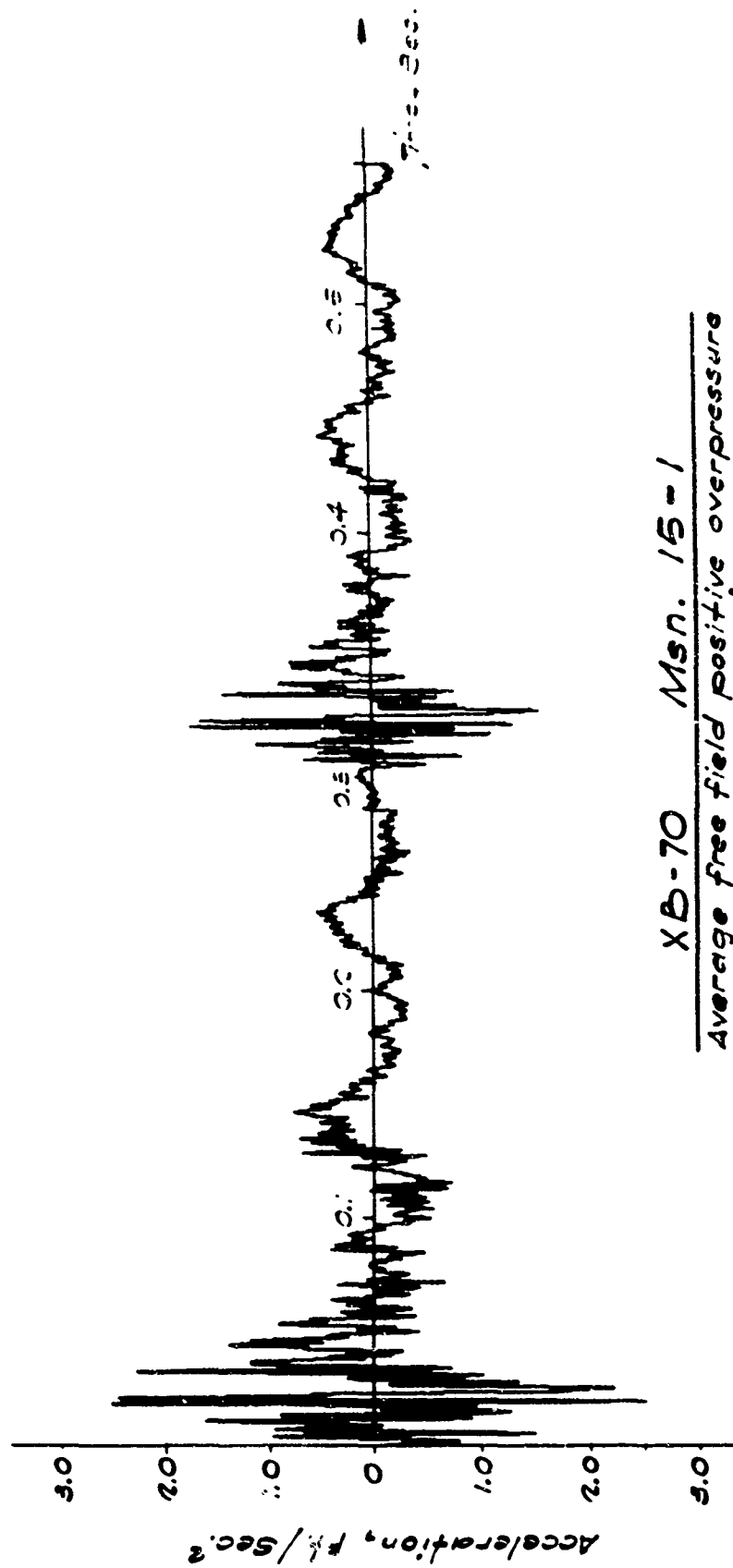
FIG.
8-1

XB-70   Msn. 15-1

Average free field positive overpressure
= 2.16 p.s.i.

EAST-WEST   RACKING   ACCELERATION
AT ROOF LINE OF N.E. CORNER OF HOUSE E-1
(CHANNEL 201)

FIG.
8-2
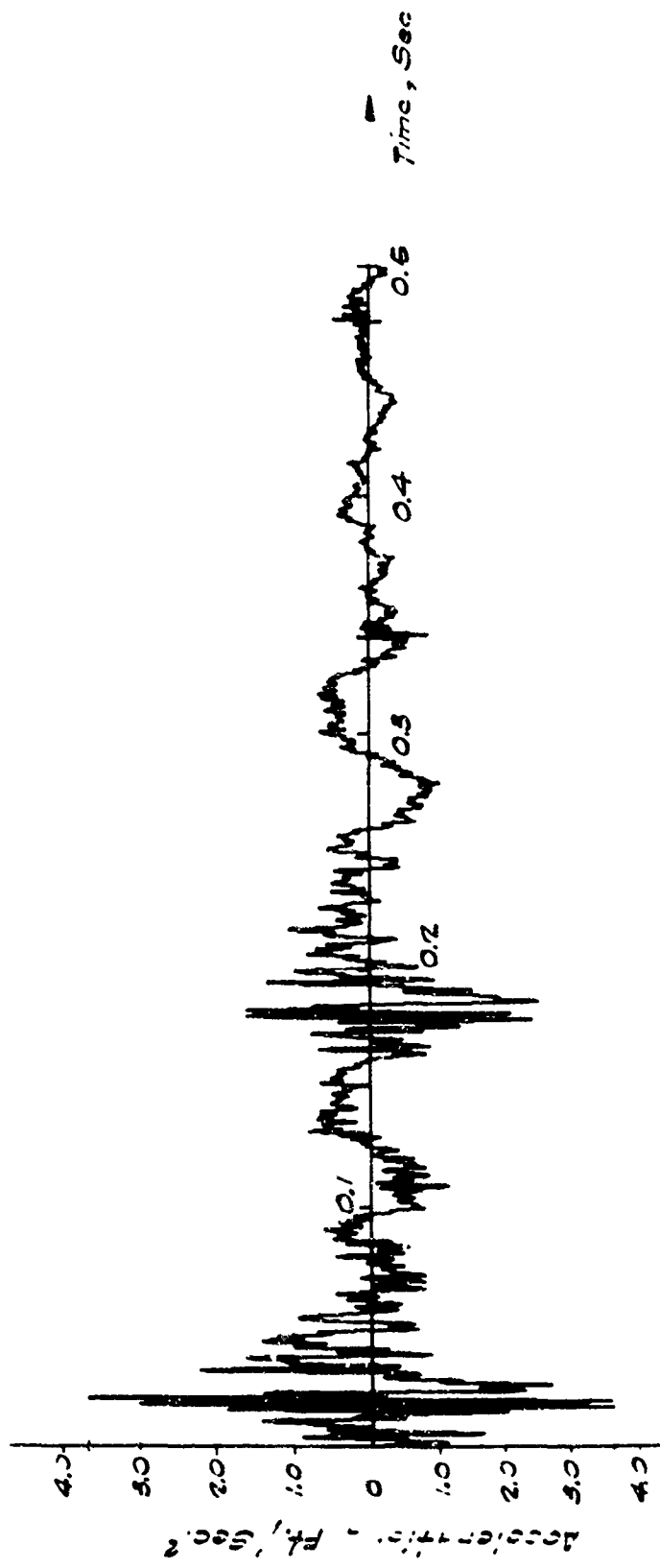
B-58   Msṇ. 15-2

Average free field positive overpressure
= 2.54 p.s.f.

EAST-WEST RACKING ACCELERATION
AT ROOF LINE OF N.E. CORNER OF HOUSE E-1
(CHANNEL 201)

FIG.
3-3

F-104 Msn. 15-3

Average free field positive overpressure = 2.61 p.s.f.

EAST-WEST RACKING ACCELERATION
AT ROOF LINE OF N.E. CORNER OF HOUSE E-1
(CHANNEL 201)

FIG. 8-4
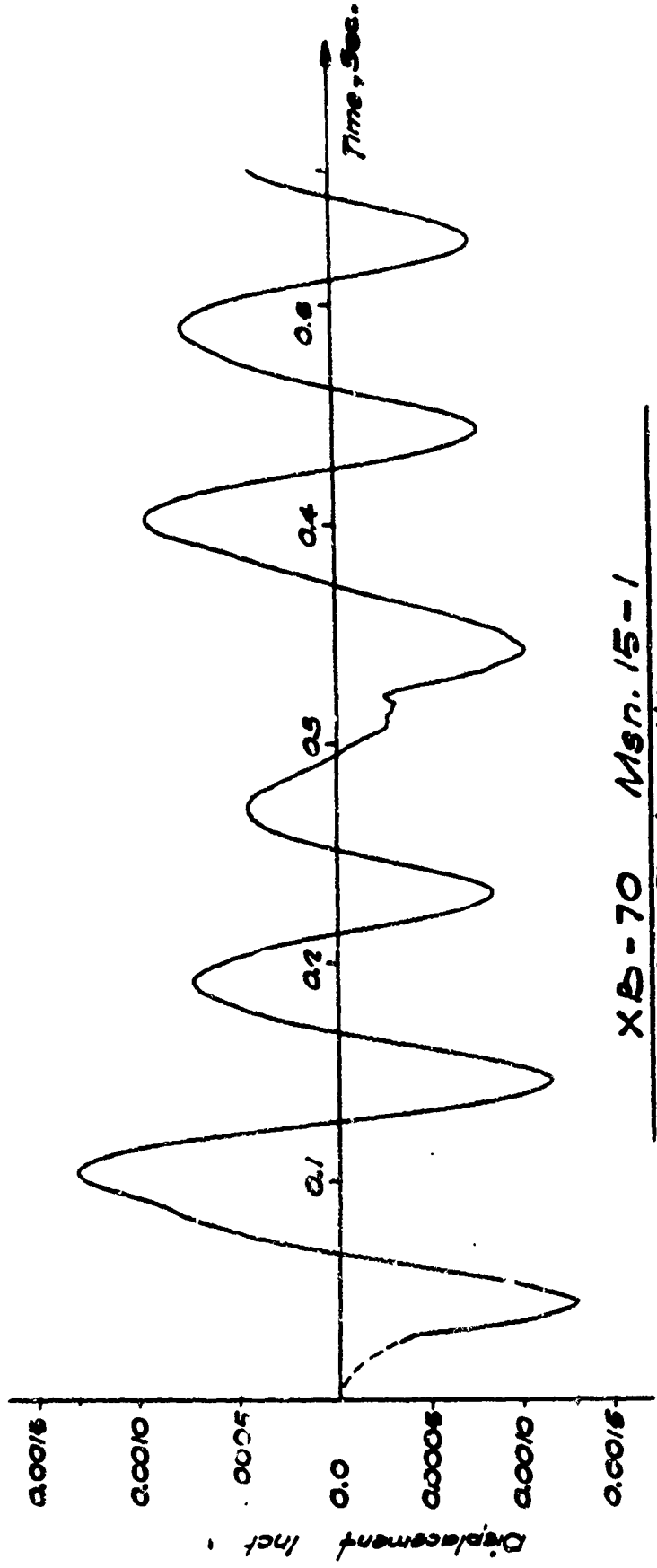
8.15

XB-70 Msn. 15-1

Average free field positive overpressure = 2.18 p.s.f.

EAST-WEST RACKING DISPLACEMENT AT ROOF LINE OF N.E. CORNER OF HOUSE B-1 (CHANNEL 201)

FIG. 8-5

B-58   Msn. 15-2

Average free field positive overpressure
= 1.34 p.s.f.

EAST-WEST   RACKING   DISPLACEMENT
AT ROOF LINE OF N.E. CORNER OF HOUSE E-1
(CHANNEL 201)

FIG.
8-6

8.17

F-104   Msn. 15-3

Average free field positive overpressure = 2.31 p.s.f.
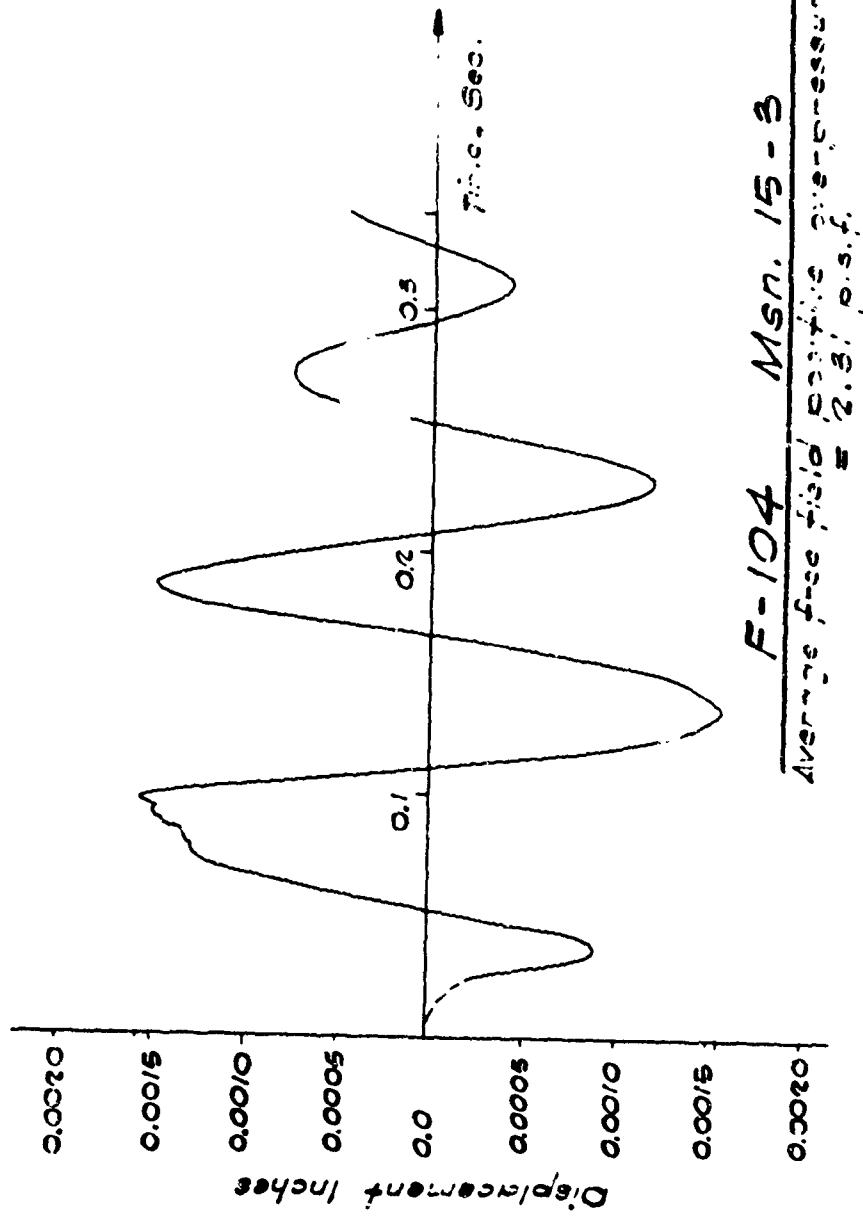
EAST - WEST RACKING DISPLACEMENT
AT ROOF LINE OF N.E. CORNER OF HOUSE E-
(CHANNEL C-25)

FIG. 8-7

8.18

PHASE I FLIGHTS

MSN	A/C	ALT	MACH	FREE FIELD PRESSURE psf
14	F-104	35.6K	1.70	1.19
46B	B-58	43.7K	1.65	1.63
13	XB-70	52.9K	1.81	2.52
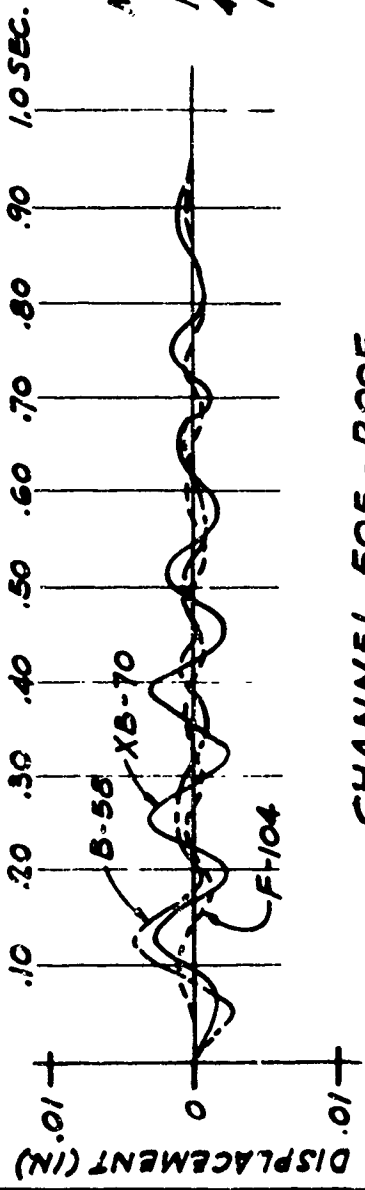
CHANNEL 505 - ROOF

PHASE I FLIGHTS

MSN	A/C	ALT	MACH	FREE FIELD PRESSURE psf
14	F-104	35.6K	1.70	1.19
46B	B-58	43.7K	1.65	1.63
13	XB-70	52.9K	1.81	2.52
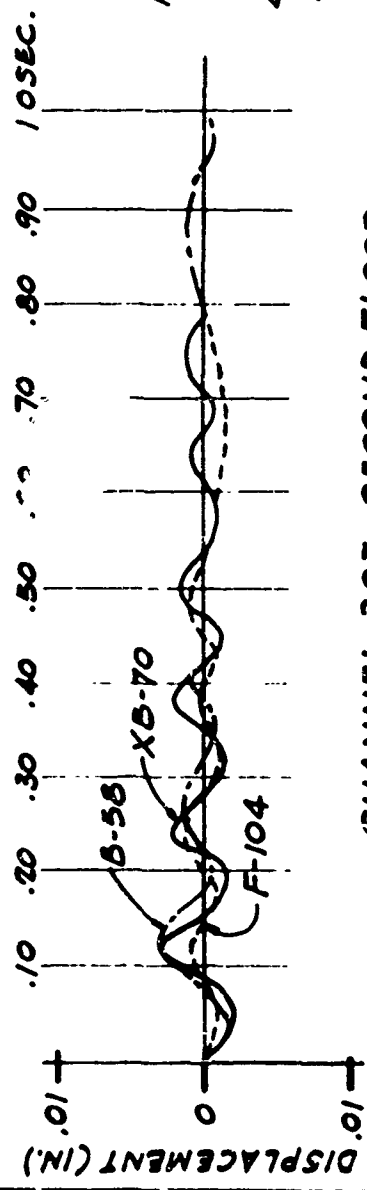
CHANNEL 307 - SECOND FLOOR

RACKING DISPLACEMENTS N-S ~ E-2

FIG.
8-8
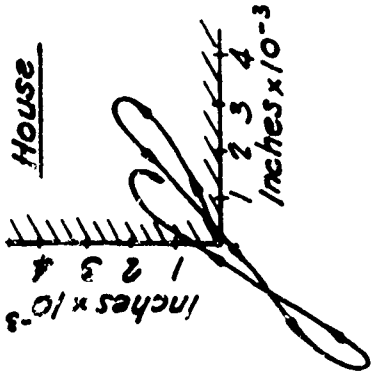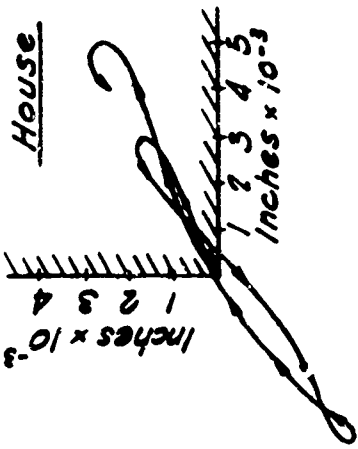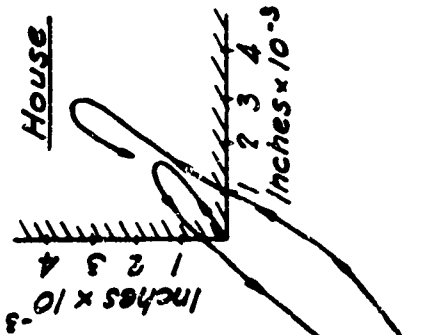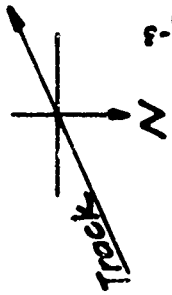
FIG.
8-8

Aircraft	F-104	B-58	XB-70
Mission	13-3	13-1	13-2
Avg. Peak Pressure	2.01 psf	2.21 psf	2.00 psf
Avg. Rise Time	0.0053 sec.	0.0049 sec.	0.0079 sec.

RACKING DISPLACEMENT AT ROOF LINE OF NORTHEAST CORNER OF TWO STORY HOUSE E-2

FIG. 8-9

PRESSURE SIGNATURES, HOUSE E-I

XB-70 Mach = 1.80, Duration = 0.287 sec., Mission 13-2
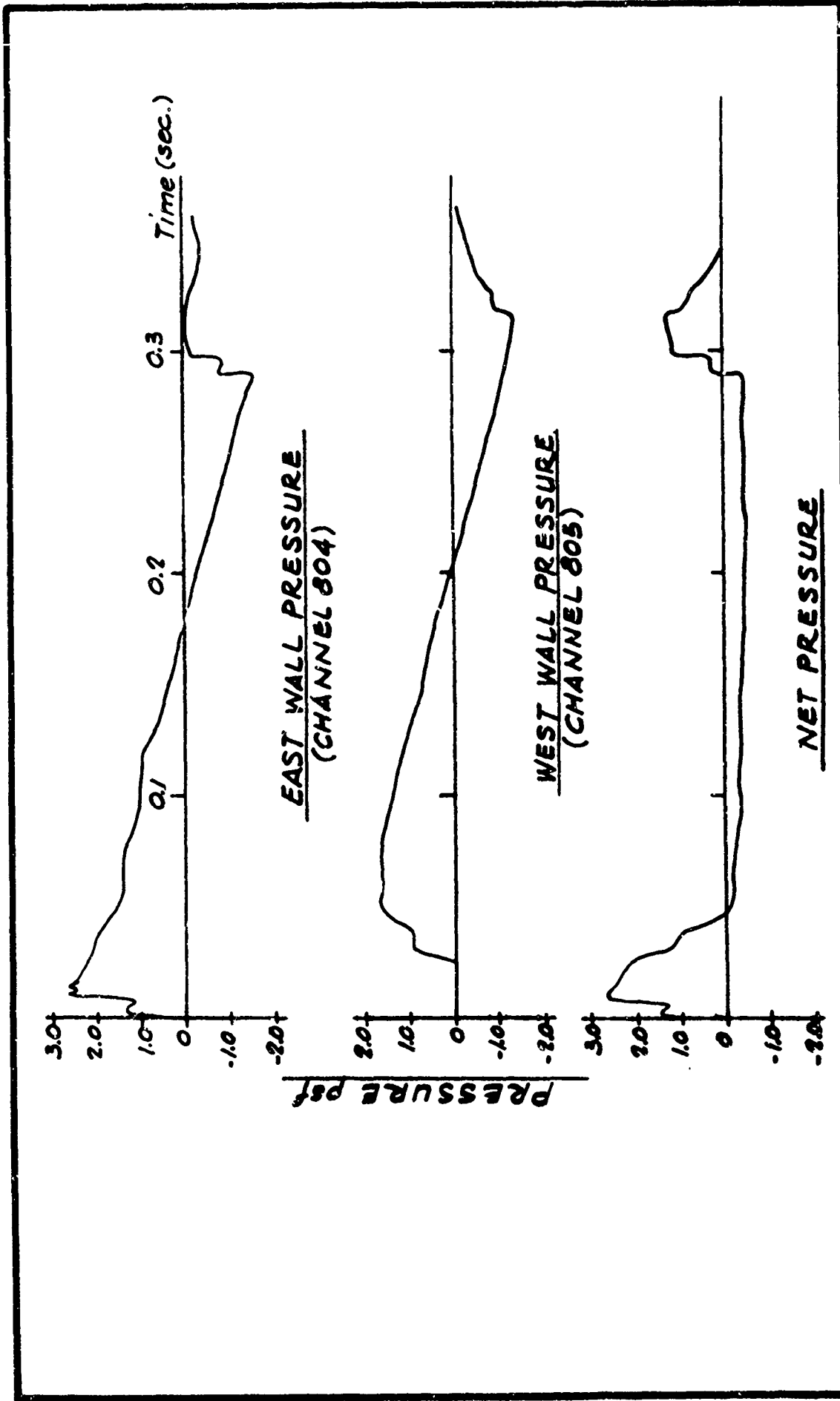
FIG.
8-10

PRESSURE SIGNATURES, HOUSE E-l
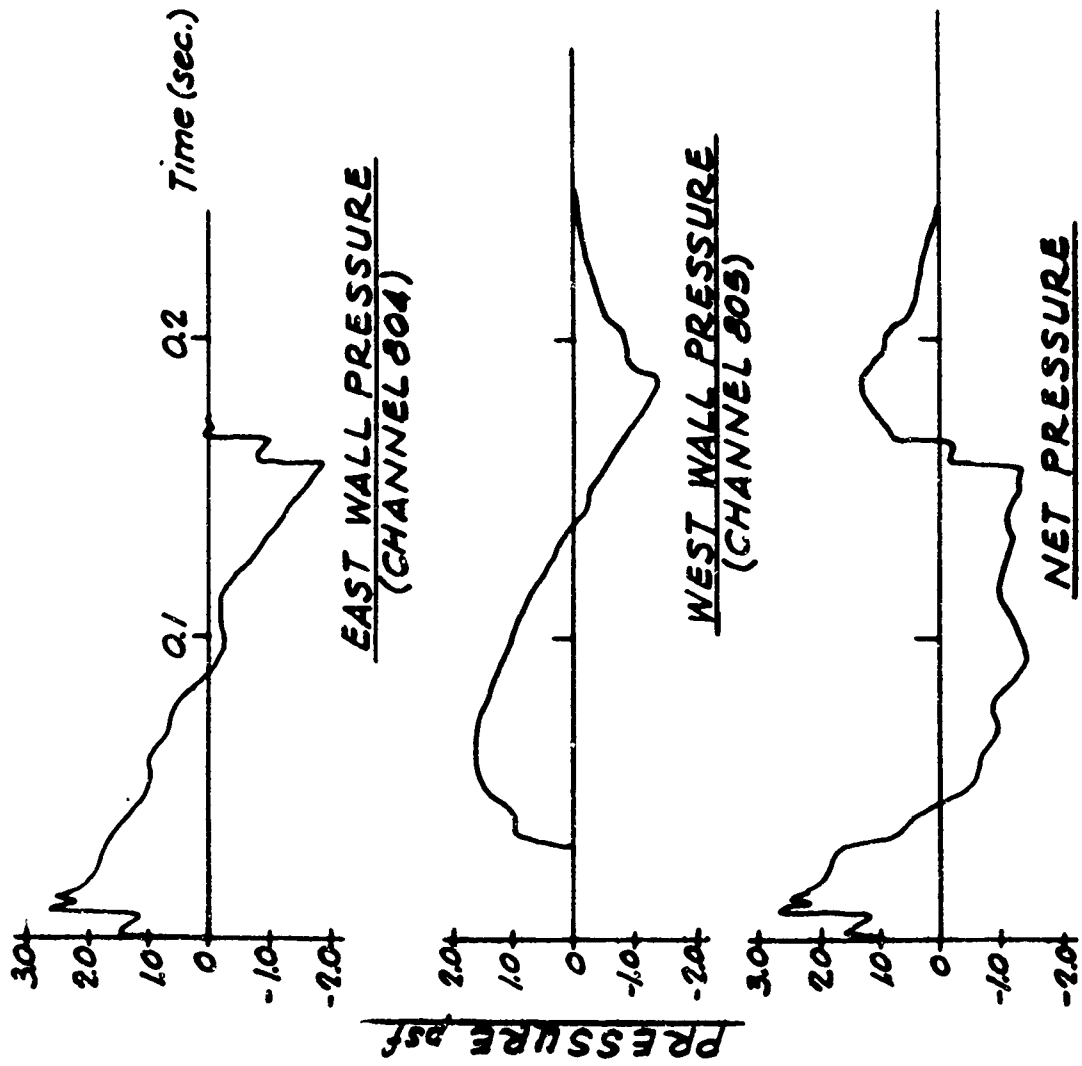
B-58   Mach. = 1.65   Duration = 0.159 sec., Mission 13-1

FIG.
8-11

FIG.
8-11

PRESSURE SIGNATURES, HOUSE E-1
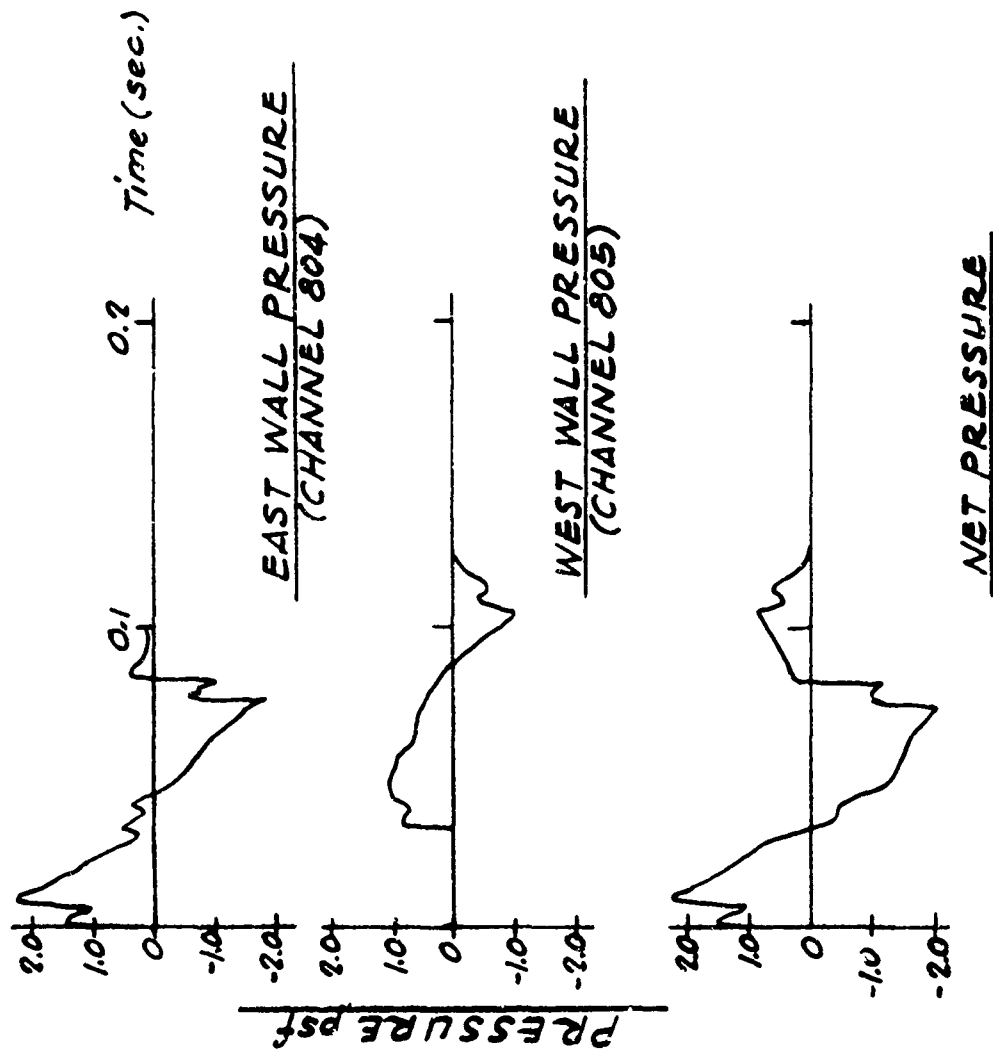
F-104   Mach = 1.40, Duration = 0.074 sec., Mission 13-3

FIG.
8-12
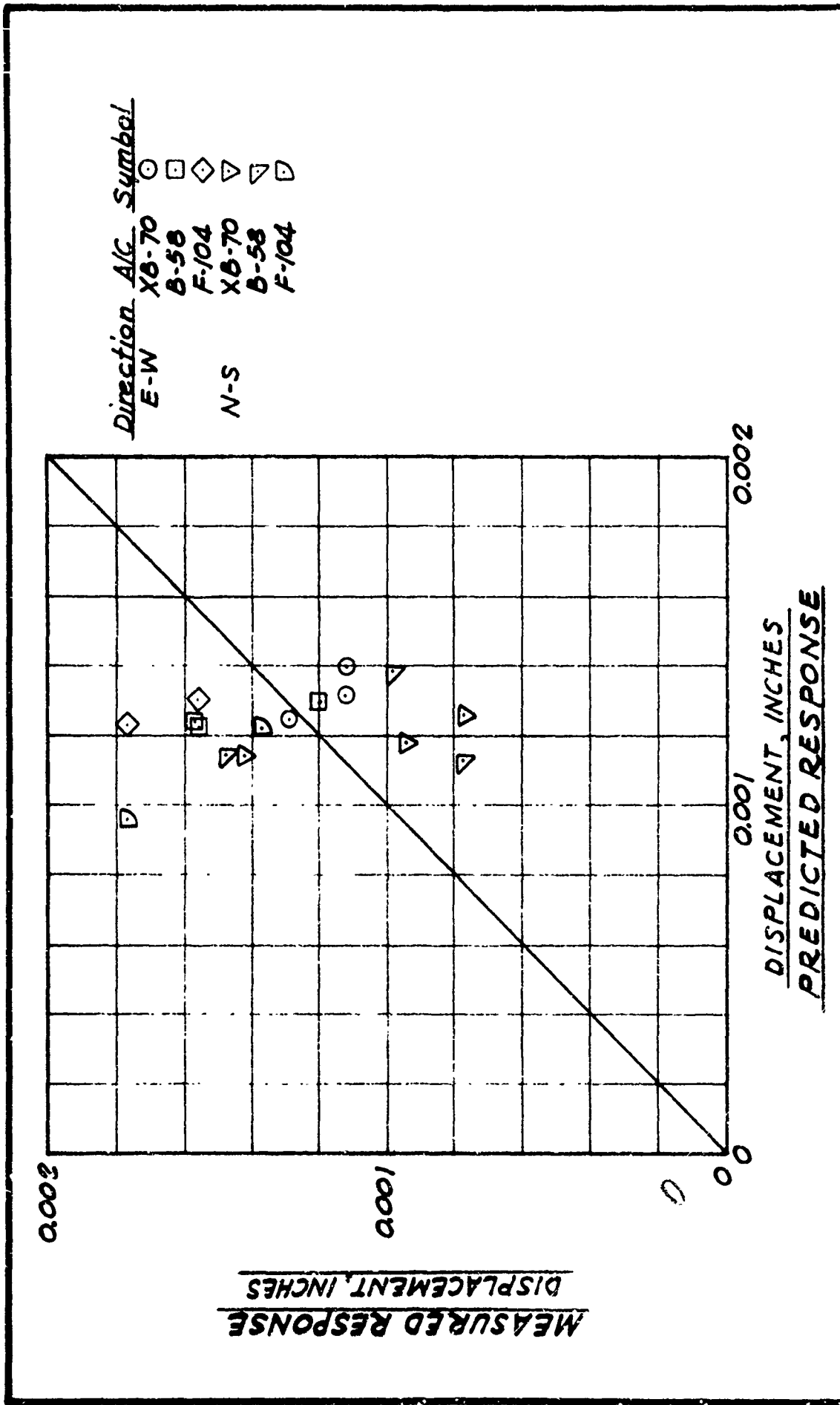
MEASURED RESPONSE vs PREDICTED RESPONSE
BASED ON FREE FIELD SIGNATURES, RACKING, HOUSE E.1

FIG.
8-13

8.24

IX. STRUCTURE DAMAGE

The advent of supersonic aircraft and the accompanying sonic booms have produced undesirable side effects. Two of these effects are the irritation of people when subjected to a sonic boom and the damage to structures and structure elements caused by the sudden changes in over-pressure produced by the sonic boom. The reactions of people are covered by reports by other participants in the Edwards Program. However, there would appear to be a link between a person's fear of structure damage when a boom occurs and his irritation about the boom. In this connection, educa-tion of the public with regard to what damage actually occurs versus feared damage from sonic booms would be beneficial.

In addition to helping reduce personal irritation with sonic booms, the process of adjudicating complaints and claims of sonic boom damage would be helped immeasurably if more knowledge and data were available regarding sonic boom damage. It is doubtful that sufficient data can be obtained to prove whether all damage claimed from sonic booms was or was not directly caused by a boom. Therefore, data and procedures should be developed to establish most likely or most probable causes of damage.

Since 1955 there have been over $18 million claimed damages from sonic boom. During FY 1966 nearly 5,000 claims were filed. As time passes, more sonic booms will be generated as more supersonic flights are made and the number of damage complaints and claims will increase accordingly. The number of complaints could possibly be reduced if more were known about what actual damage does occur.

The ultimate objective of the studies of structure response to sonic booms is to understand the mechanism of failure under sonic boom loading to that damage claims can be properly evaluated. Failure implies that the load-ing has exceeded the ultimate strength of the structure element in question. Therefore, the objective could be divided into two parts: description of loading mechanism and prediction of magnitude of loading, and description of the strength of a structure element and prediction of its ultimate strength.

9.1

The knowledge gained through these analyses was sufficient to properly describe the loading mechanism. Mathematical and statistical models, some derived expressly for the Edwards study, can be used in predicting the load on a structure element, thus eliminating extensive instrumentation. The response of a structure or structure element can now be predicted with a good degree of accuracy. NASA has developed reliable methods for predicting the magnitude of overpressure. The analyses of Edwards free field signature data indicated that the Dynamic Amplification Factor (DAF) is influenced by the ratio of the peak negative overpressure (absolute value) to the peak positive overpressure. The studies also indicated that DAF is affected by the ratio of rise time, T_I, boom duration, τ. This ratio appears to increase with increase in lateral offset of the flight track.

Review of the location of damage complaints at Milwaukee, Chicago, Pittsburgh, St. Louis and Oklahoma City indicated that often there are more complaints at some distance either side of the flight track than there are directly under the track. In all cases the complaints are spread over a fairly wide area. Figure 9-1 illustrates one possible cause for this lateral spread of complaints. Figure 9-1(a) shows the decay of overpressure with lateral offset. Figure 9-1(b) indicates how the ratio P_2/P_I may decrease with offset (as shown in Chapter V values of maximum DAF similarly decrease). Figure 9-1(c) illustrates the trend of the ratio T_I/τ as indicated by the analysis of Edwards data. Figure 9-1(d) indicates the possible combined effect of the two ratios on DAF. The amount of data recorded near the two test house structures at Edwards AFB was not sufficient to clearly define the trend of the variations in T_I and P_2/P_I. Additional free field signatures of comparable missions of XB-70 and B-58 aircraft were recorded by NASA for varying offsets of the aircraft during the Edwards testing. It is recommended that these signatures be analysed to determine if trends in the two ratios P_2/P_I and T_I/τ can be established and hence determine the resulting effects on DAF values. These analyses could be an extension of the studies in Chapter VI. The results would also help establish the effective width of the "boom swath" laid down by supersonic aircraft and hence the number of structures exposed to potential damaging conditions. These data together with boom propagation and signature prediction methods developed by NASA should result in a method for predicting load magnitude for level flights with a good degree of accuracy.

9.2

The sonic boom tests at Edwards AFB were not designed to study the damage of test structures due to sonic booms, and no damage was observed in the test houses. However, it may be inferred from a study of the magnitudes of the deformations obtained during the test flights that damage of a properly designed and constructed house due to low magnitude booms (on the order of 2 psf) is extremely unlikely. The reasoning behind this statement is given in the following discussion of the two types of structural response; plate (lateral displacement) and racking (in-plane displacement).

The maximum magnitudes of the plate displacements for both the walls and the large galss window in Test House E-1 were considerably below the levels required to cause damage. The maximum displacement was measured for the DR, E-2 wall and was 0.034 inches (Chapter VII). This displacement corresponded to a calculated stress in the gypsum board on the interior of the wall that was less than 2 percent of the failure stress of gypsum board. The maximum stress as determined from the strain records in the E-1 garage window was 790 psi, whereas the average flexural strength of regular plate glass can be taken as 6000 psi[33].

The racking displacements for both of the test houses were also less than the levels necessary to cause damage to either plaster or glass. The peak racking displacements at the roof lines of the northeast corners of the Test Houses E-1 and E-2 were less than 0.002" and 0.005" respectively. That these magnitudes were less than those required to produce damage to plaster or gypsum board walls has been substantiated by several series of previous tests. Sonic boom tests at White Sands[2] indicated that sonic boom overpressures of from 7 to 10 psf were required before any damage was observed in similar type structures. (It should be noted that the damage criteria was a crack that could be detected with a magnifying glass.) In addition, a series of laboratory racking tests[22] of 8' by 8' stud wall panels with gypsum board wall covering (with and without openings) demonstrated that a minimum deflection of 0.16" could be obtained before any cracks were observed. It was estimated that the racking displacements of the test houses caused by the sonic booms could have been increased by at least five times before any noticeable damage would have occurred.

The extremely low racking displacements obtained at Edwards AFB and
White Sands for nominal 2 psf sonic booms also indicated that glass damage
due to a racking mode of failure is extremely unlikely and, in fact, should
not occur. Previous laboratory tests[23] indicated that it is conservative to
take 1/16" per foot of height (1/4" for a 4' high window) as the allowable
racking deflection for a conventionally mounted window. In these tests, it
was found that for nominal as-installed clearances of from 1/4" to 1/2", the
total racking displacement before failure of the glass for a square window
4' by 4' varied from 1/2" to 2". The magnitude of deformation at failure
obtained in these tests was compared with the results of the previously
mentioned wall racking tests and the White Sands tests. It was concluded
that considerable plaster damage should occur before any glass damage occurs
due to racking deformation of the structure.

Based on the reasoning in the previous discussion, it was concluded
that damage in either a plate or racking mode of failure to a properly de-
signed and constructed house due to low magnitude sonic booms (on the order
of 2 psf) is extremely unlikely. However, more than this conclusion is
needed to fully understand the problem of damage due to sonic booms. The
mechanism of the loading has been well established by the EAFB tests and
others, but little data is available on the strength of in-place materials
and modes of failure of elements. The following questions therefore remain
unanswered:

1. For complaints of sonic boom damage, what is the condition and
environment of the structure in which the damage occurred? What is its age,
strength, and level of maintenance? The statistical description of the
strength of a structure element and prediction of its ultimate strength de-
pend on many factors. The strength of a material can be obtained from labora-
tory tests. However, it is reasonable to assume that the failure strength of
the material, once it is a part of a structure, may be different from its
strength in the laboratory. There are many environmental conditions of a
structure that could affect the failure strength of material in place as a
structure element. Age and history of loading, differential shrinkage and/or
settlement of the structure, large temperature differentials, weathering ef-
fects, humidity changes, wind loading, installation techniques, and other
factors can have major effects on the failure point of an element.

9.4

2. Did the sonic boom act as a trigger? This may be extremely important because the stresses due to sonic booms of low pressure levels may be extremely small. Is it possible that the damaged element was stressed to the verge of failure prior to the boom due to the method of installation, shrinkage, settlement, temperature differentials or other factors?

3. What is the relationship of damage caused by sonic boom to damage caused by natural phenomena such as wind, earthquake, and weathering? Was the element exposed to possible damage by wind loading or other phenomena? Why do windows and walls withstand high velocity winds and yet apparently break under low overpressure booms? What were the overpressures at the time of damage? Does sonic boom damage occur with higher or lower frequency in elements (e.g., ceilings) that are not normally subjected to loading by natural forces.

The answers to the above questions must be obtained before the following can be determined:

1. What is the mode of failure of structure elements due to sonic boom loading?

2. What damage is actually caused by sonic booms? If damage is not caused by sonic boom, what does cause it? What is the most likely cause of damage?

3. At what overpressure level will there be a minimum expenditure on damage claims?

Thus, it is evident that more knowledge is required about the environmental strength and characteristics of structure elements - especially those that have been claimed as failures due to boom loading. The criterion for evaluating damage claims should be based on an evaluation of the most probable causes of failure knowing the environmental conditions of the element and the sonic boom loading on the element.

9.5

SUMMARY OF FINDINGS

This chapter presented a review of the results of the tests at Edwards and tests by others as applied to damage from sonic boom of low magnitudes (in the order of 2 psf). The following findings were derived:

1. Damage to properly designed and constructed houses from low magnitude sonic booms is extremely unlikely.

2. Damage should not occur to structure elements such as glass windows from racking motions caused by low magnitude sonic booms.

3. Other causes may result in many complaints or claims even at low levels.

4. Further data is needed on modes of failure of structure elements in order to evaluate damage and determine the most likely cause of damage.

P_1 = Peak positive overpressure
P_2 = Peak negative overpressure (absolute value)

T_1 = Rise time
τ = Boom duration

For XB-70, M = 2.0 @ 60,000 ft.
Gross weight 400,000 lbs.

Lateral distance from flight track, statute miles

(a) P_1
(b) P_2/P_1
(c) T_1/τ
(d) $R \times DAF$
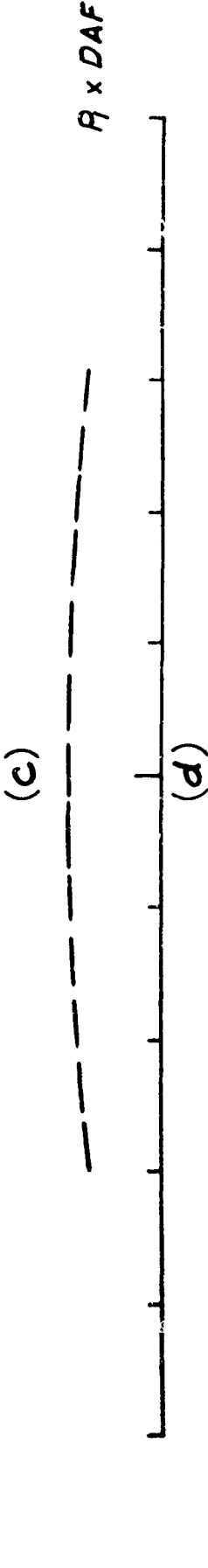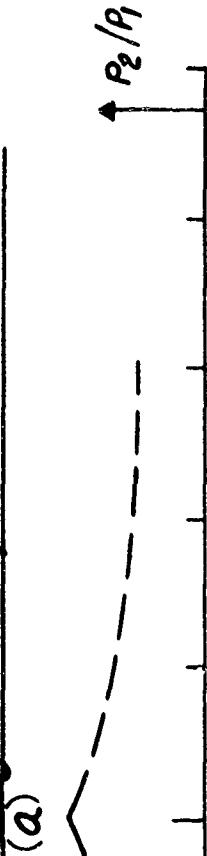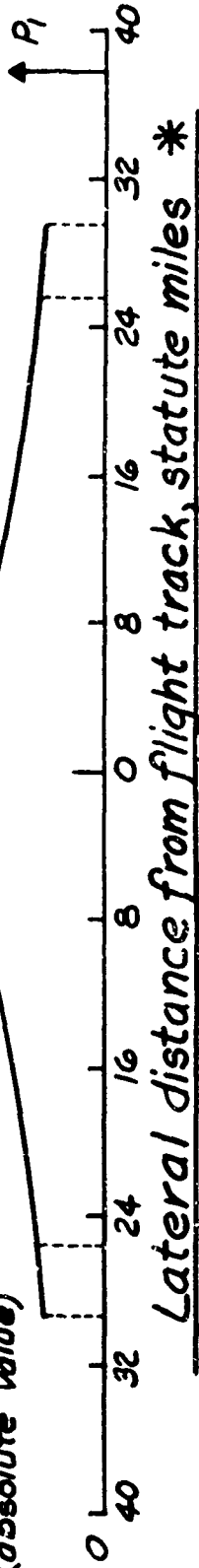
* See reference 34

POSSIBLE EFFECT OF OFFSET ON DAMAGE PREDICTION

FIG. 9-1

9.7

X. GENERALIZED DAF SPECTRUM

In the preceding chapters it was found that the response of a structure element could be computed by using free field overpressures and the DAF computed from the free field signatures. It was also found that the DAF spectra calculated by using a wave model described by free field signature parameters P_1, P_2, T_1 and T_2 (Figure 6-1) were equal to the DAF spectra obtained from digitized free field signatures. The purpose of the study discussed in this chapter was to derive a generalized DAF spectrum to use in predicting the response of a structure element when only the nominal free field overpressure and the type of aircraft were known.

To fulfill this purpose different non-linear regression models, see Appendix A, were fitted through DAF spectra computed from digitized free field signatures for XB-70, B-58 and F-104 missions. A total of 630 data points were used for the XB-70 missions, 540 for the B-58, and 350 for the F-104. The asymptotic behavior of these regression models was studied with the following results. For the XB-70 missions the asymptotes converged to a value of 2, for the B-58 to a value of 2 and for the F-104 to a value of 2.15. The upper frequency for which these models were computed was 50 cps. An effective cutoff in the lower frequencies was determined at the DAF value of 1. Using the signature wave model, lower frequency intercepts were calculated for free field signatures with durations equal to 0.4 and 0.5 seconds.

It was assumed in deriving this generalized DAF spectrum that 1) the free field signatures recorded in the E-2 cruciform microphone array could be considered as representative of future supersonic missions and, 2) the wave model derived for XB-70, B-58 and F-104 signatures could be extended to signatures with durations longer than 0.3 seconds.

The plotted values of the asymptotes represented the DAF spectrum. Since the modeling was done using statistical methods, the standard deviations of the asymptotes were readily determined and used in the calculation of the confidence interval. The dashed lines above and below the spectrum in Figure 10-1 represented a 95% confidence interval. This meant that there was a 95% probability that the peak values of the DAF spectrum were observed within the limits of the interval and that there was a 97.5% probability that all values of the DAF spectrum would be below the top line of the interval.

The generalized DAF spectrum could be used to obtain a prediction of the response of a known structure element. For example, knowing that an F-104 will fly at supersonic speed and will generate a sonic boom with a nominal overpressure of 2 psf, the response of a structure element can be predicted by multiplying the overpressure of 2 psf by a DAF of 2.15 and then dividing this product by the stiffness of the structure element. It should be emphasized that the DAF of 2.15 for F-104 applies only when the natural frequency of the element is greater than 4.4 cps and smaller than 50 cps. If a more detailed answer is desired and if the free field signature parameters (P_1, P_2, T_1, T_2) have been measured, a DAF spectrum can be computed from the wave model and the response then obtained from the corresponding DAF and the measured overpressure.

SUMMARY OF FINDINGS

The purpose of the study discussed in this chapter was to derive a generalized DAF spectrum for use in predicting the response of a structure element when only the nominal overpressure and the type of aircraft were known. The data used in the analyses were measured by five microphones arranged in a cruciform array located near structure E-2 for the comparable missions of XB-70/B-58/F-104 aircraft (flighTs flown within a few minutes of each other). The following findings resulted from the study:

1. A generalized DAF spectrum was obtained by studying the asymptotic behavior of DAF spectra computed from digitized free field signature data.

2. When the nominal pressure signature of a sonic boom is known, the generalized DAF spectrum can be used to predict the nominal response of a known structure element.

3. The magnitudes of the generalized DAF spectrum for different durations (Figure 10-1) were:

10.2

Duration of Boom in Seconds	Range of Natural Frequencies in cps	Generalized DAF Magnitude
0.5	0.8 to 50	2.0
0.4	1.1 to 50	2.0
0.3	1.5 to 50	2.0
0.2	2.1 to 50	2.0
0.1	4.4 to 50	2.15

4. If a DAF spectrum is desired that is more detailed than the generalized DAF spectrum, and if the free field signature parameters (P_1, P_2, T_1, T_2) have been measured, a DAF spectrum can be computed from the wave model as described in Chapter VI.

GENERALIZED DAF SPECTRUM

FIG.
10-1

10.4

XI. DAMAGE COMPLAINT INVESTIGATIONS

During the planning phases of the Edwards Test Program it became evi-
dent that many of the supersonic missions would subject a large number of
buildings and structures at Edwards AFB and in communities near Edwards to
sonic booms. Based on past experience, some damage was expected to occur.
Therefore, to provide a fairly reliable basis for determining the extent of
glass damage caused by the test program, a survey was made of all glass win-
dows and doors in buildings and structures at Edwards. Provisions were also
made to have an engineering-investigator inspect each complaint received from
Edwards and the adjacent communities. The results of the glass survey are
presented in the following text. There were many more complaints due to
Phase I than Phase II missions as the supersonic flight paths were quite
different during the two phases. Therefore, the complaints received and in-
vestigated are discussed in two parts, Phase I and Phase II. The results of
the investigations of the on-site (Edwards AFB) and off-site complaints are
then analysed. The chapter ends with a summary of findings and conclusions.

SURVEY OF GLASS WINDOWS AT EDWARDS AFB

Prior to the test program, a survey was conducted of all glass panes in
structures located at Edwards AFB. Survey forms were sent to occupants of
the 2,226 residential units on the Base. Of these, 567 or about 25 percent
returned completed forms showing a total of 101 cracked glass panes. Based
on these returns, it was estimated then that there were about 404 cracked
panes out of the total of 49,730 window panes (including glass doors). The
total number of glass panes in the residential units was determined from draw-
ings of the structures which were made available by Base Civil Engineering.
In addition to the residential units, all buildings and facilities used for
Base Operations were surveyed. Survey forms were sent to the custodians of
the 2,912 buildings located on the Base. All forms were returned and re-
ported a total of 60,660 panes of glass. 269 cracked panes and 25 broken or
missing panes were reported. Table 11-1 lists the number of housing and
building units, the total number of glass panes, and the number of broken and
missing panes reported in the survey. The number of panes per person and size

---

All figures and tables are placed at the end of this chapter.

group differ from those found in San Antonio[30] where 56 percent of the glass panes were 0 to 2 square feet, 43 percent were 2 to 9 square feet, 0.8 percent were 9 to 40 square feet, and 0.2 percent were over 40 square feet. Based on an average of about four persons per residential unit plus occupants in bachelor quarters, a resident population of about 10,000 people was calculated for Edwards AFB. Using this population and all buildings on the Base, there is an average of 11 window panes per person, or, using residential housing only, there is an average of five panes per person. In San Antonio there was an overall average of 19 panes per person.

COMPLAINTS FROM PHASE I MISSIONS

Description of Mission Flight Paths

Two different headings were flown by most of the aircraft during the three weeks of Phase I test missions. From 3 June through 12 June, missions were flown from east to west on a straight course heading of 245° magnetic from a point several miles east of the test structures E-1 and E-2 to a point just past the structures. Missions from 13 June through 23 June were flown east to west at 233° magnetic. The supersonic "racetrack" course shown in Figure 11-1 was flown by B-58 aircraft from 3 June through 12 June. The B-58 aircraft maintained essentially constant speed throughout the racetrack pattern. Radar plots indicated that all aircraft did not follow the precise radius of turn indicated. In addition, the flight tracks of many missions were not plotted after the aircraft started the turn to the north. Therefore, for many damage complaints, aircraft mission and location were not available. During this first period, the closest distance from flight track to the Lancaster test structure, L-2, was about 13 miles. The distances to most of Lancaster, Quartz Hill and Palmdale were greater. A total of 47 B-58 missions at Mach 1.5 to 1.65 were flown over this racetrack course. The F-104 and F-106 aircraft slowed to subsonic speed shortly after passing over the test structures. Table 11-2 lists the number of supersonic missions for each aircraft for the 3 June to 12 June period.

Figure 11-2 shows the scheduled supersonic racetrack course flown by B-58 aircraft during the period 13 June to 23 June. The distance from the flight track to the Lancaster test structure for the 233° magnetic track was reduced to about 8 miles. The distances to the rest of Lancaster, Quartz Hill and Palmdale were similarly reduced. A total of 47 B-58 missions at speeds of

Mach 1.5 to 1.65 were flown over this course. The number of supersonic missions for each aircraft for the 13 June through 23 June period are listed in Table 11-2.

Location and Types of Damage

Complaints from people other than those living at Edwards AFB were received by the Base Claims Office and daily summaries of the complaints were furnished to Blume personnel during the test flight period. Base Civil Engineering received complaints from personnel occupying residential housing on the Base, and two complaints of boom noise were received at the Air Force Plant, Palmdale. The total number of complaints received and initially attributed to Phase I of the Edwards Test Program were as follows:

Office Receiving Complaint	Number of Complaints-Phase I
Edwards AFB - Claims Office	51
Edwards AFB - Civil Engineering	8
Air Force Plant 42, Palmdale	2
	61

Complaints were classified as to type of damage as shown in Table 11-3. Table 11-4 lists the location of all Phase I complaints arranged chronologically by date of occurrence of damage. Complaints were investigated by an engineering investigator with AFLC Forms 666, 669, and 670 (see Figures 11-3, 11-4, and 11-5) used for recording the results of the investigations. The orientation of the damage incurred in each structure was also noted.

Comparison of Damage with Aircraft Mission

The engineer's investigation reports were analysed together with the mission log and the radar plots to determine if the type and speed of aircraft and location of flight path could be correlated with the damage. The missions on a given day were flown with only a short time interval between them and therefore in most cases it was r ᵗ possible to pinpoint a specific boom as the cause of damage at a particular location. The major problem was that a person filing a complaint could usually give only an estimate of the time of occurrence of the boom which caused the damage. This time estimate often spanned an hour and occasionally a whole morning. In addition, many of the radar plots did not show the entire supersonic track of each aircraft.

11.3

A few of the plots were started before Barstow while many were stopped at the turn point of the racetrack course. The analysis of the damage complaints and aircraft missions was first divided into two sections that corresponded to the different flight track headings: 3 June through 12 June - 245° magnetic, and 13 June through 23 June - 233° magnetic.

3 June through 12 June - 245° Magnetic (Figure 11-1)

Table 11-4 lists all complaints received during Phase I. Sixteen complaints were received that were attributable to the 3 June through 12 June period, for an average of 0.31 complaints per mission. Figure 11-1 shows the locations and types of complaints.

In two instances during the 3 to 12 June period, specific booms were related to damage:

Barstow - 7 June - A large window was reported broken at about 0930. The radar plot showed a B-58 aircraft maneuvering to get on the correct track and heading at about the time of the reported damage. On the radar plot Barstow was less than five miles south of the track of this aircraft.

Edwards AFB Housing - 8 June   bric-a-brac complaint was received from the Base housing area   ning damage to a figurine that fell off a shelf at 0908. Mission log data showed a boom from a B-58 at 0908 at Radar Control which is a short distance from the housing area. The flight was displaced five miles north from the flight track over the test structures or almost directly over the Base housing area. A free field overpressure of 3.17 psf was recorded near test house E-2 on the Base.

13 June through 23 June - 233° Magnetic (Figure 11-2)

The number of complaints increased from sixteen for the 3 to 12 June period to 45 for the 13 to 23 June period. Table 11-4 lists all complaints received and Figure 11-2 shows the locations and types of complaints for this period. For this period there was an average of 0.56 complaints per mission as compared to 0.31 for the 3 to 12 June period.

During the 13 to 23 June period, over half of the complaints occurred on two days. Twenty-four complaints were reported on 20 and 21 June. All of the complaints from the Quartz Hill area, one from Lake Isabella, four from Lancaster and six from Tehachapi were reported for these two days. All missions on these two days were flown by B-58 aircraft with a number of missions

11.4

having nominal 3 psf design overpressures. Average overpressures recorded
at Edwards AFB showed three booms over 3 psf, eight over 2.5 psf, four over
2.0 psf, and all other missions except four over 1.5 psf. Average over-
pressures recorded near the test structure L-2 (Lancaster) exceeded 2 psf for
two missions (2.04 and 2.35 psf), were between 1 and 2 psf for eight missions,
and were less than 1 psf for eight missions. The radar plots indicated a
B-58 aircraft descending before reaching Rosamond at 0935, 20 June. Complaints
were received from Quartz Hill and Lancaster that claimed damage before and
after this time. The radar plots indicated several other B-58 aircraft on
20 and 21 June descending while in the vicinity of Tehachapi. These air-
craft could not be identified as to mission numbers.

Three complaints were received for damage due to test program booms on
14 and 15 June. No damage complaints were received for 16 June. Only F-104
supersonic missions were flown on these three days. As noted previously,
F-104 missions normally slowed to subsonic speed shortly after passing over
the test houses at the Base. Therefore, the number of complaints would be
expected to be less as fewer buildings were exposed to booms. The maximum
average overpressure recorded near test structure E-2 at Edwards for these
three days was 3.96 psf at 0915 on 15 June 1966. The maximum overpressure
recorded at L-2 was 1.21 psf on 14 June 1966.

For the missions flown on 233° magnetic, two specific missions could be
related to specific damage:

> Tehachapi - 20 June - The Postmistress happened to be looking at a clock
> opposite her desk at the time a boom broke a window in the U. S. Post
> Office. At the same time, a window was broken in a department store
> located in the same building. The time was noted as 1043. The radar
> plot indicated a B-58 aircraft at this time had just turned to the east
> a short distance beyond Tehachapi.
> Lake Isabella - 20 June - A window was reported broken at approximately
> 0915. The radar plot showed a B-58 aircraft in a supersonic turn in
> the vicinity of Lake Isabella at 0900. This was approximately 30 miles
> north of the scheduled return leg of the track.

3 June through 23 June - both flight tracks.

The complaints for both periods and all aircraft headings were tabulated
in Tables 11-5, 11-6, and 11-7. Table 11-5 compared the type of damage and
period during which damage occurred. There were 83 incidents of damage of all
types reported during Phase I. Table 11-6 compared the number of damage inci-

dents with geographical location. Aircraft missions, date of occurrence of alleged damage, number of valid complaints, and the maximum average over-pressure measured near E-2 and L-2 were compared in Table 11-7. Of the forty incidents of valid glass damage, all but four were attributed to B-58 missions. The term incident denotes one damaged pane of glass or one piece of bric-a-brac. Of the four incidents possibly attributable to F-104 missions, two occurred on days when only F-104 aircraft flew test missions and the other two damage incidents occurred at Edwards AFB on a day when both B-58 and F-104 missions were flown. For the incidents of valid damage other than glass, one of bric-a-brac damage occurred on a day of F-104 missions and in a location probably overflown by these missions. No incidents of damage could be directly attributed to XB-70 missions.

In summary, 90 percent of the incidents of valid glass damage (engineering investigator found damage could have been caused by sonic boom) and 89.5 per-cent of all incidents of valid damage were attributed to B-58 missions. Of these valid damage incidents possibly caused by B-58 missions, approximately 60 percent occurred on days when the maximum average positive overpressure exceeded 3 psf. One important unknown factor was the actual overpressure adjacent to the damaged elements. This could have a major bearing on the cause of damage as the B-58 aircraft were turning and in some cases descending at supersonic speeds over or near the areas where the damage occurred; "super-boom" overpressures greatly exceeding those measured near E-2 and L-2 could have been produced.

For Phase I, there was a total of 61 complaints involving 83 incidents of damage. Of the total, 48 incidents of damage, or 58 percent, appeared to be valid after investigation (damage possibly caused by a sonic boom). For 25 of the 52 glass damage incidents, repairs had been made or the glass removed prior to the arrival of the engineer-investigator. The cause of the cracks in the glass therefore could not be definitely established to be from causes other than sonic boom. Seventy percent of the valid complaints were made by owners of the structures involved. Eighteen claims have been filed with the Edwards AFB Claims Office. Sixteen of these claims have been paid for a total of $2,199.93. One claim is still pending.

COMPLAINTS FROM PHASE II MISSIONS

All supersonic missions during Phase II of the test program were flown from east to west on a 245° magnetic heading. Missions except those by the

XB-70 were scheduled to slow to subsonic speeds shortly after passing over the test structures on the Base. The XB-70 missions normally made gentle turns to the north after passing over the test structures E-1 and E-2. As a result, a much smaller number of buildings were subjected to test program sonic booms and few areas were overflown by aircraft making turns or other maneuvers at supersonic speeds.

Table 11-8 lists by date of occurrence and location of damage the eleven complaints that could be attributed to flights during the 31 October 1966 through 17 January 1967 period (Phase II). Five glass damage complaints were recorded. Three of the eleven complaints were for damage that occurred on days when no test program flights were flown. Damage incidents by location and by type were compared in Tables 11-5 and 11-6.

After investigation, seven of the incidents of damage were recommended for payment if claims were filed; five could be assigned to test program flights and two were apparently caused by SR-71 flights on 1 December. Four of the five damage incidents attributable to program flights were for glass damage and one was for bric-a-brac. XB-70 missions appeared to have been the cause for two of the glass damage incidents while B-58 missions apparently caused the other two. The bric-a-brac incident was traced to an XB-70 flight. As of June 22, 1967, three claims have been filed and $55.27 has been paid for two approved claims. One claim is still unsettled (awaiting information from claimant).

A tabulation was made in Table 11-9 of the complaints received, aircraft missions flown, and the range of maximum average overpressures measured near E-2. Two (50%) of the incidents of valid glass damage were attributed to B-58 missions making a supersonic turn over Mojave. Average overpressures recorded at Edwards AFB showed four booms over 3 psf, five over 2.5 psf, three over 2 psf, and all other missions except two over 1.5 psf. The percent of total glass damage incidents attributed to B-58 missions during Phase II was nearly half (55%) of the percentage found during Phase I. This difference was largely due to the change in the supersonic flight plan for the B-58 aircraft. In Phase I all B-58 aircraft flew on a supersonic racetrack course, whereas during Phase II the aircraft slowed to subsonic speed shortly after passing E-1 and E-2. Therefore, fewer buildings were subjected to B-58 sonic booms and the booms were not normally produced by aircraft maneuvering at supersonic speeds. The number of incidents of damage attributed to XB-70 missions is not surprising as there were seventeen supersonic missions flown during Phase II versus only three during Phase I.

11.7

EVALUATION OF DAMAGE COMPLAINTS FROM PHASES I AND II

There were 72 complaints involving 96 incidents of damage received during Phases I and II of the test program. After investigation, 55 of the incidents appeared to be valid (damage that could have been caused by sonic boom test program). An incident of damage denotes one cracked or broken glass pane, or one category of other type of damage (cracked plaster or cracked stucco, etc., Table II-3). Thirty-seven, or 72.5 percent, of the valid incidents of damage were reported by owners of the property involved. The remainder of the complaintants were renters. Eighty percent of the valid complaints were for glass damage, 5.5 percent for plaster or stucco, and 14.5 percent for damage to bric-a-brac and other fallen objects. Glass damage was by far the major source of complaints. Therefore, additional analyses of the glass complaints were made.

The combined population of Palmdale, Lancaster, Rosamond, Quartz Hill and Tehachapi is about 55,000. Assuming 19 window panes per person[30], a total of about 1,045,000 panes were subjected to sonic boom. Assuming 11 panes per person (based on the total number of window panes at Edwards AFB) a total of 605,000 panes of all sizes in these communities were subjected to sonic booms. The latter total figure was used for the analyses of damage incidents rather than the former for three reasons. First, the distribution of glass sizes was felt to be more similar to those at Edwards AFB because the type of residential construction at Edwards is similar to the surrounding area. Secondly, the proportion of glass sizes 0 to 2 square feet was much less and 9 to 40 square feet was much greater than those found at San Antonio[30]. Many residential units in the areas surrounding Edwards have large windows (2.5' x 6' to 4' x 6') and sliding glass doors. As a result there are more 9 to 40 square feet panes and fewer 0 to 2 square feet. The third reason for using the lower number of panes per person was that complaints and incidents of valid damage per million boom-pane exposures would be based on a more conservative figure for glass population. A boom-pane exposure is one pane subjected to one boom.

Table II-10 lists the total number of glass panes for communities adjacent to Edwards, the number of complaints of damage received, and number of panes in each size damaged by sonic boom. The number of damaged panes per million total boom-pane exposures was also calculated for each glass size group. 114 sonic booms were used in this calculation, based on three XB-70 and 94 B-58 missions during Phase I and 17 XB-70 supersonic missions during Phase II. The

Century series fighter missions were not included as most of these aircraft slowed to subsonic speeds soon after passing the test structures. The B-58 missions during Phase II similarly reduced speeds. Information regarding the headings for the YF-12 and SR-71 missions was not released and therefore it was not known what areas were overflown outside of Edwards. They were therefore excluded.

Table II-II presents a tabulation of the glass panes and complaints of glass damage at Edwards AFB. 357 sonic booms were used to calculate the boom-pane exposure as all supersonic test missions measured and recorded near E-2 during Phases I and II passed near most of the structures on the Base.

The glass panes at Edwards AFB were surveyed prior to start of test missions while those in adjacent communities were not. The types of construction, particularly the residential units, for both areas are very similar. The size distribution of glass panes in residential units therefore should be similar for both areas. The communities adjacent to Edwards had a total of 69.0 million boom-pane exposures. The Base had 39.4 million boom-pane exposures during the test program plus millions of boom-pane exposures from other than test program missions. The complaints of glass damage of all sizes at Edwards totalled 0.203 panes per million exposures while from the adjacent communities they totalled 0.566 panes per million exposures; a rate 2.8 times greater. The number of panes possibly damaged by test program booms were 0.127 per million boom-pane exposures at Edwards versus 0.464 damaged panes per million boom-pane exposures in the adjacent communities; or 3.7 times the Edwards rate. The Edwards rate exceeded that found in the adjacent communities; in one glass size group (0 to 2 square feet), 0.076 to 0.015 damaged panes per million boom-pane exposures.

Certain conclusions could be drawn from these results. The glass panes at Edwards were surveyed prior to the test missions and their condition determined. This survey was made to eliminate as far as possible any confusion that might arise in recognizing boom damage versus damage ca sed by differential shrinkage or differential settlement of a structure. Some of the complaints received from EAFB housing were for damage obviously not caused by test program booms. Therefore, I. was concluded that the remain. g glass damage at EAFB that occurred during the test program was most likely caused by a boom.

A second possible conclusion was that the glass panes at Edwards have been subjected to so many sonic booms over the years that the "weak sisters"

were broken prior to the test program. A more convincing explanation for the difference in rates of damaged panes was that the missions apparently causing nearly 90 percent of the glass damage were B-58 aircraft maneuvering at supersonic speed. All aircraft were on straight courses while passing over the Base and therefore the Edwards structures were not subject to possible super booms created by maneuvering aircraft. It was therefore concluded that the rates of glass damage per million boom-pane exposures at Edwards should be used for predicting future glass damage from level supersonic flights with similar overpressure levels rather than the rates determined from investigation of glass damage complaints in the communities adjacent to Edwards.

The valid incidents of glass damage were also examined on the basis of type of frames, previous condition and orientation, Tables 11-12. Eleven of the damaged panes had been installed in wooden frames and thirty-one in aluminum frames. There was no correlation between type of frame and damage. Based primarily on statements of the complainants and partly on visual inspection (if the glass was still in place) all glass panes were in good condition prior to the time of boom damage. No relationship of orientation of damaged panes to aircraft producing the boom was possible as there was not sufficient information available to definitely determine location of the boom-producing aircraft.

It is of interest to note that no damage from sonic booms occurred in either test structure E-1 or E-2. This can be explained by the fact that the construction of the structures was completed just prior to the start of test missions. The structures were less than one year old at the end of the test program. Therefore the window mounting details were in good condition; there was little time for differential settlement to occur in the structures, and the structures had not been subjected to repeated weathering effects.

SUMMARY OF FINDINGS

The preceding text has discussed the results of a survey of all glass panes in structures at Edwards AFB and the results of investigations and analyses of damage complaints received during Phases I and II. Overpressure measurements were made by instruments located about two miles from most of the structures on the Base. However, no overpressure measurements were available for the communities adjacent to the Base where the largest number of damage complaints were reported; therefore direct comparisons of damage and

overpressure were not possible. Based on detailed analyses of the avialable
data, the following findings are presented:

1. The rate of valid glass damage in Edwards AFB Buildings, all of
which had been condition surveyed prior to the test program, was 0.127 panes
damaged per million boom-pane exposures or 27 percent of the rate for buildings
in communities adjacent to Edwards which were not condition surveyed prior to
test missions.

2. During Phase I, the 110,390 glass panes in structures at Edwards
were subjected to more booms from test missions than were the 605,000 glass
panes in the adjacent communities; however, the aircraft while over Edwards
were flying straight courses and then made turns at supersonic speeds over
adjacent communities. Some focusing of the boom overpressure (or super booms)
may therefore have been produced with peak overpressures greatly exceeding
those produced on the Base.

3. During Phase I, 90 percent of the incidents of valid glass damage
(engineering investigator determined damage could have been caused by sonic
boom) were attributable to B-58 missions. The remaining 10 percent were
apparently due to F-104 missions.

4. The valid glass damage rate per mission during Phase I was 8.8 times
the rate during Phase II when aircraft generally flew straight courses while
at supersonic speeds.

5. The numᵣ of complaints received decreased from 61 during Phase I to
11 during Phase II. This large decrease in number of complaints can be attrib-
uted to two factors: a) the B-58 aircraft made turns and other maneuvers at
supersonic speeds over several communities adjacent to Edwards AFB during
Phase I, and b) during Phase II the XB-70 flew supersonically on a relatively
straight course over a few of the cities adjacent to Edwards.

6. For all incidents of damage recorded during Phases I and II, 60.5
percent were for glass damage.

7. Fifty-eight percent of all incidents of damage received during Phases
I and II were listed as valid. Of these valid incidents, 80 percent were for
glass, 5.5 percent for plaster or stucco, 0.0 percent for structural, and 14.5
percent for bric-a-brac or other fallen object damage.

8. Glass damage was repaired or the broken glass removed for 55 percent of the glass damage incidents before the engineering investigator could investigate the alleged damage and hence, the validity of all glass damage could not be definitely established.

9. Damaged glass panes ranged in size from 1.3 square feet to 82.5 square feet. 2.7, 43.2, 43.2 and 10.9 percent of the incidents of damage occurred in the 0-2, 2-9, 9-40 and over 40 square feet size groups respectively.

10. No sonic boom damage was observed in the test structures prior to or after the test flights. There were minor shrinkage cracks in the test structures prior to start of test flights. However, no discernible extension or widening of these cracks was observed although observations were made and recorded daily.

11. As the condition of the glass panes at Edwards AFB was determined prior to the Test Program, the number of damaged panes caused by booms from test missions should be a reliable indicator of valid glass damage to be expected from future level supersonic flights generating sonic boom peak overpressures of 2 to 3 psf. The rate was one damaged pane per 7.9 million boom-pane exposures.

12. A large percentage (from 57 to 84 percent) of future valid incidents of damage from sonic boom should be for glass.

TABLE II-1

TABULATION OF GLASS PANE SURVEY
OF BUILDINGS AND STRUCTURES AT EDWARDS AFB

Structures	Number of Units	Size of Glass Panes In Square Feet					Cracked Panes Reported	Broken or Missing Panes Reported
		0-2	2-9	9-40	Over 40	Total		
Base Housing	2,226 a)	3,500	19,720	26,510	0	49,730	404 b)	0
Base Operation Buildings	2,912	21,647	29,696	6,773	2,544	60,660	269	25
Total	5,138	25,147	49,416	33,283	2,544	110,390	673	25
Percent of Total		22.8	44.7	30.2	2.3	100.00		

a) Determined from drawings of Base Housing.

b) Based on 101 cracked panes reported on the 25% of forms returned.

TABLE II-2

SUMMARY-PHASE I SUPERSONIC MISSIONS

Aircraft	Dates	No. of Missions	Primary Heading	Comments
B-58	3-12 June	47	245° Mag	Racetrack Course
XB-70	3-12 June	3	245° Mag (1@262°M)	Straight Course
F-104	3-12 June	1	-	Straight Course
B-58	13-23 June	47	233° Mag	Racetrack Course
F-104	13-23 June	34	233° Mag	Straight Course

a) From Mission Log, Edward, Phase I, Appendix D.

c) Not available

11.13

TABLE 11-3
CLASSIFICATION OF TYPES OF COMPLAINTS

Notation	Type of Complaint
1.	Glass Damage - Window and/or Door
2.	Glass Damage - Miscellaneous,(Auto, Mirror)
3.	Plaster or Stucco Damage - Cracks
4.	Plaster or Stucco Damage - Fallen
5.	Structural Damage
6.	Fallen Object Damage - Bric-a-brac
7.	Fallen Object Damage - Miscellaneous (Fixtures, lamps, mirrors, etc.)
8.	Miscellaneo Damage (TV, Bathroom fixtures, etc.)
9.	Noise Complaint - No Damage
10.	Information Call - No Damage

TABLE 11-4

SUMMARY OF COMPLAINTS ATTRIBUTED TO PHASE I [a]

(All dates are 1966)

Time of Occurrence of Damage		Date Complaint Received	Complaint Number	Location	Type of Claim [b]		Own-Rent	Results of Investigation	
Date	Time				No.	Explanation		A/D	Remarks
1965	NA	NA	56	EAFB	1	Glass- Window(1)	NA	D	Damage occurred prior to program
Prior to Program		9 Jun	59	Barstow	1	Glass- Window(1)	O	D	Damage occurred prior to program
6 Jun	1000-1030	1 Aug	61	Lancaster	7	Fallen Mirror	O	NA	No Claim filed
6 Jun	1000-2000	6 Jun	1	Tehachapi	1	Glass – Window(1)	O	D	Previous damage
6 Jun	1000-2000	6 Jun	3	Lancaster	1	Glass – Window (2)	O	A	Will not file claim
					7	Fallen Picture		A	
6 Jun	0900-1100	9 Jun	6	Rosamond	3	Plaster and Stucco	O	D	Probably shrinkage and settlement
6 Jun	NA	6-10 Jun	57	EAFB	1	Glass – Window (1)	R	D	Broken by B-B gun
6 Jun	AM	9 Jun	7	Barstow	3	Stucco	O	D	Probably shrinkage and settlement
6 Jun	NA	6-10 Jun	55	EAFB	1	Glass-Window (3)	R	–	Insufficient data available
6 Jun	AM	20 Jun	22	Tehachapi	1	Glass – Window (1) and door (1)	R	A	Claim filed and paid

11.15

TABLE 11-4 (Continued)

Time of Occurrence of Damage		Date Complaint Received	Complaint Number	Location	Type of Claim		Own- Rent	Results of Investigation	
Date	Time				No.	Explanation		A/D	Remarks
6 Jun	NA	6-10 Jun	52	EAFB	1	Glass-Window (1)	R	A	Possibly caused by program
7 Jun	0930-1030	7 Jun	2	Barstow	1	Glass-Window (1)	R	A	Claim filed
7 Jun	0900-1100	9 Jun	6	Rosamond	See	6 June			
7 Jun	AM	9 Jun	7	Barstow	See	6 June			
7 Jun	AM	20 Jun	22	Tehachapi	1	Extended crack in door- See 6 June			
8 Jun	0908	8 Jun	4	EAFB	6	Figurine on shelf	R	A	Claim filed and paid
8 Jun	0900-1100	9 Jun	6	Rosamond	See	6 June			
8 Jun	AM	9 Jun	7	Barstow	See	6 June			
8 Jun	0930	27 Jun	44	Barstow	3	Stucco	C	D	Previous cracks, probably shrinkage
9 Jun	0900-1100	9 Jun	6	Rosamond	See	6 June			
9 Jun	AM	9 Jun	7	Barstow	See	6 June			

TABLE II-4 (Continued)

Time of Occurrence of Damage		Date Complaint Received	Complaint Number	Complaint Location	Type of Claim		Own-Rent	Results of Investigation	
Date	Time				No.	Explanation		A/D	Remarks
9 Jun	AM	10 Jun	8	Lancaster 7		Lamp on shelf	NA	-	Information call, did not investigate
9 Jun	0930	13 Jun	12	Tehachapl 3		Plaster	O	A	Claim filed and paid
9 June	1400	9 June	13	EAFB 8		Shattered porch light globe	R	D	Time reported does not coincide with program flights
6-11 Jun	-	21 Jun	5	Lancaster 10		No damage	O	-	Owner just warned
11-17 Jun	NA	22 Jun	32	Lancaster 8		TV (Protective glass on picture tube)	O	D	Probably will not file claim
13 Jun	AM	13 Jun	9	Palmdale 1		Glass-Window (2)	O	A	
13 Jun	0953	13 Jun	10	Lancaster 1		Glass-Window (1)	O	A	Claim filed and paid
13 Jun	AM	14 Jun	14	Tehachapl 1		Glass-Window (1)	O	A	Claim filed
13 Jun	1000-2000	20 Jun	15	Lancaster 5		Exposed ceiling beams twisted	O	D	Warping and shrinkage
13 Jun	NA	13 Jun	11	Rosamond 6		Dishes on shelf	O	A	
			4			Plaster	O	D	Damage occured prior to program
13-17 Jun	NA	17 Jun	18	Tehachapl 1		Glass-Window (2)	O	D	Old paint in crack
14-15 Jun	0915	21 Jun	31	Lancaster 7		Clock on wall	O	A	

11.17

TABLE 11-4 (Continued)

Time of Occurrence of Damage		Date Complaint Received	Complaint Number	Location	Type of Claim		Own-Rent	Results of Investigation	
Date	Time				No.	Explanation		A/D	Remarks
14 Jun	1200	24 Jun	60	Lancaster 7		Light fixture-glass	NA	NA	NA
14 Jun	1600-1615	15 Jun	50	EAFB 1		Glass-Window (2)	R	A	
20 Jun	1030-1100	20 Jun	16	Tehachapi 1		Glass-Window (1)	O	A	
20 Jun	1022	21 Jun	19	Tehachapi 1		Glass-Window (1)	O	A	Claim filed and paid
20 Jun	1043	20 Jun	21	Tehachapi 1		Glass-Window (1)	O	A	Claim filed and paid
20 Jun	1044	20 Jun	22	Tehachapi 1		Glass-Window (1)	R	A	Claim filed and paid
20 Jun	1000	20 Jun	25	Lancaster 1		Glass-Window (1)	R	A	Approve 75% payment previous cracks.
20 Jun	NA	14 Jul	26	Lancaster 1		Glass-Window (2)	O	A	Negotiate settlement
20 Jun	AM	21 Jun	27	Quartz Hill 7		Light fixture	O	D	
20 Jun	1045	20 Jun	28	Quartz Hill 1		Glass-Door (1)	O	A	
20 Jun	1015	22 Jun	17	Tehachape 1		Glass-Window (1)	O	A	Claim filed and paid

TABLE 11-4 (Continued)

Time of Occurrence of Damage		Date Complaint Received	Complaint Number	Complaint Location	Type of Claim		Own-Rent	Results of investigation	
Date	Time				No.	Explanation		A/D	Remarks
20 Jun	NA	6 July	45	Tehachapi	5	Brick Pillar, 27" high supporting wood fence rails	O	D	Will not file claim
20 Jun	0910	20 Jun	29	Quartz Hill	1	Glass-Window (2)	O	A	
20 Jun	0910	20 Jun	33	Lancaster	1	Glass-Window (2)	O	A	Claim filed and paid
20 Jun	AM	24 Jun	37	Quartz Hill	1	Glass-Window (1)	O	A	
20 Jun	0915	20 Jun	38	Lake Isabella	1	Glass-Window (1) Glass-Window (1)	O	A D	Damage occurred prior to program
20-21 Jun	AM	21 Jun	42	Quartz Hill	1 7	Glass-Window (2) Medical type office scale fell	O	A –	No claim
20 Jun		22 Jun	34	Lancaster	3	Stucco	O	D	Previous cracks, probably shrinkage
21 Jun	AM	21 Jun	20	Tehachapi	1	Glass-Window (1)	O	A	Claim filed and paid

11.19

TABLE 11-4 (Continued)

Time of Occurrence of Damage		Date Complaint Received	Complaint Number	Complaint Location	Type of Claim		Own- Rent	A/D	Results of Investigation Remarks
Date	Time				No.	Explanation			
21 Jun	1315	21 Jun	30	Lancaster	3 7	Plaster-ceiling Light fixture fell from ceiling	O	A A	Will not file claim
21 Jun	NA	23 Jun	40	Lancaster	3	Plaster-ceiling	O	A	Partially approve – 50% (Previous water damage). Claim filed and paid
21 Jun	0905	22 Jun	41	Lancaster	5	Attic access cover fell – molding supports loose	O	–	Information call, will not file claim
21 Jun	0910	21 Jun	46	Tehachapi	1	Glass-Window (2)	O	A	
21 Jun	NA	21 Jun	48	Quartz Hill	9	Noise	NA	–	(Complaint through AF Plant 42)
21 Jun	NA	21 Jun	54	EAFB	1	Glass-Windows (1?)	R	D	Insufficient data available
21 Jun	0905-0945	21 Jun	49	Lake Hughes	9	Noise	NA		(Complaint through AF Plant 42)
22 Jun	NA	24 Jun	51	EAFB	1	Glass-Window (2)	R	A	

TABLE 11-4 (Continued)

Time of Occurrence of Damage — Date	Time	Date Complaint Received	Complaint Number	Complaint Location	Type of Claim — No.	Explanation	Own-Rent	A/D	Results of Investigation Remarks
23 Jun	NA	23 Jun	53	EAFB	1	Glass-Window (1?)	R	D	Insufficient data available
23 Jun	0845	23 Jun	24	EAFB	2	Glass-Auto Windshield	O	-	Complaint withdrawn
23 Jun	0955	24 Jun	58	Tehachapi	1	Glass-Window (1)	R	A	Claim filed and paid
23 Jun	0855	23 Jun	23	Tehachapi	1	Glass-Window (1)	R	A	
23 Jun	0912-1256	23 Jun	35	Palmdale	1	Glass-Window (1)	R	A	Partial payment, previous crack
Jun	NA	22 Jun	36	Lancaster	3	Stucco and Plaster	O	D	Previous cracks and patching, evidence of settlement. Will not file claim
1965-66	NA	22 Jun	39	Quartz Hill	5	Concrete irrigation pipe, splitting in longitudinal seam at beginning of irrigation period	O	-	Information call, will not file claim

TABLE II-4 (Continued)

Time of Occurrence of Damage		Date		Complaint	Type of Claim		Own-		Results of Investigation
Date	Time	Complaint Received	Complaint Number	Location	No.	Explanation	Rent	A/D	Remarks
NA	NA	27 Jun	43	Palmdale	5	Small concrete block reservoir-cracks	O	D	Poorly done project, old cement used for slab and mortar. Some fill under front end of reservoir washed out. Will not file claim
NA	NA	7 Jul	47	Lancaster	1 5	Glass-Window (3) Cracked mortar around tile	O	A D	

a) Notation

NA — Information not available

A — Claim approved. Engineering investigator found damage could have been caused by sonic boom from test program flights.

D — Claim denied. Engineering investigator judged that damage was not caused by sonic boom from test program flights.

O — Owner reporting claim

R — Renter reporting claim

b) Refer to Table II-3 for classification of types of claims. Quantity in parentheses indicates number of damaged panes.

TABLE 11-5

DAMAGE INCIDENTS BY TYPE AND TEST PROGRAM PERIOD

(A complaint may involve several incidents and types of damage)

Complaint Classification (See Table 11-4)		PHASE I								PHASE II	
		Track @245° Mag. 3 June 66 - 12 June 66		Track @ 233° Mag. 13 June 66 - 23 June 66		Date Not Available		Total		Track @245° Mag. 31 Oct 66-17 Jan 67	
No.	Type	Number	Percent	Number	Percent	Number	Percent	Number	Percent	Number	Percent
1	Glass-Window and/or Door	11	52.3	36	57.8	5	55.6	52	62.8	6	46.1
2	Glass - Miscellaneous	0	0	1	1.9	0	0	1	1.2	0	0
3	Plaster or Stucco-Cracks	4	19.0	3	5.7	1	11.1	8	9.6	2	15.4
4	Plaster or Stucco-Fallen	0	0	1	1.9	0	0	1	1.2	0	0
5	Structural	0	0	3	5.7	3	33.3	6	7.2	0	0
6	Fallen Object-Bric-A-Brac	1	4.8	1	1.9	0	0	2	2.4	1	7.7
7	Fallen Object-Miscellaneous	3	14.3	5	9.4	0	0	8	9.6	4	30.8
8	Miscellaneous	1	4.8	1	1.9	0	0	2	2.4	0	0
9	Noise Complaint-No Damage	0	0	2	3.8	0	0	2	2.4	0	0
10	Information Call-No Damage	1	4.8	0	0	0	0	1	1.2	0	0
	TOTAL	21	100.0	53	100.0	9	100.0	83	100.0	13	100.0

11.23

TABLE 11-6

DAMAGE INCIDENTS BY LOCATION AND TEST PROGRAM PERIOD

(A complaint may involve several incidents and types of damage)

Location	PHASE I 3 June 66 - 12 June 66 Track @245° Mag		13 June 66 - 23 June 66 Track @ 233° Mag		Date Not Available		Total		PHASE II 31 Oct 66 - 17 Jan 67 Track @245° Mag.	
	Number	Percent	Number	Percent	Number	Percent	Number	Percent	Number	Percent
Barstow	3	14.3	0	0	1	11.1	4	4.8	0	0
EAFB	7	33.3	7	13.2	1	11.1	15	18.0	3	23.1
Lake Hughes	0	0	1	1.9	0	0	1	1.2	0	0
Lake Isabella	0	0	2	3.8	0	0	2	2.4	0	0
Lamont	0	0	0	0	0	0	0	0	1	7.7
Lancaster	6	28.6	15	28.2	5	55.6	26	31.4	4	30.7
Mojave	0	0	0	0	0	0	0	0	2	15.4
Palmdale	0	0	3	5.7	1	11.1	4	4.8	0	0
Rosamond	1	4.8	2	3.8	0	0	3	3.6	3	23.1
Quartz Hill	0	0	9	17.0	1	11.1	10	12.0	0	0
Tehachapi	4	19.0	14	26.4	0	0	18	21.8	0	0
TOTALS	21	100.0	53	100.0	9	100.0	83	100.0	13	100.0

TABLE 11-7

TABULATION OF DAMAGE INCIDENTS VERSUS MISSIONS AND MEASURED PEAK OVERPRESSURES

FOR PHASE 1

Column groups:
- **Missions Flown[a]** — XB-70, B-58, F-104
- **Number of Incidents of[b],[c]** — Damage by Type (1–10) with total T
- **Valid Incidents of[d]** — Damage by Type (1–8) with total T
- **Range of Maximum Average Positive Overpressures** — @L-2(psf), @E-2(psf)

Date	XB-70	B-58	F-104	N1	N2	N3	N4	N5	N6	N7	N8	N9	N10	N-T	V1	V2	V3	V4	V5	V6	V7	V8	V-T	@L-2(psf)	@E-2(psf)
4 June	1		1											0									0	NA[e]	1.19–2.53
5 June	1	11		10		2				2				14	5						1		6	0.57–0.94	1.64–3.45
7 June		10		1										1	1								1	0.64–1.47	0.98–3.42
8 June	1	12				1			1					2						1			1	0.11–1.13	1.65–3.35
9 June		14				1			1	1				3			1						1	0.39–1.66	1.55–4.04
13 June		8	2	4		1			1		1			7	4						1		5	0.97–1.50	1.83–2.97
14 June			6	2							1			3	2								2	0.42–1.21	1.33–2.84
15 June			8											0									0	0.45	1.19–3.96
16 June			3											0									0	NA	1.43–1.79
20 June		10		16		1			1		1			19	15								15	0.53–1.56	1.38–3.13
21 June		13		4		2				1	1	2		10	3		2				1		6	0.48–1.54	1.17–3.23
22 June		9	8	2										2	2								2	0.14–2.00	1.00–3.76
23 June		7	7	4	1									5	3								3	0.30–2.13	1.26–5.81
Unknown[f]				9				3	1		2		2	17	5					1			6		
Totals	**3**	**94**	**35**	**52**	**1**	**8**		**3**	**6**	**2**	**8**	**2**	**2**	**83**	**40**	**0**	**3**	**0**	**0**	**2**	**3**	**0**	**48**		

11.25

TABLE 11-7 (Continued)

a) From Mission Log, Edwards Phase I, Appendix D

b) See Table 11-3 for classification of types of complaints

c) Some complaints were for more than one type of damage and/or more than one pane of glass.

d) Engineering investigator found damage could have been caused by sonic boom.

e) Not available.

f) Complaint not assignable to any one day.

11.2f

TABLE 11-8

SUMMARY OF COMPLAINTS ATTRIBUTED TO PHASE II [a)]

(Dates are 1966 unless noted)

Time of Occurrence of Damage		Date Complaint Received	Complaint Number	Complaint Location	Type of Claim [b)]		Own-/Rent	A/D	Results of Investigation Remarks
Date	Time				No.	Explanation			
10 Nov	NA	10 Nov	62	Lancaster	1	Glass-Window (1)	O	A	XB-70 8 miles south of designed track
16 Nov	1150	16 Nov	63	Mojave	1	Glass-Window (1)	R	A	B-58 turning over Mojave
23 Nov	1035	25 Nov	64	Lancaster	7	Clock fell from wall	O	A	XB-70 1.3 miles north of residence
23 Nov	1004 & 1150	28 Nov	69	Lancaster	3	Plaster-Ceiling	R	D	Not boom damage
1 Dec	1040	1 Dec	65	EAFB	7	Clock-Kitchen	R	A	Not caused by program flights
					7	Clock-Dining Room		D	Not boom damage
1 Dec	0130-1515	1 Dec	66	EAFB	6	Plate hung on wall	R	A	Not caused by program flights
8 Dec	1230	8 Dec	67	Rosamond	1	Glass-Window (2)	O	D	Extremely poor conditions B-58 over Rosamond
8 Dec	1239	8 Dec	68	Rosamond	7	Suitcases fell off of shelf, striking washing machine and bird cage	O	D	Not caused by program flight

TABLE 11-8 (Continued)

Time of Occurrence of Damage		Date Complaint Received	Complaint Number	Complaint Location	Type of Claim			Own-		Results of Investigation
Date	Time				No.	Explanation		Rent	A/D	Remarks
8 Dec	1200	15 Dec	70	Mojave	1		Glass-Window (1)	O	A	B-58 over Mojave
17 Jan 1967	1015-1020	17 Jan 1967	72	Lamont	1		Glass-Window (1)	O	A	XB-70 turning over Lamont (Approx. 7 mi. south of Bakersfield)
NA	NA	3 Jan 1967	71	Lancaster	3		Plaster	O	D	Not boom damage. Water stains evident at cracks. Damage not related to any particular boom

a) Notation

NA   Information not available

A   Claim approved. Engineering investigator found damage could have been caused by sonic boom from test program flights.

D   Claim denied. Engineering investigator judged that damage was not caused by sonic boom from test program flights.

O   Owner reporting claim

R   Renter reporting claim

b) Refer to Table 11-3 for classification of types of claims. Quantity in parentheses indicates number of damaged panes.

TABLE 11-9

TABULATION OF DAMAGE INCIDENTS VERSUS MISSIONS
AND MEASURED PEAK OVERPRESSURES
FOR PHASE II

Date[a]	Missions Flown[b]			Number of Incidents[c],[d] — Damage by Type											Valid Incidents[e] — Damage by Type									Range of Maximum Average Positive Overpressures
	XB-70	B-58	F-104	1	2	3	4	5	6	7	8	9	10	T	1	2	3	4	5	6	7	8	T	@E-2 (psf)
10 Nov	2	2	2	1										1	1								1	1.54-3.51
16 Nov		10		1										1	1								1	2.22-370
23 Nov	2	2	1			1				1				2							1		1	2.41-3.27
1 Dec[f]									1	2				3						1	1		2	-
8 Dec		12		3						1				4	1								1	1.36-3.19
17 Jan	2	2	1	1										1	1								1	1.39-2.39
Unknown						1								1									0	-
Totals	6	28	4	6	0	2	0	0	1	4	0	0	0	13	4	0	0	0	0	1	2	0	7	

a) Days on which damage occurred.

b) From Mission Log, Edwards Phase I, Appendix D

c) See Table 11-3 for classification of types of complaints.

d) Some complaints were for more than one type of damage and/or more than one pane of glass.

e) Engineering Investigator found damage could have been caused by sonic boom.

f) No program flights this day.

11.29

TABLE 11-10

SIZE DISTRIBUTION OF DAMAGED GLASS
IN STRUCTURES IN COMMUNITIES ADJACENT TO
EDWARDS AIR FORCE BASE[a]

Glass size in sq. ft.	Distribution				Total
	0-2	2-9	9-40	Over 40	
Number of panes[b]	-	-	-	-	605,000
Number of exposures, millions[c]	-	-	-	-	69.0
Panes claimed damaged	1	19	15	4	39
Panes claimed damaged per million exposures	0.015	0.276	0.217	0.058	0.566
Panes possibly damaged by sonic booms[d]	1	15	12	4	32
Panes possibly damaged by sonic booms per million exposures[d]	0.015	0.217	0.174	0.058	0.464

Notes

a) Lancaster, Palmdale, Quartz Hill, Rosamond and Tehachapi

b) 55,000 population times 11 panes per person or total of 605,000 panes.

c) Based on 114 supersonic missions (3 XB-70 and 94 B-58 during Phase I and 17 XB-70 during Phase II).

d) Engineering investigator found damage could have been caused by sonic boom.

11.30

TABLE 11-11

SIZE DISTRIBUTION OF DAMAGED GLASS

IN STRUCTURES AT EDWARDS AFB

	Distribution				Total
Glass size in sq. ft.	0-2	2-9	9-40	Over 40	
Number of Panes from Surveys					
Base Housing	3,500	19,720	26.510	0	49,730
Base Operations Buildings	21,647	29,696	6,773	2,544	60,660
Total	25,147	49,416	33,283	2,544	110,390
Number of Exposures, Millions[a]	–	–	–	–	39.4
Panes claimed damaged	3	1	4	0	8
Panes claimed damaged per million exposures	0.076	0.025	0.102	0	0.203
Panes possibly damaged by sonic booms[b]	0	1	4	0	5
Panes possibly damaged by sonic booms per million exposures[b]	0	0.025	0.102	0	0.127

Notes

a) Based on 357 supersonic missions (Phase I: YF-12, 2; SR-71, 3; XB-70, 3; B-58, 94, F-104, 35; F-106, 18; for a total of 155. Phase II: XB-70, 17; B-58, 69; F-104, 85; SR-71, 31; for a total of 202).

b) Engineering investigator found damage could have been caused by sonic boom.

TABLE 11-12

COMPLAINTS OF GLASS DAMAGE THAT OCCURRED DURING PHASES I & II

Complaint Number	Location	Size Width ft.	Ht. ft.	Area Sq.ft.	Glass	Frame	Orien- tation	Previous Condition	Instal- lation	Approval
PHASE I										
1	Tehachapi	3.8	6.2	23.5	P	?	S	Cracked	Hor.Sliding	D
2	Barstow	8.5	9.7	82.5	P	Al	SE	Good	Fixed	A
3	Lancaster	2.1	1.3	2.7	W	N/A	N/A	N/A	N/A	N/A
		2.1	1.3	2.7	W	N/A	N/A	N/A	N/A	N/A
9	Palmdale	1.5	4.0	6.0	W	Al	S	Cracked	Fixed	A
		1.5	4.0	6.0	W	Al	S	Good	Crackout	A
10	Lancaster	3.0	3.3	9.9	W	Al	E	Good	Hor.Sliding	A
14	Tehachapi	3.6	4.5	16.2	W	Wood	W	Good	Fixed	A
16	Tehachapi	3.0	3.6	10.8	W	Al	N	Good	Fixed	A
17	Tahachapi	2.5	2.5	6.3	W	Wood	E	Good	Vert.Sliding	A
18	Tehachapi	1.3	2.5	3.2	W	Wood	E	Cracked?	Fixed	D
		1.3	2.5	3.2	W	Wood	E	Cracked?	Fixed	D
19	Tehachapi	3.0	3.0	9.0	W	Al	W	Good	Fixed	A
20	Tehachapi	3.0	3.0	9.0	W	Al	W	Good	Fixed	A
21	Tehachapi	7.5	5.6	42.0	P	Al	E	Good	Fixed	A
22	Tehachapi	9.2	6.8	62.5	P	Al	E	Good	Fixed	A
		9.2	8.3	21.1	P	Al	E	Good	Fixed	A
		3.0	6.8	20.3	P	Al	E	Good	Door	A
23	Tenachapi	3.8	6.3	23.9	P	Al	S	Good	Fixed	A

11.32

TABLE 11-12 (Continued)

Complaint Number	Location	Size		Area Sq.ft.	Glass	Frame	Orien- tation	Previous Condition	Instal- lation	Approval
		Width ft.	Ht. ht.							
PHASE I (Continued)										
25	Lancaster	4.5	6.0	27.0	P	Al	W	Cracked	Hor.Sliding	A,75%
26	Lancaster	4.0	8.0	32.0	Three layer laminated	Wood	W	Good	Fixed	A
		3.0	8.0	24.0	"	Wood	E	Good	Fixed	A
28	Quartz Hill	2.0	2.5	5.0	W	Al	W	Good	Hor.Sliding	A
29	Quartz Hill	8.0	1.0	2.0	W	Wood	N	Good	Vert.Sliding	A
		2.0	2.0	4.0	W	Wood	N	Good	Fixed	A
33	Lancaster	1.5	4.0	6.0	W	Al	S	Good	Crankout	A
		1.5	3.0	4.5	N	Al	W	Good	Crankout	A
35	Palmdale	9.0	7.0	63.0	P	Al	N	Cracked	Fixed	A
37	Quartz Hill	3.0	3.0	9.0	W	Al	E	Good	Fixed	A
38	Lake Isabella	2.0	3.8	7.6	W	Ai	E	Good	Hor.Sliding	A
42	Quartz Hill	2.0	2.2	4.4	W	Wood	E	Good	Vert.Sliding	A
		1.0	1.3	1.3	W	Wood	S	Good	Fixed	A
46	Tehachapi	1.3	2.6	3.4	W	Wood	E	Good	Vert.Sliding	A
		2.2	2.3	5.1	W	Wood	E	Good	Vert.Sliding	A
47	Lancaster	2.0	4.0	8.0	W	Al	S	Good	Crankout	A
		1.5	3.0	4.5	W	Al	S	Good(?)	Crankout	A
		1.5	3.0	4.5	W	Al	S	Good(?)	Crankout	A

TABLE II-12 (Continued)

Complaint Number	Location	Size Width ft.	Size Ht. ft.	Area Sq.ft.	Glass	Frame	Orientation	Previous Condition	Installation	Approval
PHASE I (Continued)										
50	EAFB	2.9	3.9	11.0	W	Al	W	N/A	Fixed	A
		1.4	3.8	5.3	W	Al	N	N/A	N/A	A
51	EAFB	2.9	3.8	11.0	W	Al	E	N/A	Fixed	A
		2.9	3.8	11.0	W	Al	W	N/A	Hor.Sliding	A
52	EAFB	2.9	3.8	11.0	W	Al	E	N/A	Fixed	A
55	EAFB	1.0	1.3	1.3	W	Steel	N	N/A	Crankout+	N/A
		1.0	1.3	1.3	W	Steel	N	N/A	Crankout+	N/A
		1.0	1.3	1.3	W	Steel	N	N/A	Crankout+	N/A
58	Tehachapi	6.7	6.1	40.8	P	Wood	E	Good	Fixed	A
PHASE II										
62	Lancaster	1.8	3.8	6.9	W	Al	E	Good	Fixed	A
63	Mojave	1.8	3.9	7.0	W	Al	E	Good	Crankout	A
67	Rosamond	3.8	6.3	23.9	P	Al	S	Poor	Hor.Sliding	D
		3.8	6.3	23.9	P	Al	S	Poor	Fixed	D
70	Mojave	10.1	4.7	47.5	P	Al	W	Good	Fixed	A
72	Lamont	1.8	3.8	6.9	W	Al	S	Good	Hor.Sliding	A

11.34
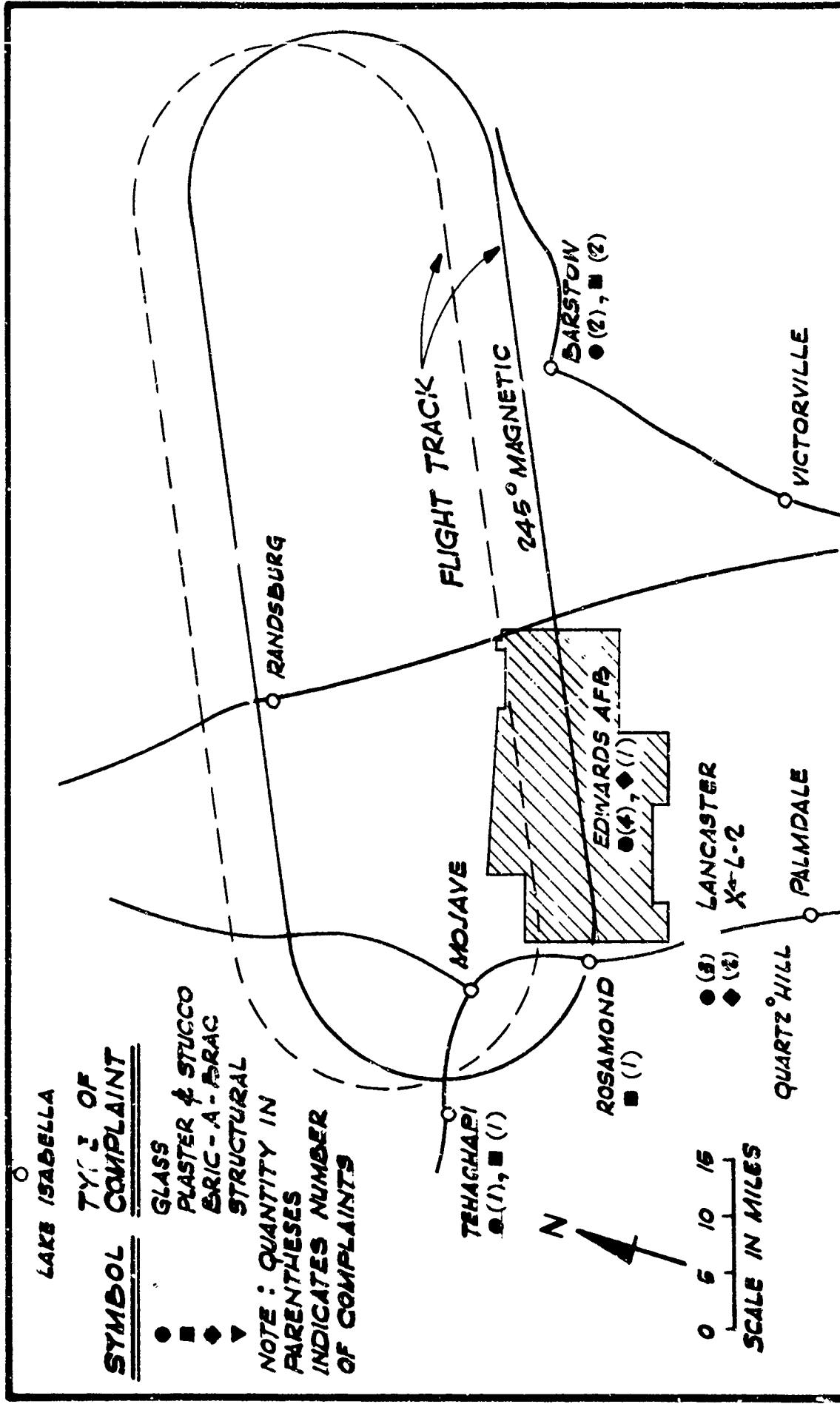
SONIC BOOM DAMAGE COMPLAINT LOCATIONS

3 JUNE 1966 - 12 JUNE 1966

FIG. 11-1
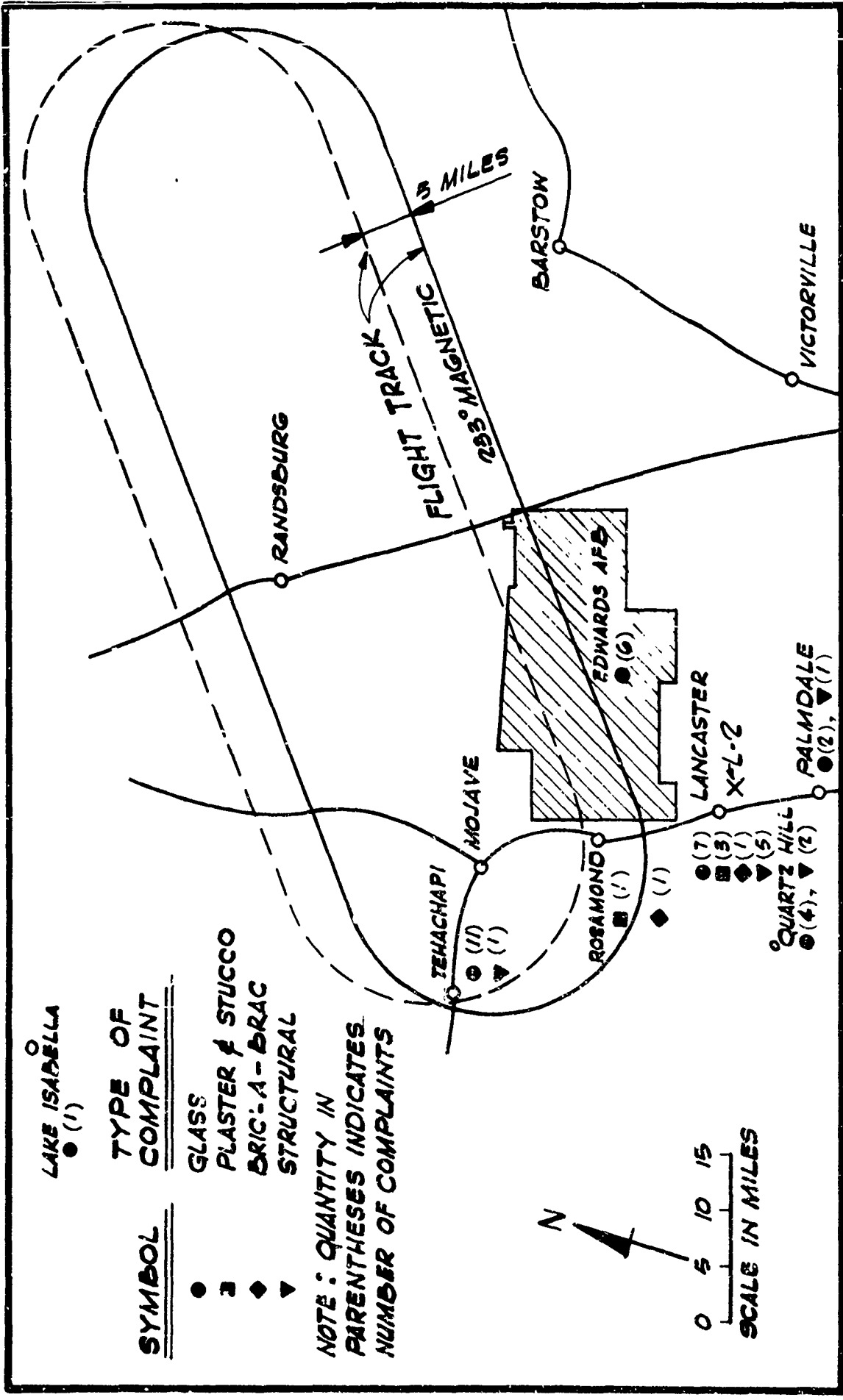
FIG. 11-1

SONIC BOOM DAMAGE COMPLAINT LOCATIONS
13 JUNE 1966 - 23 JUNE 1966

FIG. 11-2

FIGURE 11-3

INVESTIGATOR'S SONIC BOOM DAMAGE REPORT *(Write legibly or type)*

1. Name of claimant(s)	2. Address	3. Claim or complaint number
		4. Date property inspected

5. Contact ....
....or claimant at the
following phone number: ....

6. Location of damaged property:

7. DATA PERTAINING TO THE SONIC BOOM:
a. Has a sonic boom been verified at time and date alleged?...............................if so
b. Altitude of aircraft: ....
c. Speed of aircraft: ....
d. Type of aircraft: ....
e. Do local police have records of sonic boom complaints?............................if so, give details: ....
....
....
f. If sonic boom not verified, what steps were taken to verify boom? ....
....

8. PROCEDURAL MATTERS: (if applicable)
a. Is the Standard Form 95 submitted in three(3) copies? ....
b. Has the Standard Form 95 been signed in ink by claimant (also wife in joint claim)? ....
c. Has claimant specifically specified on claim form the amount claimed? ....
d. If claimant is a corporation, has the claim form been properly executed and does the file contain an authority to file claim
(if SF 95 not signed by an officer of the corporation)? ....
e. If claim is in excess of $1,000 and involves realty, does file contain a statement of title showing that the claimant owns the
property? ....
f. Is this damage covered by insurance?...................... If so, has claimant filed a claim with the insurance company? ....
g. If claimant is an insurance company does file contain proof of loss or subrogation agreement? ....
h. Has claimant submitted necessary itemized estimate(s) or paid bill? ....
i. In glass damage cases, does the estimate or bill take into consideration salvage value and discount rates? ....
....

9. GENERAL INFORMATION:
a. Time and date when boom supposedly occurred: ....
b. If multiple booms, are any identified by time and date? ....
....
c. Did anyone actually see damage occur?......................If so, list name and attach statements: ....
....
....
d. When was damage first discovered? ....
e. Were windows and doors open or closed? ....
f. Did the person who experienced the boom report that mobile objects in the building were shaken, moved or otherwise
affected? How? ....
g. List names and addresses of anyone else in the immediate area, other than claimant known to have sustained damage at the
same time as these claimants: ....
....
....
....

AFLC FORM SEP 65 **666**

AFLC- WPAFB-OCT 65 20M

FIGURE 11-3 (Continued)

10. NAMES AND ADDRESSES OF PERSONS INTERVIEWED: (attach statements)

....

....

....

11. Has damage been repaired? .... If so, when?	12. Age of building and how determined:

13. Type of property damaged and general description of the damage: ....

....

....

....

....

....

....

14. DETAILS PERTAINING TO SURROUNDING COMMUNITY:
   a. Type of terrain: ....
   b. Type of surrounding community: ....
   c. State whether or not there were present any other potential causes of the claimed damage, such as: Inclement weather, seismic disturbance, heavy truck traffic, railway traffic, explosions, soil conditions, or any other and distance of this factor from claimant's property: ....

....

....

....

....

15. DATA PERTAINING TO EXTERIOR OF PROPERTY:
   a. Type of construction and size of building: ....

....

   b. Type of roofing and condition: ....

....

   c. Type of foundation and conditions: ....

....

   d. Condition of sidewalks: ....

....

16. DATA PERTAINING TO INTERIOR OF PROPERTY:
   a. Was any settlement noted? ....

....

   b. Type of construction of walls and ceilings (wood lath and plaster, wallboard, tile or other): ....

....

   c. Condition of plaster, wallboard, or tile: (Is damage old or recent?) ....

....

   d. Are walls and ceilings papered, painted or tiled? ....

....

   e. Location and type of cracks (identify on photos and draw diagram of damaged area on AFLC Form 670) ....

....

....

....

....

   f. When was damage area last decorated and what was the extent of redecoration? ....

....

....

11.38

FIGURE 11-5 (Continued)

17. Describe general condition of the property: ....
....
....

18. Type of glass damage, if any (identify on photos and draw diagrams on AFLC Form 669). Describe type of glass, dimensions including thickness, extent and type of preexisting damage: ....
....
....
....
....
....
....
....
....

19. FINDINGS AND RECOMMENDATIONS:

Approve: .... Deny: .... Partially approve in the amount of $.................... ....

(In your discussion be specific as to when the damage occurred in relation to the time when the sonic boom occurred. Set out your opinion as to the cause of the damage. If the damage was partially caused by sonic boom set forth percentage you believe attributable to sonic booms and your rationale for arriving at this conclusion. Use a continuation sheet if necessary):
....
....
....
....
....
....
....
....
....
....
....
....
....
....
....
....
....
....
....
....
....
....
....
....

20. Any other comments: ....
....
....
....
....
....

Date	Typed Name, Rank, Title, and Organization of Inspectors:	Signature

FIGURE 11-4

SONIC BOOM – GLASS DIAGRAMS
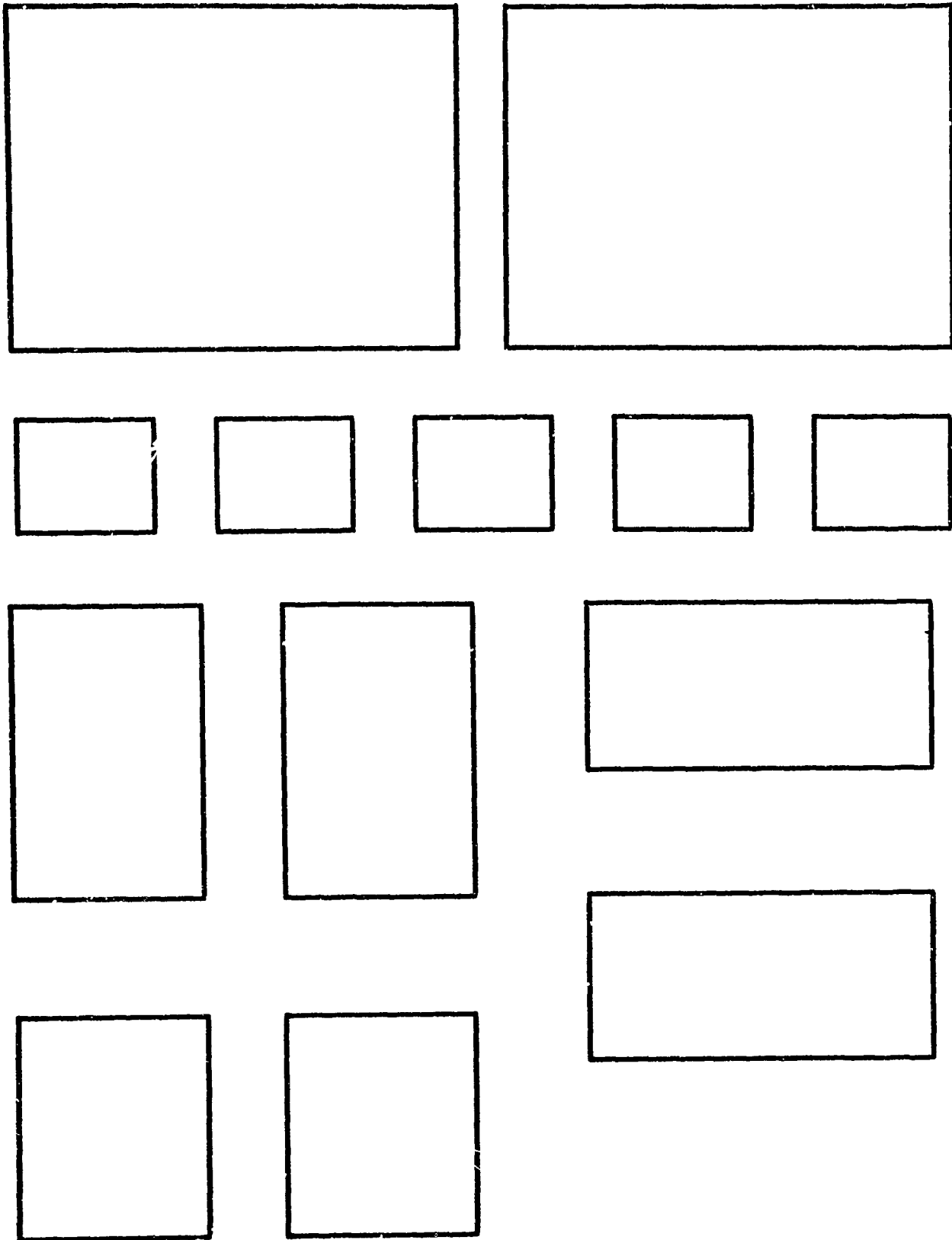
FIGURE 11-5

SONIC BOOM – INTERIOR DIAGRAMS

_____ ROOM

N

W   E

CEILING PLAN S

W   E

N WALL

E   W

S WALL

N   S

E WALL

S   N

W. WALL

_____ ROOM

N

W   E

CEILING PLAN S

W   E

N WALL

E   W

S WALL

N   S

E WALL

S   N

W WALL

AFLC FORM SEP 65 670   PC 4600
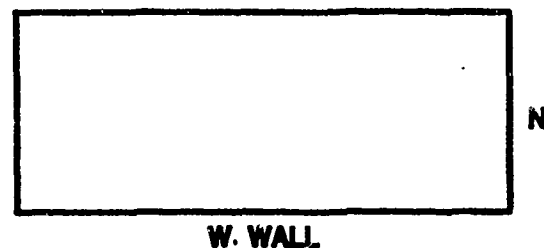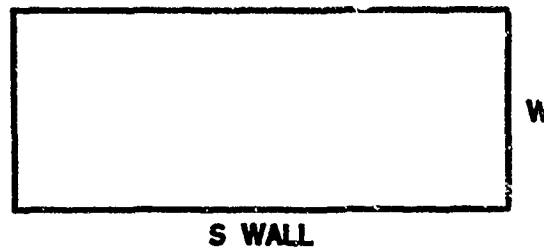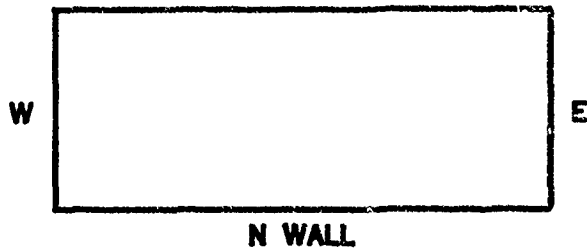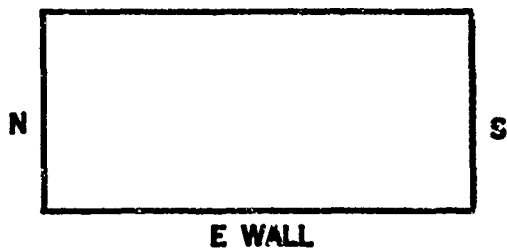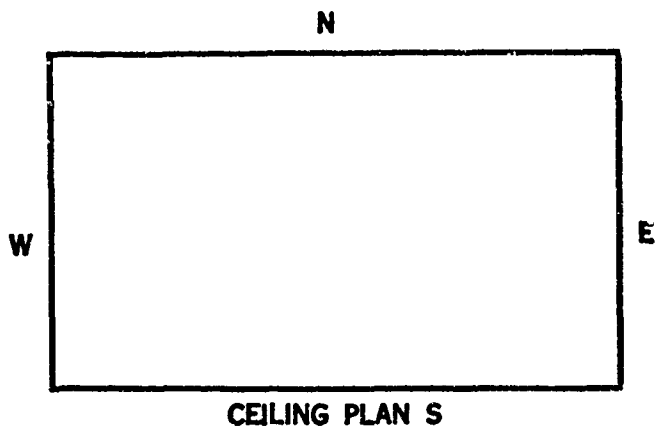
AFLC–WPAFB–OCT 65 12M
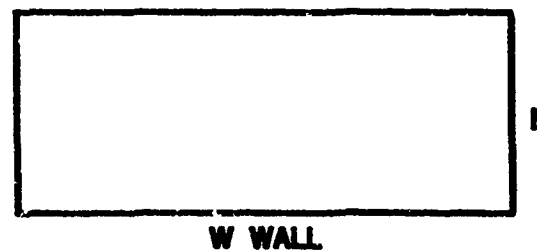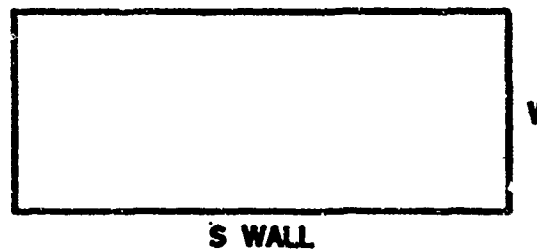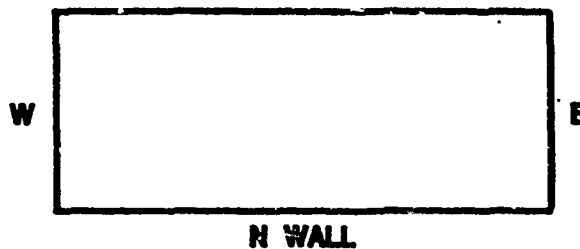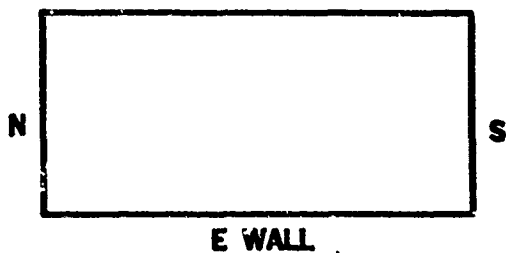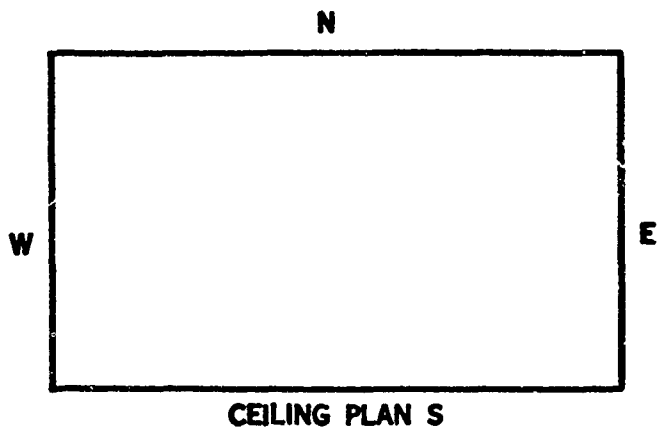
BIBLIOGRAPHY

BIBLIOGRAPHY

1. STRUCTURAL RESPONSE TO SONIC BOOMS, SST 65-1, Volumes 1 and 2 (AD610822)
    Final Report. Prepared for FAA by Andrews Associates, Inc., and Hudgins,
    Thompson, Ball and Associates, Inc., Oklahoma City, Oklahoma, February,
    1965. Contract FA-64-AC-6-526.

2. STRUCTURAL REACTION PROGRAM NATIONAL SONIC BOOM STUDY PROJECT, SST 65-15,
    Volumes 1 and 2. Prepared for FAA by John Blume & Associates Research
    Division, San Francisco, April 1965. Contract FA-SS-65-12.

3. THE EFFECTS OF SONIC BOOM ON STRUCTURAL BEHAVIOR, SST 65-18, Final Report.
    Prepared for FAA by Wiggins, J.H., John A. Blume & Associates Research
    Division, San Francisco, October 1965. Contract FA-SS-65-12.

4. DESIGN OF MULTISTORY REINFORCED CONCRETE BUILDINGS FOR EARTHQUAKE MOTIONS,
    Blume, J.A., Newmark, N.M. and Corning, L.H., Portland Cement Associa-
    tion, 1961.

5. INTRODUCTION TO STRUCTURAL DYNAMICS, Biggs, J.M., McGraw-Hill, 1964.

6. STRUCTURAL DESIGN FOR DYNAMIC LOADS, Norris, Hansen, Holley, Biggs,
    Namyet, Ninami. McGraw-Hill, 1959.

7. ENGINEERING VIBRATIONS, Jacobsen, L.S. and Ayre, R.S., McGraw-Hill, 1958.

8. VIBRATION PROBLEMS IN ENGINEERING, Timoshenko, S., and Young, D.H.,
    D. Van Nostrand, Third Edition, 1959.

9. DYNAMICS OF STRUCTURES, Hurty, W.C. and Rubinstein, M.F. Prentice-Hall,
    1964.

10. AN INTRODUCTION TO THE DYNAMICS OF FRAME STRUCTURES, Rogers, G.L., John
    Wiley & Son, 1959.

11. THE EQUIVALENT STATIC ACCELERATIONS OF SHOCK MOTIONS, Walsh, J.P. and
    Blake, R.E., Proceedings Society Experimental Stress Analysis, Volume
    6, No. 2, 1949.

12. GROUND SHOCK DUE TO RALEIGH WAVES FROM SONIC BOOMS, Baron, Bleich and
    Wright. ASCE, Engineering Mechanics Research, October 1966.

13. ADVANCED DYNAMICS, Timoshenko, and Young, D.H., McGraw-Hill, 1948.

14. ENGINEERING STATISTICS, Bowker, A.H. and Lieberman, G.J., Prentice-
    Hall, 1963.

15. INTRODUCTION TO THE THEORY OF STATISTICS, Mood, A.M. and Graybill, F.A.
    McGraw-Hill, 1963.

16. SAMPLING TECHNIQUES, Cochran, W.G., John Wiley & Son, 1963.

17. STATISTICAL THEORY WITH ENGINEERING APPLICATIONS, Hald, A., John Wiley
     & Son, 1962.

18. RESPONSE OF TEST STRUCTURES TO SELECTED SONIC BOOMS, Blume, John A.,
     Presentation to OST Committee, 26 September 1966.

19. VIBRATION RESPONSES OF TEST STRUCTURE NO. I DURING THE EDWARDS AIR
     FORCE BASE PHASE OF THE NATIONAL SONIC BOOM PROGRAM. Findley, D.S.,
     Huckel, V. and Henderson, H.R., Langley Working Paper No.288, NASA,
     September 1966.

20. VIBRATION RESPONSES OF TEST STRUCTURE NO. 2 DURING THE EDWARDS AIR FORCE
     BASE PHASE OF THE NATIONAL SONIC BOOM PROGRAM. Findley, D.S., Huckel,
     V., and Henderson, H.R., Langley Working Paper No. 259, NASA, September
     1966.

21. REINFORCED CONCRETE SHEAR WALL ASSEMBLIES, Benjamin, J.R. and Williams,
     H.A., Proceedings of the ASCE, August 1960.

22. FIRST PROGRESS REPORT ON RACKING TESTS OF WALL PANELS, prepared for the
     Nevada Operations Office, U.S. Atomic Energy Commission by John A. Blume
     & Associates Research Division, San Francisco, August 1966. Contract
     AT (26-I)-99.

23. BEHAVIOR OF WINDOW PANELS UNDER IN-PLANCE FORCES, Bouwkamp, J.G.
     Report to the Division of Architecture, Division of Public Works, State
     of California, February 1960.

24. STATICALLY INDETERMINATE STRUCTURES. Benjamin, J.R., McGraw-Hill, 1959.

25. THEORETICAL STUDY OF STRUCTURAL RESPONSE TO NEAR-FIELD AND FAR-FIELD
     SONIC BOOMS; Wiggins, J.H. and Kennedy, B., Final Report prepared for
     National Sonic Boom Evaluation Office, October, 1966. Contract No.
     AF49(638)-1777.

26. COMPUTATION OF THE PRESSURE-TIME HISTORY OF A SONIC BOOM SHOCK WAVE
     ACTING ON A GLASS WINDOW IN A BUILDING. Zumwalt Glen W., Prepared
     under Contract No. NASI-5813 for National Aeronautics and Space
     Administration.

27. ACOUSTICAL AND VIBRATIONAL STUDIES RELATING TO AN OCCURRENCE OF SONIC
     BOOM INDUCED DAMAGE TO A WINDOW GLASS IN A STORE FRONT. Lowery, Richard
     L. and Andrews, Dan K,. Prepared under Contract No. NASA-5813 for
     National Aeronautics and Space Administration.

28. FORMULAS FOR STRESS AND STRAIN, Roark, R.J., McGraw-Hill, 1965.

29. LETTER FROM DR. JAMES R. YOUNG, Stanford Research Institute, Menlo Park,
     California. Dated 16 June 1967.

30. EVALUATION OF WINDOW PANE DAMAGE INTENSITY IN SAN ANTONIO RESULTING
     FROM EXPLOSION AT MEDINA FACILITY OF NOVEMBER 13, 1963, Southwest
     Research Institue Report.

31. SONIC BOOM EXPERIMENTS AT EDWARDS AIR FORCE BASE. Working draft of Interim Report by National Sonic Boom Evaluation Office (to be published).

32. LATERAL-SPREAD SONIC-BOOM GROUND-PRESSURE MEASUREMENTS FROM AIRPLANES AT ALTITUDES TO 75,000 FEET AND AT MACH NUMBERS TO 2.0, Maglieri, D.J., Parrott, T.L., Hilton, D.A., and Copeland, W.L. NASA Technical Note NASA TN D-2021, NASA, November, 1963.

33. GLASS PRODUCTS RECOMMENDATIONS-STRUCTURAL, Technical Service Report No. 101, Pittsburgh Plate Glass Co., Pittsburgh, Pa., March 1964.

34. PRELIMINARY RESULTS OF XB-70 SONIC BOOM FIELD TESTS DURING NATIONAL SONIC BOOM EVALUATION PROGRAM, Maglieri, D.J., Huckel, V., Henderson, H.R., and Putman, T., Langley Working Paper LWP-382, Langley Research Center, NASA, March 9, 1967.

GLOSSARY OF TERMS

GLOSSARY OF TERMS

A — peak deflection

A_j — digitized acceleration values

b — height of plate (window)

C_j — coefficients obtained from Simpson's rule

C_v — coefficient of variation

c — damping coefficient

D — plate stiffness $= \dfrac{Et^3}{1-v^2}$

DAF — dynamic amplification factor

E — elastic modulus

F, f — forcing function

I — moment of inertia

K — stiffness

L — length of beam or plate

M, m — mass

m — subscript referring to m^{th} normal mode

n — sample size

n — subscript referring to n^{th} normal mode

P — total load , an element

$P()$ — probability

P_a — atmospheric pressure

P_i — inside pressure

P_n — net pressure $(P_n = P_o - P_i)$

P_o — outside pressure

P_1 — peak positive overpressure

P_2 — peak negative pressure

PF — participation factor

p — $\sqrt{\omega^2 - \beta^2}$

q — distributed load on an element

r — subscript referring to r^{th} mass

S — sample standard deviation

s^2 — sample variance

T — natural period

T_1 — rise time (time from start of boom to peak positive overpressure)

T_2 — time from start of boom to peak negative pressure

t — plate thickness

t — time

V — enclosed volume

w — displacement (perpendicular to surface of window plate), see also Δ

x — coordinate (of point on window plate)

x — displacement (see also Δ)

$\dot{x}$ — velocity

$\ddot{x}$ — acceleration

x_i — the ith sample

$\bar{x}$ — sample mean

β — percent of critical damping

Δ — displacement

ϵ — strain

ν — Poisson's ratio

τ — time from start to end of boom

ϕ — deflected shape

ω — natural circular frequency

APPENDIX A

STRUCTURAL AND STATISTICAL PRINCIPLES

STRUCTURAL AND STATISTICAL PRINCIPLES

The structural and statistical principles used in the analyses of structural response data and free field signature data in this report are reviewed in this Appendix. Equations are derived where deemed desirable. References are given as required.

STRUCTURAL PRINCIPLES

The primary purpose of the structural analyses presented in this report was to compare measured response with predicted response. Measured response was determined from instrumented test structures and predicted response was calculated using structural principles presented herein. To evaluate the predicted response of a structure or structure element to a sonic boom dynamic loading, the properties of idealized structures were represented by mathematical models. In the formulation of these models, it was assumed that the structure remained elastic and that the damping losses were proportional to the relative velocity between masses or to the velocity of each mass relative to the ground. The idealized structure, which was a multi-degree of freedom system, was then modeled by independent single-degree of freedom systems. Each normal mode of vibration of the multi-degree of freedom system was treated as an independent single degree of freedom system. The single-degree of freedom system was related to the multi-degree of freedom system by the modal participation factor. There were as many natural frequencies as there were elements of the multi-degree of freedom system and each mode of vibration was excited by the disturbing force to a degree determined by the element's modal participation factor.

The following is a brief derivation of the equations for a single-degree of freedom system and an explanation of how the single-degree of freedom system is related to the multi-degree of freedom system.

Single Degree of Freedom System

The equilibrium equation of a single degree of freedom damped system subjected to an arbitrary forcing function, $f(t)$, is:

$$m\ddot{x} + c\dot{x} + kx = f(t) \qquad \text{(A-1)}$$

where:

m = mass

c = damping coefficient

k = stiffness

$\ddot{x}$ = acceleration

$\dot{x}$ = velocity

x = displacement

Dividing Equation (A-1) by m, letting $\frac{c}{m} = 2\beta$, and $\frac{k}{m} = \omega^2$, Equation (A-1) becomes:

$$\ddot{x} + 2\beta \dot{x} + \omega^2 x = \frac{f(t)}{m} \qquad (A-2)$$

It should be noted that when $\omega = \beta$, the motion is critically damped; that is, the motion loses its vibratory character. The value of the damping coefficient, c, is then $\frac{c}{2m} = \sqrt{\frac{k}{m}}$. Thus $c = 2\sqrt{km}$.

When a system is 2% critically damped the damping coefficient, c, is equal to:

$$c = 0.04 \sqrt{km}$$

If it is assumed in the solution of Equation (A-2) that P is the peak value of the disturbing force, the term $P/m\omega^2$ or nce $m\omega^2 = k$ the term P/k can be factored out of the solution to obtain:

$$x(t) = \frac{P}{k} \cdot DAF \qquad (A-3)$$

where DAF is the Dynamic Amplification Factor and P/k is the static deflection of a structure element subjected to a load P. The DAF therefore represents the influence of a dynamic load or the change of the magnitude of the load with time.

The magnitude of the DAF for a given structural element also depends upon the element's natural frequency, stiffness, and damping. Natural frequency is the number of vibrations per second resulting when an element is displaced from its at rest position and released; stiffness is an element's resistance to displacement or rotation; damping is the measure of a system's capacity to absorb energy and cause vibrations produced by a disturbance such as a sonic boom to diminish as the time after the disturbance increases.

An example of a DAF spectrum has been plotted in Figure A-1 for a typical N-type pressure wave. In this illustration, the DAF has been plotted on the

A.2

vertical scale and the natural frequencies, in cycles per second, of struc-
ture elements have been plotted on the horizontal scale. A graph of this
type can be used in the following manner. Suppose that this graph repre-
sented the DAF spectrum for a supersonic aircraft mission and it is desired
to compute the maximum deflection of a wall panel for a sonic boom peak dy-
namic pressure of, say 2 psf. The natural frequency of the wall panel could
be determined by calculation or measurement. Assume that the value obtained
was 20 cps. Then the value of the DAF can be scaled from the graph and is
equal to 1.75. The stiffness, k, of the element could also be determined by
calculation or measurement, and assume that the value obtained was k = 200 psf/in
(which includes a correction to account for the fact that the wall is a distrib-
uted mass). Then the dynamic displacement would be:

$$\Delta \text{ dynamic} = \frac{P}{k} \times DAF = \frac{(2 \text{ psf})}{(200 \text{ psf/in})} \times 1.75$$

$$\Delta \text{ dynamic} = 0.0175 \text{ in.}$$

Multi-Degree of Freedom System

To obtain the response of a multi-degree of freedom system, where each
normal mode is treated as an independent one-degree of freedom damped system,
the modal equation is derived[4,5] by energy methods:

$$\ddot{x}_n + 2\beta_n \dot{x}_n + \omega_n^2 x_n = \frac{\Sigma F_r \phi_{rn}}{\Sigma M_r \phi_{rn}^2} \qquad (A-4)$$

where the subscript r represents a lumped mass, subscript n a mal mode,
F_r a forcing function on mass r, M_r a mass, and ϕ_{rn} the def   shape of mass r
in the nth mode. Solving Equation (A-4) we obtain:

$$x_{rn}(t) = \frac{P(max)}{m_r \omega_n^2} \cdot (DAF)_n \cdot (PF)_{rn} \qquad (A-5)$$

where $(PF)_{rn}$ is the participation factor of mass r in the nth mode. Equation
(2-6) can be rewritten thus:

$$x_{rn}(t) = \frac{P(max)}{m_r \omega_{rn}^2} (DAF)_n \qquad (A-6)$$

where:

$$\omega_{rn}^2 = \frac{\omega_n^2}{(PF)_{rn}}$$

The concept of DAF is widely used and whether the forcing function is a

A.3

load, an acceleration, a velocity or a displacement, it has been called Dynamic Load Factor[6,5], Load Response Spectrum[7], Magnification Factor[8], Dynamic Magnification Factor[9], acceleration, velocity and displacement Response Spectrum[10,4] and Shock Spectrum[11,12].

When the forcing function is given in digital form, the response of a single-degree of freedom damped system is[13]:

$$x(t) = \frac{P}{k} \cdot p \cdot \frac{\Delta t}{3} \cdot \sum_{J=o}^{I} C_J A_J \, e^{-\beta p \, (I-J)\Delta t} \, \sin p(I-J)\Delta t \qquad (A-7)$$

where:

$$p = \sqrt{\omega^2 - \beta^2}$$

A_J = digitized input value, normalized with respect to P

C_J = coefficients obtained from Simpson's Rule.

STATISTICAL PRINCIPLES

Statistical methods were used to estimate the true value of observations resulting from the same phenomena, to compare various parameters, and to provide a degree of confidence in the conclusions made from analyses of data.

In order to estimate the true value of observations resulting from the same phenomena, the mean, the variance, the standard deviation and the coefficient of variation were computed.

The sample mean (average) $\bar{x}$, is a measure of central tendency corresponding to the center of gravity in a mechanical system. It is mathematically expressed as:

$$\bar{x} = \frac{\Sigma x_i}{n} \qquad (A-8)$$

where x_i is the ith observation in a sample of size n.

The sample variance, s^2, is a measure of the spread or dispersion of the observations about the mean and corresponds to the moment of inertia in a mechanical system. The mathematical expression of the sample variance is:

$$s^2 = \frac{\Sigma(x_i - \bar{x})^2}{n - 1} \qquad (A-9)$$

The sample standard deviation is defined as the square root of the variance and corresponds to the radius of gyration measured from the center of gravity in a mechanical system. The sample mean and the sample standard devi-

A.4

ation have the same units as the observations.

Another measure of the spread of the data is the sample coefficient of variation. This dimensionless quantity is defined as the ratio of the sample standard deviation to the sample mean:

$$C_v = \frac{s}{\bar{x}} \qquad (A-10)$$

Statistical tests were used to verify each hypothesis which could be rejected or accepted. If it was rejected an alternate hypothesis was accepted. There are, however, two types of errors in hypothesis testing: the rejection of a true hypothesis, type I error, and the acceptance of a false hypothesis, type II error. The probability of committing an error of type I is denoted by α and is called the level of significance of the test; the probability of committing an error of type II is denoted by β and is equal to one minus the power of the test. The probability of accepting a true hypothesis, $(1-\alpha)$, can be called the confidence level of the test. More generally, the confidence level can be defined as the probability that the conclusion is correct.

In order to test the hypothesis that the mean of a normally distributed random variable was equal to a specified value, μ_o, against the alternate hypothesis that the mean was greater than μ_o, the following t statistic was used[14,15]:

$$t = \frac{(\bar{x} - \mu_o) \sqrt{n}}{s} \qquad (A-11)$$

If $t \leq t_{\alpha;n-1}$, the hypothesis of equality was accepted. If $t > t_{\alpha;n-1}$, the hypothesis of equality was rejected and the alternate hypothesis, $\bar{x} > \mu_o$, accepted.

In order to test the hypothesis that the means of two normally distributed random variables were equal against the alternate hypothesis that one of the means was greater than the other, the following t statistic was used:

$$t = \frac{\bar{x}_1 - \bar{x}_2}{\sqrt{\dfrac{s_1^2}{n_1} + \dfrac{s_2^2}{n_2}}} \qquad (A-12)$$

A.5

If $t \leq t_{\alpha;\nu}$, the hypothesis of equality was accepted. If $t > t_{\alpha;\nu}$, the hypothesis of equality was rejected and the alternative hypothesis, $\bar{x}_1 > \bar{x}_2$, was accepted.

It was often required to express the relationship between two variables in order to predict the outcome of one by knowing the other. The general equation expressing the relationship was given by a non-linear regression model[17]:

$$f(y) = a + b_1 \, (g_1 \, (x) - \overline{g_1(x)}) + \ldots + b_n(g_n(x) + \overline{g_n(x)}) \qquad (A-13)$$

where a, b_1, b_2, ... b_n were constants calculated from observations and $f(y)$ was any function of y such as y, $\frac{1}{y}$, $\log y$, y^n, $g_1(x)$, $g_2(x)$, $g_n(x)$ were any function of x such as $\frac{1}{x}$, $\log x$, x^n. The more basic model was the linear regression:

$$y = a + b_1 \, (x - \bar{x}) \qquad (A-14)$$

Another model was the second order polynominal:

$$y = a + b_1 \, (x - \bar{x}) + b_2 \, (x^2 - \bar{x}^2) \qquad (A-15)$$

Once the model was fitted through the data it was possible to calculate the standard deviation of y for a given value of x. For the linear model:

$$S_y = \left[s^2 \, (\frac{1}{n} + \frac{(x - \bar{x})^2}{\Sigma(x_i - \bar{x})^2}) \right]^{\frac{1}{2}} \qquad (A-16)$$

$$s^2 = \frac{\Sigma(y_i - \bar{y})^2 - \left[\dfrac{\Sigma(x_i - \bar{x})(y_i - \bar{y})}{\Sigma(x_i - \bar{x})^2} \right]^2}{n-2} \qquad (A-17)$$

The predicted value was obtained from the regression model, as for the linear model given in Equation (A-14). A prediction was usually accompanied by a range. In the regression analysis the range was given as a confidence interval, or the probability that a future observation would lie within the upper and lower values given. A confidence interval of 95%, for example, meant that there was a 95% probability that any observation lies within the upper and lower value.

TYPICAL SONIC BOOM PRESSURE SIGNATURE
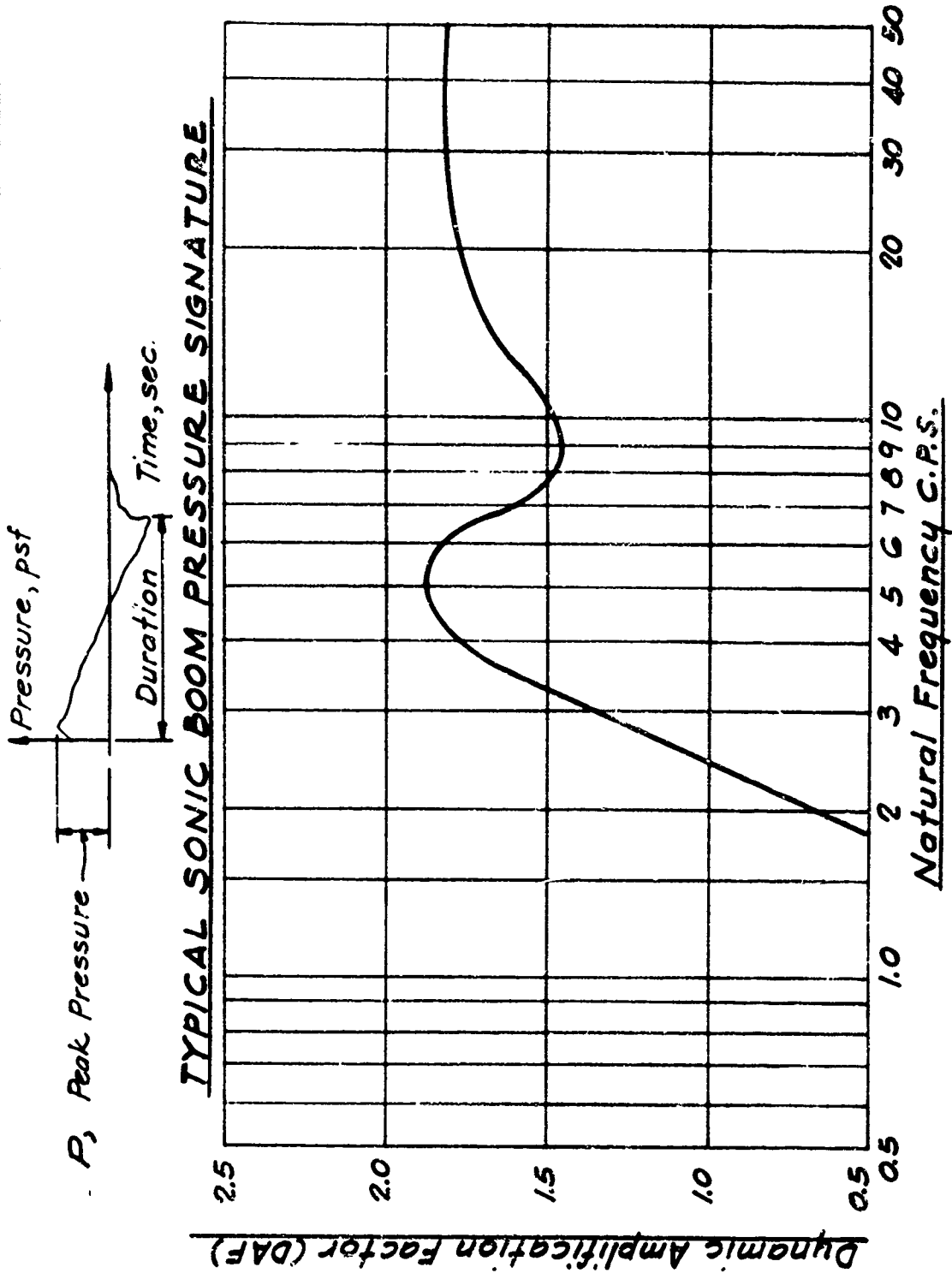
EXAMPLE OF A DAF SPECTRUM FOR A 2% DAMPED SYSTEM

FIG. A-1

A.7

APPENDIX B

INSTRUMENTATION LOCATIONS, SYSTEMS, AND FREQUENCY RESPONSE

FOR

TEST STRUCTURES E-1, E-2 AND E-3 AND
FREE FIELD MICROPHONES (CRUCIFORM ARRAY)

APPENDIX B

INSTRUMENTATION LOCATIONS, SYSTEMS, AND FREQUENCY RESPONSE
FOR
TEST STRUCTURES E-1, E-2, AND E-3 AND
FREE FIELD MICROPHONES (CRUCIFORM ARRAY)

Contents   Page

LEGEND

The following is an explanation of notations and abbreviations used in this Appendix:

Symbol	Item
MA	Acoustic Microphone (20 - 10,000 cps)
M	Pressure Microphone (0.1 - 10,000 cps)
ML	Pressure Microphone (0.1 - 10,000 cps)
MLC	Pressure Microphone (0.02 - 10,000 cps)
A	Low Frequency Accelerometer (dc - 500 cps)
A P	High Frequency Accelerometer (100 - 2000 cps)
SG	Strain Gage (2000 cps)
S	Strain Gage (2000 cps)
D	Displacement (5 - 100 cps)
TR	Tape Recorder
BR	Bedroom
FR	Family Room
KIT	Kitchen
LR	Living Room

INSTRUMENTATION LOCATION - STRUCTURE E-I*

(See Fig. B-I & B-2)

Transducer	Tape Recorder	Channel	Location
MAI	TR-I	101	In center of LR suspended 6 feet from floor.
MA2	TR-I	102	In center of FR-KIT area suspended 6 feet from floor.
MA3	TR-I	103	Center BRI suspended 6 feet from floor.
MA4	TR-I	104	BRI movable.
MA5	TR-I	105	FR-KIT area, movable.
MA7	TR-I	113	Outside subject group
AI	TR-3	304	On concrete block in LR.
A2	TR-3	305	On concrete block FR-KIT area.
A3	TR-I	106	On concrete block BRI (vertical)
A5	TR-2	201	At top plate on E wall at NE corner (East-West (acceleration).
A6	TR-2	203	At top plate on N wall at NE corner (North-South (acceleration).
AII	TR-2	202	BRI E wall, mid-height center stud (horizontal).
MLI	TR-8	803	Outside N wall above plate.
ML2	TR-8	804	Outside E wall.
ML3	TR-2	204	BRI next to AII.
ML4	TR-2	205	Center ceiling attic side above FR-KIT area.
ML5	TR-8	805	Outside W wall of garage at plate line.
ML6	TR-8	806	Outside S wall above plate line, center.
SG3	TR-2	207	Center big window (garage) (axis horizontal).
MA8	TR-2	209	Trigger mike in field.

*Refer to Legend, Page B.I, for explanation of notation and abbreviation.

TABLE B-2

INSTRUMENTATION LOCATION – STRUCTURE E-2[*]

(See Figs. B-3 through B-5)

Transducer	Tape Recorder	Channel	Location
MA1	TR-1	107	Between LR and DR 6 feet above floor.
MA2	TR-1	108	Over center in KIT 6 feet above floor.
MA3	TR-1	109	Center of BRI 6 feet above floor
MA4	TR-1	110	Center of FR 6 feet up.
MA5	TR-1	111	Movable FR-KIT-DR.
MA6	TR-1	112	Movable FR-KIT-DR.
A1P	TR-3	306	On concrete block FR.
A2P	TR-3	307	Movable FR-KIT-DR area. (Dinette window 10/31)
A5P	TR-3	308	Movable FR-KIT-DR area. (Pantry louver door 10/31)
A6P	TR-3	309	Movable FR-KIT-DR area. (Cabinet door 10/31)
A9P	TR-3	310	On concrete block BRI. (N-S Direction) - Movable.
A10P	TR-3	311	Movable FR-KIT-DR area. (Side of stove 10/31)
A11P	TR-3	312	Movable FR-KIT-DR area. (Dining room window 10/31)
A12P	TR-3	313	On concrete block BRI. (E-W direction) - Movable.
A1	TR-3	301	On concrete block DR.
A2	TR-3	302	On concrete block FR.
A5	TR-4	401	On exterior at roof plate line on N side of NE corner.
A6	TR-4	403	On exterior at roof plate line on E side of NE corner.
A7	TR-4	405	On exterior at second floor plate line on N side of NE cnr.
A8	TR-4	407	On exterior at second floor plate line on E side of NE cnr.
A9	TR-4	402	On bottom chord of roof truss approx. over center of BRI.
A11	TR-4	404	On center stud at mid-height on E wall of DR.
A12	TR-4	406	On center stud at mid-height on N wall of BRI.
SG41	TR-2	206	Located on large plate glass window garage entrance.
SG42	TR-2	208	Located on large plate glass window garage entrance.
SG43	TR-2	210	Located on large plate glass window garage entrance.
SG44	TR-2	212	Located on large plate glass window garage entrance.
D1	TR-4	411	Adjacent to A5 with same axis.
D2	TR-4	412	Adjacent to A6 with same axis.
ML2	TR-4	408	Suspended between LR and DR adjacent to MA1.
ML3	TR-4	409	Located in attic above BRI.
ML4	TR-4	410	Suspended below ceiling center BRI.
ML11	TR-8	811	Outside E wall middle of second story.
ML12	TR-8	812	Outside E wall middle of first story, outside of DR.
ML13	TR-8	810	Outside on W wall above garage roof.
ML14	TR-8	809	Outside W garage wall above plate line.
ML15	TR-8	801	Center of roof N side.
ML16	TR-8	802	Center of high roof's side.
ML17	TR-8	807	Outside N wall middle of second story.
ML18	TR-8	808	Outside S wall mid-second story, midway between porch roof and eave line.

[*] Refer to Legend, Page B.1, for explanation of notation and abbreviation.

TABLE B-3

INSTRUMENTATION LOCATION - BOWLING ALLEY E-3*

(See Fig. B-6)

Transducer	Tape Recorder	Channel	Location
A1H	TR-5	501	Top of steel column (interior of building) East-West racking acceleration.
A2H	TR-5	502	Top of steel column (south side) East-West racking accel.
A3H	TR-5	503	Top of steel column (south side) North-South racking accel.
A4H	TR-5	504	Top of steel column (west side) North-South racking accel.
A5V	TR-5	505	Center of roof girder, vertical acceleration of girder.
M2	TR-5	512	Interior - 3 feet below roof.
M4	TR-5	513	Exterior - above roof.
S1L	TR-5	507	Strain gage on bottom flange of roof girder at centerline.
S2L	TR-5	508	Strain gage on bottom flange of roof girder at 1/4 point.
S3L	TR-5	509	Strain gage on bottom flange of purlin at centerline.

TABLE B-4

INSTRUMENTATION LOCATION - FREE FIELD MICROPHONES

(CRUCIFORM ARRAY)*

(See Fig. B-7)

Transducer	Tape Recorder	Channel	Location
MLC1	TR-6	601	East corner cruciform array.
MLC2	TR-6	603	North corner cruciform array.
MLC3	TR-6	605	West corner cruciform array.
MLC4	TR-6	607	South corner cruciform array.
MLC5	TR-6	609	Bottom of mast, center cruciform array.
MLC6	TR-6	611	Top of mast, center cruciform array.

*Refer to Legend, Page B.1, for explanation of notation and abbreviation.

INSTRUMENTATION SYSTEMS

The measuring systems involved the following equipment:

TAPE RECORDERS TR-1 through TR-5

MA-System (Acoustic Microphone)

Microphones - B & K Model 4134
Power Supplies - B & K Model 2801
Amplifiers - Burr-Brown Model 9860

Low Frequency System

Accelerometers - Kistler Model 303M10
Control Panels - NASA built

ML-System (Pressure Microphones)

Microphones - Photocon Model 464
Signal Conditioning - Photocon Dynagage Model DG-605
Amplifiers - Burr-Brown Model 9860

Strain Gage System

Strain Gage - Micro-Systems Type PAI-16-350
Amplifier Box - NASA built, using Fairchild ADF-1 Amplifier

High Frequency System

Accelerometers - Endevco Model 2219E
Amplifiers - Glennite Model KA-1006

Velocity System (Displacement System)

Velocity Transducer - MB Model MB-124
Amplifier - CEC System D
Power Supply - CEC Model 2-105A

Tape Recorders - CEC VR-3300 (30 ips)
Direct Write Oscillographs - CEC Model 5-124
Galvanometer Driver Amplifiers - CEC Model 163
Oscilloscopes - Hewlett-Packard Model 140A
Squelch circuits and selector modules as designed and
   fabricated by NASA Langley Research Center.

TAPE RECORDER TR-6

ML-System

        Microphones - Photocon PRP-464-15D (Modified by partly plugging
                        vent hole to extend low frequency response)
        Signal Conditioning - Photocon DG-605D Dynagage
        Amplifier - Burr-Brown Model 9077A
        Tape Recorder - CEC VR-3300 (30 ips)

TAPE RECORDER TR-8

ML-System

        Microphones - Altec 21BR-150
        Signal Conditioning - Photocon 600D Dynagage
        Amplifier - Ampex 15770-1
        Tape Recorder - Ampex CP100
        Direct Write Oscillographs - CEC 5-124

TABLE 8-6

TRANSDUCER FREQUENCY RESPONSE AND ACCURACY

Transducer	Frequency Response	Accuracy
Acoustic Microphones (MA)	20-10,000 cps	$\pm$ 2.1 db
Pressure Microphones (ML) (TR-2, 4, 5, and 8)	0.1-10,000 cps	$\pm$ 2.1 db
Pressure Microphones (MLC) (TR-6)	0.02-10,000 cps	$\pm$ db
Low Frequency Accelerometers (A)	dc-500 cps	$\pm$ 5%
High Frequency Accelerometers (A P)	100-2000 cps	$\pm$ 12%
Strain Gages (SG, S)	2000 cps	$\pm$ 2%
Displacement (D)	5-100 cps	$\pm$ 2%

700 FT. △

245° MAG.
FLIGHT TRACK

BEDROOM
NO. 1.

FAMILY
ROOM -

GARAGE

MAG.
NORTH

LIVING
ROOM

(OUTSIDE SUBJECT
GROUP)

○ STRAIN GAGE
▫ ACCELEROMETER
△ MICROPHONE (20-10,000 CPS)
◮ MICROPHONE (0.1-10,000 CPS)
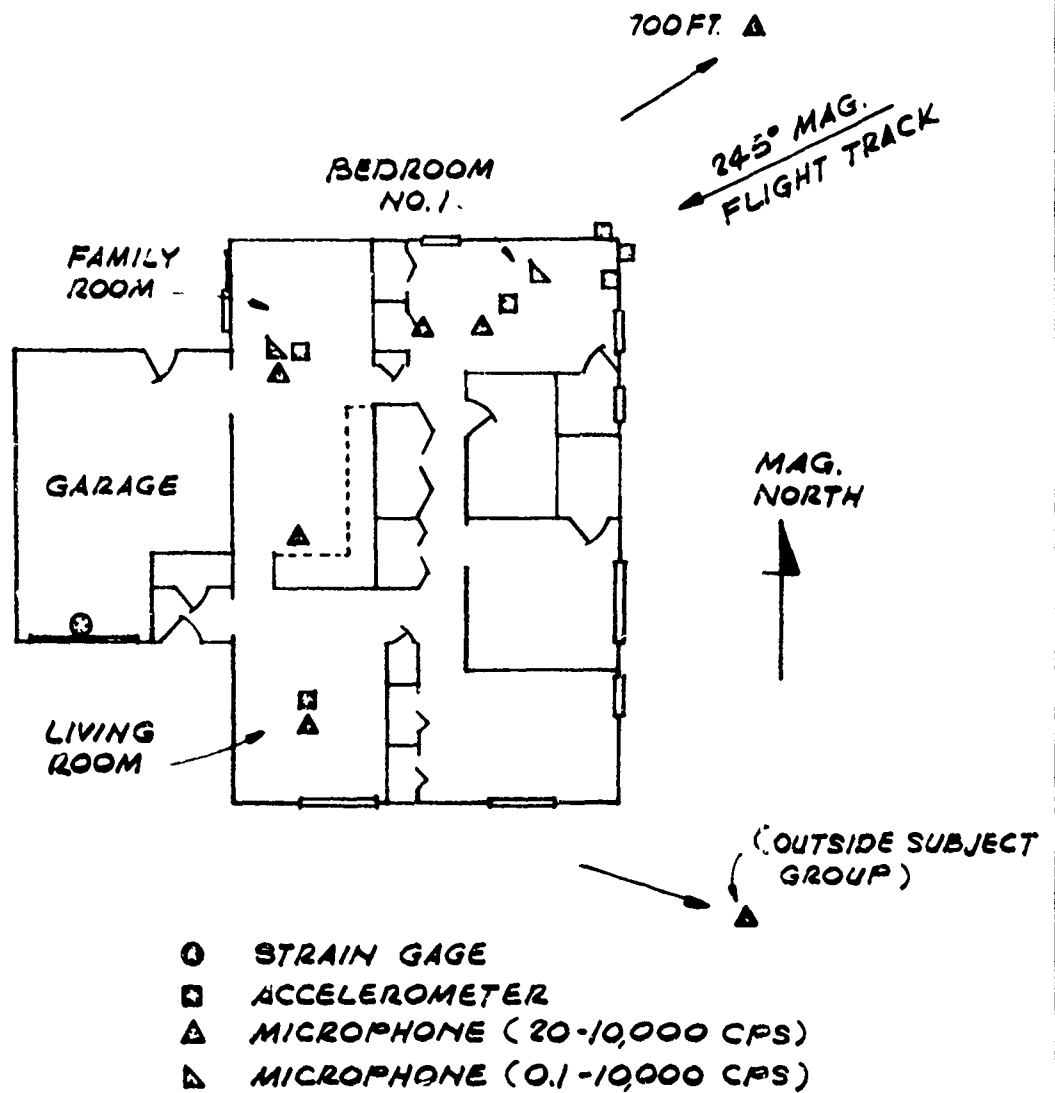
FIG. B-1 INSTRUMENTATION LOCATION,
STRUCTURE E-1 FLOOR PLAN
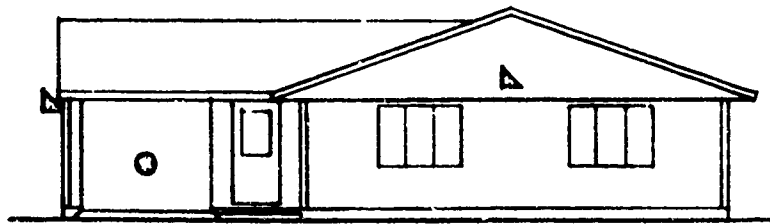
SOUTH
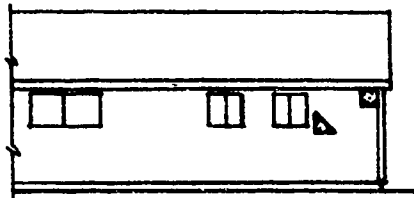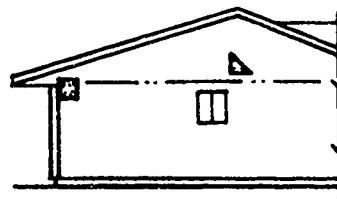
PART EAST   PART NORTH

ELEVATIONS

O STRAIN GAGE
▫ ACCELERROMETER
▲ MICROPHONE (0.1 - 10,000 CPS)

FIG. B-2 INSTRUMENTATION LOCATION,
STRUCTURE E-1 ELEVATION

245° MAG.
FLIGHT TRACK
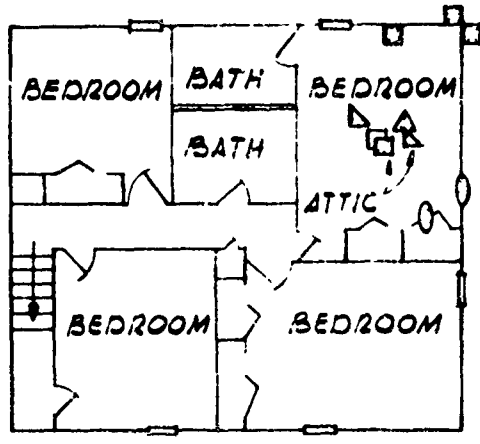
SECOND FLOOR
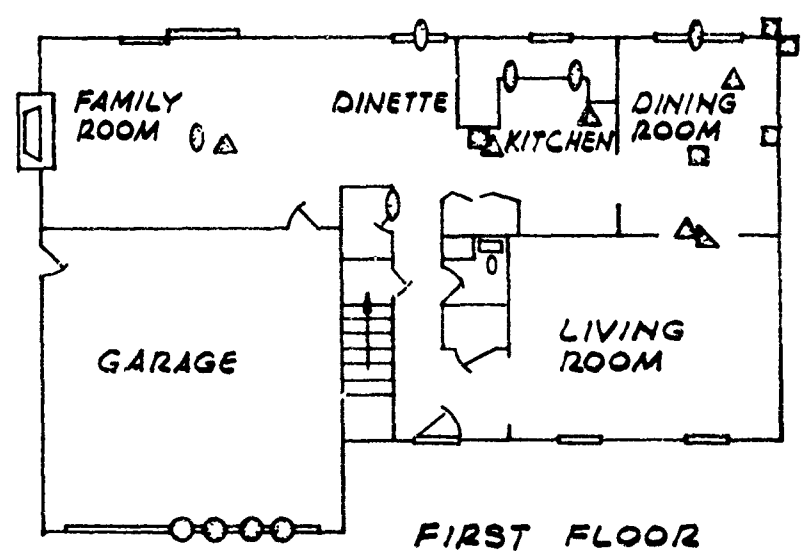
FIRST FLOOR

○ STRAIN GAGE
□ ACCELEROMETER
△ MICROPHONE (20 - 10,000 CPS)
◁ MICROPHONE (0.1 - 10,000 CPS)
◊ HF ACCELEROMETER

MAG.
NORTH

FIG. B-3 INSTRUMENTATION LOCATION,
STRUCTURE E-2 FLOOR PLAN

b.10
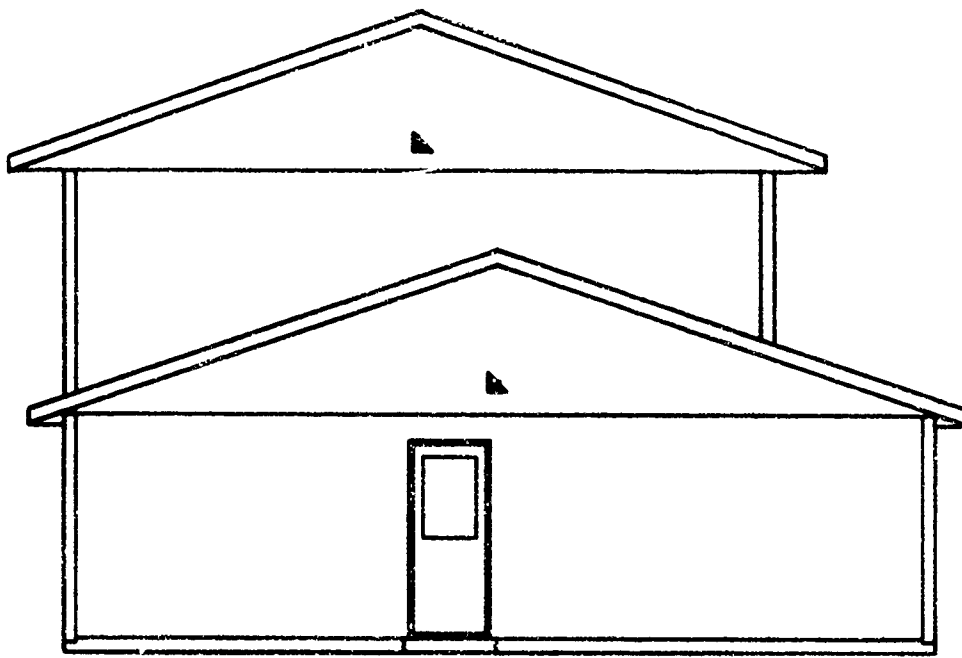
WEST ELEVATION

▲ MICROPHONE (0.1-10,000 CPS)

FIG. B-4 INSTRUMENTATION LOCATION

STRUCTURE E-2 ELEVATION

ML 15 NORTH SIDE
ML 16 SOUTH SIDE

PLATE
LINE

ML 17 NORTH SIDE
ML 18 SOUTH SIDE

NORTH ELEVATION

PLATE
LINE
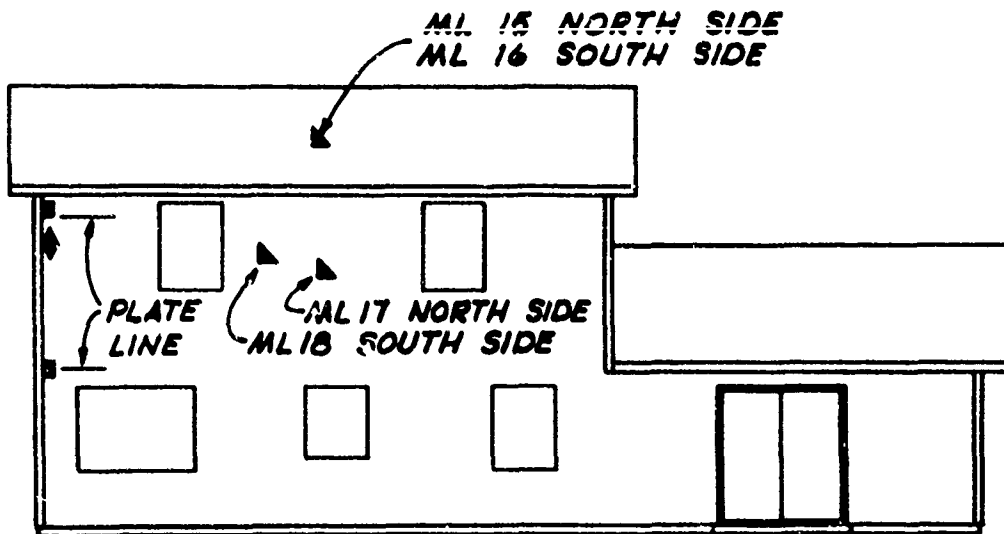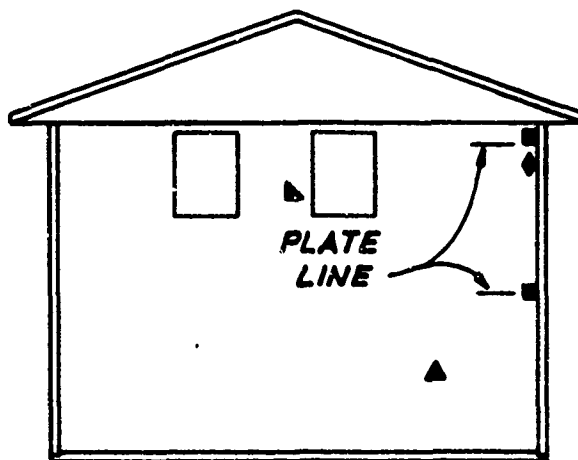
EAST ELEVATION

■ ACCELEROMETER
▲ MICROPHONE (0.1-10,000 CPS)
♦ DISPLACEMENT GAGE

FIG. B-5 INSTRUMENTATION LOCATION
STRUCTURE E-2 ELEVATION

SECTION A-A

PLAN
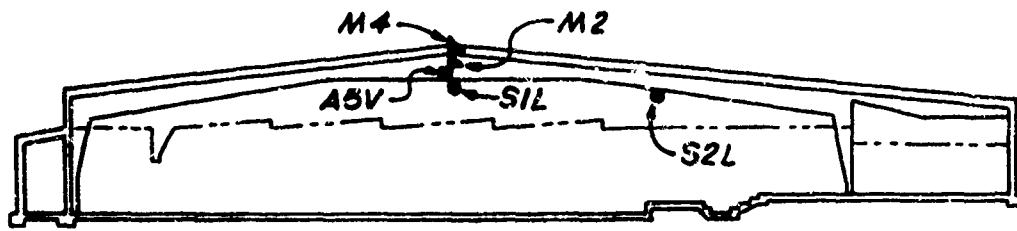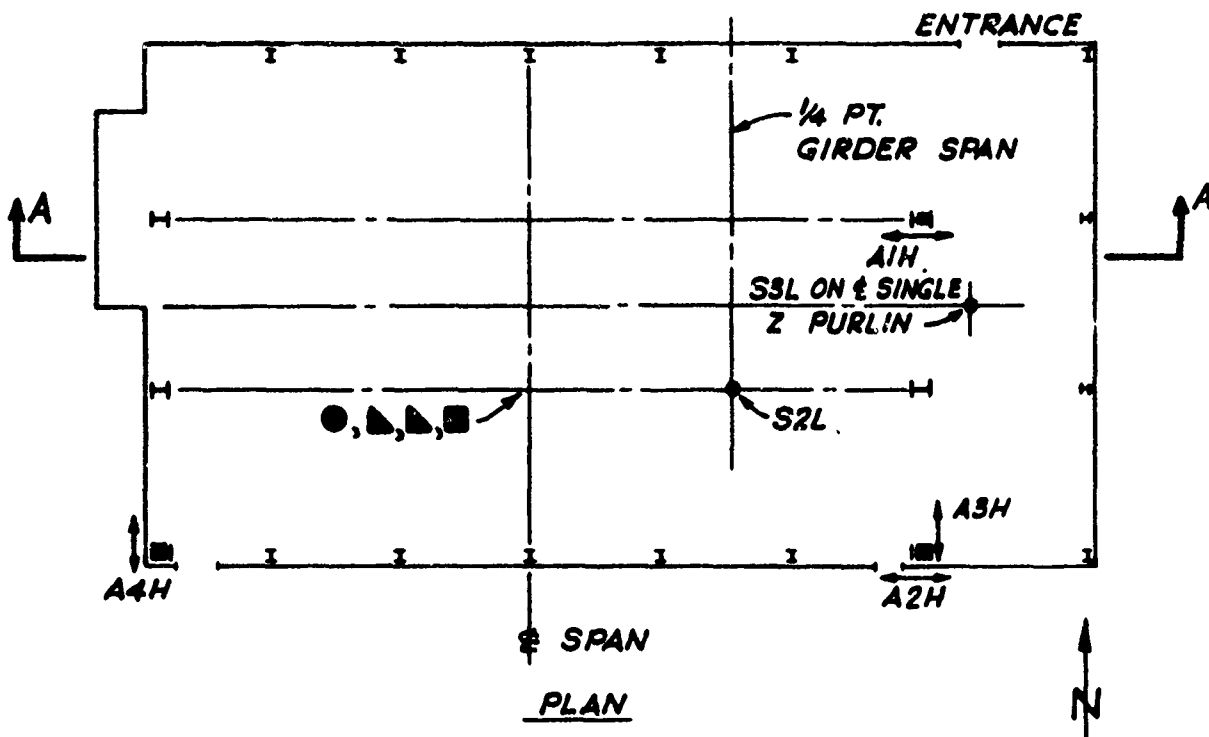
■   ACCELEROMETERS

▲   MICROPHONES

●   STRAIN GAGES

FIG. B-6   INSTRUMENTATION LOCATION

STRUCTURE E-3
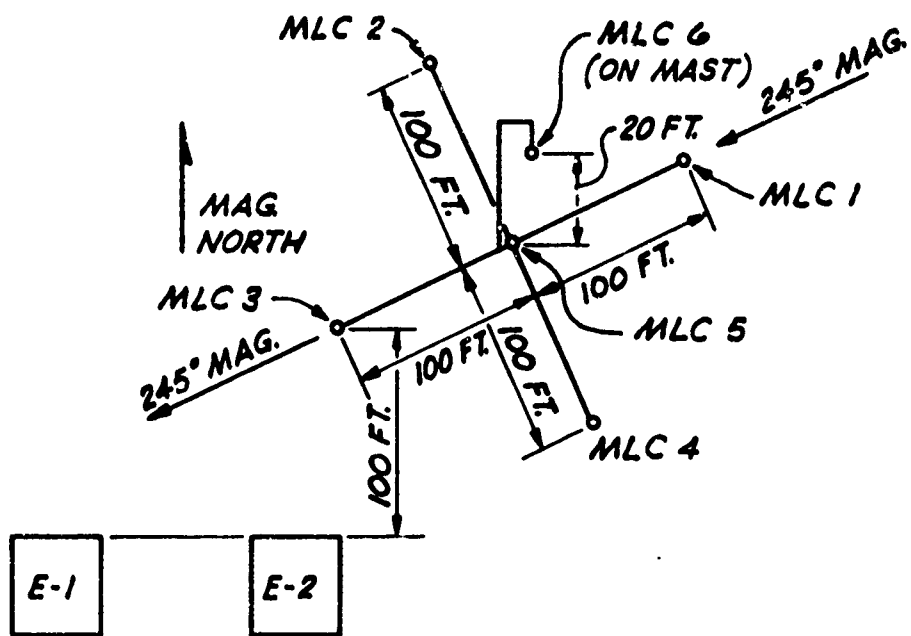
FIG. B-7   INSTRUMENTATION LOCATION
FREE   FIELD   MICROPHONES
(CRUCIFORM   ARRAY)

B.14

APPENDIX C

INSTRUMENT CALIBRATION PROCEDURES

C. INSTRUMENT CALIBRATION PROCEDURES

The following general procedures were followed for calibrating instrumentation installed in E-1, E-2 and E-3:

1. All equipment was left in the "Power On" condition, except tape recorders which were turned off over weekends only.

2. All instrumentation channels were calibrated prior to and immediately after each day's run. Calibration commenced at 0600 on run days.

3. Use of voice annotations was held to a minimum to maintain IRIG timing on the tapes.

4. On each run day, personnel were informed, prior to calibrating, of values to set on the various channels. Variations in gain settings were recorded on the log sheet for the particular mission.

5. All pertinent data, including unusual conditions or events, were recorded on the appropriate data sheets.

TAPE RECORDERS TR-1, 2, 3, 4, 5 AND 6

Photocon Microphone Calibration

1. Tune Dynagage.

2. Set Dynagage at attenuation of "18".

3. Set Burr Brown Amplifier at 18 dB.

4. Balance Dynagage for "Zero Output".

5. Install the proper adaptor on the driver unit of the Model PC-125 calibrator.

6. Check the battery condition of the PC-125 by turning the function control to "Bat. Check". If the meter reads below the line marked "Bat. Check", recharge the batteries for a minimum of 12 hours. If the meter reads above the "Bat. Check" line, proceed as follows:

7. Set the "DB SPL" control to 120 dB, turn the function control to "Operate" and adjust the "SPL ADJ" control until the "SPL" meter reads 0 dB.

8. Adjust Burr Brown amplifier gain to obtain a "2vPP" signal at tape recorder input for SPL of 120 dB.

9. Alternately switch calibrator "on & off" and check balance and gain settings. The system is now ready to make the day's calibration and record on tape. NOTE: After system calibration is on tape, DO NOT retune Dynagage.

10. When flight settings are made, leave Dynagage at "18". Add or subtract as needed in Burr Brown amplifier. (Always stay 1 dB under the assigned level - if the difference is an odd number.)

C.1

ii. Continually check the Dynagage tuner for dc balance.

12. **DO NOT** rebalance system after the command "Recorders On" is given.

13. Only one (1) variable will be used to obtain the desired SPL, if possible.

14. A 2 V PP signal will be the equivalent of 120 dB SPL.

NOTE: If the tuning meter should read high throughout the entire tuning range, it indicates that the link circuit is open. If this happens, the transducer cable and its connectors should be inspected. If the meter stays near the middle of the scale during tuning, a short in the transducer cable or in the transducer itself is indicated.

Accelerometer Calibration

1. Set accelerometer voltage at "± 28 volts dc".

2. Set accelerometer amplifier voltage at "± 15 volts dc".

3. Check output voltage when switch is in "Amplifier" position.

4. Balance output to "Zero" with balance pot, adjust dc balance and check with digital voltmeter.

5. Run a current insertion calibration on the sensitivity range selected for the day's flight, using table below as a guide:

Accelerometer Sensitivity	External Calibrate Box
0.05 g	8 micro amps
0.1 g	16 micro amps
0.2 g	20 micro amps
0.5 g	20 micro amps
1.0 g	20 micro amps

Current Insertion Calibrating Procedure

1. Insert the phone jack of the external insertion box into front of accelerometer control panel.

2. Record "Zero" voltage on data sheet.

3. With the calibrate switch of the external calibrate box in the "Positive" position, adjust the balance pot to give the required current level as listed in step 4 above. Record the voltage, then switch to the "Negative" calibrate position and record the voltage on your data sheet.

4. Record calibrate 0, +, and - signals on tape recorder.

Strain Gage Calibration

1. Check system for proper sensitivity range card. (Register Board.)

2. Check output voltage (amplifier balance) when switch is in "Dummy Gage"

position. (Should be "Zero".)

4. If calibrate voltage varies more than 20-millivolts from original calibration, call to attention of project engineer.

5. Switch to "Active Gage" position and zero active bridge.

6. Check calibrate voltages with digital voltmeter. (Record on data sheet.) Record calibrate signal on tape recorder.

Bruel & Kjaer Microphone Calibration

1. Set Burr Brown Amplifier (Model 9860) at 100 dB.

2. Install the proper adapter on the driver unit of Model PC-125 calibrator. (Photocon unit.)

3. Check the battery condition of the PC-125 by turning the function control to "Bat. Check". If the meter reads below the line marked "Bat. Check", recharge the batteries for a minimum of 12 hours. If the meter reads above the "Bat. Check" line, proceed as follows:

4. Set the "dB SPL" control to 100 dB, turn the function control to "Operate" and adjust the "SPL ADJ" control until the "SPL" meter reads zero dB.

5. Verify that the two 100 dB settings produce a 1.5 volt p-p ($\pm$ 10%) reading on the oscilloscope. (Note: If scope indicates greater than $\pm$ 10%, set unit's knob to produce 1.5 volts ($\pm$ 10%) and then reset knob by means of a set screw, to zero).

6. Verify that oscillograph deflection is approximately 0.5 in. with the two 100 dB settings.

7. For data runs, set amplifier gain knobs in accordance with the published schedule for each individual mission. (Normally, these settings were determined by SRI and were different for each noise and each boom mission.) The dial settings then become the "calibration" for each mission. (Examples: If dials indicate 177 dB, the 1.5 volt p-p signal of step 5 above equals 117 dB. If dials indicate 83 dB, 1.5 volts p-p = 83 dB.

High Frequency Accelerometer Calibration

1. Set oscillator to 1000 Hz (cps).

2. Plug oscillator into "Oscillator" terminal on Datacraft calibration panel

3. Plug scope into "Monitor" terminal on Datacraft calibration panel.

4. Set selector switch on Datacraft panel to proper channel, and set toggle switch to "Input".

5. Adjust amplitude control on oscillator until proper mv/g level is read on scope (400 mv/g accelerometers are being used). Correct input voltages will be assigned each day.

6. Reset toggle switch on calibration panel to "Output". Adjust gain control on that panel until output reads 2.0 volts p-p on the scope.

C.3

7. Repeat for other channels, turning selector switch to proper channel each time.

TAPE RECORDER TR-8

In order to ensure recordings of the Sonic Boom pressure within the linear range of the instrumentation system, and utilize the optimum dynamic range of the equipment, a proper system sensitivity must be established. Experience has shown that the actual measured pressure to nominal anitcipated pressure can vary in the order of 1.5. Therefore, a system sensitivity calibration should take into account this possible increased overpressure. Thus, given a 2 PSF nominal peak overpressure, the system should be set for 3 PSF full scale.

The following procedure gives a system sensitivity of 3 PSF peak.

1. Set DC amplifiers gain controls on channels 1-6 to -20 dB position and adjust oscillograph galvanometers for 1" centers across the paper. Apply 40 cps cal tone at 0.5 volts rms to channels 1 through 6, one at a time. Adjust oscillograph sensitivity potentiometers for a 1" deflection peak-peak. The oscillograph is now adjusted for a 3 PSF peak value.

2. Reset DC amplifier gains (channels 1-6) to 0 db position and switch transducer balance switches to position #2. Energize tape recorder and place in record mode. Apply 400 cps to channels 7-12, one at a time, and adjust FM reproduce amplifiers to 0.5 volts rms output. Read this output on channels 1-6, channel 1 corresponding to channel 7, channel 2 to channel 8, etc.

3. Return channels 1-6 DC amplifiers to +20 db level and switch transducer balance switches back to position #1.

4. A system end-to-end calibration is now obtained by applying the acoustic calibrator to each transducer. As each channel is checked, adjust the transducer sensitivity potentiometers for 0.234 volts rms (0.7 PSF peak) on VTVM. The tape recorder is now adjusted for a 3 PSF peak value. Record this signal, with appropriate annotations, on the tape recorder. The system is now ready for operation.

5. A system end-to-end post calibration is accomplished by repeating step 4, but no adjustments are made.

6. Sensitivity adjustment: Should the booms continually exceed the 3 PSF peak overpressure range, a greater dynamic range can be adjusted accordingly.

When system sensitivity other than 3 PSF peak are desired, system adjustments as illustrated below, can be made.

1. For a 4 PSF boom (nominal), let 1 volts rms = 6 PSF peak, then X volts rms = 0.7 PSF peak (calibrator), X = 0.117 volts rms.

C.4

With calibrator applied, adjust the transducer sensitivity potenti-
ometers to obtain this reading for each channel. The 400 cps insert
at 0.5 volts rms is now equivalent to 6 PSF peak to peak.

2. Oscillograph: For 6 PSF peak value, now read out values using "60"
   scale. Using 400 cps insert, adjust for 1" peak to peak deflection
   as previously.

3. An alternative method is shown below:

   For a - 6 db attenuation
   then: 6 db = 20 log X
         log X = 0.3
   or   X = 2
   Therefore, new system sensitivity is:
         $(2) \cdot 3$ PSF = 6 PSF

   The disadvantage of this method is that only - 3 db steps are avail-
   able on the dynagages, thus for any value other than - 6 db the peak
   value becomes a fractional number and direct readout is difficult.
   i.e.:

   For - 3 db of attenuation
   then: 3 db = 20 log X
         log X = 0.15
         X = 1.41
   so new range becomes $(1.41) \cdot (3)$ = 4.23 PSF peak.

C.5

APPENDIX D

MISSION LOG

Contents	Page

LEGEND

The following is an explanation of notations and abbreviations used in Mission Log Tables D-1 and D-2.

1.	DATE	Day, Month, Year
2.	MSN	Mission Identification Number
3.	A/C	Aircraft
4.	ALT, KFT, MSL	Altitude, 1000 ft. above Mean Sea Level
5/	MACH OR SPD	Mach Number for supersonic aircraft or Speed in Knots per Hour for subsonic aircraft.
6.	EPR, TKFF, (LDG)	Engine Power Ratio, Takeoff. If ratio is for landing, it is shown in parenthesis.
7.	HDG	Heading, degrees measured clockwise from magnetic north.
8.	OFFSET	Offset from track, North or South. Table D-1, offset is given in miles. Table D-2, offset is given in 1,000 ft. Table D-2, L = left or south, R = right or north.
9.	BOOM TIME	Observed boom time or time overhead for subsonic aircraft at house E-2, ZULU. Local time is ZULU minus eight hours.

D.1

TABLE D-1

MISSION LOG - EDWARDS PHASE I*

DATE DY MO YR	MSN	A/C	ALT KFT MSL	MACH OR SPD	EPR	HDG	OFF-SET N/S	BOOM TIME HR MN SC ZULU*
4 JUN 66	14	F-104	35.6	1.7				
4 JUN 66	13	XB-70	52.9	1.81		243	2.5N	17 28 00
6 JUN 66	39	B-58	31.4	1.25		244	4.64N	16 00 00
6 JUN 66	39B	KC-135	10.3		1.6			
6 JUN 66	70	B-58	43.9	1.60		245	0.55N	16 08 51
6 JUN 66	70B	KC-135	5.4		1.5			
6 JUN 66	40	B-58	31.4	1.48		246	0.20N	16 18 40
6 JUN 66	40B	KC-135	5.4		1.5			
6 JUN 66	71	B-58	44.2	1.59		245	5.00N	16 30 00
6 JUN 66	71B	KC-135	3.3		1.5			
6 JUN 66	41	B-58	31.3	1.45		247	0.17N	16 34 44
6 JUN 66	41B	KC-135	3.3		1.5			
6 JUN 66	72	B-58	43.9	1.55		244	4.85N	16 43 55
6 JUN 66	72B	KC-135	2.8		1.5			
6 JUN 66	74	B-58	32.4	1.30		242	.72S	17 01 52
6 JUN 66	74B	KC-135	8.3		2.35			
6 JUN 66	44	B-58	43.4	1.57		245	5.00N	17 11 00
6 JUN 66	44B	KC-135	8.3		2.35			
6 JUN 66	75	B-58	31.8	1.46		248		17 17 00
6 JUN 66	75B	KC-135	3.3		2.35			
6 JUN 66	42	B-58	43.3	1.53		245		17 24 40
6 JUN 66	42B	KC-135	2.8		2.35			
6 JUN 66	22	XB-70	72.0	2.83		262	4.10N	17 26 00
6 JUN 66	73	B-58	31.9	1.43		247	0.25N	17 31 30
6 JUN 66	73B	KC-135	2.5		2.35			
7 JUN 66	76A	B-58	31.6	1.48		241	1.09S	16 10 40
7 JUN 66	76B	KC-135	4.3		2.35			
7 JUN 66	45A	KC-135	3.0		2.35			
7 JUN 66	45B	B-58	43.7	1.70		244	4.95N	16 23 50
7 JUN 66	77A	KC-135	3.0		2.35			
7 JUN 66	77B	B-58	31.7	1.51		244	0.10S	16 32 12
7 JUN 66	46A	KC-135	2.6		2.35			
7 JUN 66	46B	B-58	43.7	1.65		246	5.42N	16 40 05
7 JUN 66	48A	B-58	38.7	1.31		245	5.23N	17 11 20
7 JUN 66	48B	KC-135	3.0		2.35			
7 JUN 66	79A	B-58	31.6	1.52		244	0.12N	17 22 20
7 JUN 66	79B	KC-135	2.6		2.35			
7 JUN 66	49A	B-58	43.3	1.43		252	4.68N	17 28 15
7 JUN 66	49B	KC-135	4.3		2.35			
7 JUN 66	80A	B-58	31.6	1.53		244	0.25N	17 38 45
7 JUN 66	80B	KC-135	3.0		2.35			
7 JUN 66	50A	B-58	43.3	1.43		245	5.00N	17 47 37
7 JUN 66	50B	KC-135	8.3		2.35			
7 JUN 66	81A	B-58	31.4	1.49		245	0.06S	17 56 25
7 JUN 66	81B	KC-135	4.3		2.35			

*Refer to Legend, Page D.1 for explanation of notations and abbreviations.

D.2

DATE DY MO YR	MSN	A/C	ALT KFT MSL	MACH OR SPD	EPR	HDG	OFF-SET N/S	BOOM TIME HR MN SC ZULU
8 JUN 66	1	XB-70	31.8	1.38		246	5.02S	15 19 00
8 JUN 66	43A	B-58	42.4	1.62		245	5.24N	16 00 22
8 JUN 66	43B	KC-135	14.3		2.35			
8 JUN 66	75A	B-58	31.2	1.44		244	0.23N	16 06 45
8 JUN 66	75B	KC-135	8.3		2.35			
8 JUN 66	42A	B-58	43.3	1.67		247	4.85N	16 14 50
8 JUN 66	42B	KC-135	2.8		1.5			
8 JUN 66	73A	B-58	31.2	1.50		245	0.10N	16 24 20
8 JUN 66	73B	KC-135	2.5		1.5			
8 JUN 66	41A	B-58	43.2	1.60		246	5.32N	16 30 10
8 JUN 66	41B	KC-135	5.3		1.5			
8 JUN 66	72A	B-58	31.2	1.49		245	0.16N	16 38 45
8 JUN 66	72B	KC-135	2.8		1.5			
8 JUN 66	57	KC-135	3.3		1.5			
8 JUN 66	57B	B-58	37.6	1.66		248	5.90N	17 05 10
8 JUN 66	80RA	KC-135	2.8		1.5			
8 JUN 66	80RB	B-58	31.3	1.46		247	0.14N	17 12 30
8 JUN 66	56RA	KC-135	5.3		1.5			
8 JUN 66	56RB	B-58	43.0	1.84		244	5.14N	17 21 22
8 JUN 66	87	KC-135	3.3		1.5			
8 JUN 66	87	B-58	31.4	1.49		245	0.40N	17 28 30
8 JUN 66	55RA	KC-135	10.3		1.5			
8 JUN 66	55RB	B-58	43.2	1.64		244	5.16N	17 36 10
8 JUN 66	86RA	KC-135	5.3		1.5			
8 JUN 66	86RB	B-58	31.4	1.49		229		17 45 00
9 JUN 66	86SA	KC-135	5.3		1.5			
9 JUN 66	86SRB	B-58	31.0	1.50		246	0.25N	16 08 30
9 JUN 66	55SA	KC-135	10.3		1.5			
9 JUN 66	55SRB	B-58	35.7	1.69		244	5.17N	16 19 20
9 JUN 66	87SA	KC-135	3.3		1.5			
9 JUN 66	87SRB	B-58	31.0	1.53		244	0.08S	16 25 58
9 JUN 66	56SA	KC-135	5.3		1.5			
9 JUN 66	56SRB	B-58	43.3	1.72		243	4.70N	16 34 50
9 JUN 66	80SA	KC-135	2.8		1.5			
9 JUN 66	80SRB	B-58	31.0	1.53		245	0.06N	16 41 40
9 JUN 66	57SA	KC-135	3.3		1.5			
9 JUN 66	57SRB	B-58	43.1	1.70		244	5.23N	16 49 10
9 JUN 66	41SA	B-58	42.9	1.52		240	4.87N	17 07 54
9 JUN 66	41SB	KC-135	5.3		1.5			
9 JUN 66	73SA	B-58	31.7	1.50		243	0.49S	17 16 15
9 JUN 66	73SB	KC-135	2.5		1.5			
9 JUN 66	42SA	B-58	43.1	1.52		241	4.69N	17 23 54
9 JUN 66	42SB	KC-135	2.8		1.5			
9 JUN 66	75SA	B-58	31.7	1.55		246		17 31 23
9 JUN 66	75SB	KC-135	8.3		2.35			

DATE DY MO YR	MSN	A/C	ALT KFT MSL	MACH OR SPD	EPR	HDG	OFF-SET N/S	BOOM TIME HR MN SC ZULU
9 JUN 66	43SA	B-58	43.0	1.68		243	4.62N	17 39 00
9 JUN 66	43SB	KC-135	14.3		2.35			17 57 00
9 JUN 66	42SA	B-58	43.3	1.70		244	4.92N	17 57 00
9 JUN 66	42SB	KC-135	2.8		1.5			
9 JUN 66	46SA	B-58	42.9	1.68		246	4.74N	18 11 10
9 JUN 66	46SB	KC-135	3.3		2.35			
9 JUN 66	72SA	B-58	31.3	1.53		248	0.63N	18 22 10
9 JUN 66	72SB	KC-135	2.8		1.5			
13 JUN 66	18A	B-58	37.7	1.64		231	0.09S	16 46 43
13 JUN 66	18B	B-58	49.6	1.66		234	0.36S	16 49 22
13 JUN 66	21A	B-58	37.8	1.69		230	0.21S	17 00 16
13 JUN 66	21B	B-58	49.2	1.72		231	0.35S	17 02 48
13 JUN 66	26A	F-104	21.2	1.40		231	0.08N	17 12 35
13 JUN 66	26B	F-104	29.7	1.60			0.64S	17 13 45
13 JUN 66	29A	B-58	49.3	1.67		233	0.03N	18 06 25
13 JUN 66	29B	B-58	38.1	1.67		232	0.11S	18 07 35
13 JUN 66	32A	B-58	49.8	1.64		235	0.53N	18 20 25
13 JUN 66	32B	B-58	38.0	1.67		233		18 21 10
14 JUN 66	26A	F-104						16 08 00
14 JUN 66	26B	F-104	29.9	1.54		238	.10S	16 10 50
14 JUN 66	38A	F-104						17 45 00
14 JUN 66	38B	F-104	29.7	1.52		233		17 45 45
14 JUN 66	37A	F-104	29.7	1.49		231		17 57 30
14 JUN 66	37B	F-104	21.1	1.39		231	0.02S	17 58 40
15 JUN 66	1XA	F-104	14.1	1.21		236	0.47N	16 14 50
15 JUN 66	1XB	F-104	28.1	1.50		233	0.13N	16 16 40
15 JUN 66	2XA	F-104	29.7	1.32		237	0.66N	16 21 40
15 JUN 66	2XB	F-104	14.1	1.20		233	0.22N	16 22 10
15 JUN 66	3XA	F-104	29.1	1.58		234	0.17N	16 38 25
15 JUN 66	3XB	F-104	14.2	1.15		235	0.18N	16 39 55
15 JUN 66	4XA	F-104	14.1	1.28		235	0.18N	16 47 15
15 JUN 66	4XB	F-104	29.9	1.62		233	0.44S	16 48 20
16 JUN 66	27A	F-104	29.3	1.65		230	0.10S	15 56 25
16 JUN 66	27B	F-104	20.5	1.40		228	0.26S	15 57 50
16 JUN 66	5X	F-104	29.7	1.65		344	0.25E	16 04 25
20 JUN 66	48A	B-58	41.3	1.55		232	2.20N	15 54 50
20 JUN 66	48B	KC-135	5.3		1.5			
20 JUN 66	79A	B-58	32.1	1.45		232	1.90S	16 08 00
20 JUN 66	79B	KC-135	3.3		1.5			
20 JUN 66	53A	B-58	42.7	1.59		232	5.00N	16 18 54
20 JUN 66	53B	KC-135	4.3		2.35			
20 JUN 66	84A	B-58	31.2	1.43		236		16 27 10
20 JUN 66	84B	KC-135	3.0		2.30			
20 JUN 66	54A	B-58	43.0	1.59		230	4.87N	16 35 40
20 JUN 66	54B	KC-135	3.0		2.30			
20 JUN 66	59A	KC-135	12.0		2.35			

D.4

MISSION LOG - EDWARDS PHASE I (Continued)

DATE			MSN	A/C	ALT KFT MSL	MACH	EPR	HDG	OFF-SET N/S	BOOM TIME HR MN SC ZULU
DY	MO	YR								
20	JUN	66	59B	B-58	43.4	1.41		233	5.00N	17 10 00
20	JUN	66	98A	KC-135	6.0		2.35			
20	JUN	66	98B	B-58	31.3	1.50		233		17 15 45
20	JUN	66	60A	KC-135	6.0		2.35			
20	JUN	66	90A	KC-135	6.0		2.35			
20	JUN	66	90B	B-58	31.8	1.55		230	0.17S	17 32 00
20	JUN	66	85A	B-58	32.3	1.45		231	4.35N	17 40 00
20	JUN	66	85B	KC-135	2.6		2.30			
20	JUN	66	93A	KC-135	2.6		2.30			
20	JUN	66	93B	B-58	32.1	1.55		231	0.17S	17 47 50
21	JUN	66	89A	KC-135	2.5		1.5			
21	JUN	66	89B	B-58	31.8	1.46		232	0.12N	16 01 55
21	JUN	66	58A	KC-135	2.8		1.5			
21	JUN	66	58B	B-58	43.6	1.67		233	5.12N	16 11 02
21	JUN	66	99A	KC-135	4.3		2.35			
21	JUN	66	99B	B-58	31.7	1.47		233	0.17N	16 17 05
21	JUN	66	66A	KC-135	2.8		1.5			
21	JUN	66	66B	B-58	39.9	1.59		233	5.00N	16 25 17
21	JUN	66	100A	KC-135	3.0		2.35			
21	JUN	66	100B	B-58	31.8	1.46		232	0.14S	16 30 23
21	JUN	66	68A	KC-135	8.3		2.35			
21	JUN	66	68B	B-58	44.1	1.62		232	4.83N	16 39 19
21	JUN	66	69A	B-58	39.4	1.39		233	5.00N	17 29 35
21	JUN	66	69B	KC-135	4.3		2.35			
21	JUN	66	48A	B-58	43.1	1.60		232	5.00N	17 44 12
21	JUN	66	48B	KC-135	5.3		1.5			
21	JUN	66	40A	B-58	43.8	1.65		235	5.40N	17 56 55
21	JUN	66	40B	KC-135	5.3		1.5			
21	JUN	66	60A	KC-135	8.3		2.35			
21	JUN	66	60B	B-58	43.9	1.64		233	5.16N	18 08 59
21	JUN	66	61A	KC-135	4.3		2.35			
21	JUN	66	61B	B-58	43.3	1.62		232	4.76N	19 37 19
21	JUN	66	101A	KC-135	2.6		2.35			
21	JUN	66	101B	B-58	31.7	1.50		233		19 51 15
21	JUN	66	85A	B-58	31.7	1.50		234	0.22N	20 05 50
21	JUN	66	85B	KC-135	2.6		2.35			
22	JUN	66	28A	B-58	37.0	1.63		234	0.18N	16 13 27
22	JUN	66	28B	F-104	20.8	1.35		233	0.16S	16 13 43
22	JUN	66	19A	B-58	37.2	1.64		233	0.24N	16 28 15
22	JUN	66	19B	F-104	29.5	1.42		233	0.20S	16 30 05
22	JUN	66	6X	B-58	43.6	1.60		259	1.34S	16 48 24
22	JUN	66	30A	B-58	37.4	1.65		230	0.20S	17 43 34
22	JUN	66	30B	F-104	29.7	1.37		232	0.16S	17 44 38
22	JUN	66	34A	F-104	29.6	1.39		233		17 56 06
22	JUN	66	34B	B-58	43.4	1.61		230	4.00N	17 57 06
22	JUN	66	24A	B-58	43.3	1.60		233	5.06N	18 10 37
22	JUN	66	24B	F-104	20.9	1.36		231	0.23S	18 11 26

TABLE D-1

MISSION LOG - EDWARDS PHASE I (Continued)

DY	MO	YR	MSN	A/C	ALT KFT MSL	MACH	EPR	HDG	OFF-SET N/S	HR	MN	SC ZULU
22	JUN	66	35A	B-58	43.4	1.60		225	0.92S	18	21	21
22	JUN	66	35B	F-104	21.1	1.28		235	0.25N	18	22	47
22	JUN	66	25A	F-104	21.9	1.39		233	0.21N	18	36	39
22	JUN	66	25B	B-58	43.2	1.59		233	4.89N	18	37	59
22	JUN	66	23A	F-104	29.7	1.51		237	0.34N	18	50	21
22	JUN	66	23B	B-58	37.4	1.63		232	0.50N	18	52	05
23	JUN	66	17A	B-58	37.6	1.6.		231	0.39N	15	46	08
23	JUN	66	17B	F-104	21.6	1.40		227	0.46S	15	48	00
23	JUN	66	22A	F-104	29.3	1.40		232		15	59	59
23	JUN	66	22B	B-58	43.4	1.67		229	4.25N	16	00	40
23	JUN	66	31A	B-58	37.5	1.64		231	0.12N	16	12	14
23	JUN	66	31B	F-104	21.3	1.39		232		16	12	21
23	JUN	66	33A	B-58	43.2	1.64		232	5.02N	16	21	38
23	JUN	66	33B	F-104	29.8	1.49		230	0.10S	16	22	04
23	JUN	66	20A	F-104	21.5	1.37		233	0.19N	19	51	20
23	JUN	66	20B	B-58	37.4	1.65		233	0.10N	19	54	17
23	JUN	66	36A	F-104	20.9	1.39		230	0.37S	20	05	15
23	JUN	66	36B	B-58	37.4	1.66		231	0.25S	20	06	26
23	JUN	66	7X	F-104	29.6	1.55		258	0.29S	20	18	18
23	JUN	66	6X2	B-58	43.5	1.67		258	9.86N	20	21	21

D.6

TABLE D-2
MISSION LOG
EDWARDS PHASE II *

DATE DY MO YR	MSN	A/C	ALT KFT MSL	MACH OR SPD (LDG)	EPR TKFF	HDG SET	OFF-SET L/R.K	OBS DY	BOOM HR	TME S (ZULU)	REMARKS	
23 NOV 66	1-1	XB-70	37.2	1.46		243	L10.3	327			001	1
23 NOV 66	1-2	F-104									961 NO RDR	1
23 NOV 66	1-3	B-58	32.4	1.4		240	L 7.2	327	18		J57	1
23 NOV 66	1-4	F-104	18.6	1.3		241	R 2.2	327	18	38 14	762	1
10 NOV 66	2-1	XB-70	37.3	1.48		236	L37.6	314	19	09 15	001	1
10 NOV 66	2-2	F-104									NODATA E1231	1
10 NOV 66	2-3	B-58	33.0	1.50		257	L 7.5	314	19	11 42	S19	1
10 NOV 66	2-4	F-104						314	19	15 32	763 NO RDR	1
12 DEC 66	3-1	B-58	32.4	1.5		247	R 7.8	346	18	27 31	N26	1
12 DEC 66	3-2	XB-70	37.6	1.5		246	L 0.9	346	18	31 42	001	1
12 DEC 66	3-4	F-104	17.8	1.3		245	L 2.3	346	18	38 51	763	1
16 DEC 66	4-1	B-58	32.0	1.5		247	R 1.9	350	15	53 46	N46	1
16 DEC 66	4-2	XB-70	38.6	1.5		246		350	15	57 49	001	1
12 DEC 66	5-1	B-58	36.3	1.65		245	R63.3	346	17	59 12	N26	1
12 DEC 66	5-2	XB-70	59.1	2.49		246	R12.9	346	18	05 31	001	1
12 DEC 66	5-3	WC135B	1.8		1.76	068	L 0.8	346	18	07 23	L13	1
20 DEC 66	6-1	B-58	35.5	1.65		244	R40.4	354	19	56 00	662	1
20 DEC 66	6-2	XB-70	60.0	2.5		248	R67.9	354	20	00 07	001	1
20 DEC 66	6-3	WC135B	3.7		1.76	76		354	20	01 48	667	1
13 JAN 67	7-1	B-58	35.8	1.62		241	R38.7	013	18	06 55	L50	1
13 JAN 67	7-2	DC-8	3.7		1.76	068		013	18	15 02	01U	1
13 JAN 67	7-3	XB-70	60.3	2.5		249	R71.3	013	18	17 20	001	1
17 JAN 67	8-1	B-58	35.5	1.65		<65	L 3.3	017	17	47 50	W50	1
17 JAN 67	8-2	DC-8	3.6		1.67	074	L 0.7	017	17	51 55	01U	1
17 JAN 67	8-3	XB-70	60.0	2.5		246	R68.2	017	17	53 09	001	1
10 NOV 66	9-1	XB-70	59.4	2.51		245	R32.1	314	18	35 11	001	1
10 NOV 66	9-2	B-58	40.4	1.65		249	R 1.7	314	18	38 03	S19	1
10 NOV 66	9-3	F-104	21.1	1.14		249	R 2.0	314	18	44 25	748	1
23 NOV 66	10-1	XB-70	59.7	2.46		246	L13.3	327	18	00 01	001	1
23 NOV 66	10-2	B-58	32.4	1.32		242	L 6.0	327	18	06 12	J57	1

DATE DY MO YR	MSN	A/C	ALT KFT MSL	MACH OR SPD (LDG)	EPR TKFF	HDG SET	OFF-SET L/R.K	OBS DY	BOOM HR.MN SC	TME ZULU	REMARKS	

*Refer to Legend, Page D.1 for explanation of notations and abbreviations.

D.7

TABLE D-2   MISSION LOG - EDWARDS PHASE II (Continued)

DATE DY MO YR	MSN	A/C	ALT KFT MSL	MACH OR SPD	EPR TKFF (LDG)	HDG SET	OFF-SET L/R,K	OBS DY	BOOM TME HR MN SC ZULU	REMARKS
16 DEC 66	11-1	F-104	20.8	1.4		244	L 1.5	350	15 19 18	755	1
16 DEC 66	11-2	B-58	40.2	1.65		246	R 0.8	350	15 24 42	N46	1
16 DEC 66	11-3	XB-70	59.4	2.5		245		350	15 29 05	001	1
4 JAN 67	12-1	B-58	39.2	1.65		245	L 2.1	004	20 38 05	P62	1
4 JAN 67	12-2	XB-70	60.3	2.5		246	L .2	004	20 40 52	001	1
4 JAN 67	12-3	F-104	22.0	1.42		246	R 6.7	004	20 46 22	817	1
3 NOV 66	13-1	B-58	35.9	1.65		244	L 2.5	307	18 51 03	L50	1
3 NOV 66	13-2	XB-70	60.2	1.80		244	R 6.4	307	18 56 33	001	1
3 NOV 66	13-3	F-104	20.0	1.40		240	R 3.4	307	18 57 13	817	1
20 DEC 66	14-1	XB-70	59.7	1.8		247	R 0.2	354	20 22 37	001	1
20 DEC 66	14-2	B-58	38.8	1.53		245	R 4.7	354	20 25 26	662	1
20 DEC 66	14-3	F-104	21.4	1.3		243	R 1.4	354	20 28 25	316	1
13 JAN 67	15-1	XB-70	60.6	1.8		248	R 9.5	013	18 42 32	001	1
13 JAN 67	15-2	B-58	39.6	1.65		252		013	18 44 43	L50	1
13 JAN 67	15-3	F-104	20.2	1.4		242	R 0.2	013	18 27 48	319	1
17 JAN 67	16-1	B-58	39.7	1.65		247	R 3.0	017	18 16 09	W50	1
17 JAN 67	16-2	XB-70	59.7	1.8		245	R 0.7	017	18 18 53	001	1
17 JAN 67	16-3	F-104	20.6	1.4		250	R 5.0	017	18 41 27	961	1
31 OCT 66	17-1	F-104	31.2	1.60		252	R 7.0	304	16 30 14	314	1
31 OCT 66	17-2	B-58	48.5	1.61		248	R 4.0	304	16 34 09	L19	1
31 OCT 66	18-1	B-58	47.3	1.57		250	L 1.4	304	15 57 27	L19	1
31 OCT 66	18-2	F-104	31.0	1.61		247	R 1.2	304	16 58 37	755	1
31 OCT 66	19-1	F-104	30.5	1.64		250	R 5.0	304	17 59 33	314	1
31 OCT 66	19-2	B-58	38.9	1.46		244	L 1.2	304	18 02 54	L65	1
31 OCT 66	20-1	B-58	43.9	1.55		251	R 2.4	304	18 29 09	L65	1
31 OCT 66	20-2	F-104	31.0	1.65		249		304	18 29 20	755	1

DATE DY MO YR	MSN	A/C	ALT KFT MSL	MACH OR SPD	EPR TKFF (LDG)	HDG SET	OFF-SET L/R,K	OBS DY	BOOM TME HR MN SC ZULU	REMARKS
8 NOV 66	21-1	B-58	47.6	1.60		244	L 1.3	312	16 29 35		1
8 NOV 66	21-2	WC135B			1.76					CFF COURSE	1
8 NOV 66	22-1	B-58	47.5	1.65		243	L 2.0	312	16 56 13		1
8 NOV 66	22-2	WC135B	3.9	250	1.76	68					1
8 NOV 66	23-1	B-58	47.8	1.65		246	R 1.4	312	17 14 51		1
8 NOV 66	23-2	WC135B	3.3	235	1.76	62					1
8 NOV 66	24-1	B-58	47.7	1.65		250	R 3.9	312	17 40 35		1
8 NOV 66	24-2	WC135B	5.4	230	1.76	73	R .1				1
8 NOV 66	25-1	B-58	46.8	1.65		247	R 1.0	312	18 02 58		1
8 NOV 66	25-2	WC135B	3.9	215	1.76	78	R .1				1

TABLE D-2 MISSION LOG – EDWARDS PHASE II (Continued)

DATE DY MO YR	MSN	A/C	ALT KFT MSL	MACH OR SPD (LDG)	EPR TKFF	HDG OFF-SET L/R,K	OBS BOOM TME DY HR MN SC ZULU	REMARKS
8 NOV 66	26-1	B-58	47.9	1.50		244	312 18 11 41	1
8 NOV 66	26-2	WC135B	3.2	222	1.76	77		1
8 NOV 66	27-1	WC135B	3.1	245	1.76	73		1
8 NOV 66	27-2	B-58	47.4	1.65		247 R .8	312 18 30 07	1
8 NOV 66	28-1	WC135B	3.9	235	1.76	59		1
8 NOV 66	28-2	B-58	48.0	1.65		248 R 4.1	312 18 37 55	1
8 NOV 66	29-1	WC135B	5.3	230	1.76	65 R .1		1
8 NOV 66	29-2	B-58	47.4	1.65		249 R 2.0	312 18 54 26	1
8 NOV 66	30-1	WC135B	3.1	245	1.76	65		1
8 NOV 66	30-2	B-58	47.5	1.65		254 R 6.5	312 19 17 41	1

DATE DY MO YR	MSN	A/C	ALT KFT MSL	MACH OR SPD (LDG)	EPR TKFF	HDG OFF-SET L/R,K	OBS BOOM TME DY HR MN SC ZULU	REMARKS
8 NOV 66	31-1	WC135B	3.9	225	1.76	55		1
8 NOV 66	31-2	B-58	47.0	1.60		244 L 1.3	312 19 52 41	1
8 NOV 66	32-1	WC135B	5.2	235	1.76	77 L .1		1
8 NOV 66	32-2	B-58	48.0	1.65		242 L 2.3	312 20 20 44	1
16 NOV 66	33-1	B-58	36.2	1.65		241 L 5.5	320 16 30 18	M85 1
16 NOV 66	33-2	WC135B	3.2		1.76	060 L 0.4	320 16 31 42	1
16 NOV 66	34-1	B-58	36.0	1.65		240 L 4.2	320 16 58 12	M85 1
16 NOV 66	34-2	WC135B	4.4		1.76	236 L 0.8	320 16 59 33	1
16 NOV 66	35-1	B-56	36.4	1.63		247 R 1.5	320 17 18 37	M83 1
16 NOV 66	35-2	WC135B	4.4		1.76	066 L 0.2	320 17 19 59	1
16 NOV 66	36-1	B-58	36.2	1.64		245	320 17 45 38	M63 1
16 NOV 66	36-2	WC135B	3.2		1.76	066	320 17 47 10	1
16 NOV 66	37-1	B-58	36.0	1.65		248 R 2.1	320 18 09 56	M85 1
16 NOV 66	37-2	WC135B	3.1		1.76	062 L 0.2	320 18 08 15	1
16 NOV 66	38-1	B-58	35.9	1.64		239 L 8.9	320 18 31 39	M85 1
16 NOV 66	38-2	WC135B	4.4		1.76	072 L 0.2	320 18 30 54	1
16 NOV 66	39-1	B-58	35.7	1.65		244 R 0.7	320 18 51 56	M85 1
16 NOV 66	39-2	WC135B	4.3		1.76	083 L 0.7	320 18 49 30	1
16 NOV 66	40-1	B-58	36.2	1.64		248 R 2.2	320 19 01 57	M83 1
16 NOV 66	40-2	WC135B	3.1		1.76	072 L 0.3	320 18 59 22	1

DATE DY MO YR	MSN	A/C	ALT KFT MSL	MACH OR SPD (LDG)	EPR TKFF	HDG OFF-SET L/R,K	OBS BOOM TME DY HR MN SC ZULU	REMARKS
17 NOV 66	41-1	B-58	36.3	1.65		247 R 3.5	321 18 16 40	M85 1
17 NOV 66	41-2	WC135B	4.3		1.76	077	321 18 17 37	1

D.9

TABLE D-2

MISSION LOG – EDWARDS PHASE II (Continued)

DATE DY MO YR	MSN	A/C	ALT KFT MSL	MACH OR SPD	EPR TKFF (LDG)	HDG	OFF-SET L/R,K	OBS DY	BOOM TME HR MN SC (ZULU)	REMARKS	
21 NOV 66	42-1	B-58	3.0		1.76	063	L 1.2	325	19 00 11	J57 NO RDR	1
21 NOV 66	42-2	WC135B	3.1		1.76	065	L 0.6	325	19 01 13	666	1
21 NOV 66	43-1	WC135B	3.1			245	L 2.9	325	19 19 48	666	1
21 NOV 66	43-2	B-58	35.9	1.65		245		325	19 23 53	J57	1
21 NOV 66	44-1	WC135B	4.3		1.76	062	L 0.7	325	19 30 47	666	1
21 NOV 66	44-2	B-58	36.4	1.65		250	L 3.5	325	19 31 58	J18	1
21 NOV 66	45-1	B-58	36.0	1.63		246		325	19 54 19	J18	1
21 NOV 66	45-2	WC135B	4.3		1.76	077	L 1.3	325	19 55 12	666	1
21 NOV 66	46-1	B-58	35.9	1.55		246	L 1.6	325	20 37 14	J57	1
21 NOV 66	46-2	WC135B	3.0		1.76	065	L 0.3	325	20 37 55	666	1
21 NOV 66	47-1	WC135B	3.1		1.76	074	L 0.6	325	21 00 26	666	1
21 NOV 66	47-2	B-58	35.8	1.65		244	L 2.5	325	21 02 53	J57	1
21 NOV 66	48-1	WC135B	4.3		1.76	083	L 0.5	325	21 13 02	666	1
21 NOV 66	48-2	B-58	36.0	1.65		247	L 0.4	325	21 15 01	J18	1
15 NOV 66	49-1	WC135B	2.8	240	1.76	63	L 0.2	319	18 18 28	L49	1
15 NOV 66	49-2	F-104	16.6	1.15		245	R 0.8	319	18 21 13	316	1
15 NOV 66	50-1	WC135B	3.3	232	1.76	68	L 0.1	319	18 31 46	L49	1
15 NOV 66	50-2	F-104	16.4	1.22		245	L 0.6	319	18 34 46	763	1
DATE DY MO YR	MSN	A/C	ALT KFT MSL	MACH OR SPD	EPR TKFF (LDG)	HDG	OFF-SET L/R,K	OBS DY	BOOM TME HR MN SC (ZULU)	REMARKS	
29 NOV 66	51-1	WC135B	2.7		1.76	72		333	16 32 15	671	1
29 NOV 66	51-2	F-104	16.6	1.30		246	R 4.0	333	16 34 06	755	1
6 DEC 66	52-1	F-104	17.0	1.30		248	R 6.2	340	17 34 17	C12	1
6 DEC 66	52-2	WC135B	2.7		1.76	74	L 1.7	340	17 34 55	667	1
6 DEC 66	53-1	F-104	17.1	1.30		74	L 1.0	340	17 44 23	C12	1
6 DEC 66	53-2	WC135B	3.4		1.76	93	L 1.0	340	17 45 31	667	1
7 DEC 66	54-1	F-104	16.5	1.3		244	L 0.8	341	17 10 18	C14	1
7 DEC 66	54-2	WC135B	2.8		1.76	63	L 2.2	341	17 12 01	667	1
21 DEC 66	55-1	F-104	16.9	1.3		243	R 1.9	355	16 33 30	211	1
21 DEC 66	55-2	WC135B	2.7		1.76	68		355	16 35 38	567	1
9 DEC 66	56-1	F-104	16.5	1.28		246	R 2.2	343	18 29 42	763	1
9 DEC 66	56-2	WC135B						343	18 30 31	L20	1
9 DEC 66	57-1	F-104	16.0	1.29		240	R 0.8	343	18 37 54	763	1
9 DEC 66	57-2	WC135B	2.5		1.76	71	L 0.2	343	18 39 48	L20	1
20 DEC 66	58-1	WC135B	2.5		1.76	73	R 0.2	354	17 40 24	667	1
20 DEC 66	58-2	F-104	16.8	1.3		246	R10.8	354	17 41 58	755	1
20 DEC 66	59-1	WC135B	3.4		1.76	74		354	17 50 26	667	1
20 DEC 66	59-2	F-104	16.6	1.34		247	R 8.0	354	17 50 17	755	1
21 DEC 66	60-1	WC135B	2.8		1.78	66	L	355	16 20 49	667	1

D.10

TABLE D-2   MISSION LOG – EDWARDS PHASE II (Continued)

DATE DY MO YR	MSN	A/C	ALT KFT MSL	MACH OR SPD (LDG)	EPR TKFF	HDG OFF-SET L/R,K	OBS DY ZULU	BOOM TME HR MN SC	REMARKS
21 DEC 66	60-2	F-104	17.1	1.28		245 L	.8 355	16 22 31	812 1
15 NOV 66	61-1	F-104	29.6	1.65		247 R 3.1	319	16 55 19	763 1
15 NOV 66	61-2	WC135B	3.4	242	1.76	61 L 0.3	319	16 56 14	L49 1
30 NOV 66	62-1	F-104	30.3	1.66		246 L .5	334	16 27 50	316 1
30 NOV 66	62-2	WC135B	4.2		1.76	72 L .2	334	16 29 22	665 1
30 NOV 66	63-1	F-104	29.6	1.62		242 L .9	334	18 32 57	316 1
30 NOV 66	63-2	WC135B	6.6		1.76	64 L .6	334	18 34 22	665 1
29 NOV 66	64-1	WC135B	6.5		1.76	69 L 0.5	333	16 58 31	671 1
29 NOV 66	64-2	F-104	29.4	1.65		248 R 3.0	333	16 59 48	748 1
6 DEC 66	65-1	WC135B	4.4		1.75	68 L 1.2	340	17 27 17	667 1
6 DEC 66	65-2	E-104	29.7	1.60		244 L 0.1	340	17 30 17	C11 1
6 DEC 66	66-1	WC135B	3.4			245 R 2.2	340	17 54 54	667 1
6 DEC 66	66-2	F-104	30.1	1.64			340	17 57 09	C13 1
7 DEC 66	67-1	F-104	29.6	1.65		245 L 2.9	341	17 00 26	C13 1
7 DEC 66	67-2	WC135B	3.3		1.76	70 L 1.8	341	17 02 52	667 1
21 DEC 66	68-1	F-104	29.7	1.64		249 R 5.1	355	16 44 18	212 1
21 DEC 66	68-2	WC135B	4.0		1.76	72 R .2	355	16 46 12	667 1
9 DEC 66	69-1	F-104	29.6	1.67		246 R 1.2	343	16 58 08	817 1
9 DEC 66	69-2	WC135B	6.2			70 L 0.9	347	17 00 05	L20 1
20 DEC 66	70-1	WC135B	6.4		1.76	77 R 0.6	354	16 40 56	567 1
20 DEC 66	70-2	F-104	29.8	1.65		246	354	16 40 13	755 1

DATE DY MO YR	MSN	A/C	ALT KFT MSL	MACH OR SPD (LDG)	EPR TKFF	HDG OFF-SET L/R,K	OBS DY ZULU	BOOM TME HR MN SC	REMARKS
20 DEC 66	71-1	WC135B	4.4		1.76	74 R 0.2	354	16 02 08	667 1
20 DEC 66	71-2	F-104	30.5	1.52		244 L 0.1	354	16 03 53	316 1
20 DEC 66	72-1	WC135B	4.5		1.75	75	354	17 11 36	667 1
20 DEC 66	72-2	F-104	34.3	1.42		245 R 5.1	354	17 15 45	811 1
30 NOV 66	73-1	F-104	50.1	1.51		248 R 2.3	334	17 16 24	748 1
30 NOV 66	73-2	WC135B	4.2		1.76	68	334	17 17 36	665 1
15 NOV 66	74-1	F-104	50.5	1.5		247 R 4.2	319	16 27 48	763 1
15 NOV 66	74-2	WC135B	6.4	224	1.64	70 L 0.9	319	16 29 49	L49 1
30 NOV 66	75-1	F-104	49.6	1.5		246 R .9	334	18 41 52	763 1
30 NOV 66	75-2	WC135B	11.2		1.76	66 L .8	334	18 42 37	665 1
29 NOV 66	76-1	WC135B	10.6		1.76	75 L 0.2	333	18 22 34	671 1

D.11

TABLE D-2 MISSION LOG – EDWARDS PHASE II (Continued)

DATE DY MO YR	MSN	A/C	ALT KFT MSL	MACH OR SPD	EPR TKFF (LDG)	HDG	OFF-SET L/R,K	OBS DY	BOOM TME HR MN SC ZULU	REMARKS	
29 NOV 66	76-2	F-104	50.4	1.52		245	R 0.9	333	18 26 13	755	1
29 NOV 66	77-1	WC135B	6.4		1.76	63	R 0.1	333	18 29 42	671	1
29 NOV 66	77-2	F-104	48.8	1.51		244	L 0.6	333	18 33 10	316	1
7 DEC 66	78-1	WC135B	4.1		1.76	69	L 1.4	341	16 29 11	667	1
7 DEC 66	78-2	F-104	50.0	1.5		246	R 1.3	341	16 31 09	C11	1
7 DEC 66	79-1	F-104	50.4	1.5		246	R 1.8	341	16 45 32	C12	1
7 DEC 66	79-2	WC135B	4.2		1.76	62	L 1.2	341	16 46 38	667	1
21 DEC 66	80-1	F-104	49.2	1.5		244	R .2	355	16 53 33	213	1
21 DEC 66	80-2	WC13ɔB	6.2		1.76	70	L .9	355	16 54 17	667	1

DATE DY MO YR	MSN	A/C	ALT KFT MSL	MACH OR SPD	EPR TKFF (LDG)	HDG	OFF-SET L/R,K	OBS DY	BOOM TME HR MN SC ZULU	REMARKS	
21 DEC 66	81-1	F-104	49.4	1.51		245	R .9	355	17 04 14	214	1
21 DEC 66	81-2	WC135B	10.4		1.76	66	L .6	355	17 05 55	667	1
9 DEC 66	82-1	WC135B	10.3		1.76	71	R 1.2	343	16 38 05	L20	1
9 DEC 66	82-2	F-104	50.5	1.5		245	R 3.0	343	16 39 30	763	1
20 DEC 66	83-1	WC135B	6.5		1.76	73	R 0.2	354	16 50 00	667	1
20 DEC 66	83-2	F-104	50.2	1.5		245	R 1.9	354	16 53 45	316	1
21 DEC 66	84-1	WC135B	4.3		1.78	69	L .2	355	16 02 55	c67	1
21 DEC 66	84-2	F-104	49.5	1.56		247	R 3.2	355	16 06 14	J14	1
16 NOV 66	85-1	B-58	36.0	1.63		248	R 3.4	320	19 24 59	M83	1
16 NOV 66	85-2	WC135B	3.1		1.76	075	L 0.3	320	19 24 02		1
16 NOV 66	86-1	B-58	36.1	1.64		251	R 3.3	320	19 44 23	M83	1
16 NOV 66	86-2	WC135B	3.1		1.76	070		320	19 43 31		1
17 NOV 66	87-1	B-58	36.4	1.65		246	R 2.5	321	17 29 39	M85	1
17 NOV 66	87-2	WC135B	3.2		1.76	067	L 0.5	321	17 30 33		1
17 NOV 66	88-1	B-58	36.3	1.65		244	R 5.5	321	17 55 10	M85	1
17 NOV 66	88-2	WC135B	3.1		1.76	072	L 0.5	321	17 56 27		1

DATE DY MO YR	MSN	A/C	ALT KFT MSL	MACH OR SPD	EPR TKFF (LDG)	HDG	OFF-SET L/R,K	OBS DY	BOOM TME HR MN SC ZULU	REMARKS	
4 JAN 67	113-1	B-58	39.1	1.65		246	L .7	004	21 04 47	P62	1
4 JAN 67	113-2	XB-70	60.3	1.8		247	L .1	004	21 05 53	001	1
4 JAN 67	113-3	F-104	20.6	1.4		246	R 1.2	004	21 25 44	755	1
2 DEC 66	117-1	F-104	26.4	1.65		251	R 5.0	336	17 48 18	817	1
2 DEC 66	117-2	B-58	48.0	1.65		244	L 1.9	336	17 48 26	B85	1
2 DEC 66	118-1	B-58	48.7	1.65		247	R 2.0	336	18 23 02	B85	1
2 DEC 66	118-2	F-104	26.1	1.60		248	R 4.1	336	18 25 11	763	1

D.12

TABLE D-2

MISSION LOG – EDWARDS PHASE II (Continued)

DATE DY MO	MSN	A/C	ALT KFT MSL	MACH OR SPD (LDG)	EPR TKFF	HDG	OFF-SET L/R,K	OBS BOOM TME DY	HR	MN	SC	REMARKS
7 DEC	66119-1	F-104	26.4	1.65		240	5.9	341	19	00	19	314
8 NOV	66121-1	B-58	47.4	1.66		250	R 7.4	312	19	40	38	RERUN 21-1
8 NOV	66171-2	WC135B	5.2	260	1.76	51	R .1					RERUN 21-2
8 DEC	66122-1	B-58	48.6	1.65		244	R 2.2	342	17	10	28	V26
8 DEC	66122-2	WC135B	3.4		1.76	71	L 0.3	342	17	12	32	667
8 DEC	66123-1	B-58	47.6	1.51		249	L 4.9	342	17	23	15	V49
8 DEC	66123-2	WC135B	2.7		1.76	68	L 0.6	342	17	25	24	667
8 DEC	66124-1	B-58	48.2	1.65		244	L 0.9	342	17	49	36	V49
8 DEC	66124-2	WC135B	4.2		1.76	69	L 0.3	342	17	51	27	667
8 DEC	66125-1	B-58	48.2	1.65		242		342	18	04	16	V62
8 DEC	66125-2	WC135B	3.4		1.76	72	L 0.3	342	18	06	40	667
8 DEC	66126-1	B-58	50.2	1.65		242	L 4.2	342	18	29	28	V62
8 DEC	66126-2	WC135B	2.7		1.76	66	L 0.3	342	18	31	25	667
8 DEC	66127-1	WC135B	2.8		1.76	74	L 0.3	342	18	41	43	667
8 DEC	66127-2	B-58	49.0	1.65		241	R 3.5	342	18	44	40	V26
8 DEC	66128-1	WC135B	3.3		1.76	69	L 0.3	342	18	08	11	667
8 DEC	66128-2	B-58	41.6	1.4		244		342	18	10	06	V49
8 DEC	66129-1	WC135B	4.1		1.76	71	L 0.5	342	19	22	23	667
8 DEC	66129-2	B-58	48.8	1.65		244	R 0.8	342	19	24	42	V26
8 DEC	66130-1	WC135B	2.8		1.76	72	L 0.6	342	19	37	26	667
8 DEC	66130-2	B-58	48.4	1.65		247	R 1.8	342	19	39	02	V49
8 DEC	66131-1	WC135B	3.4		1.76	76	L 0.6	342	19	54	43	667
8 DEC	66131-2	B-58	48.5	1.65		246	R 1.2	342	19	55	35	V62
8 DEC	66132-1	WC135B	4.1		1.76	75	L 0.6	342	20	18	14	667
8 DEC	66132-2	B-58	48.3	1.65		241	L 4.5	342	20	18	26	V62
15 NOV	66149-1	WC135B	3.0	234	1.76	65	L 0.2	319	17	17	29	L49
15 NOV	66150-1	WC135B	5.1	226	1.76	67	L 0.5	319	18	00	35	L49
15 NOV	66161-2	WC135B	3.8	230	1.76	67	L 0.5	319	17	03	48	L49
21 DEC	66172-1	WC135B	3.3		1.76	68	L .5	355	17	22	15	667
21 DEC	66172-2	F-104	29.0	1.65		245	R 6.4	355	17	23	18	314
15 NOV	66174-2	WC135B	5.2	232	1.76	57	L 0.4	319	16	37	21	L49

DATE DY MO YR	MSN	A/C	ALT KFT MSL	MACH OR SPD (LDG)	EPR TKFF	HDG	OFF-SET L/R,K	OBS BOOM TME DY HR MN SC ZULU				REMARKS
8 DEC 66221-1		B-58	47.2	1.4		246	R 3.9	342	16	43	36	V26
8 DEC 66221-2		WC135B	4.1		1.76	70	L 0.3	342	16	43	38	667
15 NOV 66249-1		WC135B	3.0	232	1.76	66	L 0.1	319	17	24	13	L49
15 NOV 66250-1		WC135B	3.8	227	1.76	63	L 0.2	319	18	08	44	L49
15 NOV 66261-2		WC135B	3.8	230	1.76	67	L 0.6	319	17	10	48	L49
15 NOV 66274-2		WC135B	5.2	248	1.76	58	L 1.1	319	16	45	14	L49

D.13

TABLE D-2   MISSION LOG - EDWARDS PHASE II (Continued)

DATE DY MO YR	MSN	A/C	ALT KFT MSL	MACH OR SPD	EPR TKFF (LDG)	HDG OFF-SET L/R,K	OBS BOOM TIME DY HR MN SC ZULU	REMARKS	
15 NOV 66350-1		WC135B	5.2	247	1.76	60 L 0.8	319 18 39 23	L49	1
15 NOV 66450-1		WC135B	2.5	252	1.76	63 L 0.1	319 18 46 23	L49	1
3 NOV 66	SR-1	SR-71						COND C	1
3 NOV 66	SR-2	SR-71						COND C	1
17 NOV 66	SR-3	SR-71						COND G	1
17 NOV 66	SR-4	SR-71						COND E	1
29 NOV 66	SR-6	SR-71					333 20 29 47	COND E	1
29 NOV 66	SR-7	SR-71					333 22 55 24	COND F	1
30 NOV 66	SR-8	SR-71					334 20 40 37	COND E	1
1 DEC 66	SR-9	SR-71					335 19 54 11	COND A	1
1 DEC 66	SR-10	SR-71					335 20 26 30	COND E	1
1 DEC 66	SR-11	SR-71					335 20 43 35	COND E	1
8 DEC 66	SR-12	SR-71					342 18 48 19	COND E	1
8 DEC 66	SR-13	SR-71					342 20 34 27	COND E	1
9 DEC 66	SR-14	SR-71					343 21 48 10	COND E	1
12 DEC 66	SR-15	SR-71					346 23 34 20	COND E	1
16 DEC 66	SR-19	SR-71						COND E	1
16 DEC 66	SR-20	SR-71						COND F	1
16 DEC 66	SR-21	SR-71						COND E	1
20 DEC 66	SR-23	SR-71					354 21 39 17	COND F	1
21 DEC 66	SR-24	SR-71						COND F	1
21 DEC 66	SR-25	SR-71						COND F	1
4 JAN 67	SR-26	SR-71						COND D	1

NOTE: Flight data for SR-71 missions not available for release at this time.
Each condition (COND) represents a certain altitude, Mach number, etc.

D.14

APPENDIX E

TYPICAL INSTRUMENT LOCATION LOG

(For 15 November 1966)

TYPICAL INSTRUMENT LOCATION LOG*

DATE DY MO YR	CHNL	HOUSE INSTR	INST TYPE	LOCATION	P.
15 NOV 66	101	1 MA1	ACOUSTIC	CNTR LR SUSP 6 FT ABV FLR	1 3
15 NOV 66	102	1 MA2	ACOUSTIC	CNTR FR-KIT SUSP 6 FT ABV FLR	1 3
15 NOV 66	103	1 MA3	ACOUSTIC	CNTR BR1 SUSP 6 FT ABV FLR	1 3
15 NOV 66	104	1 MA4	ACOUSTIC	BR1 FRONT OF CLOSET MOVABLE	1 3
15 NOV 66	105	1 MA5	ACOUSTIC	FR-KIT FRONT OF RANGE MOVABLE	1 3
15 NOV 66	106	1 A3	LF ACCEL	CONC BLK FLR BR1 AXIS VERT	1 3
15 NOV 66	107	2 MA1	ACOUSTIC	BTWN LR AND BR SUSP 6 FT ABV FLR	1 3
15 NOV 66	108	2 MA2	ACOUSTIC	CNTR KIT SUSP 6 FT ABV FLR	1 3
15 NOV 66	109	2 MA3	ACOUSTIC	CNTR BR1 SUSP 6 FT ABV FLR	1 3
15 NOV 66	110	2 MA4	ACOUSTIC	CNTR FR	1 3
15 NOV 66	111	2 MA5	ACOUSTIC	FR-KIT-DR KIT STOVE	1 3
15 NOV 66	112	2 MA6	ACOUSTIC	FR-KIT BR-BR SUSP 6 FT ABV FLR NR CHINA CLOS	1 3
15 NOV 66	113	1 MA7	ACOUSTIC	OUTSIDE SUBJECT GROUP	1 3
15 NOV 66	114		ACOUSTIC	IRIG B TIME CODE AND VOICE	1 3

DATE DY MO YR	CHNL	HOUSE INSTR	INST TYPE	LOCATION	P
15 NOV 66	201	1 A5	LF ACCEL	ROOF PLATE LINE E WALL NE CRNR (E-W ACCEL)	1 3
15 NOV 66	202	1 A11	LF ACCEL	BR1 E WALL (N-S ACCEL)	1 3
15 NOV 66	203	1 A6	LF ACCEL	ROOF PLATE LINE N WALL NE CRNR (N-S ACCEL)	1 3
15 NOV 66	204	1 ML3	PRESSURE	BR1 E WALL NEXT TO A11	1 3
15 NOV 66	205	1 ML4	PRESSURE	FR-KIT CNTR CLG ATTIC SIDE	1 3
15 NOV 66	206	2 SG41	STRAIN	GARAGE WNDW 3RD FROM CNTR	1 3
15 NOV 66	207	1 SG2	STRAIN	GARAGE CNTR LARGE WINDOW	1 3
15 NOV 66	208	2 SG42	STRAIN	GARAGE WNDW 2ND FROM CNTR	1 3
15 NOV 66	209	2 MA8	ACOUSTIC	TRIGGER MIKE	1 3
15 NOV 66	210	2 SG43	STRAIN	GARAGE WNDW 1ST FROM CNTR	1 3
15 NOV 66	211			SPARE	1 3
15 NOV 66	212	2 SG44	STRAIN	GARAGE WNDW CENTER	1 3
15 NOV 66	213			SPARE	1 0
15 NOV 66	214			IRIG B TIME CODE AND VOICE	3 3

DATE DY MO YR	CHNL	HOUSE INSTR	INST TYPE	LOCATION	P
15 NOV 66	301	2 A1	LF ACCEL	FR FLR CONC BLK AXIS VERT	1 3
15 NOV 66	303	2 A3	LF ACCEL	BR1 BED CONC BLK AXIS EAST-WEST	2 3
15 NOV 66	302	2 A2	LF ACCEL	FR FLR CONC BLK AXIS VERT BETW KIT AND FR	1 3
15 NOV 66	304	1 A1	LF ACCEL	FR FLR CONC BLK AXIS VERT	1 3
15 NOV 66	305	1 A2	LF ACCEL	FR-KIT FLR CONC BLK AXIS VERT	1 3
15 NOV 66	306	2 A1P	HF ACCEL	FR FLR CONC BLK AXIS VERT	1 3

*Refer to Legend, Appendix B, for explanation of notation and abbreviations.

E.1

TYPICAL INSTRUMENT LOCATION LOG (Continued)

DATE (DY MO YR)	CHNL	HOUSE INSTR	INST TYPE	LOCATION		
15 NOV 66	307	2 A2P	HF ACCEL	FR-KIT-DR MOVABLE KIT RNDW BETW KIT AND FR	1	3
15 NOV 66	308	2 A5P	HF ACCEL	AIR COND DOOR	2	3
15 NOV 66	309	2 A6P	HF ACCEL	FR-KIT-DR MOVABLE KIT CABNT DOOR ABV SINK LFFT	1	3
15 NOV 66	310	2 A9P	HF ACCEL	RFI CLOSET DOOR	2	3
15 NOV 66	311	2 A10P	HF ACCEL	KIT CABINET	2	3
15 NOV 66	312	2 A11P	HF ACCEL	FR-KIT-DR MOVABLE DR CNTR N WINDOW	1	
15 NOV 66	313	2 A12P	HF ACCEL	RFI EAST WNDW	2	
15 NOV 66	314			IRIG B TIME CODE AND VOICE	P	3

DATE (DY MO YR)	CHNL	HOUSE INSTR	INST TYPE	LOCATION		
15 NOV 66	401	2 A5	LF ACCEL	ROOF PLATE LINE N WALL NF CORNER (N-S ACCEL)	1	3
15 NOV 66	402	2 A9	LF ACCEL	BR1 CNTR CLG BOTT CHORD ROOF TRUSS	1	3
15 NOV 66	403	2 A6	LF ACCEL	ROOF PLATE LINE E WALL NF CORNER (E-W ACCEL)	1	3
15 NOV 66	404	2 A11	LF ACCEL	DR E WALL MID HT CNTR STUD	1	3
15 NOV 66	405	2 A7	LF ACCEL	2ND FLR PLATE LINE N WALL NE CRNR (N-S ACCEL)	1	3
15 NOV 66	406	2 A12	LF ACCEL	BR1 N WALL MID HT CNTR STUD	1	3
15 NOV 66	407	2 A8	LF ACCEL	2ND FLR PLATE LINE E WALL NE CRNR (E-W ACCEL)	1	3
15 NOV 66	408	2 ML2	PRESSURE	BTWN LR AND DR SUSP 6 FT ABV FLR	1	3
15 NOV 66	409	2 ML3	PRESSURE	BR1 ATTIC	1	3
15 NOV 66	410	2 ML4	PRESSURE	BR1 CNTR CLG SUSP 2 IN BELOW CLG	1	3
15 NOV 66	411	2 D1	DISPL	ADJACENT TO A5 WITH SAME AXIS	1	3
15 NOV 66	412	2 D2	DISPL	ADJACENT TO A6 WITH SAME AXIS	1	3
15 NOV 66	413			SPARE	0	3
15 NOV 66	414			IRIG B TIME CODE AND VOICE	P	3

DATE (DY MO YR)	CHNL	HOUSE INSTR	INST TYPE	LOCATION		
15 NOV 66	501	3 A1H	LF ACCEL	TOP STEEL COL INTERIOR OF BLDG E-W RACKING	1	3
15 NOV 66	502	3 A2H	LF ACCEL	TOP STEEL COL SOUTH SIDE E-W RACKING	1	3
15 NOV 66	503	3 A3H	LF ACCEL	TOP STEEL COL SOUTH SIDE N-S RACKING	1	3
15 NOV 66	504	3 A4H	LF ACCEL	TOP STEEL COL WEST SIDE N-S RACKING	1	3
15 NOV 66	505	3 A5H	LF ACCEL	CENTER OF ROOF GRDR HORZ ACCEL	1	3
15 NOV 66	506			BLANK	0	3
15 NOV 66	507	3 S1L	STRAIN	BOTT FLANGE ROOF GIRDER AT CENTERLINE	1	3
15 NOV 66	508	3 S2L	STRAIN	BOTT FLANGE ROOF GIRDER AT 1/4 POINT	1	3
15 NOV 66	509	3 S3L	STRAIN	BOTT FLANGE ROOF PURLIN AT CENTERLINE	1	3
15 NOV 66	510			BLANK	0	3
15 NOV 66	511			BLANK	0	3
15 NOV 66	512	3 M2	PRESSURE	INTERIOR 3 FT BELOW ROOF	1	3
15 NOV 66	513	3 M4	PRESSURE	EXTERIOR ABV ROOF	1	3
15 NOV 66	514			IRIG B TIME CODE	P	3

DATE (DY MO YR) | CHNL | HOUSE INSTR | INST TYPE | LOCATION

E.2

TYPICAL INSTRUMENT LOCATION LOG (Continued)

DATE DY-MO	YR	CHNL HOUSE INSTR	INST TYPE	LOCATION		
15 NOV	66	601	2 MLC1 PRESSURE	EAST CORNER CRUCIFORM ARRAY	1	C 3
15 NOV	66	602		PLANK	0	C 3
15 NOV	66	603	2 MLC2 PRESSURE	NORTH CORNER CRUCIFORM ARRAY	1	C 3
15 NOV	66	604		PLANK	0	C 3
15 NOV	66	605	2 MLC3 PRESSURE	WEST CORNER CRUCIFORM ARRAY	1	C 3
15 NOV	66	606		PLANK	0	C 3
15 NOV	66	607	2 MLC4 PRESSURE	SOUTH CORNER CRUCIFORM ARRAY	1	C 3
15 NOV	66	608		PLANK	0	C 3
15 NOV	66	609	2 MLC5 PRESSURE	CENTER BOTTOM MAST CRUC ARRAY	1	C 3
15 NOV	66	610		PLANK	0	C 3
15 NOV	66	611	2 MLC6 PRESSURE	CENTER TOP MAST CRUCIFORM ARRAY	1	C 3
15 NOV	66	612		VOICE		
15 NOV	66	613		100KC REFERENCE SIGNAL		
15 NOV	66	614		IRIG B TIME CODE	P	3

DATE DY-MO	YR	CHNL HOUSE INSTR	INST TYPE	LOCATION		
15 NOV	66	801	2 ML15 PRESSURE	OUTSIDE CNTR HIGH ROOF N SIDE	1	C 3
15 NOV	66	802	2 ML16 PRESSURE	OUTSIDE CNTR HIGH ROOF S SIDE	1	C 3
15 NOV	66	803	1 ML1 PRESSURE	OUTSIDE N WALL AV PLATE	1	C 3
15 NOV	66	804	1 ML2 PRESSURE	OUTSIDE E WALL	1	C 3
15 NOV	66	805	1 ML5 PRESSURE	OUTSIDE W WALL GARAGE AT PLATE LINE	1	C 3
15 NOV	66	806	1 ML6 PRESSURE	OUTSIDE S WALL CNTR ABV PLATE LINE	1	C 3
15 NOV	66	807	2 ML17 PRESSURE	OUTSIDE N WALL MIDDLE 2ND STORY	1	C 3
15 NOV	66	808	2 ML18 PRESSURE	OUTSIDE S WALL MIDDLE 2ND STORY	1	C 4
15 NOV	66	809	2 ML14 PRESSURE	OUTSIDE W WALL GARAGE ABV PLATE LINE	1	C 3
15 NOV	66	810	2 ML13 PRESSURE	OUTSIDE W WALL ABOVE GARAGE ROOF	1	C 3
15 NOV	66	811	2 ML11 PRESSURE	OUTSIDE E WALL MIDDLE OF 2ND STORY	1	C 3
15 NOV	66	812	2 ML12 PRESSURE	OUTSIDE E WALL MIDDLE OF 1ST STORY OUTSIDE DR	1	C 3
15 NOV	66	813		VOICE		
15 NOV	66	814		IRIG B TIME CODE (CP-100 REVERSED IRIG HEAD)		3

E.3

APPENDIX F

SUMMARY OF FREE FIELD OVERPRESSURE DATA

The following is an explanation of notations and abbreviations used in this Appendix:

Table F-1   Summary of Data from Free Field Microphones located near E-2, Phase I.

1. Date   Month, Day, Year.
2. Mission No.   Mission identification number
3. Altitude   Altitude above mean sea level in feet.
4. Microphone No.   See Legend and Figure B-7 Appendix B.
5. Δp Peak positive overpressure
6. Δt Time from start of boom to negative peak in seconds (Figure F-1)

Table F-2   Summary of Data from Free Field Microphones located near L-2, Phase I.

1. Date   Month, Day, Year.
2. Mission No.   Mission identification number
3. Altitude   Altitude above mean sea level in feet.
4. Average Peak overpressure   Average peak positive overpressure in psf.

Table F-3   Summary of Data from Free Field Microphones located near
            E-2, Phase II.

1. MSN   Mission identification number

2. CHNL   Tape recorder-channel number, Appendix B.

3. HOUSE,   House number and instrument designation,
   INSTR.   Figure B-7, Appendix B.

4. TYPE   Waveform type code number, Figure F-1.

5. PEAK   Peak amplitudes, psf, Figure F-1.
   AMPLITUDES

6. RISE TIME   Rise Time, sec.

7. PERIOD   Time from start of boom to negative peak, sec,
                      (Δt, Figure F-1).

8. WAVE ANGLE   Angle between overpressure wave front and
                      ground, degrees.

9. GND SPD   Wave front speed at ground level, ft/sec.
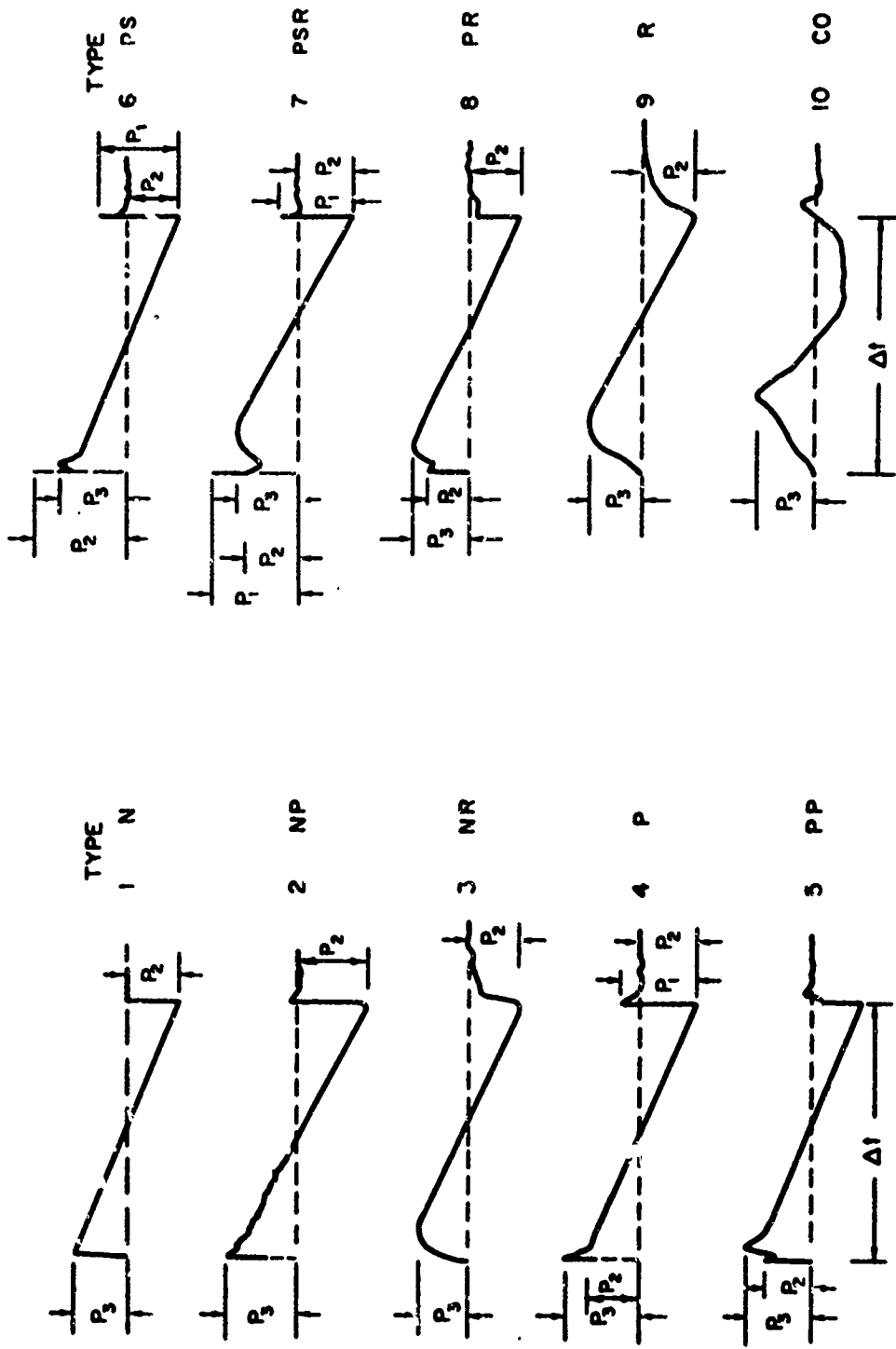
FIG. F-1 SONIC BOOM WAVEFORM CATEGORIES

Table F-1

SUMMARY OF DATA FROM FREE FIELD MICROPHONES LOCATED NEAR E-2, PHASE I [1]

Date	Mission No.	Aircraft	Altitude ft	Mach No.	Microphone No. **	Δp lb/ft^2	Δt sec.	Rise Time sec.
6-4-66	14	XB-70	52,920	1.81	MLC-1	2.37	.250	.0125
					MLC-5	--	--	--
					MLC-6	1.36	--	--
					MLC-2	2.59	.250	.007
					MLC-3	2.72	.250	.006
					MLC-4	2.42	.250	.0035
6-3-66	22	XB-70	72,000	2.83	MLC-1	1.65	.3175	.0055
					MLC-5	1.64	.3175	.007
					MLC-6	.814	--	--
					MLC-2	1.53	.3175	.005
					MLC-3	1.68	.3175	.005
					MLC-4	1.70	.3175	.007
6-8-66	1	XB-70	31,850	1.38	MLC-1	Noise	--	--
					MLC-5	2.35	.233	.03
					MLC-6	2.10	--	--
					MLC-2	2.28	.234	.032
					MLC-3	2.08	.233	.03
					MLC-4	2.38	.234	.028
6-6-66	39		No Boom					
	70	B-58	43,900	1.6	MLC-1	1.97	.185	.005
					MLC-5	1.88	.185	.024
					MLC-6	1.01	--	--
					MLC-2	2.23	.185	.002
					MLC-3	1.72	.185	.007
					MLC-4	1.98	.1845	.023
	40	B-58	31,400	1.48	MLC-1	3.55	.1573	.010
					MLC-5	3.36	.157	.0115
					MLC-6	1.78	--	--
					MLC-2	3.21	.157	.007
					MLC-3	3.63	.157	.0065
					MLC-4	3.52	.157	.015
	71	B-58	44,200	1.59	MLC-1	1.65	.179	.012
					MLC-5	1.88	.179	.017
					MLC-6	.930	--	--
					MLC-2	1.72	.179	.012
					MLC-3	1.76	.178	.006
					MLC-4	1.78	.179	.016
	41	B-58	31,340	1.45	MLC-1	2.49	.154	.016
					MLC-5	2.56	.154	.017
					MLC-6	1.24	--	--
					MLC-2	2.33	.154	.015
					MLC-3	2.43	.154	.018
					MLC-4	2.64	.1535	.016
	72	B-58	43,920	1.55	MLC-1	1.51	.172	.006
					MLC-5	2.64	.172	.005
					MLC-6	1.63	--	--
					MLC-2	2.09	.174	.001
					MLC-3	2.02	.172	.003
					MLC-4	1.78	.171	.005

[1] Refer to Legend, Page F.I for explanation of notations and abbreviations.

F.4

Table F-1 (Continued)

Date	Mission No.	Aircraft	Altitude ft	Mach No.	Microphone No. **	Δp lb/ft^2	Δt sec.	Rise Time sec.
6-6-66	43	B-58	Missed Boom					
	74	B-58	32,440	1.3	MLC-1	3.16	.195	.014
					MLC-5	3.20	.194	.010
					MLC-6	1.67	--	--
					MLC-2	3.12	.194	.001
					MLC-3	3.33	.194ɔ	.006
					MLC-4	3.09	.194	.009
	44	B-58	43,400	1.57	MLC-1	1.58	.197	.007
					MLC-5	1.96	.196	.0005
					MLC-6	1.16	--	--
					MLC-2	1.53	.196	.006
					MLC-3	1.65	.195	.0005
					MLC-4	1.90	.1955	.004
	75	B-58	31,840	1.46	MLC-1	2.67	.157	.006
					MLC-5	3.00	.1575	.004
					MLC-6	2.02	--	--
					MLC-2	3.02	.157	.001
					MLC-3	4.94*/3.33	.157	.0005*/.001
					MLC-4	3.05	.1575	.0035
	42	B-58	43,300 1.53 10 N. mi East		MLC-1	1.83	.1835	.0065
					MLC-5	1.80	.183	.0065
					MCL-6	.930	--	--
					MCL-2	1.58	.183	.007
					MLC-3	1.65	.1825	.011
					MLC-4	1.98	.1835	.0065
	73	B-58	31,860	1.43	MLC-1	2.95	.160	.006
					MLC-5	5.44*/3.72	.160	.0005*/.001
					MLC-6	2.29	--	--
					MLC-2	3.12	.160	.0005
					MLC-3	3.03	.160	.006
					MLC-4	3.25	.160	.004
6-7-66	76-A	B-58	31,560	1.48	MLC-1	2.88	.164	.0065
					MLC-5	2.81	.1635	.006
					MLC-6	1.61	--	--
					MLC-2	3.10	.164	.008
					MLC-3	4.51	.164	.0015
					MLC-4	3.47	.1635	.004
	45-B	B-58	43,660	1.70	MLC-1	1.75	.1715	.005
					MLC-5	2.01	.172	.0085
					MLC-6	1.06	--	--
					MLC-2	2.29	.171	.001
					MLC-3	2.27	.172	.0055
					MLC-4	1.96	.171	.009
	77-B	B-58	31,680	1.51	MLC-1	2.48	.156	.011
					MLC-5	2.75	.156	.010
					MLC-6	1.48	--	--
					MLC-2	3.26	.155	.005
					MLC-3	3.24	.156	.005
					MLC-4	2.71	.1565	.027

Table F-1 (Continued)

Date	Mission No.	Aircraft	Altitude ft	Mach No.	Microphone No.**	Δp lb/ft²	Δt sec.	Rise Time sec.
6-7-60	46-B	B-58	43,720	1.65	MLC-1	1.35	.1715	.0005
					MLC-5	1.82	.172	.011
					MLC-6	.84	---	--
					MLC-2	1.40	.171	.003
					MLC-3	1.81	.170	.006
					MLC-4	1.71	.172	.006
	48-A		No Boom					
	79-A	B-58	31,600	1.52	MLC-1	2.57	.170	.028
					MLC-5	2.49	.1695	.029
					MLC-6	1.16	--	--
					MLC-2	2.45	.169	.027
					MLC-3	2.45	.1695	.014
					MLC-4	2.66	.169	.017
	49-A	B-58	43,340	1.43	MLC-1	1.41	.211	.040
					MLC-5	1.49	.212	.032
					MLC-6	1.42	--	--
					MLC-2	1.33	.2075	.024
					MLC-3	1.39	.212	.045
					MLC-4	1.59	.2115	.035
	80-A	B-58	31,600	1.53	MLC-1	2.59	.156	.0085
					MLC-5	2.59	.1555	.0115
					MLC-6	1.35	--	--
					MLC-2	3.10*/2.48	.1555	.001/.003
					MLC-3	2.60	.1565	.019
					MLC-4	3.11	.1555	.014
	50-A	B-58	43,340	1.43	MLC-1	.930	.197	.0105
					MLC-5	.938	.192	.020
					MLC-6	.483	--	--
					MLC-2	1.02	.197	.045
					MLC-3	.908	.1995	.023
					MLC-4	1.15	.196	.049
	81-A	B-58	31,400	1.49	MLC-1	1.75	.151	.053
					MLC-5	2.07	.1505	.042
					MLC-6	.516	--	--
					MLC-2	1.80	.150	.050
					MLC-3	1.97	.151	.034
					MLC-4	2.29	.150	.047
6-8-66	43-A	B-58	42,380	1.62	MLC-1	--	--	--
					MLC-5	1.70	.177	.015
					MLC-6	1.53	--	--
					MLC-2	1.74	.174	.012
					MLC-3	1.73	.176	.014
					MLC-4	1.63	.175	.012
	75-A	B-58	31,200	1.44	MLC-1	--	--	--
					MLC-5	3.52	.156	.0055
					MLC-6	1.75	--	--
					MLC-2	3.18	.156	.0115
					MLC-3	3.37	.1565	.009
					MLC-4	3.15	.157	.007

Date	Mission No.	Aircraft	Altitude ft	Mach No.	Microphone No. **	Δp lb/ft^2	Δt sec.	Rise Time sec.
6-8-66	42-A	B-58	43,260	1.67	MLC-1	--	--	--
					MLC-5	2.09	.179	.009
					MLC-6	1.18	--	--
					MLC-2	2.73	.179	.006
					MLC-3	2.34	.179	.0035
					MLC-4	2.06	.179	.008
	73-A	B-58	31,200	1.5	MLC-1	--	--	--
					MLC-5	2.35	.147	.0155
					MLC-6	1.23	--	--
					MLC-2	2.23	.147	.011
					MLC-3	2.16	.146	.014
					MLC-4	2.23	.147	.016
	41-A	B-58	43,200	1.6	MLC-1	--	--	--
					MLC-5	1.74	.166	.006
					LLC-6	.963	--	--
					MLC-2	3.03	.166	.005
					MLC-3	1.82	.166	.006
					MLC-4	1.91	.167	.006
	72-A	B-58	31,200	1.49	MLC-1	--	--	--
					MLC-5	2.96	.144	.006
					MLC-6	1.58	--	--
					MLC-2	2.88	.145	.004
					MLC-3	3.24	.144	.002
					MLC-4	2.55	.145	.004
	57-RB	B-58	37,600	1.66	MLC-1	--	--	--
					MLC-5	1.78	.161	.023
					MLC-6	.832	--	--
					MLC-2	2.18	.162	.003
					MLC-3	1.51	.163	.030
					MLC-4	1.67	.162	.0085
	80-RB	B-58	31,300	1.46	MLC-1	--	--	--
					MLC-5	2.52	.161	.005
					MLC-6	1.31	--	--
					MLC-2	2.58	.160	.014
					MLC-3	2.64	.160	.0075
					MLC-4	3.15	.161	.0025
	56-RB	B-58	43,040	1.64	MLC-1	--	--	--
					MLC-5	2.61	.171	.004
					MLC-6	1.40	--	--
					MLC-2	2.08	.171	.0135
					MLC-3	1.90	.169	.008
					MLC-4	2.06	.171	.0065
	87-RB	B-58	31,440	1.49	MLC-1	--	--	--
					MLC-5	3.09	.148	.0175
					MLC-6	1.66	--	--
					MLC-2	4.27	.148	.001
					MLC-3	2.81	.148	.006
					MLC-4	3.19	.148	.017

Table F-1 (Continued)

Date	Mission No.	Aircraft	Altitude ft	Mach No.	Microphone No. **	Δp lb/ft^2	Δt sec.	Rise Time sec.
6-8-66	55-RB	B-58	43,200	1.64	MLC-1	--	--	--
					MLC-5	2.18	.170	.003
					MLC-6	1.71	--	--
					MLC-2	2.63	.169	.0125
					MLC-3	2.68	.166	.0015
					MLC-4	2.06	.169	.0055
	86-RB	B-58	31,360	1.49	MLC-1	--	--	--
					MLC-5	2.87	.144	.009
					MLC-6	1.62	--	--
					MLC-2	2.63	.144	.011
					MLC-3	3.03	.144	.0055
					MLC-4	2.48	.144	.006
6-9-66	86-SRB	B-58	31,000	1.5	MLC-1	3.52	.153	.0055
					MLC-5	3.72	.153	.005
					MLC-6	1.94	--	--
					MLC-2	4.09	.153	.0045
					MLC-3	5.32	.152	.005
					MLC-4	3.31	.1525	.004
	55-SRB	B-58	35,720	1.69	MLC-1	1.42	.1395	.032
					MLC-5	1.46	.1395	.030
					MLC-6	.74	. --	--
					MLC-2	1.43	.1405	.030
					MLC-3	1.75	.1395	.0085
					MLC-4	1.56	.1405	.031
	87-SRB	B-58	31,000	1.53	MLC-1	3.02	.147	.015
					MLC-5	2.93	.146	.006
					MLC-6	1.58	--	--
					MLC-2	3.12	.1455	.005
					MLC-3	3.72	.1465	.006
					MLC-4	4.02	.146	.001
	56-SRB	B-58	43,300	1.72	MLC-1	3.11	.1605	.002
					MLC-5	2.64	.161	.005
					MLC-6	1.34	--	--
					MLC-2	2.46	.1615	.0035
					MLC-3	2.98	.162	.0075
					MLC-4	2.63	.161	.004
	80-SRB	B-58	31,000	1.53	MLC-1	2.79	.1405	.006
					MLC-5	3.12	.140	.007
					MLC-6	2.18	-	-
					MLC-2	2.46	.140	.021
					MLC-3	3.61	.140	.003
					MLC-4	2.63	.1405	.024
	57-SRB	B-58	43,100	1.70	MLC-1	1.60	.1505	.0085
					MLC-5	1.56	.1495	.0055
					MLC-6	.838	--	--
					MLC-2	1.99	.150	.012
					MLC-3	2.12	.150	.004
					MLC-4	1.94	.150	.018

Table F-1   (Continued)

Date	Mission No.	Aircraft	Altitude ft	Mach No.	Microphone No. **	Δp lb/ft^2	Δt sec.	Rise Time sec.
6-9-66	41-SA	B-58	42,920	1.52	MLC-1	1.75	.180	.011
					MLC-5	2.93	.1805	.001
					MLC-6	1.74	--	--
					MLC-2	1.79	.1805	.005
					MLC-3	2.23	.181	.0045
					MLC-4	2.19	.1805	.002
	73-SA	B-58	31,720	1.50	MLC-1	3.05	.156	.017
					MLC-5	2.83	.1555	.0045
					MLC-6	1.47	--	--
					MLC-2	2.69	.155	.0045
					MLC-3	3.61	.155	.014
					MLC-4	2.76	.155	.018
	42-SA	B-58	43,060	1.52	MLC-1	1.99	.1755	.015
					MLC-5	2.04	.176	.018
					MLC-6	1.21	--	--
					MLC-2	2.23	.176	.005
					MLC-3	2.49	.176	.0175
					MLC-4	2.08	.176	.0015
	75-SA	B-58	31,680	1.55	MLC-1	3.68	.149	.003
					MLC-5	4.01*/3.34	.1485	.001*/.005
					MLC-6	1.81	--	--
					MLC-2	2.99	.1488	.003
					MLC-3	4.24	.1485	.012
					MLC-4	3.78	.149	.004

Note   72-SA Aborted

Date	Mission No.	Aircraft	Altitude ft	Mach No.	Microphone No. **	Δp lb/ft^2	Δt sec.	Rise Time sec.
	43-SA	B-58	43,000	1.68	MLC-1	3.50	.157	.003
					MLC-5	2.35	.1565	.001
					MLC-6	1.17	--	--
					MLC-2	2.99	.157	.004
					MLC-3	2.31	.157	.001
					MLC-4	3.01	.157	.002
	42-SA	B-58	43,300	1.70	MLC-1	1.87	.1645	.007
					MLC-5	2.07	.166	.011
					MLC-6	1.01	--	--
					MLC-2	1.66	.1645	.017
					MLC-3	2.05	.1655	.011
					MLC-4	1.81	.1665	.013
	46-SA	B-58	42,900	1.68	MLC-1	1.69	.156	.022
					MLC-5	1.69	.1555	.008
					MLC-6	.972	--	--
					MLC-2	2.26	.1565	.007
					MLC-3	2.83	.156	.006
					MLC-4	1.97	.1565	.0205
	72-SA	B-58	31,320	1.53	MLC-1	2.19	.1455	.0145
					MLC-5	2.29	.145	.016
					MLC-6	1.17	-	-
					MLC-2	1.89	.145	.0095
					MLC-3	2.57	.145	.017
					MLC-4	2.16	.1455	.019

F.9

Table F-1 (Continued)

Date	Mission No.	Aircraft	Altitude ft	Mach No.	Microphone No.**	Δp lb/ft²	Δt sec.	Rise Time sec.
8-13-66	18-A	B-58	37,740	1.64	MLC-1	2.59	.1605	.005
					MLC-5	3.36*/2.77	.1605	.0004/.0008
					MLC-6	1.85	--	--
					MLC-2	2.71	.160	.0035
					MLC-3	2.83	.160	.0003
					MLC-4	2.78	.160	.004
	18-B	B-58	49,600	1.66	MLC-1	2.16	.1935	.0005
					MLC-5	1.96	.1955	.005
					MLC-6	1.04	--	--
					MLC-2	1.88	.195	.0055
					MLC-3	2.00	.1955	.007
					MLC-4	2.31	.1955	.0035
	21-A	B-58	37,840	1.69	MLC-1	3.00	.1455	.0005
					MLC-5	2.55	.146	.0065
					MLC-6	1.34	--	--
					MLC-2	2.76	.146	.0035
					MLC-3	2.98	.146	.004
					MLC-4	2.94	.146	.005
	21-B	B-58	49,160	1.72	MLC-1	1.83	.195	.0045
					MLC-5	1.84	.195	.004
					MLC-6	.936	--	--
					MLC-2	1.83	.1945	.0045
					MLC-3	1.98	.195	.004
					MLC-4	2.03	.195	.0045
	29-A	B-58	49,300	1.67	MLC-1	1.83	.195	.0055
					MLC-5	2.01	.195	.0035
					MLC-6	1.04	--	--
					MLC-2	1.73	.1955	.004
					MLC-3	2.03	.195	.0055
					MLC-4	1.84	.1955	.013
	29-B	B-58	38,140	1.67	MLC-1	3.56*/2.93	.156	.0002*/.001
					MLC-5	3.07	.156	.0045
					MLC-6	1.52	--	--
					MLC-2	2.58	.1555	.0035
					MLC-3	2.66	.156	.009
					MLC-4	3.33*/3.22	.156	.0002*/.001
	32-A	B-58	49,820	1.64	MLC-1	1.85*/1.80	.1825	.0002*/.005
					MLC-5	1.91	.1825	.005
					MLC-6	1.10	--	--
					MLC-2	1.91	.1825	.004
					MLC-3	1.91	.182	.004
					MLC-4	1.93	.1825	.004
	32-B	B-58	38,000	1.67	MLC-1	2.35	.149	.015
					MLC-5	2.40/2.50	.149	.0002/.004
					MLC-6	1.31	--	--
					MLC-2	2.06	.149	.004
					MLC-3	2.39	.149	.005
					MLC-4	2.56	.149	.0035

F.10

Table F-1 (Continued)

Date	Mission No.	Aircraft	Altitude ft	Mach No.	Microphone No.**	Δp lb/ft²	Δt sec.	Rise Time sec.
6-20-66	48-A	B-58	41,300	1.55	MLC-1	2.71	.179	.005
					MLC-5	2.61	.179	.004
					MLC-6	1.40	--	--
					MLC-2	2.52	.1785	.005
					MLC-3	2.66	.179	.005
					MLC-4	2.93	.1775	.005
	79-A	B-58	32,100	1.45	MLC-1	2.57	.1535	.002
					MLC-5	2.52	.1535	.004
					MLC-6	1.37	--	--
					MLC-2	2.27	.1535	.006
					MLC-3	2.54	.1535	.005
					MLC-4	2.50	.1535	.005
	53-A	B-58	42,700	1.59	MLC-1	1.49	.1755	.020
					MLC-5	1.49	.1755	.020
					MLC-6	.588	--	--
					MLC-2	1.39	.1755	.021
					MLC-3	1.54	.175	.023
					MLC-4	1.43	.1755	.021
	84-A	B-58	31,220	1.43	MLC-1	2.68	.1445	.0015
					MLC-5	2.58	.1445	.017
					MLC-6	1.37	--	--
					MLC-2	2.36	.1445	.004
					MLC-3	2.66	.144	.0155
					MLC-4	2.59	.1445	.019
	54-A	B-58	43,000	1.59	MLC-1	1.28	.164	.0065
					MLC-5	1.31	.1635	.0075
					MLC-6	.718	--	--
					MLC-2	1.36	.164	.005
					MLC-3	1.42	.1645	.0055
					MLC-4	1.49	.1645	.0065
	59-B	B-58	43,360	1.41	MLC-1	2.31	.2175	.007
					MLC-5	2.31	.2176	.010
					MLC-6	1.01	--	--
					MLC-2	2.21	.218	.005
					MLC-3	2.24	.218	.0075
					MLC-4	2.47	.2175	.0045
	98-B	B-58	31,340	1.50	MLC-1	3.27	.1545	.0025
					MLC-5	3.04	.1535	.005
					MLC-6	1.50	--	--
					MLC-2	2.74	.1545	.004
					MLC-3	3.25	.1545	.006
					MLC-4	2.96	.1545	.004
	60-B		No Boom					
	90-B	B-58	31,800	1.55	MLC-1	2.74	.145	.016
					MLC-5	2.76	.145	.0135
					MLC-6	1.31	--	--
					MLC-2	2.68	.1455	.004
					MLC-3	3.16	.145	.002
					MLC-4	2.62	.1455	.011

F.11

Table   F-1   (Continued)

Date	Mission No.	Aircraft	Altitude ft	Mach No.	Microphone No.**	Δp lb/ft^2	Δt sec.	Rise Time sec.
6-20-66	85-A	B-58	32,320	1.45	MLC-1	2.22	.143	.016
					MLC-5	2.37	.142	.0115
					MLC-6	1.27	--	--
					MLC-2	2.33	.1435	.0145
					MLC-3	2.66	.142	.011
					MLC-4	2.38	.1435	.016
	93-B	B-58	32,140	1.55	MLC-1	2.48	.1415	.005
					MLC-5	2.86	.1410	.008
					MLC-6	1.47	--	--
					MLC-2	2.84	.1415	.013
					MLC-3	2.92	.141	.006
					MLC-4	3.32	.1405	.0045
6-21-66	89-B	B-58	31,760	1.46	MLC-1	2.84	.151	.018
					MLC-5	2.65	.1515	.007
					MLC-6	1.46	--	--
					MLC-2	3.00	.152	.014
					MLC-3	2.67	.151	.013
					MLC-4	2.98	.1515	.012
	58-B	B-58	43,600	1.67	MLC-1	1.93	.175	.006
					MLC-5	2.20	.1745	.002
					MLC-6	1.26	--	--
					MLC-2	1.55	.175	.012
					MLC-3	1.79	.1745	.002
					MLC-4	1.91	.175	.0075
	99-B	B-58	31,700	1.47	MLC-1	2.66	.1485	.025
					MLC-5	3.54*/3.16	.149	/.007
					MLC-6	1.78	--	--
					MLC-2	2.71	.1485	.002
					MLC-3	3.19	.1485	.0015
					MLC-4	3.89	.148	.004
	66-B	B-58	39,860	1.59	MLC-1	1.13	.167	.025
					MLC-5	1.16	.1675	.006
					MLC-6	.575	--	--
					MLC-2	1.08	.1675	.0125
					MLC-3	1.14	.167	.025
					MLC-4	1.19	.1665	.030
	100-B	B-58	31,760	1.46	MLC-1	3.55	.147	.0025
					MLC-5	2.96	.1465	.004
					MLC-6	1.39	--	--
					MLC-2	2.46	.1465	.005
					MLC-3	2.48	.146	.010
					MLC-4	3.54	.1465	.005
	68-B	B-58	44,080	1.62	MLC-1	1.32	.1675	.005
					MLC-5	1.44	.167	.007
					MLC-6	.732	--	--
					MLC-2	1.28	--	.012
					MLC-3	1.55	.167	.006
					MLC-4	1.44	.1665	.001

Table   F-1   (Continued)

Date	Mission No.	Aircraft	Altitude ft	Mach No.	Microphone No. **	Δp lb/ft^2	Δt sec.	Rise Time sec.
6-21-66	69-B	B-58	39,440	1.39	MLC-1	1.59	.1855	.023
					MLC-5	1.59	.186	.008
					MLC-6	.837	--	--
					MLC-2	1.58	.1855	.018
					MLC-3	1.60	.1855	.016
					MLC-4	1.66	.18¹	.013
	48-A	B-58	43,140	1.60	MLC-1	1.45	.178	.003
					MLC-5	1.57	.1775	.026
					MLC-6	.735	--	--
					MLC-2	1.16	.1775	.011
					MLC-3	1.81	.177	.002
					MLC-4	1.44	.1775	.022
	40-A	B-58	43,840	1.65	MLC-1	1.55	.171	.012
					MLC-5	1.77	.171	.006
					MLC-6	1.05	--	--
					MLC-2	1.87	.171	.005
					MLC-3	1.88	.1705	.009
					MLC-4	1.96	.171	.0065
	60-B	B-58	43,940	1.64	MLC-1	1.55	.165	.007
					MLC-5	1.46	.165	.013
					MLC-6	.759	--	--
					MLC-2	2.24	.1655	.004
					MLC-3	1.43	.1655	.017
					MLC-4	1.82	.165	.0095
	61-B	B-58	43,260	1.62	MLC-1	2.46	.1825	.008
					MLC-5	2.05	.1815	.011
					MLC-6	1.10	--	--
					MLC-2	3.32	.1815	.0025
					MLC-3	1.93	.1805	.020
					MLC-4	2.38	.181	.007
	101-B	B-58	31,700	1.5	MLC-1	2.68	.1485	.019
					MLC-5	2.68	.1485	.015
					MLC-6	1.39	--	--
					MLC-2	2.49	.148	.019
					MLC-3	2.72	.149	.001
					MLC-4	2.76	.485	.020
	85-A	B-58	31,700	1.5	MLC-1	2.23	.146	.023
					MLC-5	3.74	.146	.020
					MLC-6	1.57	--	-
					MLC-2	2.64	.1455	.00
					MLC-3	2.55	.146	.005
					MLC-4	3.12	.1455	.007
6-22-66	28-A	B-58	37,000	1.63	MLC-1	2.26	.162	.013
					MLC-5	2.73	.162	.0115
					MLC-6	1.45	--	--
					MLC-2	2.36	.163	.0345
					MLC-3	3 .	.1625	.008
					MLC-4	2.62	.162	.017

F.13

Table F-1 (Continued)

Date	Mission No.	Aircraft	Altitude ft	Mach No.	Microphone No.**	Δp lb/ft^2	Δt sec.	Rise Time sec.
6-22-66	19-A	B-58	37,200	1.64	MLC-1	2.30	.1555	.0155
					MLC-5	2.02	.156	.015
					MLC-6	1.08	--	--
					MLC-2	2.20	.156	.026
					MLC-3	1.78	.1565	.0085
					MLC-4	2.04	.156	.0135
	6-X	B-58	43,560	1.60	MLC-1	2.48	.167	.006
					MLC-5	3.36	.167	.0115
					MLC-6	2.48	--	--
					MLC-2	1.79	.1665	.0245
					MLC-3	5.06	.167	.0055
					MLC-4	4.12	.167	.016
	30-A	B-58	37,400	1.65	MLC-1	2.21	.163	.008
					MLC-5	1.92	.1635	.032
					MLC-6	1.01	--	--
					MLC-2	1.98	.163	.0185
					MLC-3	2.10	.163	.0295
					MLC-4	1.93	.1625	.0045
	34-B	B-58	43,400	1.61	MLC-1	1.44	.169	.018
					MLC-5	1.36	.170	.024
					MLC-6	.800	--	--
					MLC-2	1.74	--	.0105
					MLC-3	1.59	.170	.003
					MLC-4	1.44	.170	.0165
	24-A	B-58	43,300	1.6	MLC-1	1.58	No	.021
					MLC-5	1.59	time.	.031
					MLC-6	1.34	Could	--
					MLC-2	1.28	not	.022
					MLC-3	1.47	read.	.016
					MLC-4	1.55		.0225
	35-A	B-58	43,400	1.6	MLC-1	1.15	.165	.0225
					MLC-5	1.19	.165	.0175
					MLC-6	1.01	--	--
					MLC-2	.989	.165	.0365
					MLC-3	1.57	.1645	.0155
					MLC-4	1.35	.165	.028
	25-B	B-58	43,220	1.59	MLC-1	1.69	.179	.0135
					MLC-5	1.67	.1795	.0165
					MLC-6	.852	--	--
					MLC-2	1.23	.180	.009
					MLC-3	1.66	.1785	.0175
					MLC-4	1.44	.1795	.010
	23-B	B-58	37,440	1.63	MLC-1	2.73	.157	.0055
					MLC-5	2.45	.158	.009
					MLC-6	1.21	--	--
					MLC-2	2.05	.157	.0075
					MLC-3	2.36	.158	.0145
					MLC-4	2.60	.157	.0125

Date	Mission No.	Aircraft	Altitude ft	Mach No	Microphone No. ##	Δp lb/ft^2	Δt sec.	Rise Time sec.
6-23-66	17-A	B-58	37,600	1.64	MLC-1	2.38	.1625	.0035
					MLC-5	2.24/2.37	.162	.005/.0065
					MLC-6	1.17	--	--
					MLC-2	2.17/2.22	.162	.010/.014
					MLC-3	2.35	.162	.0045
					MLC-4	2.92	.162	.001
	22-B	B-58	43,360	1.67	MLC-1	1.13/1.43	.1685	.0025/.016
					MLC-5	1.46	.168	.0065
					MLC-6	.859	--	--
					MLC-2	1.53/1.87	.168	.0025/.0055
					MLC-3	.877/1.60	.168	.002/.010
					MLC-4	1.76	.168	.0055
	31-A	B-58	37,480	1.64	MLC-1	1.11/1.92	.155	.0025/.016
					MLC-5	1.80/1.95	.155	.007/.011
					MLC-6	.990	--	--
					MLC-2	2.12	.155	.006
					MIC-3	2.03	.154	.008
					MLC-4	1.79/1.90	.155	.0015/.015
	33-A	B-53	43,200	1.64	MLC-1	1.20	.163	.005
					MLC-5	1.20/1.28	.164	.004/.007
					MLC-6	.755	--	--
					MLC-2	1.03/1.26	.162	.0055/.013
					MLC-3	.701/1.25	.163	.002/.013
					MLC-4	1.30	.164	.006
	20-B	B-58	37,400	1.65	MLC-1	1.67/1.93	.159	.006/.019
					MLC-5	1.88	.159	.005
					MLC-6	1.07	. --	--
					MLC-2	1.97/2.27	.159	.003/.013
					MLC-3	2.26	.1595	.007
					MLC-4	2.17	.159	.0095
	36-B	B-58	37,400	1.66	MLC-1	4.37	.160	.015
					MLC-5	5.11	.1805	.006
					MLC-6	2.69	--	--
					MLC-2	4.24	.160	.0025
					MLC-3	7.65	.1595	.005
					MLC-4	6.12	.160	.005
	6X-2	B-58	43,520	1.67	MLC-1	1.61	.168	.019
					MLC-5	1.52	.168	.019
					LLC-6	--	--	--
					MLC-2	2.27	.168	.006
					MLC-3	1.51	.1675	.0135
					MLC-4	2.04	.168	.0125
6-4-66	2	F-104	No Tracking		MLC-1	1.19	.087	
					MLC-5	1.16	.087	
					MLC-6	.622	--	
					MLC-2	1.30	.087	
					MLC-3	1.26	.087	
					MLC-4	1.04	.087	

Table F-1 (Continued)

Date	Mission No.	Aircraft	Altitude ft	Mach No.	Microphone No. **	Δp lb/ft^2	Δt sec.	Rise Time sec.
6-13-66	26-A	F-104	21,200	1.4	MLC-1	1.75	.0735	.0055
					MLC-5	1.74	.073	.0055
					MLC-6	.883	--	--
					MLC-2	1.88	.0735	.0035
					MLC-3	1.88	.0735	.0035
					MLC-4	1.93	.074	.0035
	26-B	F-104	29,660	1.6		Missed Boom		
6-14-66	26-A	F-104	No Tracking		MLC-1	2.10	.072	
					MLC-5	2.28	.072	
					MLC-6	1.03	--	
					MLC-2	1.72	.0715	
					MLC-3	2.15	.072	
					MLC-4	2.15	.0725	
	26-B	F-104	29,920	1.54	MLC-1	1.61	.080	.0065
					MLC-5	1.43	.0795	.0055
					MLC-6	.814	--	--
					MLC-2	1.48	.079	.013
					MLC-3	1.45	.0795	.007
					MLC-4	1.43	.079	.006
	38-A	F-104	No Tracking		MLC-1	2.07	.074	.004
					MLC-5	2.10	.074	.0055
					MLC-6	1.08	--	--
					MLC-2	1.94	.0735	.006
					MLC-3	1.94	.074	.004
					MLC-4	2.35	.074	.0045
	38-B	F-104	29,700	1.52	MLC-1	1.49	.0795	.019
					MLC-5	1.36	.0785	.0135
					MLC-6	.788	--	--
					MLC-2	1.63	.079	.0085
					MLC-3	1.33	.0795	.0095
					MLC-4	1.62	.0795	.0115
	37-A	F-104	29,700	1.49	MLC-1	1.30	.079	.009
					MLC-5	1.19	.0795	.004
					MLC-6	.788	--	--
					MLC-2	1.41	.079	.004
					MLC-3	1.28	.079	.008
					MLC-4	1.56	.0795	.007
	37-B	F-104	21,080	1.39	MLC-1	3.21*/2.93	.0755	.0005*/.002
					MLC-5	2.60	.075	.004
					MLC-6	1.34	--	--
					MLC-2	2.67	.075	.0015
					MLC-3	--	--	--
					MLC-4	2.99	.075	.004
6-15-66	1X-A	F-104	14,080	1.21	MLC-1	4.24	.080	.0005
					MLC-5	3.75	.0795	.0045
					MLC-6	1.99	--	--
					MLC-2	3.17	.080	.0035
					MLC-3	4.40	.080	.0005
					MLC-4	3.48	.0795	.004

Table F-1 (Continued)

Date	Mission No.	Aircraft	Altitude ft.	Mach No.	Microphone No.**	Δp lb/ft^2	Δt sec.	Rise Time sec.
6-15-66	1X-B	F-104	28,140	1.5	MLC-1	1.32	.079	.009
					MLC-5	1.50	.079	.005
					MLC-6	.831	. --	--
					MLC-2	1.62	.0785	.0005
					MLC-3	1.36	.079	.0055
					MLC-4	1.52	.0785	.0055
	2X-A	F-104	29,700	1.32	MLC-1	1.62	.090	.014
					MLC-5	1.63	.090	.0115
					MLC-6	--	--	--
					MLC-2	1.55	.0905	.007
					MLC-3	1.69	.090	.009
					MLC-4	1.76	.0905	.0125
	2X-B	F-104	14,080	1.20	MLC-1	4.27	.079	.0035
					MLC-5	4.44	.079	.004
					MLC-6	2.13	--	--
					MLC-2	4.30	.079	.004
					MLC-3	4.40	.0795	.004
					MLC-4	4.30	.079	.0035
	3X-A	F-104	29,100	1.58	MLC-1	1.15	.075	.0135
					MLC-5	1.19	.0755	.0105
					MLC-6	.631	--	--
					MLC-2	1.39	.0745	.0105
					MLC-3	1.20	.0755	.008
					MLC-4	1.23	.075	.0095
	3X-B	F-104	14,200	1.15	MLC-1	2.35	.077	.006
					MLC-5	2.28	.077	.006
					MLC-6	1.20	--	--
					MLC-2	2.10	.077	.0115
					MLC-3	2.29	.077	.010
					MLC-4	2.17	.0775	.006
	4X-A	F-104	14,060	1.28	MLC-1	3.38	.0675	.0015
					MLC-5	3.28	.0685	.0055
					MLC-6	1.69	--	--
					MLC-2	3.20	.0675	.0035
					MLC-3	3.19	.0675	.0035
					MLC-4	3.49	.0675	.0035
	4X-B	F-104	29,880	1.62	MLC-1	3.29/2.56	.078	.0005/.004
					MLC-5	2.41	.0765	.0045
					MLC-6	1.20	--	--
					MLC-2	2.26	.077	.0045
					MLC-3	2.44	.077	.005
					MLC-4	2.46	.0775	.0035
6-16-66	27-A	F-104	29,300	1.65	MLC-1	1.28	.075	.0055
					MLC-5	1.48	.075	.004
					MLC-6	.797	. -- .	--
					MLC-2	1.54	.075	.001
					MLC-3	1.45	.075	.0055
					MLC-4	1.52	.075	.004

Table F-1   (Continued)

Date	Mission No.	Aircraft	Altitude ft.	Mach No.	Microphone No.**	Δp lb/ft^2	Δt sec.	Time Rise sec.
6-16-66	27-B	F-104	20,540	1.4	MLC-1	1.63	.074	.003
					MLC-5	1.61	.0735	.004
					MLC-6	.897	. --	--
					MLC-2	1.95	.0735	.0035
					MLC-3	1.56	.0735	.005
					MLC-4	1.58	.0735	.0035
	5-X	F-104	29,700	1.65	MLC-1	1.93	.072	.005
					MLC-5	1.79	.072	.0045
					MLC-6	.964	--	--
					MLC-2	1.64	.071	.003
					MLC-3	1.71	.0715	.0045
					MLC-4	1.71	.072	.0045
6-22-66	28-B	F-104	20,820	1.35	MLC-1	2.05	.0775	.0135
					MLC-5	2.20	.078	.0085
					MLC-6	1.34	--	--
					MLC-2	2.15	.077	.0105
					MLC-3	3.46	.078	.0065
					MLC-4	2.98	.0775	.0085
	19-B	F-104	29,500	1.42	MLC-1	1.51	.0885	.0175
					MLC-5	2.05	.089	.0025
					MLC-6	1.03	--	--
					MLC-2	1.50	.0885	.008
					MLC-3	1.94	.0885	.0095
					MLC-4	1.99	.089	.0085
	30-B	F-104	29,720	1.37	MLC-1	1.01	.093	.0215
					MLC-5	.985	.094	.0265
					MLC-6	.439	--	--
					MLC-2	.724	.092	.0385
					MLC-3	.958	.0935	.0265
					MLC-4	1.02	.093	.0290
	34-A	F-104	29,600	1.39	MLC-1	1.31	.096	.018
					MLC-5	1.29	.0965	.0225
					MLC-6	.981	. --	--
					MLC-2	1.45	.0945	.0215
					MLC-3	1.07	.0985	.011
					MLC-4	1.30	.0945	.021
	24-B	F-104	20,860	1.36	MLC-1	1.76	.0785	.012
					MLC-5	2.37*/1.69	.0775	.0005*/.0135
					MLC-6	1.06	--	--
					MLC-2	1.76	.077	.007
					MLC-3	1.99	.078	.007
					MLC-4	2.90	.0775	.0025
	35-B	F-104	21,060	1.28	MLC-1	3.02	.0815	.005
					MLC-5	2.85	.082	.0035
					MLC-6	1.43	--	--
					MLC-2	2.24	.0825	.007
					MLC-3	2.50	.0815	.007
					MLC-4	1.82	.0805	.0045

F.18

Table F-1 (Continued)

Date	Mission No.	Aircraft	Altitude ft.	Mach No.	Microphone No.**	Δp lb/ft^2	Δt sec.	Rise Time sec.
6-22-66	25-A	F-104	21,900	1.39	MLC-1	1.24	.075	.007
					MLC-5	1.36	.075	.0065
					MLC-6	.749	--	--
					MLC-2	1.42	.078	.0095
					MLC-3	1.75	.075	.0045
					MLC-4	1.46	.075	.012
	23-A	F-104	29,720	1.51	MLC-1	.993	.083	.036
					MLC-5	.985	.084	.0195
					MLC-6	.904	--	--
					MLC-2	2.17	.084	.0045
					MLC-3	1.01	.083	.0225
					MLC-4	1.24	.0845	.0135
6-23-66	17-B	F-104	21,600	1.4	MLC-1	2.31	.076	.0015
					MLC-5	1.33/2.03	.0755	.002/.007
					MLC-3	.938	. --	--
					MLC-2	1.43/1.48	.076	.002/.005
					MLC-3	1.93	.076	.0055
					MLC-4	1.82	.076	.002
	22-A	F-104	29,260	1.4	MLC-1	1.39/1.80	.083	.001/.0085
					MLC-5	1.22/1.51	.083	.0045
					MLC-6	.781	--	--
					MLC-2	1.55	.0825	.010
					MLC-3	1.28/1.43	.083	.0015/.006
					MLC-4	1.74*/1.52	.082	.001/.0045
	31-B	F-104	21,260	1.39	MLC-1	2.17	.076	.006
					MLC-5	1.02/2.08	.076	.0015/.013
					MLC-6	.547	--	--
					MLC-2	1.72/1.97	.076	.003/.0095
					MLC-3	1.93	.076	.013
					MLC-4	1.63/2.49	.076	.001/.006
	33-B	F-104	29,840	1.49	MLC-1	1.43	.084	.012
					MLC-5	1.61	.084	.011
					MLC-6	.885	--	--
					MLC-2	2.41	.084	.004
					MLC-3	1.85	.084	.010
					MLC-4	1.82/1.92	.084	.0085/.011
	20-A	F-104	21,520	1.37	MLC-1	1.86	.078	.011
					MLC-5	1.61/1.97	.080	.007/.012
					MLC-6	1.07	--	--
					MLC-2	.985/1.74	.079	.0025/.020
					MLC-3	2.14	.080	.003/.0095
					MLC-4	1.83	.079	.012
	36-A	F-104	20,860	1.39	MLC-1	1.93	.077	.002
					MLC-5	2.24	.077	.005
					MLC-6	1.26	--	--
					MLC-2	1.97/2.12	.077	.001/.0055
					MLC-3	1.85/2.14	.0765	.0045/.007
					MLC-4	1.70/2.04	.077	.003/.005

F.19

Table F-1   (Concluded)

Date	Mission No.	Aircraft	Altitude ft.	Mach No.	Microphone No.	Δp lb/ft²	Δt sec.	Rise Time sec.
6-23-66	7-X	F-104	29,640	1.55	MLC-1	1.99	.081	.008
					MLC-5	1.70	.081	.016
					MLC-6	.806	--	--
					MLC-2	3.33	.082	.0075
					MLC-3	1.27/1.56	.0815	.009/.0205
					MLC-1	1.70	.081	.0135

NOTES:

* Slash (/) denotes two peaks.

**MLC-2 moved to southeast corner of yard of concrete blockhouse after flights of June 6, 1966.

TABLE F-2
SUMMARY OF DATA FROM FREE FIELD
MICROPHONES LOCATED NEAR L-2, PHASE I[1]

Date	Mission No.	Aircraft	Altitude Ft.	Mach No.	Average Peak Pressure psf
6-6-66	70	B-58	43,400	1.60	0.94
	40	B-58	31,400	1.48	0.57
6-7-66	76A	B-58	31,500	1.48	0.94
	46B	B-58	43,720	1.65	0.64
	79A	B-58	31,600	1.52	1.47
	80A	B-58	31,600	1.53	1.21
	81A	B-58	31,400	1.49	1.03
6-8-66	43A	B-58	42,380	1.62	0.32
	75A	B-58	31,200	1.44	0.85
	42A	B-58	43,260	1.67	0.28
	73A	B-58	31,200	1.50	0.65
	41A	B-38	43,200	1.60	0.26
	72A	B-58	31,200	1.49	1.13
	57B	B-58	37,600	1.66	0.57
	56RB	B-58	43,040	1.64	0.11
	87	B-58	31,440	1.49	0.50
	55RB	B-58	43,200	1.64	0.14
	86RB	B-58	31,360	1.49	0.40

1) Refer to Legend, Page F.1, for explanation of notations and
   abbreviations.

TABLE F-2 (Continued)
SUMMARY OF DATA FROM FREE FIELD
MICROPHONES LOCATED NEAR L-2, PHASE I

Date	Mission No.	Aircraft	Altitude Ft.	Mach No.	Average Peak Pressure psf
6-9-66	55SRB	B-58	35,720	1.69	0.68
	87SRB	9-58	31,000	1.53	1.06
	80SRB	B-58	31,000	1.53	1.21
	57SRB	B-58	43,100	1.70	0.58
	41SA	B-58	42,920	1.52	1.13
	73SA	B-58	31,720	1.50	1.12
	42SA	B-58	3,060	1.52	1.21
	75SA	B-58	31,680	1.55	0.62
	43SA	B-58	43,000	1.68	1.66
	42SA	B-58	43,300	1.70	0.39
	46SA	B-58	42,900	1.68	0.53
	72SA	B-58	31,320	1.53	1.15
6-13-66	18A	B-58	37,740	1.64	1.50
	18B	B-58	49,600	1.66	1.15
	21A	B-58	37,840	1.69	1.50
	21B	B-58	49,160	1.72	1.31
	26A	B-58	21,200	1.4	0.97
	29A	B-58	49,300	1.67	1.01
	29B	B-58	38,140	1.67	1.67
	32A	B-58	49,820	1.64	1.15
	32B	B-58	38,000	1.67	1.50

TABLE F-2 (Continued

SUMMARY OF DATA FROM FREE FIELD

MICROPHONES LOCATED NEAR L-2, PHASE I

Date	Mission No.	Aircraft	Altitude Ft.	Mach No.	Average Peak Pressure psf
6-14-66	26A	F-104	20,000	1.4	1.21
	26B	F-104	29,920	1.54	0.53
	38A	F-104	20,000	1.4	0.42
	38B	F-104	29,700	1.52	0.68
	37A	F-104	29,700	1.49	0.83
	37B	F-104	21,080	1.39	0.55
6-15-66	4XB	F-104	29,880	1.62	0.45
6-20-66	48A	B-58	41,300		0.93
	53A	B-58	42,700	.9	0.86
	84A	B-58	31,220	1.43	0.53
	54A	B-58	43,000	1.59	0.53
	59B	B-58	43,360	1.41	0.53
	98B	B-58	31,340	1.50	1.53
	93B	B-58	32,140	1.55	1.56
6-21-66	89B	B-58	31,760	1.46	1.34
	58B	B-58	43,600	1.67	0.69
	99B	B-58	31,700	1.47	1.34
	66B	B-58	39,860	1.59	1.04
	100B	B-58	31,760	1.46	1.14
	68B	B-58	44,080	1.62	0.71

TABLE F-2 (Continued)
SUMMARY OF DATA FROM FREE FIELD
MICROPHONES LOCATED NEAR L-2, PHASE I

Date	Mission No.	Aircraft	Altitude Ft.	Mach No.	Average Peak Pressure psf
6-21-66	85A	B-58	31,700	1.50	1.88
	48A	B-58	43,140	1.60	0.96
	40A	B-58	43,840	1.65	0.87
	60B	B-58	43,940	1.64	0.48
	101B	B-58	31,700	1.50	1.54
6-22-66	28A	B-58	37,000	1.63	1.30
	28B	F-104	20,800	1.35	0.34
	19A	B-58	37,200	1.64	1.31
	19B	F-104	29,500	1.42	0.31
	6X	B-58	43,560	1.6	0.46
	30A	B-58	37,400	1.65	2.00
	34B	B-58	43,400	1.61	0.79
	35B	F-104	21,060	1.28	0.14
	23A	F-104	29,720	1.51	0.43
	23B	B-58	37,440	1.63	1.19
6-23-66	17A	B-58	37,600	1.64	2.13
	17B	F-104	21,600	1.40	0.70
	22A	F-.04	29,200	1.40	0.47
	22B	B-58	43,300	1.67	0.47
	31A	B-58	37,400	1.64	0.97
	31B	F-104	21,200	1.39	0.59
	33A	B-58	43,200	1.64	0.74

F.24

TABLE F-2 (Continued)
SUMMARY OF DATA FROM FREE FIELD
MICROPHONES LOCATED NEAR L-2, PHASE I[1)

Date	Mission No.	Aircraft	Altitude Ft.	Mach No.	Average Peak Pressure psf
6-23-66	33B	F-104	29,800	1.49	0.70
	20B	B-58	37,400	1.65	1.34
	36A	F-104	20,800	1.39	0.59
	7X	F-104	29.600	1.55	0.30
	6X2	B-58	43,500	1.67	0.32

F.25

Table F-3

SUMMARY OF DATA FROM FREE FIELD MICROPHONES LOCATED NEAR E-2, PHASE .(. 1)

MSN	CHNL	HOUSE	INSTR	TYPE	PEAK AMPLITUDES (PSF) POSITIVE P1	P2	P3	NEGATIVE P1	P2	RISE TIME T1 SEC	T2	PER-IOD SEC	WAVE ANGLE DEG	GND SPD FT/SEC	6
1-1	601	2	MLC1	2			3.06	2.29	2.50		.0015	.229	58.9	1342	6
1-1	603	2	MLC2	2			2.91	2.34	2.67		.0065	.229			6
1-1	605	2	MLC3	2			2.78	2.22	2.38		.005	.229			6
1-1	607	2	MLC4	2			2.86	2.18	2.64		.002	.230			6
1-1	609	2	MLC5	2			2.94	2.37	2.84		.003	.231			6
1-1	611	2	MLC6				1.44								6
1-3	601	2	MLC1	2			2.99	1.72	2.25		.005	.165	66.5	1242	6
1-3	603	2	MLC2	6		3.57	3.37	2.51	2.44	.0005	.005	.165			6
1-3	605	2	MLC3	2			2.86	1.94	2.22		.003	.165			6
1-3	607	2	MLC4	2			2.93	1.96	2.52		.007	.165			6
1-3	609	2	MLC5	2			3.24	2.27	2.44		.005	.155			6
1-3	611	2	MLC6				1.59								6
1-4	601	2	MLC1	2			2.75	3.06	2.57		.0015	.082	58.7	1351	6
1-4	603	2	MLC2	6		3.81	3.07	3.67	2.81	.0005	.004	.081			6
1-4	605	2	MLC3	4			3.85	4.29	2.62		.0005	.081			6
1-4	607	2	MLC4	2			3.21	3.58	2.86		.003	.081			6
1-4	609	2	MLC5	2			3.34	3.81	2.87		.0035	.081			6
1-4	611	2	MLC6				1.78								6
2-1	601	2	MLC1	2			2.37	1.96	1.38		.005	.237	79.4	1250	6
2-1	603	2	MLC2	3			2.23	1.87	1.48		.008	.237			6
2-1	605	2	MLC3	4			2.82	2.11	1.30		.004	.236			6
2-1	607	2	MLC4	3			2.25	1.75	1.45		.008	.237			6
2-1	609	2	MLC5	4			3.09	2.32	1.63		.006	.237			6
2-1	611	2	MLC6				1.52								6
2-3	601	2	MLC1	3			2.15	1.62	2.30		.014	.153	50.9	1626	6
2-3	603	2	MLC2	3			2.21	1.61	2.15		.017	.152			6
2-3	605	2	MLC3	3			2.32	1.83	2.14		.0075	.153			6
2-3	607	2	MLC4	8		2.10	2.40	1.52	2.30	.001	.008	.153			6
2-3	609	2	MLC5	3			2.52	1.43	2.40		.012	.153			6
2-3	611	2	MLC6				0.99								6
2-4	601	2	MLC1	4			3.96	4.22	2.76		.001	.079	54.3	1439	6
2-4	603	2	MLC2	4			3.71	4.12	2.79		.0005	.078			6
2-4	605	2	MLC3	2			3.02	3.70	2.66		.004	.079			6
2-4	607	2	MLC4	4			3.47	3.95	2.80		.002	.078			6
2-4	609	2	MLC5	2			3.41	3.93	2.93		.002	.079			6
2-4	611	2	MLC6				1.69								6

1) Refer to legend, page F.2 for explanation of notations and abbreviations.

F.26

Table F-3 (Continued)

MSN	CHNL	HOUSE INSTR	TYPE	PEAK AMPLITUDES POSITIVE			NEGATIVE		RISE TIME		PER-IOD	WAVE ANGLE	GND SPD
				P1	P2	P3	P1	P2	T1	T2			
3-1	601	2 MLC1	2			2.66	2.08	1.75		.005	.153	53.6	1476	6
3-1	603	2 MLC2	2			2.46	1.99	1.89		.0055	.153			6
3-1	605	2 MLC3	2			2.39	1.96	1.67		.005	.153			6
3-1	607	2 MLC4	2			2.68	2.23	1.92		.0035	.153			6
3-1	609	2 MLC5	2			2.56	2.10	1.90		.0055	.152			6
3-1	611	2 MLC6	2			1.30								6
3-2	601	2 MLC1	2			2.57	2.27	2.50		.005	.234	56.7	1384	6
3-2	603	2 MLC2	2			2.42	1.79	2.39		.005	.233			6
3-2	605	2 MLC3	2			2.39	2.10	2.25		.005	.234			6
3-2	607	2 MLC4	2			2.47	2.13	2.51		.0045	.234			6
3-2	609	2 MLC5	2			2.53	2.23	2.63		.004	.234			6
3-2	611	2 MLC6	2			1.30								6
3-4	601	2 MLC1	A6	2.79		2.47	2.86	2.40	.001	.004	.077	56.1	1413	6
3-4	603	2 MLC2	2			2.32	2.76	2.36		.005	.077			6
3-4	605	2 MLC3	2			2.25	2.79	2.32		.005	.077			6
3-4	607	2 MLC4	2			2.34	2.68	2.37		.004	.077			6
3-4	609	2 MLC5	2			2.42	2.76	2.33		.004	.077			6
3-4	611	2 MLC6	3			1.26								6
4-1	601	2 MLC1	3			2.30	1.87	2.04		.0135	.149	50.9	1476	6
4-1	603	2 MLC2	3			2.29	1.83	2.01		.015	.149			6
4-1	605	2 MLC3	3			2.20	1.87	1.87		.014	.149			6
4-1	607	2 MLC4	3			2.25	1.90	2.11		.014	.149			6
4-1	609	2 MLC5	3			2.19	1.81	2.02		.0125	.149			6
4-1	611	2 MLC6	3			.91								6
4-2	601	2 MLC1	2			2.57	2.24	2.27		.005	.232	55.0	1399	6
4-2	603	2 MLC2	2			2.57	2.32	2.29		.005	.232			6
4-2	605	2 MLC3	2			2.49	2.23	2.02		.005	.232			6
4-2	607	2 MLC4	2			2.39	2.11	2.29		.006	.232			6
4-2	609	2 MLC5	2			2.43	2.12	2.22		.005	.232			6
4-2	611	2 MLC6	3			1.17								6
5-1	601	2 MLC1	3			.70	.42	.62		.014	.17	75.5	1401	6
5-1	603	2 MLC2	8		.60	.70	.40	.67	.0005	.015	.1			6
5-1	605	2 MLC3	8		.60	.67	.42	.60	.001	.015	.17.			6
5-1	607	2 MLC4	2			.67	.45	.67		.0045	.173			6
5-1	609	2 MLC5	3			.67	.35	.64		.0165	.173			6
5-1	611	2 MLC6				.32								6

Table F-3 (Continued)

MSN	CHNL	HOUSE	INSTR	TYPE	PEAK AMPLITUDES POSITIVE P1	POSITIVE P2	POSITIVE P3	NEGATIVE P1	NEGATIVE P2	RISE TIME T1	T2	PERIOD	WAVE ANGLE	GND SPD	
5-2	601	2	MLC1	2			1.25	.62	.81		.005	.283	52.0	2235	6
5-2	603	2	MLC2	2			1.16	.60	.83		.006	.284			6
5-2	605	2	MLC3	2			1.14	.62	.76		.005	.283			6
5-2	607	2	MLC4	2			1.24	.62	.88		.004	.283			6
5-2	609	2	MLC5	2			1.20	.59	.82		.0045	.283			6
5-2	611	2	MLC6	2			.61								6
6-1	601	2	MLC1	3			1.29	.75	1.13		.021	.157	67.1	1533	6
6-1	603	2	MLC2	3			1.35	.83	1.21		.015	.157			6
6-1	605	2	MLC3	3			1.30	.61	1.06		.015	.157			6
6-1	607	2	MLC4	3			1.29	.70	1.21		.016	.158			6
6-1	609	2	MLC5	3			1.31	.76	1.16		.014	.158			6
6-1	611	2	MLC6	3			.532								6
6-2	601	2	MLC1	2			1.67	.95	.97		.007	.284	53.3	2128	6
6-2	603	2	MLC2	2			1.75	.98	1.00		.0065	.284			6
6-2	605	2	MLC3	2			1.91		.98		.0045	.284			6
6-2	607	2	MLC4	2			1.89	1.03	1.05		.006	.234			6
6-2	609	2	MLC5	2			1.69	.97	1.03		.0055	.284			6
6-2	611	2	MLC6	2			.874								6
7-1	601	2	MLC1	2			1.79	.91	1.30		.0055	.147	56.7	1639	6
7-1	603	2	MLC2	2			1.78	.91	1.20		.0055	.147			6
7-1	605	2	MLC3	2											6
7-1	607	2	MLC4	2											6
7-1	609	2	MLC5	2			1.67	.91	1.23		.005	.147			6
7-1	611	2	MLC6	2			.887								6
7-3	601	2	MLC1				1.33	.51	.86	.0005	.006	.264	41.3	2273	6
7-3	603	2	MLC2	5		1.17	1.34	.56	.78	.001	.004	.264			6
7-3	605	2	MLC3	5		1.24									6
7-3	607	2	MLC4				1.29	.65	.85		.0045	.264			6
7-3	609	2	MLC5	2			.679								6
7-3	611	2	MLC6												6
8-1	601	2	MLC1	2			2.44	2.14	2.25		.005	.163	45.0	1802	6
8-1	603	2	MLC2	2			2.50	2.23	2.32		.0055	.164			6
8-1	605	2	MLC3	2			2.58		2.17		.0045	.164			6
8-1	607	2	MLC4	2			2.12	2.00	2.34		.0075	.165			6
8-1	609	2	MLC5	2			2.33	2.02	2.27		.005	.165			6
8-1	611	2	MLC6	2			1.25								6

Table F-3 (Continued)

MSR	CHNL	HOUSE INSTR	TYPE	PEAK AMPLITUDES POSITIVE P1	P2	P3	NEGATIVE P1	P2	RISE TIME T1	TIME T2	PER-IOD	WAVE ANGLE	GND SPD
8-3	601	2 MLC1	3			1.39		.875		.008	.269	42.3	2439	6
8-3	603	2 MLC2	3			1.43		.930		.013	.270			6
8-3	605	2 MLC3	3			1.37		.808		.013	.270			6
8-3	607	2 MLC4	3			1.37		1.03		.008	.270			6
8-3	609	2 MLC5	3			1.37		.866		.012	.269			6
8-3	611	2 MLC6				.696								6
9-1	601	2 MLC1	7	2.10	1.65	1.94	0.83	1.13	.0005	.005	.275	30.9	2381	6
9-1	603	2 MLC2	2			2.10	0.84	1.22		.0015	.276			6
9-1	605	2 MLC3	5		2.03	2.24	0.79	1.24	.002	.005	.275			6
9-1	607	2 MLC4	2			2.06	0.89	1.25		.0035	.272			6
9-1	609	2 MLC5	2			2.10	1.06	1.30		.0035	.273			6
9-1	611	2 MLC6				0.99								6
9-2	601	2 MLC1	2			2.11	1.81	1.71	.0015	.003	.175	48.5	1538	6
9-2	603	2 MLC2	5		1.81	2.41	1.98	1.77		.005	.174			6
9-2	605	2 MLC3	6		4.51	4.16	3.32	1.70		.0005	.174			5
9-2	607	2 MLC4	2			2.34	2.06	1.94		.005	.174			6
9-2	609	2 MLC5	2			2.51	2.20	1.87		.002	.174			6
9-2	611	2 MLC6				1.32								6
9-3	601	2 MLC1	2			1.60	1.92	1.58		.0055	.085	59.0	1333	6
9-3	603	2 MLC2	2			1.71	1.85	1.48		.0065	.085			6
9-3	605	2 MLC3	3			1.41	1.66	1.39		.009	.084			4
9-3	607	2 MLC4	2			1.37	1.69	1.47		.0075	.084			6
9-3	609	2 MLC5	2			1.61	1.75	1.59		.0085	.085			6
9-3	611	2 MLC6				0.75								6
10-1	601	2 MLC1	2			2.32	1.01	1.54		.004	.262	28.4	2469	6
10-1	603	2 MLC2	2			2.41	1.17	1.70		.005	.263			6
10-1	605	2 MLC3	2			2.33	1.07	1.54		.005	.263			6
10-1	607	2 MLC4	2			2.47	1.11	1.75		.004	.263			6
10-1	609	2 MLC5	2			2.52	1.19	1.75		.0035	.263			6
10-1	611	2 MLC6				1.20								6
10-2	601	2 MLC1	3			3.16	2.10	2.35		.0135	.185	73.8	1163	6
10-2	603	2 MLC2	3			3.29	2.26	2.65		.0055	.185			6
10-2	605	2 MLC3	3			3.03	2.30	2.68		.017	.185			6
10-2	607	2 MLC4	3			3.44	2.03	2.69		.016	.185			6
10-2	609	2 MLC5	3			3.42	2.18	2.65		.014	.185			6
10-2	611	2 MLC6				1.47								6

Table F-3 (Continued)

MSN	CHNL	HOUSE INSTR	TYPE	POSITIVE P1	POSITIVE P2	POSITIVE P3	NEGATIVE P1	NEGATIVE P2	RISE TIME T1	RISE TIME T2	PERIOD	WAVE ANGLE	GND SPD	
11-1	601	2 MLC1	2			2.12	2.47	2.12		.004	.073	50.2	1515	6
11-1	603	2 MLC2	2			1.98	2.35	2.01		.005	.073			6
11-1	605	2 MLC3	5		1.72	1.89	2.26	1.95		.0045	.073			6
11-1	607	2 MLC4	2			1.96	2.32	2.04		.0045	.074			6
11-1	609	2 MLC5	2			2.09	2.42	2.04		.0045	.074			6
11-1	611	2 MLC6	2			.93								6
11-2	601	2 MLC1	3			1.94	1.57	1.83		.005	.171	47.4	1533	6
11-2	603	2 MLC2	3			1.84	1.54	1.79		.005	.171			6
11-2	605	2 MLC3	3			1.80	1.49	1.66		.005	.170			6
11-2	607	2 MLC4	3			1.87	1.51	1.96		.0045	.170			6
11-2	609	2 MLC5	2			1.87	1.52	1.76		.0045	.171			6
11-2	611	2 MLC6				.84								6
11-3	601	2 MLC1	2			2.23	1.33	1.59		.0045	.278	28.4	2381	6
11-3	603	2 MLC2	2			2.04	1.23	1.59		.005	.278			6
11-3	605	2 MLC3	2			2.12	1.29	1.52		.0045	.278			6
11-3	607	2 MLC4	2			2.12	1.34	1.59		.0045	.278			6
11-3	609	2 MLC5	2			1.95	1.19	1.60		.0045	.278			6
11-3	611	2 MLC6				.99								6
12-1	601	2 MLC1	2			2.40	1.57	1.85		.006	.171	47.3	1538	6
12-1	603	2 MLC2	2			2.32	1.51	1.88		.0055	.172			6
12-1	605	2 MLC3	5		2.21	2.43	1.54	1.84		.005	.172			6
12-1	607	2 MLC4	2			2.32	1.60	2.08	.002	.006	.171			6
12-1	609	2 MLC5	A5	2.92	2.07	2.51	1.40	1.87	.001	.004	.172			6
12-1	611	2 MLC6				1.28								6
12-2	601	2 MLC1	2			2.21	1.41	1.71		.0045	.290	27.9	2439	6
12-2	603	2 MLC2	2			2.14	1.51	1.71		.005	.289			6
12-2	605	2 MLC3	2			2.29	1.57	1.73		.005	.289			6
12-2	607	2 MLC4	2			2.28	1.65	1.72		.005	.290			6
12-2	609	2 MLC5	2			2.04	1.46	1.66		.005	.290			6
12-2	611	2 MLC6				.98								6
12-3	601	2 MLC1	2	1.88	1.74	1.88	1.99	1.85		.0045	.076	51.2	1460	6
12-3	603	2 MLC2	A5		2.00	1.88	2.51	2.00	.0005	.006	.076			6
12-3	605	2 MLC3	5			2.16	2.30	2.00	.001	.0055	.076			6
12-3	607	2 MLC4	2			2.16		2.01		.005	.076			6
12-3	609	2 MLC5	A6		2.19	2.01	2.13	1.93	.001	.005	.076			6
12-3	611	2 MLC6				1.01								6

F-.30

Table F-3 (Continued)

MSN	CHNL	HOUSE INSTR	TYPE	POSITIVE P1	POSITIVE P2	POSITIVE P3	NEGATIVE P1	NEGATIVE P2	RISE TIME T1	RISE TIME T2	PERIOD	WAVE ANGLE	GND SPD	
13-1	601	2 MLC1	3			2.31	1.59	1.82		.006	.159	47.7	1581	6
13-1	603	2 MLC2	2			2.17				.005	.160			6
13-1	605	2 MLC3	5		1.92	2.19	1.41	1.67	.001	.005	.159			6
13-1	607	2 MLC4	2		2.04	2.25	1.48	1.93	.0015	.004	.158			6
13-1	609	2 MLC5	2			2.11	1.50	1.93		.0045	.158			6
13-1	611	2 MLC6				1.08								6
13-2	601	2 MLC1	3			2.00	1.21	1.59		.0075	.286	43.7	1778	6
13-2	603	2 MLC2	3			1.92				.0055	.286			6
13-2	605	2 MLC3	2			2.17	1.25	1.54		.005	.287			6
13-2	607	2 MLC4	3			1.95	1.19	1.73		.015	.287			6
13-2	609	2 MLC5	3			1.97	1.17	1.69		.0065	.287			6
13-2	611	2 MLC6				1.03								6
13-3	601	2 MLC1	2			1.87	2.16	1.92		.0055	.074	56.0	1493	6
13-3	603	2 MLC2	2			2.05	2.42	2.07		.0055	.074			6
13-3	605	2 MLC3	2			2.01	2.22	1.83		.005	.075			6
13-3	607	2 MLC4	2			2.15	2.37	1.95		.0045	.074			6
13-3	609	2 MLC5	2			1.95	2.25	1.97		.006	.075			5
13-3	611	2 MLC6				0.98								6
14-1	601	2 MLC1	3			2.02	1.22	1.65		.013	.312	43.7	1674	6
14-1	603	2 MLC2	3			2.01	1.25	1.68		.018	.312			6
14-1	605	2 MLC3	2			2.17	1.41	1.64		.006	.311			6
14-1	607	2 MLC4	2			2.26	1.36	1.79		.0045	.311			6
14-1	609	2 MLC5	2			2.11	1.29	1.78		.005	.311			6
14-1	611	2 MLC6				.933								6
14-2	601	2 MLC1	6		3.36	2.70	1.62	1.82	.0005	.0035	.156	54.6	1423	6
14-2	603	2 MLC2	2			2.53	1.59	1.86		.075	.156			6
14-2	605	2 MLC3	2			2.61	1.53	1.67		.005	.156			6
14-2	607	2 MLC4	2			2.75	1.73	2.01		.0035	.156			6
14-2	609	2 MLC5	2			2.62	1.56	1.87		.0035	.156			6
14-2	611	2 MLC6				1.26								6
14-3	601	2 MLC1	2		2.47	2.02	2.48	2.08	.0005	.005	.086	58.8	1347	6
14-3	603	2 MLC2	6			2.04	2.38	2.13		.002	.086			6
14-3	605	2 MLC3	2			1.97	2.35	2.14		.005	.086			6
14-3	607	2 MLC4	2		2.17	1.85	2.16	2.19	.0005	.002	.086			6
14-3	609	2 MLC5	2			2.20	2.62	2.23		.004	.086			6
14-3	611	2 MLC6				.963								6

Table F-3 (Continued)

MSN	CHNL	HOUSE	INSTR	TYPE	PEAK AMPLITUDES POSITIVE P1	P2	P3	NEGATIVE P1	P2	RISE TIME T1	TIME T2	PER-IOD	WAVE ANGLE	GND SPD	
15-1	601	2	MLC1	2			2.32	1.64	1.78		.0055	.296	40.4	1739	6
15-1	603	2	MLC2	2			2.23	1.62	1.83		.005	.296			6
15-1	605	2	MLC3	2			2.13	1.49	1.74		.006	.296			6
15-1	607	2	MLC4	2			2.10	1.49	1.86		.004	.295			6
15-1	609	2	MLC5	2			2.14	1.54	1.84		.0035	.295			6
15-1	611	2	MLC6	2			1.05								6
15-2	601	2	MLC1	2			2.29	1.81	2.01		.004	.163	45.7	1626	6
15-2	603	2	MLC2	2			2.32	1.91	2.03		.005	.163			6
15-2	605	2	MLC3	2			2.32	1.85	1.96		.004	.162			6
15-2	607	2	MLC4	2			2.38	1.83	2.10		.004	.163			6
15-2	609	2	MLC5	2			2.38	1.90	2.08		.0045	.162			6
15-2	611	2	MLC6	2			1.14								6
15-3	601	2	MLC1	2			2.29	2.49	2.01		.004	.073	45.9	1550	6
15-3	603	2	MLC2	5		2.23	2.29	2.44	2.09	.0005	.005	.073			6
15-3	605	2	MLC3	2			2.51	2.76	2.15		.004	.073			6
15-3	607	2	MLC4	6		2.32	2.07	2.20	2.07	.0005	.002	.074			6
15-3	609	2	MLC5	2			2.38	2.65	2.11		.004	.074			6
15-3	611	2	MLC6	2			1.20								6
16-1	601	2	MLC1	3			2.12	1.73	2.04		.007	.169	48.3	1550	6
16-1	603	2	MLC2	2			2.52	1.93	2.15		.005	.170			6
16-1	605	2	MLC3	2			2.16	1.65	1.92		.0045	.170			6
16-1	607	2	MLC4	2			2.17	1.72	2.32		.0045	.170			6
16-1	609	2	MLC5	2			2.29	1.83	2.04		.0045	.170			6
16-1	611	2	MLC6	2			1.10								6
16-2	601	2	MLC1	2			2.29	1.41	1.70		.005	.298	41.5	1739	6
16-2	603	2	MLC2	2			2.24	1.47	1.93		.0055	.299			6
16-2	605	2	MLC3	2			2.26	1.49	1.77		.0055	.298			6
16-2	607	2	MLC4	2			2.27	1.46	1.83		.005	.299			6
16-2	609	2	MLC5	2			2.41	1.56	1.92		.004	.299			6
16-2	611	2	MLC6	2			1.13								6
16-3	601	2	MLC1	2			1.95	2.06	1.81		.004	.076	54.4	1429	6
16-3	603	2	MLC2	2			2.09	2.06	1.87		.0005	.076			6
16-3	605	2	MLC3	2			1.98	2.07	1.83		.004	.076			6
16-3	607	2	MLC4	2			1.90	2.00	1.83		.004	.076			6
16-3	609	2	MLC5	2			2.16	2.20	1.89		.001	.076			6
16-3	611	2	MLC6	2			1.10								6

Table F-3 (Continued)

MSN	CHNL	HOUSE INSTR	TYPE	POSITIVE P1	POSITIVE P2	POSITIVE P3	NEGATIVE P1	NEGATIVE P2	RISE TIME T1	RISE TIME T2	PER-IOD	WAVE ANGLE	GND SPD	6
17-1	601	2	MLC1	3			1.04	0.87	1.04		.0065	.076	45.0	1667	6
17-1	603	2	MLC2	8	0.95	1.10		0.80	1.12	.0025	.006	.076			6
17-1	605	2	MLC3	3		1.08			1.01		.006	.076			6
17-1	607	2	MLC4	2		1.21			1.02		.004	.076			6
17-1	609	2	MLC5	5	1.00	1.09			1.00		.006	.075			6
17-1	611	2	MLC6	3		.60									6
17-2	601	2	MLC1	3		1.59			1.38		.009	.188	48.7	1527	6
17-2	603	2	MLC2	3		1.70					.0065				6
17-2	605	2	MLC3	3		1.59			1.46		.015	.188			6
17-2	607	2	MLC4	3		1.66			1.39		.008	.189			6
17-2	609	2	MLC5	8	1.23	1.64			1.46	.001	.0075	.189			6
17-2	611	2	MLC6	3		.91									6
18-1	601	2	MLC1	3		1.19			1.21		.015	.172	43.6	1535	6
18-1	603	2	MLC2	3		1.32					.0065	.173			6
18-1	605	2	MLC3	3		1.30			1.24		.014	.173			6
18-1	607	2	MLC4	3		1.25			1.25		.0085	.173			6
18-1	609	2	MLC5	3		1.30			1.30		.008	.172			6
18-1	611	2	MLC6	3		.70									6
18-2	601	2	MLC1	2		1.14		1.12	1.00		.001	.072	44.4	1702	6
18-2	603	2	MLC2	2		1.19		1.46	1.15		.005	.073			6
18-2	605	2	MLC3	2		1.19		1.37	1.06		.004	.072			6
18-2	607	2	MLC4	2	1.02	1.15			1.07	.005	.004	.073			6
18-2	609	2	MLC5	2	1.14	1.16		1.27	1.11	.0015	.0045	.072			6
18-2	611	2	MLC6	2		.68									6
19-1	601	2	MLC1	2		1.47			1.21		.0045	.074	49.3	1639	6
19-1	603	2	MLC2	2		1.44			1.29		.005	.074			6
19-1	605	2	MLC3	2		1.44		1.30	1.09		.0045	.075			6
19-1	607	2	MLC4	2		1.71		1.64	1.39		.005	.075			6
19-1	609	2	MLC5	2		1.42			1.23		.0045	.074			6
19-1	611	2	MLC6	3		.74									6
19-2	601	2	MLC1	3		2.03			1.72		.007	.155	52.6	1455	6
19-2	603	2	MLC2	3		2.19			1.76		.006	.154			6
19-2	605	2	MLC3	7	2.41	2.12	2.24	1.37	1.68	.001	.005	.154			6
19-2	607	2	MLC4	3		1.55		1.06	1.45		.005	.154			6
19-2	609	2	MLC5	2		2.18			1.79		.0035	.154			6
19-2	611	2	MLC6	2		1.02									6

Table F-3 (Continued)

MSN	CHNL	HOUSE	INSTR	TYPE	POSITIVE P1	POSITIVE P2	POSITIVE P3	NEGATIVE P1	NEGATIVE P2	RISE TIME T1	RISE TIME T2	PER-IOD	WAVE ANGLE	GND SPD	
20-1	601	2	MLC1	3			1.77	1.16	1.40		.005	.161	52.3	1470	6
20-1	603	2	MLC2	5		1.75	1.92	1.11	1.38	.0015	.0055	.161			6
20-1	605	2	MLC3	2			1.70	1.16	1.42		.005	.161			6
20-1	607	2	MLC4	3			1.98		1.77		.005	.161			6
20-1	609	2	MLC5	3			1.82	1.23	1.47		.004	.161			6
20-1	611	2	MLC6				.92								6
20-2	601	2	MLC1	3			1.24		1.28		.005	.074	47.0	1695	6
20-2	603	2	MLC2	3			1.24		1.44		.005	.073			6
20-2	605	2	MLC3	2			1.27		1.27		.005	.073			6
20-2	607	2	MLC4	2			1.45		1.52		.0045	.074			6
20-2	609	2	MLC5	1			1.32		1.40		.005	.074			6
20-2	611	2	MLC6				.68								6
21-1	601	2	MLC1	3			1.08	0.43	0.90		.013	.189	51.2	1471	6
21-1	603	2	MLC2	8		0.84	1.00	0.40	0.84	.003	.032	.189			6
21-1	605	2	MLC3	8		0.62	0.875	0.54	0.76	.002	.0055	.189			6
21-1	607	2	MLC4	3			0.929	0.51	0.91		.0075	.189			6
21-1	609	2	MLC5	8		0.76	0.907	0.47	0.74	.0025	.014				6
21-1	611	2	MLC6				0.53								6
22-1	601	2	MLC1	5		1.01	1.66	1.25	1.10	.0015	.006	.173	47.6	1587	6
22-1	603	2	MLC2	3			1.48	1.27	1.12		.011	.173			6
22-1	605	2	MLC3	2			1.53	1.16	1.04		.0075	.173			6
22-1	607	2	MLC4	2			1.73	1.47	1.15		.002	.174			6
22-1	609	2	MLC5	5		1.35	1.56	1.21	1.15	.0025	.0075	.174			6
22-1	611	2	MLC6				0.82								6
23-1	601	2	MLC1	3			1.44	1.07	1.45		.0065	.190	49.8	1538	6
23-1	603	2	MLC2	2			1.77	1.38	1.57		.0025	.190			6
23-1	605	2	MLC3	3			1.55		1.46		.020	.190			6
23-1	607	2	MLC4	3			1.62	1.02	1.51		.015	.190			6
23-1	609	2	MLC5	3			2.50	1.07	1.44		.017	.190			6
23-1	611	2	MLC6				0.69								6
24-1	601	2	MLC1	2			1.22	0.76	0.92		.004	.177	45.0	1667	6
24-1	603	2	MLC2	2			1.53	1.03	1.09		.010	.177			6
24-1	605	2	MLC3	2			1.26	0.74	0.94		.0055	.176			6
24-1	607	2	MLC4	2			1.39	0.94	1.15		.005	.176			6
24-1	609	2	MLC5	2			1.33	0.89	1.00		.0075	.176			6
24-1	611	2	MLC6				0.69								6

Table F-3 (Continued)

MSN	CHNL	HOUSE	INSTR	TYPE	POSITIVE P1	POSITIVE P2	POSITIVE P3	NEGATIVE P1	NEGATIVE P2	RISE TIME T1	RISE TIME T2	PER-IOD	WAVE ANGLE	GND SPD	6
25-1	601	2	MLC1	3			1.74	1.07	1.25		.012	.186	45.0	1600	6
25-1	603	2	MLC2	7	2.00	1.77	1.91	1.38	1.55	.0005	.0135	.185			6
25-1	605	2	MLC3	3			1.62	1.14	1.41		.014	.186			6
25-1	607	2	MLC4	7	2.16	1.63	2.05	1.60	1.44	.0006	.0135	.186			6
25-1	609	2	MLC5	4			2.21		1.36		.001	.185			6
25-1	611	2	MLC6				0.93								6
26-1	601	2	MLC1	2	2.08	1.83	2.08		1.54	.0005	.005	.196	53.7	1471	6
26-1	603	2	MLC2	2			2.15	1.41	1.58		.0025	.196			6
26-1	605	2	MLC3	2		1.87	2.27	1.18	1.53	.0015	.004	.196			6
26-1	607	2	MLC4	2			2.31	1.60	1.75		.0015	.196			6
26-1	609	2	MLC5	2			2.28		1.70		.0045	.196			6
26-1	611	2	MLC6	2			1.27								6
27-2	601	2	MLC1	2			1.39	1.07	1.30		.003	.174	48.6	1600	6
27-2	603	2	MLC2	2			2.19	1.38	1.62		.005	.174			6
27-2	605	2	MLC3	2			1.58	0.94	1.31		.003	.174			6
27-2	607	2	MLC4	2			2.05	1.28	1.76		.008	.175			6
27-2	609	2	MLC5	5		1.80	2.03	0.91	1.47	.0025	.006	.175			6
27-2	611	2	MLC6				1.00								6
28-2	601	2	MLC1	3			1.25	0.70	1.15		.004	.175	45.9	1613	6
28-2	603	2	MLC2	8		1.34	1.45	0.81	1.40	.002	.0075	.175			6
28-2	605	2	MLC3	8		1.16	1.25	0.74	1.21	.002	.015	.175			6
28-2	607	2	MLC4	5		1.65	1.67		1.38	.0005	.004	.174			6
28-2	609	2	MLC5	8			1.33	0.76	1.18		.002	.174			6
28-2	611	2	MLC6				0.84								6
29-2	601	2	MLC1	2			1.65	1.36	1.22		.0055	.195	46.4	1587	6
29-2	603	2	MLC2	5		1.60	1.67	1.41	1.48	.0045	.015	.195			6
29-2	605	2	MLC3	2			1.50	1.35	1.25		.005	.195			6
29-2	607	2	MLC4	3			1.57	1.59	1.28		.008	.195			6
29-2	609	2	MLC5	2			1.56	1.37	1.7		.005	.195			6
29-2	611	2	MLC6				0.84								6
30-2	601	2	MLC1	4			2.03	1.83	1.51		.0035	.186	46.9	1660	6
30-2	603	2	MLC2	5		2.17	3.16	2.34	1.51	.0005	.002	.186			6
30-2	605	2	MLC3	4			1.70	1.21	1.38		.005	.186			6
30-2	607	2	MLC4	4			2.96	2.51	1.45		.0015	.187			6
30-2	609	2	MLC5	2			1.77	1.56	1.44		.012	.187			6
30-2	611	2	MLC6				0.92								6

Table F-3 (Continued)

MSN	CHNL	HOUSE INSTR	TYPE	PEAK AMPLITUDES POSITIVE P1	P2	P3	NEGATIVE P1	P2	RISE TIME T1	T2	PERIOD	WAVE ANGLE	GND SPD	
31-2	601	2 MLC1	2			1.73	0.92	1.47		.0025	.187	48.6		6
31-2	603	2 MLC2	3			1.86	1.07	1.72		.025	.187			6
31-2	605	2 MLC3	3			1.58	1.01	1.52		.022	.187			6
31-2	607	2 MLC4	3			1.73		1.51		.010	.187			6
31-2	609	2 MLC5	5		1.74	1.78	0.94	1.51	.001	.022	.187			6
31-2	611	2 MLC6				1.37								6
32-2	601	2 MLC1	5		1.76	1.73	1.13	1.34	.001	.013	.179	49.0		6
32-2	603	2 MLC2	5		1.34	1.74	0.91	1.58	.001	.0075	.179			6
32-2	605	2 MLC3	2			1.77		1.36		.011	.178			6
32-2	607	2 MLC4	2			2.00		1.55		.0025	.180			6
32-2	609	2 MLC5	5		1.36	1.78	1.24	1.44	.0015	.005	.179			6
32-2	611	2 MLC6				0.92								6
33-1	601	2 MLC1	3			2.61	1.39	2.06		.0125	.168	50.0	1460	6
33-1	603	2 MLC2	3			2.26	1.48	2.17		.0175	.169			6
33-1	605	2 MLC3	2			2.48	1.93	2.01		.007	.169			6
33-1	607	2 MLC4	2			2.80	2.41	2.29		.0075	.168			6
33-1	609	2 MLC5	3			2.29	1.54	2.11		.0155	.168			6
33-1	611	2 MLC6				1.26								6
34-1	601	2 MLC1	3			2.97	2.31	1.98		.011	.155	50.4	1504	6
34-1	603	2 MLC2	5		3.23	3.38	2.26	2.05	.001	.0055	.155			6
34-1	605	2 MLC3	2			4.20	2.96	2.04		.0035	.154			6
34-1	607	2 MLC4	2			3.44	2.50	2.35		.008	.154			6
34-1	609	2 MLC5	2			3.62	2.41	2.05		.004	.154			6
34-1	611	2 MLC6				1.79								6
35-1	601	2 MLC1	3			2.68	1.29	1.98		.0165	.163	50.0	1527	6
35-1	603	2 MLC2	5		1.87	2.55	1.39	1.99	.0005	.005	.162			6
35-1	605	2 MLC3	6		2.99	2.41	1.20	1.75		.001	.162			6
35-1	607	2 MLC4	2			2.77	1.40	2.13		.005	.163			6
35-1	609	2 MLC5	2			2.53	1.15	1.96		.003	.163			6
35-1	611	2 MLC6				1.36								6
36-1	601	2 MLC1	99	NO DATA FAILURE OF RECORDER										6
36-1	603	2 MLC2	99	NO DATA FAILURE OF RECORDER										6
36-1	605	2 MLC3	99	NO DATA FAILURE OF RECORDER										6
36-1	607	2 MLC4	99	NO DATA FAILURE OF RECORDER										6
36-1	609	2 MLC5	99	NO DATA FAILURE OF RECORDER										6
36-1	611	2 MLC6	99	NO DATA FAILURE OF RECORDER										6

Table F-3 (Continued)

MSN	CHNL	HOUSE INSTR	TYPE	PEAK AMPLITUDES POSITIVE P1	P2	P3	NEGATIVE P1	P2	RISE TIME T1	T2	PER- IOD	WAVE ANGLE	GND SPD	6
37-1	601	2 MLC1	6		3.78	2.83	2.20	1.98	.001	.0005	.162	50.4	1504	6
37-1	603	2 MLC2	5		2.20	2.65	1.51	1.99		.005	.163			6
37-1	605	2 MLC3	3			2.26	1.64	1.75		.007	.163			6
37-1	607	2 MLC4	2			2.44	1.65	2.01		.004	.162			6
37-1	609	2 MLC5	3			2.32	1.66	1.87		.004	.162			6
37-1	611	2 MLC6				1.23								6
38-1	601	2 MLC1				3.45	2.94	2.28		.004	.159	54.3	1439	6
38-1	603	2 MLC2				3.98	3.53	2.29		.003	.159			6
38-1	605	2 MLC3			2.85	3.98	2.92	2.23	.001	.004	.158			6
38-1	607	2 MLC4				3.41	3.02	2.38		.008	.158			6
38-1	609	2 MLC5				3.71	3.32	2.32		.003	.159			6
38-1	611	2 MLC6				2.39								6
39-1	601	2 MLC1				2.90	2.24	1.87	.0025	.005	.158	52.3	1470	6
39-1	603	2 MLC2			2.90	3.08	2.41	2.05	.001	.0055	.158			6
39-1	605	2 MLC3				2.66	1.86	1.75		.008	.158			6
39-1	607	2 MLC4				3.08	2.44	2.10		.007	.158			6
39-1	609	2 MLC5				3.02	2.44	2.08		.004	.158			6
39-1	611	2 MLC6				1.46								6
40-1	601	2 MLC1				3.75	2.61	2.28		.002	.160	49.0	1538	6
40-1	603	2 MLC2				2.99		2.20		.0025	.160			6
40-1	605	2 MLC3				3.10	2.23	1.86		.005	.160			6
40-1	607	2 MLC4			4.39	3.84	2.77	2.47	.0005	.001	.160			6
40-1	609	2 MLC5				3.74	2.53	2.26		.001	.160			6
40-1	611	2 MLC6				1.69								6
41-1	601	2 MLC1	2			2.74	1.68	1.59		.0015	.157	51.1	1538	6
41-1	603	2 MLC2	2			2.42		1.90		.005	.157			6
41-1	605	2 MLC3	2			2.30		1.77		.004	.157			6
41-1	607	2 MLC4	2			2.45	1.81	2.00		.0055	.158			6
41-1	609	2 MLC5	2			2.67	1.92	1.96		.001	.158			6
41-1	611	2 MLC6				1.44								6
42-1	601	2 MLC1	2			2.60	1.35	1.96		.007	.168	50.2	1515	6
42-1	603	2 MLC2	2			2.33	1.75	2.02		.006	.168			6
42-1	605	2 MLC3	6		3.32	2.56	1.93	1.69	.001	.0025	.168			6
42-1	607	2 MLC4	2			2.24	1.57	2.03		.0055	.168			6
42-1	609	2 MLC5	2			2.32	1.57	1.91		.013	.168			6
42-1	611	2 MLC6	3			1.18								6

Table F-3 (Continued)

MSN	CHNL	HOUSE INSTR	TYPE	POS P1	POS P2	POS P3	NEG P1	NEG P2	RISE T1	RISE T2	PERIOD	WAVE ANGLE	GND SPD	
43-2	601	2 MLC1	5		3.04	3.28	2.03	1.93	.001	.0055	.155	49.1	1504	6
43-2	603	2 MLC2	4			3.59	1.56	1.87		.0005	.156			6
43-2	605	2 MLC3	2			2.33	1.06	1.59		.0055	.155			6
43-2	607	2 MLC4	2			2.74	1.78	1.96		.007	.156			6
43-2	609	2 MLC5	2			2.92		1.87		.0055	.156			6
43-2	611	2 MLC6				1.42								6
44-2	601	2 MLC1	2			2.74	1.82	2.13		.006	.167	49.9	1527	6
44-2	603	2 MLC2	3			2.40	1.60	2.02		.0135	.166			6
44-2	605	2 MLC3	2			2.36	1.63	1.73		.005	.167			6
44-2	607	2 MLC4	2			2.71	1.75	2.10		.002	.167			6
44-2	609	2 MLC5	A5	2.73	2.02	2.62	1.87	2.06		.0005	.167			6
44-2	611	2 MLC6				1.28								6
45-1	601	2 MLC1	2			2.64	1.76	2.03		.012	.165	50.4	1504	6
45-1	603	2 MLC2	4			2.86	1.53	1.98		.001	.166			6
45-1	605	2 MLC3	2			2.19	1.53	1.66		.005	.165			6
45-1	607	2 MLC4	5		2.17	2.46	1.21	2.14	.0035	.0135	.165			6
45-1	609	2 MLC5	2			2.54	1.80	2.02		.004	.165			6
45-1	611	2 MLC6				1.28								6
46-1	601	2 MLC1	3			2.50	1.55	1.79		.012	.166	58.7	1351	6
46-1	603	2 MLC2	2			2.44	1.53	1.75		.0075	.166			6
46-1	605	2 MLC3	4			3.39	2.16	1.73		.0015	.166			6
46-1	607	2 MLC4	2			3.06	2.10	1.99		.004	.167			6
46-1	609	2 MLC5	5		2.58	2.66	1.50	1.87	.001	.0045	.167			6
46-1	611	2 MLC6				1.62								6
47-2	601	2 MLC1	2			2.64	1.62	1.76		.006	.158	48.7	1527	6
47-2	603	2 MLC2	2			2.48	1.60	1.79		.006	.153			6
47-2	605	2 MLC3	3			1.93	1.20	1.53		.006	.157			6
47-2	607	2 MLC4	3			2.28	1.42	1.85		.008	.158			6
47-2	609	2 MLC5	2			2.25	1.53	1.80		.005	.158			6
47-2	611	2 MLC6				1.28								6
48-2	601	2 MLC1	3			2.33	1.39	2.06		.007	.165	52.3	1471	6
48-2	603	2 MLC2	2			2.71	1.98	2.06		.004	.166			6
48-2	605	2 MLC3	3			2.86	1.86	1.79		.004	.166			6
48-2	607	2 MLC4	2			2.78	1.99	2.21		.004	.166			6
48-2	609	2 MLC5	2			2.73	2.39	2.10		.0045	.166			6
48-2	611	2 MLC6				1.59								6

Table F-3 (Continued)

MSN	CHNL	HOUSE INSTR	TYPE	POSITIVE P1	POSITIVE P2	POSITIVE P3	NEGATIVE P1	NEGATIVE P2	RISE TIME T1	RISE TIME T2	PER-IOD	WAVE ANGLE	GND SPD
49-2	601	2 MLC1	5		2.70	2.70	3.02	2.86	.001	.004	.100	76.6	1190 6
49-2	603	2 MLC2	3			2.74	3.08	2.68		.005	.099		6
49-2	605	2 MLC3	5		2.47	2.53	2.91	2.72	.0015	.005	.100		6
49-2	607	2 MLC4	2			2.46		2.80		.0065	.100		6
49-2	609	2 MLC5	2			2.70	3.08	2.77		.0055	.100		6
49-2	611	2 MLC6				1.36							6
50-2	601	2 MLC1	2			3.08	3.47	2.76		.002	.085	68.4	1290 6
50-2	603	2 MLC2	5			3.14	3.29	2.80		.0025	.086		6
50-2	605	2 MLC3	5		2.35	3.07	3.22	2.72	.0005	.0045	.085		6
50-2	607	2 MLC4	5		3.52	3.80	4.11	3.02	.0005	.004	.086		6
50-2	609	2 MLC5	5		2.80	2.92	3.14	2.83	.001	.005	.086		6
50-2	611	2 MLC6	2			1.46							6
51-2	601	2 MLC1	2			3.48	4.26	3.09		.006	.078	55.5	1375 6
51-2	603	2 MLC2	5		3.38	3.55	4.68	3.31	.0025	.006	.077		6
51-2	605	2 MLC3	4			4.10	4.90	3.12		.0025	.077		6
51-2	607	2 MLC4	2			3.36	3.71	3.13		.005	.078		6
51-2	609	2 MLC5	4			4.07	4.78	3.25		.004	.078		6
51-2	611	2 MLC6				1.91							6
52-1	601	2 MLC1	5		3.14	3.51	4.62	3.14	.007	.014	.084	68.3	1290 6
52-1	603	2 MLC2	5		3.91	4.83	5.20	3.50	.0025	.0115	.084		6
52-1	605	2 MLC3	3			2.67		2.84	.0025	.0055	.084		6
52-1	607	2 MLC4	2			2.69	2.65	2.96		.0045	.084		6
52-1	609	2 MLC5	5		2.86	3.20	3.45	3.23	.004	.018	.084		6
52-1	611	2 MLC6				2.87							6
53-1	601	2 MLC1	4			5.43	6.50	3.25		.0075	.085	70.3	1303 6
53-1	603	2 MLC2	2			3.15	3.75	3.46		.0105	.085		6
53-1	605	2 MLC3	2			3.18	3.55	2.70		.013	.085		6
53-1	607	2 MLC4	2			3.39	4.17	3.19		.006	.085		6
53-1	609	2 MLC5	4			3.73	4.06	2.93		.0105	.085		6
53-1	611	2 MLC6				4.27							6
54-1	601	2 MLC1	2			4.07	4.72	3.81		.003	.079	53.7	1399 6
54-1	603	2 MLC2	2			4.17	4.52	4.10		.003	.079		6
54-1	605	2 MLC3	2			3.55	4.00	3.34		.007	.079		6
54-1	607	2 MLC4	2			3.88	4.48	3.72		.0025	.079		6
54-1	609	2 MLC5	2			3.75	4.32	3.78		.004	.079		6
54-1	611	2 MLC6				1.71							6

Table F-3 (Continued)

MSN	CHNL	HOUSE INSTR	TYPE	PEAK AMPLITUDES POSITIVE			NEGATIVE		RISE TIME		PER-IOD	WAVE ANGLE	GND SPD
				P1	P2	P3	P1	P2	T1	T2			
55-1	601	MLC1	2			2.82	3.30	2.96		.006	.076	52.3	1404	6
55-1	603	MLC2	5		2.62	2.81	3.51	2.92	.002	.0065	.077			6
55-1	605	MLC3	A6		4.10	2.92	3.56	2.78	.0005	.006	.077			6
55-1	607	MLC4	2			2.99	3.30	2.80		.0015	.077			6
55-1	609	MLC5	2			2.84	3.44	2.88		.0035	.077			6
55-1	611	MLC6				1.40								
56-1	601	MLC1	2			2.60	3.05	2.57		.0055	.081	59.2	1325	6
56-1	603	MLC2	2			2.92	3.09	2.51		.001	.081			6
56-1	605	MLC3	2			2.50	2.94	2.46		.0025	.081			6
56-1	607	MLC4	2			2.70	3.03	2.74		.004	.081			6
56-1	609	MLC5	2			2.58	2.99	2.68		.003	.081			6
56-1	611	MLC6				1.42								
57-1	601	MLC1	2			2.73	2.96	2.47		.002	.080	58.9	1342	6
57-1	603	MLC2	2			2.68	3.16	2.72		.0015	.080			6
57-1	605	MLC3	2			2.42	2.86	2.50		.002	.079			5
57-1	607	MLC4	2			2.49	2.74	2.63		.004	.079			6
57-1	609	MLC5	2			2.89	3.33	2.68		.001	.079			5
57-1	611	MLC6				1.46								
58-2	601	MLC1	2	2.61		2.15	2.22	2.04		.004	.076	60.6	1408	6
58-2	603	MLC2	A5		2.07	2.30	2.38	2.11	.0005	.005	.075			5
58-2	605	MLC3	2			2.29	2.36	2.14		.005	.076			6
58-2	607	MLC4	2			2.45	2.61	2.18		.005	.076			6
58-2	609	MLC5	2			2.43	2.50	2.16		.004	.076			6
58-2	611	MLC6				1.17								
59-2	601	MLC1	A5	2.87	2.47	2.58	2.87	2.33	.0005	.005	.075	59.3	1399	6
59-2	603	MLC2	2			2.46	2.84	2.50		.002	.075			6
59-2	605	MLC3	2			2.62	2.96	2.40		.0045	.075			6
59-2	607	MLC4	2			2.76	2.99	2.41		.0045	.075			6
59-2	609	MLC5	2			2.65	2.88	2.39		.0035	.075			6
59-2	611	MLC6				1.25								
60-2	601	MLC1	2			2.58		2.61		.005	.082	56.1	1347	6
60-2	603	MLC2	2			2.59	2.96	2.62		.005	.082			6
60-2	605	MLC3	A6		4.06	2.60	2.85	2.46	.0005	.005	.082			6
60-2	607	MLC4	2			2.54	2.69	2.69		.005	.082			6
60-2	609	MLC5	2			2.54		2.62		.0035	.082			6
60-2	611	MLC6				1.36								

Table F-3 (Continued)

MSN	'CHML HOUSE INSTR	TYPE	POSITIVE P1	POSITIVE P2	POSITIVE P3	NEGATIVE P1	NEGATIVE P2	RISE TIME T1	RISE TIME T2	PER-IOD	WAVE ANGLE	GND SPD	6
61-1	601 2 MLC1	3			1.16		1.36		.005	.078	46.4	1587	6
61-1	603 2 MLC2	3			1.18		1.32		.0055	.077			6
61-1	605 2 MLC3	2			1.26	1.38	1.28		.004	.078			6
61-1	607 2 MLC4	2			1.26		1.41		.004	.078			6
61-1	609 2 MLC5	2			1.21		1.39		.005	.078			6
61-1	611 2 MLC6				0.59								6
62-1	601 2 MLC1	2			1.81		1.76		.005	.079	41.7	1660	6
62-1	603 2 MLC2	2			1.83		1.79		.005	.079			6
62-1	605 2 MLC3	2			1.79		1.73		.005	.079			6
62-1	607 2 MLC4	2			1.73	1.69	1.79		.005	.079			6
62-1	609 2 MLC5	2			1.85		1.83		.004	.079			6
62-1	611 2 MLC6				.89								6
63-1	601 2 MLC1	2			1.79	1.67	1.70		.005	.080	44.8	1613	6
63-1	603 2 MLC2	2			1.85	1.77	1.83		.005	.080			6
63-1	605 2 MLC3	2			1.69	1.59	1.65		.005	.079			6
63-1	607 2 MLC4	2			1.75	1.63	1.79		.005	.080			6
63-1	609 2 MLC5	2			1.81	1.73	1.85		.005	.080			6
63-1	611 2 MLC6				.87								6
64-2	601 2 MLC1	2			1.55	1.91	1.72		.007	.077	47.7	1515	6
64-2	603 2 MLC2	2			1.55	1.91	1.78		.0025	.078			6
64-2	605 2 MLC3	2			1.50	1.76	1.57		.0055	.078			6
64-2	607 2 MLC4	3			1.51	1.81	1.63	.008	.008	.077			6
64-2	609 2 MLC5	3			1.49		1.62	.007	.007	.078			6
64-2	611 2 MLC6	3			.746								6
65-2	601 2 MLC1	3			1.09	.62	.83		.016	.084	73.6	1471	6
65-2	603 2 MLC2	3			.96	.48	.94		.010	.084			6
65-2	605 2 MLC3	3			1.21	.52	.99		.?18	.083			6
65-2	607 2 MLC4	3			1.19	.66	1.04		.0165	.085			6
65-2	609 2 MLC5	3			1.01	.31	.80		.013	.085			6
65-2	611 2 MLC6	3		1.13									6
66-2	601 2 MLC1	3			1.17	.91	.76		.023	.078	71.4	1498	6
66-2	603 2 MLC2	3			1.00	.92	.76		.0185	.078			6
66-2	605 2 MLC3	3			.88	.73	.69		.015	.078			6
66-2	607 2 MLC4	3			1.00	.83	.70		.022	.079			6
66-2	609 2 MLC5	2			1.07	.70	.66		.0205	.078			6
66-2	611 2 MLC6	2			.375								6

Table F-3 (Continued)

MSN	CHNL	HOUSE INSTR	TYPE	PEAK AMPLITUDES POSITIVE			NEGATIVE		RISE TIME T1	TIME T2	PER-IOD	WAVE ANGLE	GND SPD	
				P1	P2	P3	P1	P2						
67-1	601	2 MLC1	5		1.47	1.75	1.67	1.51	.005	.0095	.082	43.3	1633	6
67-1	603	2 MLC2	2			1.93	1.75	1.54		.0055	.083			6
67-1	605	2 MLC3	2			1.38	1.29	1.43		.0080	.083			6
67-1	607	2 MLC4	4			2.08	1.89	1.72		.005	.083			6
67-1	609	2 MLC5	2			1.68	1.47	1.53		.006	.083			6
67-1	611	2 MLC6				.71								6
68-1	601	2 MLC1	A6		1.71	1.63		1.56	.001	.005	.082	45.8	1619	6
68-1	603	2 MLC2	2			1.56		1.49		.005	.081			6
68-1	605	2 MLC3	5		1.39	1.62	1.48	1.71	.002	.0065	.082			6
68-1	607	2 MLC4	5		1.53	1.75	1.70	1.58	.0015	.005	.081			6
68-1	609	2 MLC5	2			1.28	1.65	1.53		.005	.081			6
68-1	611	2 MLC6				.765								6
69-1	601	2 MLC1	2			1.16	1.36	1.26		.005	.078	42.8	1660	6
69-1	603	2 MLC2	2			1.19	1.39	1.30		.0055	.078			6
6?-1	605	2 MLC3	2			1.18	1.44	1.25		.0055	.078			6
69-1	607	2 MLC4	2			1.25	1.48	1.36		.0045	.078			6
69-1	609	2 MLC5	2			1.20	1.39	1.31		.004	.077			6
69-1	611	2 MLC6				.56								6
70-2	601	2 MLC1	2			1.36		1.47		.005	.074	42.2	1695	6
70-2	603	2 MLC2	2			1.28		1.40		.0055	.074			6
70-2	605	2 MLC3	2			1.40	1.68	1.45		.005	.075			6
70-2	607	2 MLC4	2			1.40	1.52	1.42		.005	.074			6
70-2	609	2 MLC5	2			1.36	1.48	1.43		.005	.074			6
70-2	611	2 MLC6				.598								6
71-2	601	2 MLC1	2			1.42	1.31	1.56		.005	.083	44.8	1613	6
71-2	603	2 MLC2	2			1.43		1.57		.0055	.083			6
71-2	605	2 MLC3	2			1.40		1.52		.006	.083			6
71-2	607	2 MLC4	2			1.40	1.47	1.54		.006	.083			6
71-2	609	2 MLC5	2			1.41	1.27	1.32		.006	.082			6
71-2	611	2 MLC6				.670								6
72-2	601	2 MLC1	3			1.18	1.40	1.22		.014	.092	55.2	1389	6
72-2	603	2 MLC2	3			1.14	1.40	1.26		.014	.091			6
72-2	605	2 MLC3	3			1.14	1.40	1.28		.014	.091			6
72-2	607	2 MLC4	3			1.18	1.42	1.32		.013	.090			6
72-2	609	2 MLC5	3			1.17	1.31	1.24		.013	.091			6
72-2	611	2 MLC6				.550								6

Table F-3 (Continued)

MSN	CHNL	HOUSE	INSTR	TYPE	POSITIVE P1	POSITIVE P2	POSITIVE P3	NEGATIVE P1	NEGATIVE P2	RISE TIME T1	RISE TIME T2	PER- IOD	WAVE ANGLE	GND SPD	6
73-1	601	2	MLC1	3			.762	.58	.67		.007	.103	55.2	1389	6
73-1	603	2	MLC2	3			.761	.64	.72		.007	.103			6
73-1	605	2	MLC3	3			.756	.60	.68		.0065	.104			6
73-1	607	2	MLC4	3			.776	.64	.78		.008	.104			6
73-1	609	2	MLC5	3			.761	.62	.73		.0065	.103			6
73-1	611	2	MLC6				.374								6
74-1	601	2	MLC1	2			0.91	0.91	0.85		.002	.115	62.2	1316	6
74-1	603	2	MLC2	2			0.98	0.88	0.80		.007	.115			6
74-1	605	2	MLC3	2			1.06	0.97	0.86		.005	.113			6
74-1	607	2	MLC4	2			1.02	0.93	0.91		.0035	.115			6
74-1	609	2	MLC5	2			0.97	0.94	0.84		.004	.114			6
74-1	611	2	MLC6	2			0.48								6
75-1	601	2	MLC1	3			.817	.63	.78		.007	.103	55.6	1370	6
75-1	603	2	MLC2	3			.866	.70	.83		.007	.103			6
75-1	605	2	MLC3	2			.828	.67	.83		.006	.103			6
75-1	607	2	MLC4		NO DATA										
75-1	609	2	MLC5	2			.877	.71	.90		.0045	.103			6
75-1	611	2	MLC6				.406								6
76-2	601	2	MLC1	3			.845	.54	.78		.015	.106	62.4	1307	6
76-2	603	2	MLC2	3			.801		.80		.015	.105			6
76-2	605	2	MLC3	8		.542	.754	.57	.71	.002	.008	.105			6
76-2	607	2	MLC4	3			.839		.84		.0135	.105			6
76-2	609	2	MLC5	3			.821		.79		.013	.105			6
76-2	611	2	MLC6				.418								6
77-2	601	2	MLC1	2			1.10	.81	.91		.0045	.116	62.5	1299	6
77-2	603	2	MLC2	2			1.15	.88	.92		.008	.115			6
77-2	605	2	MLC3	2			1.05	.77	.85		.0065	.115			6
77-2	607	2	MLC4	2			1.04	.81	.98		.007	.115			6
77-2	609	2	MLC5	2			1.10	.79	.98		.004	.115			6
77-2	611	2	MLC6				.48								6
78-2	601	2	MLC1	5		1.96	2.19	2.06	1.25	.011	.0125	.110	63.2	1262	6
78-2	603	2	MLC2	4			2.40	2.02	1.28		.0105	.110			6
78-2	605	2	MLC3	4			2.20	2.31	1.36		.0065	.109			6
78-2	607	2	MLC4	4				3.06	1.53			.110			6
78-2	609	2	MLC5	4			2.71	2.71	1.41		.0105	.111			6
78-2	611	2	MLC6	4			1.32								6

F.43

Table F-3 (Continued)

MSN	CHNL	HOUSE INSTR	TYPE	PEAK AMPLITUDES POSITIVE P1	P2	P3	NEGATIVE P1'	P2	RISE TIME T1	TIME T2	PER-IOD	WAVE ANGLE	GND SPD	6
79-1	601	2 MLC1	8		.51	.52	.33	.46	.0075	.0175	.114	53.1	1307	6
79-1	603	2 MLC2	3			.54	.26	.48		.027	.115			6
79-1	605	2 MLC3	3			.54	.37	.50		.015	.114			6
79-1	607	2 MLC4	3			.60	.39	.54		.0105	.115			6
79-1	609	2 MLC5	3			.54	.32	.48		.023	.115			6
79-1	611	2 MLC6												6
80-1	601	2 MLC1	2			.870	.79	.70		.005	.108	54.7	1413	6
80-1	603	2 MLC2	2			.806	.70	.67		.006	.108			6
80-1	605	2 MLC3	2			.867	.72	.65		.0065	.108			6
80-1	607	2 MLC4	2			.863		.72		.0045	.108			6
80-1	609	2 MLC5	2			.864		.67		.0045	.108			6
80-1	611	2 MLC6	2			.407								6
81-1	601	2 MLC1	2			.815	.72	.62		.005	.103	51.1	1465	6
81-1	603	2 MLC2	A5	.865	.701	.760	.70	.57	.0005	.006	.103			6
81-1	605	2 MLC3	4			.878	.69	.56		.001	.103			6
81-1	607	2 MLC4	5		.803	.803	.66	.62	.0015	.0045	.103			6
81-1	609	2 MLC5	2			.876	.73	.62		.005	.103			6
81-1	611	2 MLC6				.419								6
82-2	601	2 MLC1	2			.92	.83	.71		.005	.104	53.5	1408	6
82-2	603	2 MLC2	2			.92	.75	.68		.0055	.103			6
82-2	605	2 MLC3	2			.87	.75	.67		.0055	.104			6
82-2	607	2 MLC4	2			.89	.74	.74		.006	.103			6
82-2	609	2 MLC5	2			.95	.77	.72		.004	.104			6
82-2	611	2 MLC6	2			.45								6
83-2	601	2 MLC1	2			.839	.63	.77		.0065	.106	53.1	1418	6
83-2	603	2 MLC2	2			.862	.68	.80		.006	.105			6
83-2	605	2 MLC3	2			.911	.72	.81		.006	.106			6
83-2	607	2 MLC4	2			.889	.67	.82		.005	.106			6
83-2	609	2 MLC5	2			.695	.50	.62		.005	.106			6
83-2	611	2 MLC6	2			.527								6
84-2	601	2 MLC1	2			.783	.60	.65		.0065	.102	54.5	1428	6
84-2	603	2 MLC2	2			.736	.56	.67		.006	.102			6
84-2	605	2 MLC3	5		.755	.822	.56	.70	.001	.0055	.103			6
84-2	607	2 MLC4	2			.755	.56	.70		.0045	.103			6
84-2	609	2 MLC5	2			.745	.54	.67		.005	.102			6
84-2	611	2 MLC6	2			.419								6

F. 44

Table F-3 (Continued)

MSN	CHNL	HOUSE	INSTR	TYPE	POSITIVE P1	POSITIVE P2	POSITIVE P3	NEGATIVE P1	NEGATIVE P2	RISE TIME T1	RISE TIME T2	PERIOD	WAVE ANGLE	GND SPD	
85-1	601	2	MLC1				2.24	1.39	1.80		.0025	.156			6
85-1	603	2	MLC2				2.29	1.48	1.84		.0015	.156			6
85-1	605	2	MLC3				2.04	1.24	1.68		.006	.155			6
85-1	607	2	MLC4				2.44	1.52	1.95		.0035	.156			6
85-1	609	2	MLC5		2.32	1.93	2.08	1.27	1.84	.0003	.013	.157	51.0	1563	6
85-1	611	2	MLC6				1.03								6
86-1	601	2	MLC1				2.94	2.02	1.84	.0005	.0055	.157	50.1	1521	6
86-1	603	2	MLC2			2.84	2.78	2.05	1.90		.006	.157			6
86-1	605	2	MLC3				2.30	1.42	1.61		.010	.157			6
86-1	607	2	MLC4				2.56	1.77	1.98		.003	.157			6
86-1	609	2	MLC5				2.59		1.81		.0075	.157			6
86-1	611	2	MLC6				1.30								6
87-1	601	2	MLC1	3			2.31	1.82	2.05	.001	.004	.169	50.3	1509	6
87-1	603	2	MLC2	8		2.05	2.12	1.49	2.12		.0055	.170			6
87-1	605	2	MLC3	3			2.23	1.73	2.00		.005	.170			0
87-1	607	2	MLC4	3			2.32	1.91	2.38		.007	.170			0
87-1	609	2	MLC5				2.07	1.62	2.15		.005	.170			0
87-1	611	2	MLC6				1.17								6
88-1	601	2	MLC1	2			2.41	1.49	1.92		.004	.160	51.0	1470	6
88-1	603	2	MLC2	3			2.19	1.41	1.90		.0075	.160			6
88-1	605	2	MLC3	2			2.53	1.57	1.96		.005	.160			6
88-1	607	2	MLC4	3			2.19		1.97		.02	.161			6
88-1	609	2	MLC5	2			2.26	1.36	1.88		.004	.161			6
88-1	611	2	MLC6				1.10								6
113-1	601	2	MLC1	A6		3.09	2.60	2.21	1.93	.0005	.0045	.164	50.6	1493	6
113-1	603	2	MLC2	2			2.64	1.25	1.97		.005	.164			6
113-1	605	2	MLC3	5		2.43	2.64	1.48	2.02	.001	.005	.163			6
113-1	607	2	MLC4	2			2.44	1.40	2.01		.0015	.164			6
113-1	609	2	MLC5	5		2.57	2.71	1.66	1.90	.0015	.004	.164			6
113-1	611	2	MLC6				1.49								6
113-2	601	2	MLC1	2			2.26	1.55	1.77		.005	.313	41.8	1717	6
113-2	603	2	MLC2	2			2.29	1.57	1.88		.0055	.313			6
113-2	605	2	MLC3	5		1.89	2.21	1.32	1.84	.001	.0055	.313			6
113-2	607	2	MLC4	2			2.13	1.48	1.94		.004	.313			6
113-2	609	2	MLC5	2			2.10	1.43	1.81		.004	.313			6
113-2	611	2	MLC6				1.07								6

Table F-3 (Continued)

MSN	CHNL	HOUSE INSTR	TYPE	POSITIVE P1	POSITIVE P2	POSITIVE P3	NEGATIVE P1	NEGATIVE P2	RISE TIME T1	RISE TIME T2	PER-IOD	WAVE ANGLE	GND SPD	6
113-3	601	2 MLC1	8		1.60	1.74	1.66	1.82	.001	.0065	.079	57.6	1408	6
113-3	603	2 MLC2	5		1.88	1.94	2.06	1.91	.001	.005	.078			6
113-3	605	2 MLC3	A6		2.21	2.10	2.43	2.00	.0005	.005	.078			6
113-3	607	2 MLC4	2			1.91	1.96	1.89		.002	.078			6
113-3	609	2 MLC5	2			2.04	2.13	1.84		.004	.078			6
113-3	611	2 MLC6				1.07								6
117-1	601	2 MLC1	6		5.72	3.02	3.94	2.16		.001	.077	46.2	1575	6
117-1	603	2 MLC2	7	2.97	2.06	2.73	3.13	2.23	.0015	.0035	.077			6
117-1	605	2 MLC3	5		1.23	2.25	2.50	1.79	.002	.009	.077			6
117-1	607	2 MLC4	4			2.55	2.89	1.90		.003	.077			6
117-1	609	2 MLC5	4			2.78	2.91	2.02		.0025	.078			6
117-1	611	2 MLC6				1.25								6
117-2	601	2 MLC1	2			1.97	1.35	1.47		.006	.194	53.9	1460	6
117-2	603	2 MLC2	A3			1.94		1.43		.018	.193			6
117-2	605	2 MLC3	3			1.65		1.31		.014	.193			6
117-2	607	2 MLC4	2			2.02		1.48		.007	.193			6
117-2	609	2 MLC5	A3			1.78	1.26	1.41		.0175	.193			6
117-2	611	2 MLC6				.92								6
118-1	601	2 MLC1	2			2.20	1.01	1.72		.007	.185	50.7	1550	6
118-1	603	2 MLC2	4			2.39	1.07	1.68		.005	.185			6
118-1	605	2 MLC3	4			2.29	1.02	1.60		.009	.185			6
118-1	607	2 MLC4	2			2.32	1.29	1.81		.007	.186			6
118-1	609	2 MLC5	4			2.60	1.69	1.15		.005	.186			6
118-1	611	2 MLC6				1.29								6
118-2	601	2 MLC1	6		2.15	1.78	1.55	1.89		.001	.074	44.5	1626	6
118-2	603	2 MLC2	2			1.97	1.90	2.10		.005	.075			6
118-2	605	2 MLC3	2			1.83		1.85		.007	.075			6
118-2	607	2 MLC4	3			1.64	1.10	1.79		.016	.075			6
118-2	609	2 MLC5	2			1.67	1.58	1.93		.0055	.074			6
118-2	611	2 MLC6				.81								6
119-1	601	2 MLC1	7	2.55	1.79	2.22	1.12	.87	.002	.0285	.078	44.8	1681	6
119-1	603	2 MLC2	2			2.28	1.01	.82		.006	.077			6
119-1	605	2 MLC3	6			2.04	.84	.81		.0025	.077			6
119-1	607	2 MLC4	5		2.24	2.21	1.17	.94	.003	.015	.077			6
119-1	609	2 MLC5	5		1.51	2.32	1.12	.84	.0025	.0135	.077			6
119-1	611	2 MLC6			1.77	.92								6

F-46

Table F-3 (Continued)

MSN	CHNL	HOUSE	INSTR	TYPE	POSITIVE P1	POSITIVE P2	POSITIVE P3	NEGATIVE P1	NEGATIVE P2	RISE T1	RISE T2	PERIOD	WAVE ANGLE	GND	SFC
121-1	601	2	MLC1	2			1.45	1.41	1.24		.005	.175	47.1		6
121-1	603	2	MLC2	4			1.81	1.33	1.52		.001	.175			6
121-1	605	2	MLC3	2			1.62	1.20	1.33		.005	.175			6
121-1	607	2	MLC4	4			1.97	1.63	1.60		.0065	.174			6
121-1	609	2	MLC5	4			1.75	1.42	1.47		.0075	.174			6
121-1	611	2	MLC6				0.93								6
122-1	601	2	MLC1	2			1.43	1.00	1.14		.008	.182	53.5	1481	6
122-1	603	2	MLC2	2			1.46	.84	1.16		.016	.183			6
122-1	605	2	MLC3	3			1.23		1.11		.016	.182			6
122-1	607	2	MLC4	3			1.31		1.28		.0185	.183			6
122-1	609	2	MLC5	3			1.36		1.05		.020	.183			6
122-1	611	2	MLC6												6
123-1	601	2	MLC1	4			1.90	1.24	1.38		.004	.214	55.6	1370	6
123-1	603	2	MLC2	2			1.38	1.02	1.30		.007	.215			6
123-1	605	2	MLC3	2			1.54		1.29		.004	.215			6
123-1	607	2	MLC4	2			1.66	1.26	1.45		.005	.215			6
123-1	609	2	MLC5	2			1.75	1.03	1.24		.002	.216			6
123-1	611	2	MLC6												6
124-1	601	2	MLC1	2			2.38	1.85	1.52		.006	.200	52.1	1413	6
124-1	603	2	MLC2	6		2.25	2.07	1.26	1.52	.001	.005	.199			6
124-1	605	2	MLC3	5		1.67	1.95		1.47	.001	.005	.199			6
124-1	607	2	MLC4	2			1.91	1.24	1.64		.006	.200			6
124-1	609	2	MLC5	2			2.06	1.34	1.48		.006	.199			6
124-1	611	2	MLC6												6
125-1	601	2	MLC1	8		1.16	1.85	.83	1.64	.001	.013	.204	57.8	1399	6
125-1	603	2	MLC2	3			2.05		2.05		.015	.204			6
125-1	605	2	MLC3	5		2.06	2.29	1.59	1.52	.003	.014	.205			6
125-1	607	2	MLC4	3			1.84	1.22	1.76		.015	.205			6
125-1	609	2	MLC5	2			1.94	1.43	1.55		.010	.205			6
125-1	611	2	MLC6												6
126-1	601	2	MLC1	3			1.79	.93	1.51		.018	.200	53.3	1418	6
126-1	603	2	MLC2	3			1.63	1.10	1.50		.010	.200			6
126-1	605	2	MLC3	8			1.59	.77	1.54		.015	.199			6
126-1	607	2	MLC4	3		1.37	1.67		1.62	.0025	.016	.200			6
126-1	609	2	MLC5	3			1.62		1.47		.019	.199			6
126-1	611	2	MLC6				.83								6

Table F-3 (Continued)

MSN	CHNL	HOUSE TYPE INSTR		PEAK AMPLITUDES POSITIVE			NEGATIVE		RISE TIME I1	T2	PER-IOD	WAVE ANGLE	GND SPD
				P1	P2	P3	P1	P2					
127-2	601	2 MLC1	3			1.54	1.06	1.54		.021	.198	55.5	1374	6
127-2	603	2 MLC2	3			1.44	1.02	1.50		.016	.198			6
127-2	605	2 MLC3	3			1.48	.88	1.45		.023	.198			6
127-2	607	2 MLC4	3			1.43	1.03	1.65		.008	.198			6
127-2	609	2 MLC5	3			1.44	.95	1.47		.023	.298			6
127-2	611	2 MLC6				.70								6
128-2	601	2 MLC1	2			2.42	1.89	2.13		.0065	.184	58.9	1338	6
128-2	603	2 MLC2	5		2.26	2.68	1.78	1.99	.002	.0085	.184			6
128-2	605	2 MLC3	2			2.60	1.92	1.98		.006	.184			6
128-2	607	2 MLC4	5		2.70	2.70	1.91	2.14	.002	.0055	.184			6
128-2	609	2 MLC5	2			2.68	2.01	2.11		.0065	.184			6
128-2	611	2 MLC6				1.91								6
129-2	601	2 MLC1	2			1.94	1.56	1.59		.008	.190	50.9	1476	6
129-2	603	2 MLC2	2			1.84	1.50	1.59		.0075	.190			6
129-2	605	2 MLC3	2			1.73	1.37	1.56		.006	.190			6
129-2	607	2 MLC4	3			1.65	1.58	1.69		.0145	.190			6
129-2	609	2 MLC5	2			1.80	1.39	1.62		.006	.190			6
129-2	611	2 MLC6				.90								6
130-2	601	2 MLC1	2			2.12	1.51	1.81		.006	.192	52.3	1470	6
130-2	603	2 MLC2	2			2.01	1.36	1.76		.0065	.192			6
130-2	605	2 MLC3	3			1.87	1.59	1.81		.0125	.192			6
130-2	607	2 MLC4	3			1.95	1.36	1.95		.008	.192			6
130-2	609	2 MLC5	3			1.88	1.44	1.88		.0105	.191			6
130-2	611	2 MLC6				.99								6
131-2	601	2 MLC1	2			3.25	2.19	2.85		.005	.195	54.5	1428	6
131-2	603	2 MLC2	A6		3.77	3.52	1.48	1.08		.0015	.195			6
131-2	605	2 MLC3	2			3.37	2.17	3.37		.0025	.194			6
131-2	607	2 MLC4	2			2.68	2.30	2.24		.007	.195			6
131-2	609	2 MLC5	2			3.14	2.70	2.24		.008	.195			6
131-2	611	2 MLC6				1.67								6
132-2	601	2 MLC1	2			1.49	.93	1.49		.015	.191	54.1	1449	6
132-2	603	2 MLC2	2			1.78		1.57		.014	.192			6
132-2	605	2 MLC3	2			1.65	1.10	1.45		.006	.191			6
132-2	607	2 MLC4	3			1.49	.86	1.54		.0155	.191			6
132-2	609	2 MLC5	3			1.59	.77	1.23		.017	.191			6
132-2	611	2 MLC6				.77								6

F.48

Table F-3 (Continued)

MSN	CHNL	HOUSE	TYPE INSTR		PEAK AMPLITUDES POSITIVE			NEGATIVE		RISE TIME		PER-IOD	WAVE ANGLE	GND SPD	
					P1	P2	P3	P1	P2	T1	T2				
172-2	601	2	MLC1	6		1.95	1.43	1.65	1.41	.0005	.0015	.077	45.8	1619	6
172-2	603	2	MLC2	5		1.28	1.33	1.49	1.33	.002	.005	.077			6
172-2	605	2	MLC3	5		1.35	1.42	1.57	1.46	.002	.006	.077			6
172-2	607	2	MLC4	5		1.43	1.55	1.77	1.43	.001	.0045	.078			6
172-2	609	2	MLC5	A6		1.70	1.49	1.65	1.39	.0005	.005	.078			6
172-2	611	2	MLC6				.956								6
221-1	601	2	MLC1	10			2.07								6
221-1	603	2	MLC2	10			1.46								6
221-1	605	2	MLC3	10			1.47								6
221-1	607	2	MLC4	10			1.80								6
221-1	609	2	MLC5	10			1.58								6
221-1	611	2	MLC6												6
SR-6	601	2	MLC1												6
SR-6	603	2	MLC2												6
SR-6	605	2	MLC3												6
SR-6	607	2	MLC4												6
SR-6	609	2	MLC5												6
SR-6	611	2	MLC6												6
SR-7	601	2	MLC1												6
SR-7	603	2	MLC2												6
SR-7	605	2	MLC3												6
SR-7	607	2	MLC4												6
SR-7	609	2	MLC5												6
SR-7	611	2	MLC6												6
SR-8	601	2	MLC1												6
SR-8	603	2	MLC2												6
SR-8	605	2	MLC3												6
SR-8	607	2	ML 4												6
SR-8	609	2	MLC5												6
SR-8	611	2	MLC6				1.79					.162			6
SR-9	601	2	MLC1				1.82					.162			6
SR-9	603	2	MLC2				1.80					.162			6
SR-9	605	2	MLC3				1.66					.163			6
SR-9	607	2	MLC4				1.80					.163			6
SR-9	609	2	MLC5				1.42								6
SR-9	611	2	MLC6												6

F.49

Table F-3 (Continued)

MSN	CHNL	HOUSE TYPE INSTR	PEAK AMPLITUDES POSITIVE P2 P1		NEGATIVE P1 P2		RISE TIME T1 T2		PER-IOD	WAVE ANGLE	GND SPD
SR-10	601	2 MLC1		.88					.224		6
SR-10	603	2 MLC2		.88					.224		6
SR-10	605	2 MLC3		.86					.224		6
SR-10	607	2 MLC4		.82					.224		6
SR-10	609	2 MLC5		.81					.224		6
SR-10	611	2 MLC6		.40							6
SR-11	601	2 MLC1		1.44					.220		6
SR-11	603	2 MLC2		1.33					.221		6
SR-11	605	2 MLC3		1.31					.221		6
SR-11	607	2 MLC4		1.34					.221		6
SR-11	609	2 MLC5		1.24					.221		6
SR-11	611	2 MLC6									6
SR-12	601	2 MLC1		1.06					.207		6
SR-12	603	2 MLC2		.97					.207		6
SR-12	605	2 MLC3		.99					.207		6
SR-12	607	2 MLC4		1.10					.208		6
SR-12	609	2 MLC5		1.03					.208		6
SR-12	611	2 MLC6		.44							6
SR-13	601	2 MLC1		.40							6
SR-13	603	2 MLC2		.44							6
SR-13	605	2 MLC3		.37							6
SR-13	607	2 MLC4		.44							6
SR-13	609	2 MLC5		.45							6
SR-13	611	2 MLC6		.19							6
SR-15	601	2 MLC1		.84					.210		6
SR-15	603	2 MLC2		.86					.211		6
SR-15	605	2 MLC3		.80					.210		6
SR-15	607	2 MLC4		.80					.210		6
SR-15	609	2 MLC5		.80					.210		6
SR-15	611	2 MLC6		.43					.211		6

NOTE: All data for SR-71 missions not available for release at this time.

F.50

APPENDIX G

TYPICAL ANALOG TAPE LOG

(For Tape Recorder 4, 13 January 1967)

See Appendix B for explanation

of notations and abbreviations.

TABLE G-1

<u>TYPICAL ANALOG TAPE LOG</u>

ANALOG TAPE NO. 415 DATE 13 JAN 67 TAPE RECORDER NO. 4

DATE (DY MO YR)	CHNL	HOUSE	INSTR	INST TYPE	LOCATION	P
13 JAN 67	401	2	A5	LF ACCEL	ROOF PLATE LINE N WALL NE CORNER (N-S ACCEL)	1 3
13 JAN 67	402	2	A9	LF ACCEL	BR1 CNTR CLG BOTT CHORD ROOF TRUSS	1 3
13 JAN 67	403	2	A6	LF ACCEL	ROOF PLATE LINE E WALL NE CORNER (E-W ACCEL)	1 3
13 JAN 67	404	2	A11	LF ACCEL	DR E WALL MID HT CNTR STUD	1 3
13 JAN 67	405	2	A7	LF ACCEL	2ND FLR PLATE LINE N WALL NE CRNR (N-S ACCEL)	1 3
13 JAN 67	406	2	A12	LF ACCEL	BR1 N WALL MID HT CNTR STUD	1 3
13 JAN 67	407	2	A8	LF ACCEL	2ND FLR PLATE LINE E WALL NE CRNR (E-W ACCEL)	1 3
13 JAN 67	408	2	ML2	PRESSURE	BTWN LR AND DR SUSP 6 FT ABV FLR	1 3
13 JAN 67	409	2	ML3	PRESSURE	BR1 ATTIC	1 3
13 JAN 67	410	2	ML4	PRESSURE	BR1 CNTR CLG SUSP 2 IN BELOW CLG	1 3
13 JAN 67	411	2	D1	DISPL	ADJACENT TO A5 WITH SAME AXIS	1 3
13 JAN 67	412	2	D2	DISPL	ADJACENT TO A6 WITH SAME AXIS	1
13 JAN 67	413	2	MA8	TRIGGER MIKE	IRIG B TIME CODE AND VOICE	3
13 JAN 67	414		A/C			

DATE (DY MO YR)	CHNL	HOUSE	INSTR	CAL TYPE	START DAY HR MN SC	STOP HR MN SC	START HR MN SC	STOP HR MN SC	SAMPLE RATE	FLTR CTFF
13 JAN 67	401	2	A5	PRE	013 15 29 15	15 29 16	15 29 23	15 29 24	5	
13 JAN 67	402	2	A9	PRE	013 15 30 52	15 30 53	15 30 59	15 31 00	5	
13 JAN 67	403	2	A6	PRE	013 15 33 20	15 33 21	15 33 28	15 33 29	5	
13 JAN 67	404	2	A11	PRE	013 15 41 15	15 41 16	15 41 23	15 41 24	5	
13 JAN 67	405	2	A7	PRE	013 15 42 59	15 43 00	15 43 07	15 43 08	5	
13 JAN 67	406	2	A12	PRE	013 15 44 16	15 44 17	15 44 24	15 44 25	5	
13 JAN 67	407	2	A8	PRE	013 15 45 25	15 45 26	15 45 32	15 45 33	5	
13 JAN 67	408	2	ML2	PRE	013 15 56 19	15 56 20			5	
13 JAN 67	409	2	ML3	PRE	013 16 04 58	16 04 59			5	
13 JAN 67	410	2	ML4	PRE	013 16 07 26	16 07 27			5	
13 JAN 67	411	2	D1	PRE	013 16 17 25	16 17 26			1	
13 JAN 67	412	2	D2	PRE	013 16 18 23	16 18 24			1	

DATE (DY MO YR)	MSN	A/C	ALT KFT MSL	MACH SPD (LDG)	EPR OR TKFF	HDG OFF-SET L/R,K	PMAX OR PNDB	BOOM TME DY HR MN SC ZULU	REMARKS
13 JAN 67	7-1	B-58	35.8	1.62		241 R38.7		013 18 06 55	L50
13 JAN 67	7-2	DC-8	3.7	1.76		068		013 18 15 02	010
13 JAN 67	7-3	XB-70	60.3	2.5		249 R71.3		013 18 17 20	001
13 JAN 67	15-3	F-104	20.2	1.4		242 R 0.2		013 18 27 48	319
13 JAN 67	15-1	XB-70	60.6	1.8		248 R 9.5		013 18 42 32	001
13 JAN 67	15-2	B-58	39.6	1.65		252		013 18 44 43	L50

START DIGIT STOP DIGIT LOC REMARKS

DY HR MN SEC HR MN SEC

G.1

TYPICAL ANALOG TAPE LOG (Continued)

								REMARKS	
13 JAN 67	7-1	8-58	013 18 06 55.0	18 06 56.0				FINAL E1, E2	2
13 JAN 67	7-3	XB-70	013 18 17 19.8	18 17 20.8				FINAL E1, E2	2
13 JAN 67	15-3	F-104	013 18 27 48.0	18 27 49.0				FINAL E1, E2	2
13 JAN 67	15-1	XB-70	013 18 42 32.1	18 42 33.1				FINAL E1, E2	2
13 JAN 67	15-2	B-58	013 18 44 43.5	18 44 44.5				FINAL E1, E2	2

MSN	CHNL HOUSE INSTR	PRE-CALIBRATE ATTN DB GAIN DB	+CAL	-CAL	POST-CALIBRATE RUN ATTN DB GAIN AT GN	+CAL	-CAL LEVEL	REMARKS	SAMPLE RATE SPS	FLTR CTFF
7-1	401 2 A5		.20	.20		.20	.20		4	.10
7-1	402 2 A9		.50	.50		.50	.50		4	.20
7-1	403 2 A6		.20	.20		.20	.20		4	.10
7-1	404 2 A11		1.0	1.0		1.0	1.0		4	.50
7-1	405 2 A7		.20	.20		.20	.20		4	.10
7-1	406 2 A12		.50	.50		.50	.50		4	
7-1	407 2 A8		.20	.20		.20	.20		4	.10
7-1	408 2 ML2	130.	130.	21	21	12			4	
7-1	409 2 ML3	130.	130.	18	18	12			4	
7-1	410 2 ML4	130.	130.	24	24	15			4	
7-2	401 2 A5		.20	.20		.20	.20		4	.10
7-2	402 2 A9		.50	.50		.50	.50		4	.20
7-2	403 2 A6		.20	.20		.20	.20		4	.10
7-2	404 2 A11		1.0	1.0		1.0	1.0		4	.50
7-2	405 2 A7		.20	.20		.20	.20		4	.10
7-2	406 2 A12		.50	.50		.50	.50		4	
7-2	407 2 A8		.20	.20		.20	.20		4	.10
7-2	408 2 ML2	130.	130.	21	21	12			4	
7-2	409 2 ML3	130.	130.	18	18	12			4	
7-2	410 2 ML4	130.	130.	24	24	15			4	
7-3	401 2 A5		.20	.20		.20	.20		4	.10
7-3	402 2 A9		.50	.50		.50	.50		4	.20
7-3	403 2 A6		.20	.20		.20	.20		4	.10
7-3	404 2 A11		1.0	1.0		1.0	1.0		4	.50
7-3	405 2 A7		.20	.20		.20	.20		4	.10
7-3	406 2 A12		.50	.50		.50	.50		4	
7-3	407 2 A8		.20	.20		.20	.20		4	.10
7-3	408 2 ML2	130.	130.	21	21	12			4	
7-3	409 2 ML3	130.	130.	18	18	12			4	
7-3	410 2 ML4	130.	130.	24	24	15			4	
15-1	401 2 A5		.20	.20		.20	.20		4	
15-1	402 2 A9		.50	.50		.50	.50		4	
15-1	403 2 A6		.20	.20		.20	.20		4	
15-1	404 2 A11		1.0	1.0		1.0	1.0		4	

TABLE G-1 TYPICAL ANALOG TAPE LOG (Continued)

	CHNL	HOUSE INSTR	CAL				SAMPLE RATE	FLTR CTFF
15-1	405	2 A7	.20	.20	.20	.20		4
15-1	406	2 A12	.50	.50	.50	.50		4
15-1	407	2 A8	.20	.20	.20	.20		4
15-1	408	2 ML2	130.	130.	130.	130.	18	4
15-1	409	2 ML3	130.	130.	130.	18	18	4
15-1	410	2 ML4	130.	130.	24	21		4
15-2	401	2 A5	.20	.20	.20	.20		4
15-2	402	2 A9	.50	.50	.50	.50		4
15-2	403	2 A6	.20	.20	.20	.20		4
15-2	404	2 A11	1.0	1.0	1.0	1.0		4
15-2	405	2 A7	.20	.20	.20	.20		4
15-2	406	2 A12	.50	.50	.50	.50		4
15-2	407	2 A8	.20	.20	.20	.20		4
15-2	408	2 ML2	130.	130.	130.	21	15	4
15-2	409	2 ML3	130.	130.	130.	18	15	4
15-2	410	2 ML4	130.	130.	130.	24	15	4
15-3	401	2 A5	.20	.20	.20	.20		4
15-3	402	2 A9	.50	.50	.50	.50		4
15-3	403	2 A6	.20	.20	.20	.20		4
15-3	404	2 A11	1.0	1.0	1.0	1.0		4
15-3	405	2 A7	.20	.20	.20	.20		4
15-3	406	2 A12	.50	.50	.50	.50		4
15-3	407	2 A8	.20	.20	.20	.20		4
15-3	408	2 ML2	130.	130.	130.	21	12	4
15-3	409	2 ML3	130.	130.	130.	18	12	4
15-3	410	2 ML4	130.	130.	130.	24	12	4

DATE DY MO YR	CHNL	HOUSE INSTR	CAL TYPE	START DAY	STOP HR MN SC	START HR MN SC	STOP HR MN SC	START HR MN SC	SAMPLE RATE	FLTR CTFF
13 JAN 67	401	2 A5	POST	013	19 07 41	19 07 42	19 07 48	19 07 49		5
13 JAN 67	402	2 A9	POST	013	19 09 15	19 09 16	19 09 23	19 09 24		5
13 JAN 67	403	2 A6	POST	013	19 10 33	19 10 34	19 10 40	19 10 41		5
13 JAN 67	404	2 A11	POST	013	19 12 27	19 12 28	19 12 35	19 12 36		5
13 JAN 67	405	2 A7	POST	013	19 13 52	19 13 53	19 13 59	19 14 00		5
13 JAN 67	406	2 A12	POST	013	19 15 10	19 15 11	19 15 19	19 15 20		5
13 JAN 67	407	2 A8	POST	013	19 16 29	19 16 30	19 16 39	19 16 40		5
13 JAN 67	408	2 ML2	130.	013	19 24 02	19 24 03			12	5
13 JAN 67	409	2 ML3	130.	013	19 28 26	19 28 27			12	5
13 JAN 67	410	2 ML4	130.	013	19 31 24	19 31 25			12	5
13 JAN 67	411	2 D1	POST	013	19 34 34	19 34 35				5
13 JAN 67	412	2 D2	POST	013	19 35 34	19 35 35				5

G.3

APPENDIX H

DERIVATIONS

APPENDIX H

DERIVATIONS

A. RELATION OF INSIDE PRESSURE TO OUTSIDE PRESSURE[a]

The response of the large glass window in Test House E-I was analysed to determine the relation of the inside pressure to the outside pressure. This Appendix presents the results of this analysis.

...ed that the change in the inside pressure was proportional to the ...volume inside the garage produced by deflection of the window. ...also assumed that the deflected surface of a simply supported plate mounted in a rigid airtight enclosure when subjected to a sonic boom loading was closely approximated by its first mode static deflected shape multiplied by an appropriate DAF, i.e.:

$$w = a_{11} \sin\frac{\pi x}{L} \sin\frac{\pi y}{b} g(t) \qquad \text{(H-Ia)}$$

$$w = a_{11} \sin\frac{\pi x}{L} \sin\frac{\pi y}{b} (DAF)_n \qquad \text{(H-Ib)}$$

$$w = w_s (DAF)_n \qquad \text{(H-Ic)}$$

where

$$a_{11} = \frac{16 \, L^4}{D\pi^6 \left[1 + (L/b)^2\right]^2} \qquad \text{(H-2)}$$

Here it was assumed that the DAF due to net pressure is a known quantity. A more rigorous approach to this problem without making this assumption leads to the following differential equation:

$$\dddot{f}_{11} + (A + Ct)\, \dot{f}_{11} + 2Cf_{11} = F\dot{P}_o \qquad \text{(H-3)}$$

where

$$A = \frac{D\pi^4}{\rho L^4}\left[1 + (L/b)^2\right]^2$$

---

[a] A Glossary of terms is given at the end of this Appendix.

$$C = \frac{16 \, P_a \, L^2 \, b^2}{V \pi^4}$$

$$F = \frac{4 \, L \, b}{\pi^2}$$

then

$$w = f_{11}(t) \sin\frac{\pi x}{L} \sin\frac{\pi y}{b} \tag{H-4}$$

In general $f_{11}(t)$ cannot be expressed in closed form and it is necessary to obtain the solution to (H-3) by numerical integration. In order to obtain w, it was assumed in the remainder of this discussion that $(DAF)_n$ was a known quantity.

The total volume displaced in the garage is

$$v^{1} = DAF \int_{0}^{L} \int_{0}^{b} a_{11} \sin\frac{\pi x}{L} \sin\frac{\pi y}{b} \, dy dx \tag{H-5a}$$

$$= a_{11} \frac{4 \, L \, b}{\pi^2} \, DAF \tag{H-5b}$$

Assuming pressure times volume inside the garage is constant,

$$P_a V = (P_a + P_i)(V - v^{1}) \tag{H-6}$$

Defining

$$P_n = P_o - P_i \tag{H-7}$$

Equation (H-6) becomes

$$P_n = P_o - P_a \left[\frac{v^{1}}{V-v^{1}}\right] \approx P_o - P_a \frac{v^{1}}{V} \tag{H-8}$$

The maximum displacement occurs at the center of the plate and is

$$w_n = a_{11} \, DAF \tag{H-9a}$$

$$w_n = \frac{16 \, L^4 \, P_n \, (DAF)}{D \pi^6 \left[1 + (L/b)^2\right]^2} \tag{H-9b}$$

H.2

Substituting Equations (H-5b) and (H-8) into Equation (H-9b) yields

$$w_n = B\left[P_o - \frac{P_a \ 4 \ L \ b \ w_n}{V \ \pi^2}\right] \tag{H-10a}$$

where

$$B = \frac{16 \ L^4 \ (DAF)}{D\pi^6\left[1 + (L/b)^2\right]^2}$$

Solving for w_n gives

$$w_n = \frac{P_o \ B}{1 + \dfrac{4}{\pi^2} \dfrac{P_a \ B \ L \ b}{V}} \tag{H-10b}$$

Noting that

$$w_o = P_o \ B \tag{H-11}$$

Equation (H-7b) can be written

$$\frac{w_n}{w_o} = \frac{1}{1 + \dfrac{4 \ P_a \ B \ L \ b}{\pi^2 \ V}} \tag{H-12}$$

Since

$$\frac{P_n}{P_o} = \frac{w_n}{w_o} \tag{H-13}$$

The inside pressure is

$$P_i = P_o \ \frac{\dfrac{4 \ P_a \ B \ L \ b}{\pi^2 \ V}}{1 + \dfrac{4}{\pi^2} \dfrac{P_a \ B \ L \ b}{V}} \tag{H-14}$$

which can be rewritten as

$$P_i = P_o \ \frac{P_a \ B}{P_a \ B + \dfrac{\pi^2 V}{4Lb}} \tag{H-15}$$

H.3

GLOSSARY OF TERMS

E   = modulus of elasticity

L,b = plate dimensions

t   = plate thickness

ν = Poisson's ratio

P   = pressure

DAF = dynamic amplification factor

V   = volume of enclosure

V^{I} = change in volume

ρ = mass per unit area

P_{a} = atmospheric pressure

t   = time

w   = lateral deflection of plate

K   = effective stiffness

$\cdot$ = $\dfrac{d\ (\ )}{dt}$

D   = window stiffness = $\dfrac{Et^{3}}{12(1 - \nu^{2})}$

Subscripts

i   = inside

o   = outside

n   = net

s   = static

H.4

DOCUMENT CONTROL DATA - R&D

(Security classification of title, body of abstract and indexing annotation must be entered when the overall report is classified)

1 ORIGINATING ACTIVITY *(Corporate author)*	2a. REPORT SECURITY CLASSIFICATION
John A. Blume & Associates Research Division 612 Howard Street San Francisco, California 94105	UNCLASSIFIED
	2b GROUP

3. REPORT TITLE

Response of Structures to Sonic Booms Produced by XB-70, B-58 and F-104 Aircraft

4. DESCRIPTIVE NOTES *(Type of report and inclusive dates)*

Final Report

5. AUTHOR(S) *(Last name, first name, initial)*

Blume, John A., Sharpe, Roland L., Kost, Garrison, and Proulx, Jacques

6. REPORT DATE	7a. TOTAL NO. OF PAGES	7b. NO. OF REFS
July 1967		34

8a. CONTRACT OR GRANT NO.	9a. ORIGINATOR'S REPORT NUMBER(S)
AF 49(638)-1739	
b. PROJECT NO.	
c.	9b. OTHER REPORT NO(S) *(Any other numbers that may be assigned this report)*
d.	

10. AVAILABILITY/LIMITATION NOTICES

Qualified requesters may obtain copies of this report from DDC.
Others may obtain copies of this report from the Clearinghouse for Federal
Scientific and Technical Information, Dept. of Commerce.

11. SUPPLEMENTARY NOTES	12. SPONSORING MILITARY ACTIVITY
	National Sonic Boom Evaluation Office United States Air Force 1400 Wilson Blvd. Arlington, Virginia 22209

13. ABSTRACT

The response of test structures and structure elements to sonic booms produced by XB-70, B-58 and F-104 aircraft was studied. These aircraft produced sonic booms of different signature durations. They were flown at several flight track offsets, altitudes and Mach numbers so as to generate different overpressure levels and signature characteristics. Free field signature data and the effects of free field signature parameters on structural response were analysed. Studies were made of the plate response (lateral deformation) and racking response (in-plane deformation) of the test structures. Damage complaints resulting from the test missions were investigated and the results analysed. The implications of the magnitudes of the responses of the test structures and the investigation of the damage claims resulting from the test missions on possible damage caused by supersonic flights were discussed.

DD FORM 1473
1 JAN 54

14. KEY WORDS	LINK A		LINK B		LINK C	
	ROLE	WT	ROLE	WT	ROLE	WT
Sonic boom						
Overpressure						
Structure response						
Racking response						
Plate response						
Window response						
Damage evaluation						
XB-70 aircraft						
B-58 aircraft						
F-104 aircraft						

INSTRUCTIONS

1. ORIGINATING ACTIVITY: Enter the name and address of the contractor, subcontractor, grantee, Department of Defense activity or other organization (corporate author) issuing the report.

2a. REPORT SECURITY CLASSIFICATION: Enter the overall security classification of the report. Indicate whether "Restricted Data" is included. Marking is to be in accordance with appropriate security regulations.

2b. GROUP: Automatic downgrading is specified in DoD Directive 5200.10 and Armed Forces Industrial Manual. Enter the group number. Also, when applicable, show that optional markings have been used for Group 3 and Group 4 as authorized.

3. REPORT TITLE: Enter the complete report title in all capital letters. Titles in all cases should be unclassified. If a meaningful title cannot be selected without classification, show title classification in all capitals in parenthesis immediately following the title.

4. DESCRIPTIVE NOTES: If appropriate, enter the type of report, e.g., interim, progress, summary, annual, or final. Give the inclusive dates when a specific reporting period is covered.

5. AUTHOR(S): Enter the name(s) of author(s) as shown on or in the report. Enter last name, first name, middle initial. If military, show rank and branch of service. The name of the principal author is an absolute minimum requirement.

6. REPORT DATE: Enter the date of the report as day, month, year; or month, year. If more than one date appears on the report, use date of publication.

7a. TOTAL NUMBER OF PAGES: The total page count should follow normal pagination procedures, i.e., enter the number of pages containing information.

7b. NUMBER OF REFERENCES: Enter the total number of references cited in the report.

8a. CONTRACT OR GRANT NUMBER: If appropriate, enter the applicable number of the contract or grant under which the report was written.

8b, 8c, & 8d. PROJECT NUMBER: Enter the appropriate military department identification, such as project number, subproject number, system numbers, task number, etc.

9a. ORIGINATOR'S REPORT NUMBER(S): Enter the official report number by which the document will be identified and controlled by the originating activity. This number must be unique to this report.

9b. OTHER REPORT NUMBER(S): If the report has been assigned any other report numbers (either by the originator or by the sponsor), also enter this number(s).

10. AVAILABILITY/LIMITATION NOTICES: Enter any limitations on further dissemination of the report, other than those imposed by security classification, using standard statements such as:

(1) "Qualified requesters may obtain copies of this report from DDC."

(2) "Foreign announcement and dissemination of this report by DDC is not authorized."

(3) "U. S. Government agencies may obtain copies of this report directly from DDC. Other qualified DDC users shall request through

_____ ."

(4) "U. S. military agencies may obtain copies of this report directly from DDC. Other qualified users shall request through

_____ ."

(5) "All distribution of this report is controlled. Qualified DDC users shall request through

_____ ."

If the report has been furnished to the Office of Technical Services, Department of Commerce, for sale to the public, indicate this fact and enter the price, if known.

11. SUPPLEMENTARY NOTES: Use for additional explanatory notes.

12. SPONSORING MILITARY ACTIVITY: Enter the name of the departmental project office or laboratory sponsoring (paying for) the research and development. Include address.

13. ABSTRACT: Enter an abstract giving a brief and factual summary of the document indicative of the report, even though it may also appear elsewhere in the body of the technical report. If additional space is required, a continuation sheet shall be attached.

It is highly desirable that the abstract of classified reports be unclassified. Each paragraph of the abstract shall end with an indication of the military security classification of the information in the paragraph, represented as (TS), (S), (C), or (U)

There is no limitation on the length of the abstract. However, the suggested length is from 150 to 225 words.

14. KEY WORDS: Key words are technically meaningful terms or short phrases that characterize a report and may be used as index entries for cataloging the report. Key words must be selected so that no security classification is required. Identifiers, such as equipment model designation, trade name, military project code name, geographic location, may be used as key words but will be followed by an indication of technical context. The assignment of links, rules, and weights is optional.